Smooth Muscle Differentiation from Human Umbilical Cord Derived Mesenchymal Stem Cells
miRNA-involved Mechanism and Potential Application for Vascular Tissue Engineering

Gu, Wenduo

Awarding institution:
King's College London

Smooth Muscle Differentiation from Human Umbilical Cord Derived Mesenchymal Stem Cells: miRNA-involved Mechanism and Potential Application for Vascular Tissue Engineering

By

Wenduo Gu

A thesis submitted to King's College London

For the degree of

Doctor of Philosophy

Cardiovascular Division

Faculty of Life Sciences & Medicine

King's College London

September 2017

In Dedication to My Family and Friends

Abstract

Tissue engineered vascular grafts with long term patency are in great need in the clinics. An accessible source of human smooth muscle cell (SMC) is important for constructing functional vascular grafts. Human mesenchymal stem cells from the umbilical cord (UCMSCs) exhibit multi-lineage differentiation abilities, including the potential to differentiate towards vascular lineages such as SMCs. MicroRNAs (miRNAs) are short non-coding regulatory RNAs. They widely participate in regulation of stem cell differentiation and may play an important role in SMC differentiation. Understanding how to generate SMCs from UCMSCs as well as its underlying mechanism might greatly contribute to our knowledge of manufacturing functional vascular grafts.

We hypothesise that vascular grafts could be generated with SMCs differentiated from human UCMSCs, and further explore the role of miRNAs in the differentiation process. We utilised transforming growth factor β 1 (TGFβ1) to stimulate the UCMSCs differentiation towards SMCs. A panel of SMC markers including αSMA, SM22, Calponin and SMMHC were highly upregulated both at the gene expression and the protein level at day 5 of TGFβ1 treatment. Micro-RNA (miR) array analysis showed that miR-503 was increased at early time points (6 h and 24 h) after TGFβ1 treatment, which was confirmed by TaqMan microRNA assay. We further demonstrated that miR-503 mimics promoted SMC differentiation both at the gene expression and the protein level and miR-503 inhibitors downregulated SMC markers at the protein level. Smad7, which is a negative regulator of TGFβ1-related signalling pathways, was identified to be a direct target of miR-503 by luciferase reporter experiments. The expression level of miR-503 was Smad4-dependent as shown by the Smad4 knockdown experiments. Also, Smad4 was demonstrated to be enriched at the promoter region of miR-503 as shown by Chromatin immunoprecipitation experiments.

In addition to miR-503, miR-222-5p was also downregulated in the differentiation process. The gain-of-function study with the treatment of miR-222-5p mimics

significantly inhibited the induction of SMC markers Calponin and αSMA both at the gene expression and protein level during differentiation. αSMA was confirmed to be a direct target of miR-222-5p. Moreover, ROCK2, which could mediate SMC differentiation through RhoA/ROCK pathway, was downregulated by miR-222-5p mimics both at the gene expression and protein level. The 3'-UTR segment of ROCK2 was identified to be a direct target of miR-222-5p.

Finally, SMCs differentiated from UCMSCs exhibited the ability to migrate into decellularised mouse aorta grafts. Seeding of the cells onto the decellularised scaffold gave rise to vascular graft with smooth muscle layer that is comparable to its analog of the native vessel. In conclusion, we demonstrated the potential of using hUCMSCs-derived SMCs to generate vascular grafts which are in critical need in the clinics.

Table of Contents

Declaration

I, Wenduo Gu, declare that the work included in this thesis is all from myself. I have been involved in the design, planning, conduct of all experiments, and the thesis writing.

Expert assistance has been provided in some aspects of the project by the following colleagues from the Cardiovascular Division of King's College London.

Dr. Yanhua Hu performed the *in vivo* part of the Matrigel plug angiogenesis assay.

Acknowledgements

First and foremost, I would like to express gratitude to Professor Qingbo Xu for the opportunity to study for my PhD degree. I would also like to thank him for the academic input, time and energy he contributed in nurturing me to be a young scientist. Furthermore, his life advice has influenced me in all aspects.

I would like to thank Dr. Xuechong Hong for her academic support throughout the PhD program. I would also like to thank Dr. Yanhua Hu for all kinds of help, especially with *in vivo* animal experiments.

I also wish to thank all present and past lab members for their help and support. Special thanks to Dr. Shirin Issa Bhaloo, Dr. Alexandra Le Bras, Dr. Witold Nowak, Dr. Ka Hou Lao, Dr. Ana Moraga, Mr Yao Xie, Ms Peiyi Luo, Ms Ada Sera Kurt, and Mr Zhichao Ni for their support as well as the precious memories about the group birthday celebrations, dinners, drinks, trips and film activities which always bright my day. I would like to thank Dr. Xuechong Hong, Dr. Witold Nowak and Dr. Ka Hou Lao and Dr. Jiacheng Deng for their help in the thesis revision.

I also wish to express my gratitude to people who have helped me in life. Without them I would not be able to be where I am now. Special thanks to Qingli Huang, Jingtao Zhang and Lan Yu for their support and life guidance. I would also like to thank my friends Yun He, Yaqin Zhang, Zhichao Zheng and Yalei Zhang for their unconditional support in daily life.

Most importantly, I wish to convey my deepest thanks and gratitude to my mother, my sister and my father, for their unconditional love, for their always being by my side, and for their encouragement for me to do whatever I prefer in life and in career. Especially, I would like to thank my newborn niece Murui Wang, who has brought so many happy moments to my life in the last year of my PhD program.

Finally, I wish to thank King's - China Scholarship Council Scholarship for funding my PhD project.

List of Figures

List of Tables

Abbreviations

3’-UTR	**3’-untranslated region**
ADSCs	**adipose tissue-derived mesenchymal stem cells**
AngII	**angiotensin II**
Arl2	**ADP ribosylation factor like GTPase 2**
at-RA	**all-trans retinoic acid**
BMMSCs	**bone marrow-derived mesenchymal stem cells**
BMP4	**bone morphogenetic protein 4**
CD	**cluster of differentiation**
CDKN1B/p27^{kip1}	**cyclin-dependent kinase inhibitor 1B**
CDKN1C/p57^{kip2}	**cyclin-dependent kinase inhibitor 1C**
CFU	**colony forming unit**
ChIP	**chromatin immunoprecipitation**
CLASH	**crosslinking, ligation and sequencing of RNA hybrids**
DGCR8	**DiGeorge syndrome chromosome region 8**
dsRBD	**double-stranded RNA binding domains**
E2F3	**E2F transcription factor 3**
EC	**endothelial cell**
ECM	**extracellular matrix**
EGF	**epidermal growth factor**
ePTFE	**expanded polytetrafluoroethylene**
ERα	**estrogen receptor α**

FACS	**fluorescence-activated cell sorting**
FBS	**fetal bovine serum**
FGF	**fibroblast growth factor**
F-actin	**filamentous actin**
G-actin	**glomerular actin**
H&E	**hematoxylin and eosin**
HAT	**histone acetyltransferase**
HDAC	**histone deacetylase**
HMG2L1	**high mobility group 2 like 1**
HSC	**haematopoietic stem cell**
HUVEC	**human umbilical vein endothelial cell**
IGF	**Insulin-like growth factor**
iPSC	**induced pluripotent stem cell**
ISCT	**International Society for Cellular Therapy**
JNKs	**Jun amino-terminal kinases**
Klf4	**Krüppel-like factor 4**
L1CAM	**L1 cell adhesion molecule**
LIF	**leukaemia inhibitory factor**
MADS	**MCM1, agamous, deficiens, serum response factor**
MAPKs	**p38 mitogen-activated protein kinases**
MEF2	**myocyte enhancer factor 2**
MEM	**minimum essential medium**
miRNA	**microRNAs**

mRNA	**messenger ribonucleic acid**
MRTFs	**myocardin-related transcription factors**
MSCs	**mesenchymal stem cells**
NF- κB	**nuclear factor κ-light-chain-enhancer of activated B cells**
Nox4	**NADPH oxidase 4**
PAGE	**polyacrylamide gel electrophoresis**
PBS	**phosphate buffered saline**
PCL	**poly ε-caprolactone**
PDGF	**platelet-derived growth factor**
PELCL	**poly(ethylene glycol)-b-poly(L-lactide-co-caprolactone)**
PET	**polyethylene terephthalate**
PFA	**paraformaldehyde**
PGS	**Poly(glycerol sebacate)**
PLA	**polylactic acid**
POSS-PCU	**polyhedral oligomeric silsesquioxane poly(carbonate-urea) urethane**
PPARγ	**peroxisome proliferator-activated receptor γ**
PU	**polyurethane**
Q-PCR	**quantitative polymerase chain reaction**
RBP	**RNA-binding protein**
RISC	**RNA-induced silencing complex**
RLU	**relative luciferase unit**
RT	**reverse transcription**
SDS	**sodium dodecyl sulphate**

siRNA	**small interfering RNA**
SM22	**Smooth muscle protein 22 / transgelin**
Smad7	**mothers against decapentaplegic homolog 7**
SMC	**smooth muscle cell**
SMMHC	**smooth muscle myosin heavy chain**
Smurf2	**SMAD specific E3 ubiquitin protein ligase 2**
SPC	**sphingosylphosphorylcholine**
SRF	**serum response factor**
TCE	**TGFβ control element**
TIMP3	**tissue inhibitor of metalloproteinase 3**
TRBP	**human immunodeficiency virus type 1 transactivating response RNA-binding protein**
UCMSCs	**umbilical cord-derived mesenchymal stem cells**
uPAR	**urokinase-type plasminogen activator receptor**
αSMA	**α smooth muscle actin**

1. Introduction

The aim of my PhD project is to study the potential application of smooth muscle cells (SMCs) derived from human umbilical cord mesenchymal stem cells (hUCMSCs) in vascular tissue engineering and investigate the miRNA-related mechanism in the differentiation process. In the introduction part of this thesis, I would first introduce the major studies and concepts in the fields of mesenchymal stem cells (MSCs), differentiation of SMCs from stem cells and established mechanisms, miRNAs and vascular tissue engineering. Firstly, the discovery history and the basic biology of MSCs would be described. Secondly, the differentiation system from various stem cell types towards SMCs would be depicted. Thirdly, the differentiation mechanisms that have been illustrated in the literature would be reviewed. After that, the recognition of regulatory miRNAs in pathological and physiological conditions as well as the basic principles of miRNA functioning mode would be explored. In the end, the vascular tissue engineering approaches with the focus on the numerous stem cell types especially MSCs would be presented.

1.1. Mesenchymal stem cells (MSCs)

1.1.1. The discovery of mesenchymal stem cells

Freidenstein (Friedenstein et al., 1968) was credited for the discovery of mesenchymal stem cells in 1968. By analysing the newly formed bone tissue and haematopoietic tissue under the renal capsule after the transplantation of fragmented marrow there, his laboratory managed to determine that the bone tissue is exclusively of donor origin whereas the haematopoietic tissue is of host origin. After secondary transplantation of the donor cells isolated from the ectopic bone, they confirmed the self-renewal capacity of these cells and established the existence of what he called precursors of osteogenic tissues (Friedenstein et al., 1968). This experiment proved that precursors of osteogenic tissues are a different cell type from the previously discovered haematopoietic stem cells.

After Freidenstein's findings in 1968, he proceeded and devoted his efforts in confirming the identity of the cells that were responsible for osteogenesis of the transplanted marrow. In a series of studies (Friedenstein and Kuralesova, 1971; Friedenstein, 1980, 1995; Friedenstein et al., 1970; Friedenstein et al., 1987; Friedenstein et al., 1974; Friedenstein et al., 1976; Friedenstein et al., 1978; Latsinik et al., 1970; Owen and Friedenstein, 1988), he observed the development of fibroblast colonies in monolayer cultures of guinea pig bone marrow and confirmed the bone formation capability of these cells in diffusion chambers (Figure 1-1). He used to call these cells colony forming unit fibroblasts, osteogenic precursor cells, bone marrow stromal mechanocytes, fibroblast precursors, marrow-derived osteogenic precursors and marrow stromal fibroblasts, which are now called mesenchymal stem/stromal cells by most researchers in this field. These cells are characterised by their rapid adherence to the plastic surface, self-renewal ability and their *in vitro* colony forming capacity when seeded at a suitable density. (Landmark studies in the discovery of BMMSCs are summarised in Table 1-1)

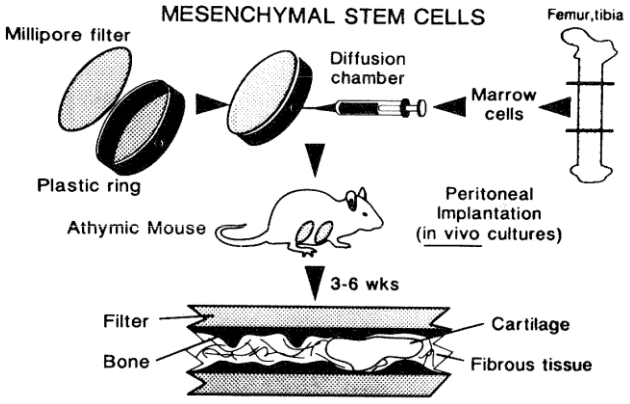

Figure 1-1 How the diffusion chamber assay works

The diffusion chamber is composed of a small plastic ring enclosed by two Millipore filters. Cells injected in the chamber remained inside as they could not pass through the filter to get mixed with the host cells outside. Body fluids (nutrients, salts, and proteins) could pass freely

through the filter. After transplantation into the peritoneal cavity of a nude mouse, the diffusion chamber was quickly surrounded by host vasculature, allowing it to serve as an *in vivo* incubator. This figure is reproduced from Arnold I. Caplan, 1991.

Table 1-1 Landmark experiments in the discovery of BMMSCs

Year	Author	Study & Finding
1867	Cohnheim	Cohnheim hypothesis: Marrow-derived fibroblast like cells could enter circulation and excavate vessels of injured tissues and take part in tissue regeneration
1868	Goujon	Osteogenesis of ectopically transplanted bone marrow
1963	Till, McCulloch and Becker	Existence of haematopoietic stem cell within the bone marrow
1966,1968,1971	Freidenstein, Tavassoli & Crosby, Maniatis	Re-observation of osteogenesis in ectopically transplanted bone marrow; Not sure whether cells responsible for osteogenesis are of the same origin of haematopoietic cells
1968	Freidenstein	Confirmation that cells for neo-bone tissue formation and haematopoietic tissue are of different origins by the method of heterogenic transplantation
1970-1995	Freidenstein	Isolation and culture of colony forming unit fibroblasts with osteogenic potential

1.1.2. Bone marrow-derived mesenchymal stem cells (BMMSCs)

With the diffusion chamber system in the 1990s, researchers managed to confirm the differentiation of bone marrow-derived mesenchymal stem cells (BMMSCs) to bone, cartilage and fibrous tissue. In the diffusion chamber with two Millipore filters enclosed by a small plastic ring, cells injected in the chamber remained inside as they could not pass through the filter to get mixed with the host cells outside. Body fluids (nutrients, salts and proteins) could pass freely through the filter. After transplantation into the peritoneal cavity of a nude mouse *in vivo*, the diffusion chamber was quickly surrounded by host vasculature, allowing it to serve as an *in vivo* incubator (Bab et al., 1986; Bennett et al., 1991; Caplan, 1991). Figure 1-1 outlines the diffusion chamber assay in a nude mice (Caplan, 1991). In addition to the use of diffusion chamber, Caplan and his group took advantage of porous calcium phosphate ceramics loaded with marrow cells and implanted them at heterotopic sites (eg. subcutaneous), with the observation of predominant bone formation, which was slightly different from the mixture of bone, cartilage and fibrous tissue formation in the diffusion chamber assay (Caplan, 1991; Ohgushi et al., 1989a, b).

By manipulating the culture conditions (Beresford et al., 1992), the cells could be induced into either adipocytic or osteogenic lineage. This is the preliminary evidence for the *in vivo* and *in vitro* differentiation of BMMSCs. Subsequently numerous studies have been conducted with various differentiation conditions. It is worth noting that, Caplan is the first to call these cells multi-potent “mesenchymal stem cells”.

1.1.3. Mesenchymal stem cells from other stromal tissues

Since the isolation of MSCs with tri-lineage differentiation potential (i.e. osteogenic, chondrogenic and adipogenic differentiation capacities) from the bone marrow, cells with similar characteristics have been isolated from multiple human tissue types including adipose tissue, synovial membrane, periodontal ligament, tendon, skin, cartilage, dental pulp, eye, gut, heart, kidney, liver, lung, muscle, pancreas, spleen, thymus, umbilical cord, placenta, aorta, vena cava, cord blood and peripheral blood (Alsalameh et al., 2004; Bi et al., 2007; Campagnoli et al., 2001; da Silva Meirelles et al., 2006; De Bari et al., 2001; Gronthos et al., 2002; Romanov et al., 2003; Salingcarnboriboon et al., 2003; Seo et al., 2004; Shi and Gronthos, 2003; Toma et al., 2005; Villaron et al., 2004; Zuk et al., 2002; Zuk et al., 2001). (The characterization of MSCs derived from various tissues are summarised in Table 1-2.)

Since the discovery of BMMSCs and later MSCs originating from tissues all over the body, MSCs have been widely used in translational researches, such as orthopaedic reconstruction, which has promising clinical potential. Some clinical trials have taken advantage of the benefits of the immune regulatory function of MSCs and have shown promising and reproducible results in immune disorders such as multiple sclerosis, graft-versus-host disease and Crohn’s disease (Prockop and Olson, 2007; Uccelli et al., 2008). Clinical benefits have also been achieved in other areas such as cardiovascular diseases (myocardial infarction and ischemia), pulmonary and neurological diseases. However, some of the results are anecdotal and not reproducible due to the lack of homogeneity, poor understanding of *in vivo* identity of MSCs and the lack of standard culture conditions. The promising therapeutic

application of MSCs in translational researches urges further efforts to be invested in elucidating the *in vivo* identity and biological function of these cells.

Umbilical cord-derived mesenchymal stem cells (UCMSCs)

UCMSCs have similar immunophenotypic characteristics and functional properties with MSCs derived from other tissues. However, source-dependent differences exist. Compared to MSCs derived from other tissues, UCMSCs display higher proliferation capacity which is a significant advantage with regard to their application potential in tissue engineering (Abu Kasim et al., 2012; Hsieh et al., 2010; Lu et al., 2006; Yu et al., 2013). UCMSCs grow faster than BMMSCs at early passages with a cell population doubling time of 24 hours over 40 hours of BMMSCs (Abu Kasim et al., 2012). Furthermore, UCMSCs demonstrate better ability to form colony forming units *in vitro* which is also a proof of their relatively better proliferation capacity compared to bone marrow nucleated cells (Lu et al., 2006).

Regarding the transcriptomic profile of UCMSCs and BMMSCs, most of the surface markers they express are common mesenchymal markers. However, unlike in BMMSCs, HLA-ABC is weakly expressed in UCMSCs, indicating that these cells might be less immunogenic than BMMSCs (El Omar et al., 2014). This immune privilege makes UCMSCs a good candidate for tissue engineering of vascular grafts, which will be grafted *in vivo* in the end.

Adipose tissue-derived mesenchymal stem cells (ADSCs)

The harvesting method of BMMSCs is invasive with a relatively low yield. ADSCs present similar properties with MSCs derived from other tissues including BMMSCs (da Silva Meirelles et al., 2006). The main advantage of ADSCs over BMMSCs is perhaps the abundance of adipose tissue which makes ADSCs readily available. Arguably, ADSCs are among the most promising MSCs for stem cell based cell therapeutics and tissue engineering (Cawthorn et al., 2012).

Table 1-2 Characterisation of MSCs derived from various sources

Tissue	Literature	Molecular characterisation	Differentiation *in vitro*
Adipose tissue	Zuk PA, 2002	FVIII 24.9%, α SMA 29.2% (ECs, SMCs, pericytes), ASO2 85.0%, vimentin 63.2% (mesenchymal markers) (IF) Positive: CD29, CD44, CD71, CD90, CD105, SH3, CD49d; Negative: CD31, CD34,CD 45	Adipogenic Chondrogenic Osteogenic Neurogenic Myogenic
Umbilical cord	Romanov YA,2003	(IF) Positive: α SMA; Negative; CD31, vWF, CD34	Adipogenic
Synovial membrane	Di Bari, 2001	(RT-PCR) Positive: CD44; Negative: CD31, CD45,CD14, CD20	Adipogenic Chondrogenic Osteogenic Myogenic
Periodontal ligament	Seo BM, 2004	(IF) Stro-1, CD146	Cementoblast-like cells Adipogenic,
Tendon	Bi Y, 2007, Salingcarnboriboon R, 2003		Osteogenic Adipogenic Tendon
Skin	Toma JG, 2005	(IF) fibronection, vimentin, nestin	Neurons Glias SMCs
Cartilage	Alsolameh S, 2004	CD105+ 95%; CD166+ 5%; CD105+/CD166+ 3.49%	Adipogenic Chondrogenic Osteogenic
Dental pulp	Shi S, 2003	Stro1 + selected cells: Positive: CD146, α SMA, 3G5	Adipocyte Neural cells
Spleen, muscle, kidney, lung, liver, brain, thymus, aorta, vein	Da Silva Meirelles L, 2006	(FACS) CD29+, CD44+, CD117-, CD49e, CD90.2: expression varies; Sca-1, CD34: decrease with passage	Adipogenic, Osteogenic, Chondrogenic
Blood	Villaron EM, 2004	(FACS) Positive: CD90, CD106, CD54, CD49b; Negative: CD105, CD56, CD34, CD133, CD104, CD62L, HLA-DR	
Cord blood	Campagnoli C, 2001	(FACS) Positive: CD29, CD44, CD105, SH3, SH4 Negative: CD45, CD34, CD14, CD68, vWF, HLA-DR	Adipogenic Osteogenic Chondrogenic

1.1.4. The minimal criteria of mesenchymal stem cells

Since 2000, there has been an explosion in the number of studies about mesenchymal stem cells. However, without standard characterisation method, obvious discrepancy across different labs existed, which made it difficult to interpret the results accurately. To solve this problem, International Society for Cellular

Therapy (ISCT) published a position statement of the minimal criteria to define multipotent mesenchymal stromal cells cultured from human tissues (Dominici et al., 2006). In this position paper, mesenchymal stem cells are defined as being adherent to the plastic surface when cultured under standard conditions. They acquire a specific phenotype and display multipotent differentiation capacity *in vitro*. (The minimal criteria of human MSCs are summarised in Table 1-3.) Concerning negative surface markers of the phenotype, CD45 (cluster of differentiation 45), CD34, CD14 or CD11b, CD79α or CD19 are used to exclude contamination of pan-leukocyte, primitive haematopoietic progenitors, monocytes/macrophages and B cells respectively in the culture. Positive expression of the surface markers merits further exploration because none of the markers are specific to mesenchymal stem cells and more markers should be explored to distinguish mesenchymal stem cells between their differentiated state and undifferentiated state.

Though the ISCT position managed to define MSCs with phenotypic markers and avoided contamination of other cell population, these criteria still could not uniquely identify all MSCs (Sabatini et al., 2005). Sabatini identified human bronchial fibroblasts exhibiting a mesenchymal stem cell phenotype and multilineage differentiation potentials in 2005. Furthermore, though these markers are used to identify mesenchymal stem cells *in vitro*, it is hard to search for mesenchymal stem cells *in situ* in tissue sections with multi-staining of them even with the most advanced multicolour fluorescence microscopes due to the *in vitro* culture artifacts and the lack of knowledge about the differences between MSCs *in vivo* and *in vitro*.

Table 1-3 The minimal criteria to characterise human MSCs

1.	**Adherence to the plastic surface in standard culture conditions**
2.	**Phenotype:** **Positive (⩾95%+): CD73, CD90, CD105; Negative (⩽2%+): CD45, CD34, CD14 or CD11b, CD79αor CD19, HLA-DR**
3.	***In vitro* differentiation capacities: osteoblasts, adipocytes, chondrocytes (demonstrated by staining of *in vitro* culture)**

Other markers used for mesenchymal stem cell characterisation include Stro-1 (Simmons and Torok-Storb, 1991), which can enrich CFU-Fs (colony forming unit fibroblasts) by approximately 100-fold in human MSCs, when combined with glycophorin A negative phenotype (to exclude erythroid progenitors). However, Stro-1 is only expressed in human tissues and there is no corresponding marker in other species. Recent findings showed that Stro-1 is expressed in the endothelium rather than in mesenchymal tissue *in vivo*, and it was induced under mesenchymal stem cell culture conditions *in vitro* (Ning et al., 2011). Additionally, it is well documented that difference exists across tissue origins and between species (Sacchetti et al., 2016). This implies the necessity of future work to discover true markers of mesenchymal stem cells and minimise artifacts of *in vitro* culture.

1.1.5. *In vivo* identity and function of mesenchymal stem cells

MSCs are a heterogeneous population reflected in the colonies they form *in vitro* which have different growth rates and morphologies ranging from fibroblast like spindle shaped cells to large spread cells. Furthermore, if the colonies are allowed to grow for a long period, heterogeneity in the colonies could be observed as well, with some of the colonies alkaline phosphate positive, some of them negative and some others positive in the centre and negative in the periphery region (Friedenstein et al., 1982). This heterogeneity might be explained by the tissues themselves which consist of numerous different cell types and therefore have diverse precursor types and are heterogeneous in nature and origin. However, *in vitro* culture of these cells seems to be at least similar concerning the phenotype and multilineage differentiation potential.

To minimise the discrepancy of reported properties of mesenchymal stem cells and increase the consistency of molecular studies and preclinical trials across different labs, characterisation of *in situ*/native mesenchymal stem cells is a prerequisite and could allow for purification of these cells which could facilitate the researches in tissue engineering applications. Approaches in searching for the *in vivo* nature, localisation and identity of mesenchymal stem cells so far include seeking for the *in vivo* MSCs with *in vitro* expressed surface markers, infusion of marked MSCs *in vivo* to track their

homing and distribution, and systemic isolation of MSCs from various tissues to evaluate their characterisation.

As discussed earlier, Stro-1 is strongly expressed in stromal cells which are clonogenic in *in vitro* cultured cells (Gronthos et al., 1994). Theoretically, the same reagent used in *in vivo* sections could establish the *in vitro* and *in vivo* relationship of mesenchymal stem cells, providing evidence of micro-anatomical niches or identity of the clonogenic cells (Bianco et al., 2001). In frozen sections stained with Stro-1, it was shown that the wall of vasculature was the main location of Stro-1 positive cells. However, the major obstacle is that most surface markers of *in vitro* cultured mesenchymal stem cell do not uniquely identify these cells, and they are still expressed in other cell types. For example, CD105 is also expressed in ECs and CD44 is also expressed in SMCs. Nonetheless, the phenotype of MSCs changes once they are cultured *in vitro* and heterogeneity of MSCs indicates that even we could characterise cells with some specific markers; it does not necessarily mean that these are all the cells that have clonogenic potential *in vitro*. As a result, characterisation of MSCs *in vivo* of their phenotypic feature closely mimics shooting a moving target in that the phenotypic print of MSCs constantly changes in response to their *in vitro* and *in vivo* microenvironment (Bianco et al., 2001).

Another strategy is to infuse MSCs *in vivo* to track the engraftment and homing of them to specific tissues. After transducing murine BMMSCs with eGFP, tagged cells were systemically injected into minimally injured mice and tissue specific differentiation of these cells was determined by RT-PCR and immunohistochemistry (Anjos-Afonso et al., 2004). The contribution of donor derived eGFP-MSCs to different cell types including hepatocytes, lung epithelial cells, myofibroblasts, and renal tubular cells was confirmed. Although this approach could provide functional information about mesenchymal stem cells in tissue regeneration, utilising it as a proof of the *in vivo* natural localisation of MSCs is inappropriate, as non-specific binding of MSCs in various tissues could not be excluded. Furthermore, there is evidence showing that MSCs are short-lived when injected intravenously into the circulation and do not pass the lungs (Eggenhofer et al., 2012).

Systemic isolation and evaluation of MSCs from different tissues represents an alternative approach (da Silva Meirelles et al., 2006). It was reported in many studies that MSCs with similar *in vitro* characterisation can be cultured from various tissues like adipose tissue, umbilical cord, tendon, synovial membrane and others. Isolation of MSCs from tissues all over the body (brain, kidney, liver, lung, spleen, bone marrow, vena cava and aorta) provides an opportunity to consistently visualise the distribution of MSCs *in vivo* (da Silva Meirelles et al., 2006). The similar but not identical phenotype of mesenchymal stem cells originating from different tissues reflects the similar origins but influences of different microenvironments. The proposed hypothesis that MSCs are tissue resident stem cells led to further investigations of their perivascular origin (Crisan et al., 2008), and this has been suggested by other studies as well (Bianco et al., 2001; Farrington-Rock et al., 2004; Shi and Gronthos, 2003). Despite the accumulating evidence indicating a perivascular origin of MSCs, disputes have also arisen, most of which lie in the use of CD146 as a perivascular surface marker and the lack of biological relevance of CD146 expression and MSC function. In addition, it is demonstrated recently that MSCs might actually contain tissue specific progenitors from different mesoderm derivatives (Sacchetti et al., 2016).

As none of the approaches provides a definite answer to the question of the *in vivo* identity of MSCs, more studies should be done to track the development origin and elucidate the *in vivo* function of MSCs.

1.2. Differentiation of stem cells towards smooth muscle lineage

1.2.1. SMC differentiation from embryonic stem cells

Developmentally, vascular SMCs originate from different embryonic stages, and form different vessels or different sections of one vessel with sharp boundaries (Majesky, 2007; Yoshida and Owens, 2005). Utilising stem cells at different embryonic stages,

in vitro systems of SMCs differentiation have been established (Xie et al., 2011b), applying treatment with all-trans retinoic acid (at-RA), TGFβ, PDGF-BB, and collagen IV coating, either alone or combined. These systems, including the cell origin, treatment, the extent of differentiation marked by SMC marker expression, and functional contractility of differentiated cells, are summarised in Table 1-4.

It is worth mentioning that each differentiation system has its own pros and cons. For example, Kamaritini E (Karamariti et al., 2013a) demonstrated that reprogrammed lung fibroblasts had the ability to differentiate into functional and contractile SMCs when treated with PDGF-BB on collagen IV coated flasks. When derived SMCs were seeded on decellularised aortic scaffold from mouse in combination with ECs, functional vessels could be formed when transplanted *in vivo*. However, it needs to be considered that the cells they use are reprogrammed embryonic lung fibroblasts transfected with the Yamanaka factors (Oct4, Sox2, Klf4 and cMyc), which could form teratomas in immunodificient mice. Pros and cons of each differentiation system should be taken into consideration and weighed carefully before choosing specific system. What is more, all these systems utilise *in vitro* culture of cells which is the intrinsic limitation, which should not be ignored when interpreting experiment results; because it is unknown to what extent these *in vitro* systems could recapitulate SMCs differentiation *in vivo*.

Table 1-4 *In vitro* SMC differentiation models from embryonic stem cells (Modified from Xie C, 2011)

Cells	Cell origin	Treatment	SMC markers	Pros	Cons	Reference
A404	Mouse P19-derived cell line with ACTA2 promoter/intron-driven puromycin-resistant gene	atRA 10^{-6}mol/L, 2 d; puromycin 0.5 μg/mL, 2-5 d	α SMA Calponin		Gene transfection	Manabe I, 2001
ESC-EB	Self-assembling 3-dimentional aggregate of mouse pluripotent stem cells grown *in vitro*	AtRA 10^{-8} mol/L, dibutyryl-cAMP $0.5x10^{-3}$ mol/L, 6 d	α SMA		Low efficiency	Drab M, 1997
ESC-EB	Mouse ESC-EB transfected with ACTA2 promotor/intron driven puromycin resistant gene	Negative selection by puramycin, overnight or for 3 days	α SMA	Potent	Risk of teratomas *in vivo*	Sinha S, 2006
ESC-EB	CD34+ vascular progenitor cells from human ESC-EB	PDGF-BB 50 ng/ml, 3 passages	α SMA SM22, Calponin	Vessel formed *in vivo*	Endothelial markers still exist	Fereira LS, 2007
ESC	Mouse, human	atRA 10^{-6} mol/L, 10 d	α SMA	Potent		Huang H, 2006
ESC	Mouse	αMEM + 10% FBS in collagen IV coated flasks, 8—12 days	α SMA SM22 Calponin			Xiao Q, 2008
Lung fibroblasts	Reprogrammed embryonic lung fibroblasts	αMEM + 10% FBS + PDGF-BB 10 ng/ml, in collagen IV coated flasks, 5 days	α SMA SM22 Calponin	Vessel formed *in vivo*	Gene transfection	Karamariti E, 2013
C3H/10T1/2	Established from mouse embryos	TGFβ1 1 ng/ml, 24-48 hours	α SMA SM22 Calponin	Rapid	Induced cells don't express Myocardin	Hirschi KK, 1998
Monc-1	Immortal mouse neural crest cell line	TGFβ1 5 ng/ml, 3 d	Smoothelin	Rapid	v-myc gene transfection	Jain MK, 1998
JoMa1	Immortal mouse neural crest cell line	TGFβ1 1 ng/ml, 6 d	α SMA Calponin		Difficult to remain undifferentiated	Maurer J, 2007

1.2.2. SMC differentiation from adult stem cells

Vascular SMCs are a major cell type in the vascular wall constituting the media layer in relatively large vessels. In various cardiovascular diseases such as coronary artery disease, SMCs play an essential role. For example, SMC accumulation is a major event during the development of atherosclerosis. Unravelling the origin of these cells prove to be an important building block in deciphering the mechanism of cardiovascular diseases for subsequent therapeutic exploration. However, conflicting data exist, with some of the reports describing the importance of adult stem cells and some others reporting importance of existing SMC.

The adult stem cell pool includes the bone marrow-derived stem cells (haematopoietic stem cells and mesenchymal stem cells) which can be mobilised to circulation, and tissue resident stem cells (vascular progenitor cells and stem cells from tissues all around the body).

It is now recognised that these SMCs might originate from transdifferentiation of other cell types such as ECs (DeRuiter et al., 1997) and fibroblasts, through phenotypic switching from SMCs in the media or differentiation from either resident stem cells or those mobilised from other tissues such as bone marrow. Transdifferentiation and the phenotypic switching will be discussed later. The evidence is also accumulating that adult stem/progenitor cells differentiate into SMCs in a variety of cardiovascular diseases, including atherosclerosis and intra vascular stent restenosis. A set of *in vivo* studies have provided evidence of the origin of tissue resident stem cells that give rise to neointimal SMCs which may contribute to atherosclerosis and restenosis.

In 2001, Han and colleagues (Han et al., 2001) confirmed that bone marrow-derived cells could contribute to SMCs in vascular healing by providing an alternative source of smooth muscle-like cells when the media was severely damaged. However, they did not elucidate whether it was the haematopoietic stem cell or the mesenchymal stem cell within the bone marrow that was responsible for the effect. Later, Shimizu (Shimizu et al., 2001) confirmed the finding of Han by transplantation of bone marrow

galactosidase-expressing cells. Sata (Sata et al., 2002) took the study one step further. They injected purified haematopoietic stem cells into mouse circulation and observed that injected cells could participate in the pathogenesis of atherosclerosis. Although they confirmed that haematopoietic stem cells had potential to differentiate into SMCs both *in vivo* and *in vitro*, they did not exclude the possibility that mesenchymal stem cells within the bone marrow could be mobilised in terms of vascular injury and take part in atherosclerosis.

However, conflicting data exist as to whether bone marrow is a source for neointimal SMCs. Bone marrow transplantation of SM-LacZ β-gal expressing cells into mice suggested that bone marrow progenitor cells did not serve as a source of SMCs (Hu et al., 2002). And later on, the same group identified a type of Sca-1(+) cells within the adventitia of aortic root and confirmed that after seeding these Sca-1(+) positive cells cultured *in vitro* onto the adventitia side of the vascular injury, the cells migrated into the media and intima and participated in atherosclerotic lesion formation and vascular repair (Hu et al., 2004).

These studies are summarised in Table 1-5. An explanation of the conflicting data is that αSMA is more sensitive than SM22 as a marker for SMC identification. Thus, the use of different markers for SMCs (α SMA, SM22 or SMMHC) in different reports made the conclusion ambiguous and the question of whether bone marrow-derived stem cells could contribute to SMC differentiation requires further investigation.

As stated earlier, several processes may contribute to SMCs presence in atherosclerotic lesions, and it remains unclear to what extent stem cells could give rise to SMCs in pathogenesis. What is now widely accepted is that the origin and residency of these stem cells requires further exploration. Using the models summarised in Table 1-5, it may be possible to elucidate detailed mechanisms of SMCs differentiation. New light might be shed on the pathological reasons behind differentiation of vascular resident stem cells into SMCs, thus providing more opportunities for new therapeutic choices in cardiovascular diseases.

Table 1-5 Studies of adult stem cell differentiation into SMCs *in vivo* and their pathological meaning

Stem cells	Study	Evidence of differentiation	Result
Bone marrow nucleated cells	Han CI, 2001	Staining of α SMA	Bone marrow-derived cells are recruited in vascular healing as a complementary source of smooth muscle-like cells when the media is severely damaged and few resident SMCs are available to affect repair.
Bone-marrow transplantation of β -galactosidase expressing cells	Shimizu K, 2001	Staining of α SMA	Host bone-marrow cells are a source of donor intimal smooth-muscle–like cells in murine aortic transplant arteriopathy
Bone marrow purified haematopoietic stem cells	Sata M, 2002	Staining of α SMA	Haematopoietic stem cells differentiate into vascular cells that participate in the pathogenesis of atherosclerosis
Bone marrow transplantation of SM-LacZ β -gal expressing cells	Hu Y, 2002	SM22-LacZ	SMCs in transplant atherosclerotic lesions are originated from recipients, but not bone marrow progenitor cells
Sca-1 (+) adventitia cells	Hu Y,2004	SM22-LacZ	When Sca-1(+) cells carrying the LacZ gene were transferred to the adventitial side of vein grafts in ApoE-deficient mice, β -gal(+) cells were found in atherosclerotic lesions of the intima, and these cells enhanced the development of the lesions
Adventitia fibroblast	Li G, 2001	__	Adventitial fibroblasts seeded on the adventitia side of vascular balloon injury would migrate to neointimal site and take part in neointimal formation

1.2.3. Phenotypic switching/plasticity of SMCs

Vascular SMCs in normal vessel walls are highly specialised cells whose contractile function controls the blood vessel tone. In physiological conditions, vascular SMCs display a contractile phenotype, remain quiescent, exhibit a low proliferation rate and synthesise minimal extracellular matrix (Owens, 1995). However, unlike skeletal or cardiac myocytes which are terminally differentiated, vascular SMCs retain the ability to undergo profound and remarkable phenotypic switching, changing from the functional contractile phenotype into the synthetic phenotype in response to

environmental cues (Ammit and Panettieri, 2001). The comparison of these two phenotypes is described in detail in Table 1-6. Briefly, SMCs exhibiting a contractile phenotype express more contractile proteins such as SM22, αSMA, Calponin and SMMHC, while synthetic SMCs express more extracellular matrix proteins and are more proliferative and migratory.

Developmentally, vascular SMCs plasticity plays a key role in the morphogenesis of blood vessels, in which, they exhibit a high rate of proliferation, migration, and production of extracellular matrix components but at the same time they still acquire contractile capabilities. Physiologically, SMC phenotypic switching represents an important capability of vascular repair, in which SMCs change from a contractile phenotype to a synthetic phenotype, migrate to the sites of vascular injury and restore vessel function.

However, when this repairing system goes too far, it may contribute to the development and progression of vascular diseases including atherosclerosis and post implantation in-stent restenosis. In atherosclerosis, vascular SMCs migrate into subintimal space and contribute to fibrous cap formation over the atherosclerotic plaques. Although SMCs could synthesise collagen to promote stabilisation of the fibrous cap, they could also release matrix metalloproteinases which might contribute to the disruption of the fibrous cap and cause subsequent arterial thrombosis. Extracellular matrixes released by SMCs located in the subintimal space could cause hyperplasia of the intima, restenosis and eventually lead to failure of the vascular intervention or reconstruction.

Before the recognition of the contribution of adult stem cells to SMCs presence in atherosclerotic lesions or at other vascular injury sites, media of the vessel was widely thought to be the major source of synthetic SMCs, which were contractile SMCs in the dedifferentiated phase (Ross and Glomset, 1976). However, it is hard to quantify which proportion of SMCs in the intima are derived from media SMCs, due to the downregulation of the specific SMC markers in the intimal SMCs and the use of αSMA staining which was not specific to identify SMCs in the lesion site (Owens et al., 2004).

Overall, the origins of intimal SMCs in atherosclerotic lesions, restenosis and other vascular injuries as well as the control of the phenotypic switching and differentiation process are very complex and further exploration is needed.

1.2.4. Transdifferentiation of SMC from other cell types

Apart from phenotypic switching and differentiation, there is also evidence that other cell sources including ECs (Arciniegas et al., 2000; Clowes et al., 1983) and adventitia fibroblasts (Sartore et al., 2001; Stenmark et al., 2000) can be transdifferentiated and act as alternative origins of SMCs.

Table 1-6 The comparison between contractile phenotype and synthetic phenotype of SMCs (Modified from Rzucidlo EM, 2007)

Difference	Contractile phenotype	Synthetic phenotype
Cell size and shape	Spindle elongated shape	Hypertrophic spread shape
ECM (extracellular matrix) production	Decreased ECM production: predominance collagen IV, laminin	Increased ECM production: Predominance collagen III, fibronection
Contractile protein expression	Increased contractile protein expression: SMMHC2, Calponin, α SMA	Decreased contractile protein expression; increased expression of osteopontin
Migration	Decreased migration: decreased MMPs, increased TIMPs	Increased migration: Increased MMP-1 and MMP3

1.3. Mechanism of smooth muscle differentiation

1.3.1. Signalling pathways

1.3.1.1. SRF – CArG-dependent regulation of SMC differentiation

Serum response factor is a MADS (MCM1, agamous, deficiens, serum response factor) box transcription factor, which binds to the highly conserved CArG cis-elements (CC(A/T)6GG) that is present within virtually all promotor or intronic sequences of SMC marker genes, including αSMA, SM22, Calponin, SMMHC, and desmin. SRF binds with CArG elements as dimers and interacts with other co-factors such as Myocardin, the Myocardin-related transcription factors (MRTFs), and some Nkx and Gata family members. The complex has the capability to regulate the

expression of SMC markers (Figure 1-2). SRF is a ubiquitously expressed protein which also regulates cardiac and skeletal muscle gene expression, as well as some early response and structural genes (Sun et al., 2006). Although expressed widely in many cell types, the relatively higher level of SRF within SMCs (and other muscle cell types) partly explains the specific regulation muscle cell specific genes (Belaguli et al., 1997; Croissant et al., 1996). The ability of SRF to bind to CArG regions of SMC genes proves to be the rate limiting factor in SMC differentiation (Manabe and Owens, 2001).

Other than Myocardin and the Myocardin-related family, the homeodomain proteins (Hox, Nkx3.1, Prx-1 and Barx2b) could also enhance SRF binding ability, while the HERP1/HEY2 (Doi et al., 2005) (a target of the Notch signalling pathway), homeodomain-only protein (HOP) and YY1 possesses the ability to inhibit it (Hautmann et al., 1997; Herring et al., 2001; Yoshida et al., 2004).

Post translationally, modification of SRF by phosphorylation changes the binding affinity of SRF with transcription factors. Arginine vasopressin increased αSMA promotor activity by phosphorylation of SRF at Ser103 by Jun amino-terminal kinases (JNKs) and p38 mitogen-activated protein kinase (MAPKs) (Garat et al., 2000). Phosphorylation at Ser162 by protein kinase Cα and at Thr159 by protein kinase A decreased αSMA promotor activity (Blaker et al., 2009; Iyer et al., 2006). Interestingly, CArG elements control the promotor activity of SRF (Belaguli et al., 1997), suggesting a positive feedback loop of the control system (Spencer and Misra, 1996). It is noteworthy that SRF-CArG regulation needs other complementary signalling mechanisms which control chromatin structure and transcription factor access to SRF and this will be discussed later.

Furthermore, the SRF-CArG regulating pathway is not sufficient for SMC specific gene expression, other *cis* elements and trans-binding factors also play a very important role in the regulation of SMC differentiation, including TGFβ control element (TCE), E box elements (CANNTG motifs) and a *cis* element referred to as a G/C repressor (Liu et al., 2003; Madsen et al., 1997; Shimizu et al., 1995). Mutation of

TCE and E box elements, which are non-CArG elements, eliminated the expression of SMC specific genes in transgenic mice (Kumar et al., 2003; Liu et al., 2003).

In summary, SMC differentiation depends on the integration of multiple regulatory pathways in which SRF-CArG *cis* elements regulation plays a critical but not exclusive role.

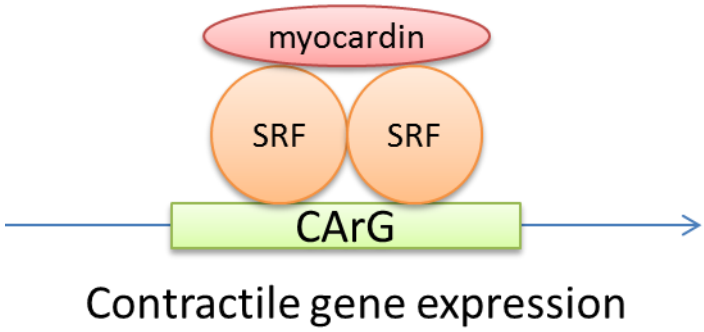

Figure 1-2 The interaction of Myocardin, SRF and the CArG elements at SMC contractile gene promotors regulates the contractile gene expression in SMCs

Myocardin and SRF binds to the highly conserved CArG cis-elements (CC(A/T)6GG) that are present within virtually all promotor or intronic sequences of SMC marker genes, including αSMA, SM22, Calponin, SMMHC, and desmin.

1.3.1.2. Myocardin-related regulation

Myocardin (935 aa) is expressed in the heart and most SMC containing tissues, and is located predominantly in the nucleus (Chen et al., 2002; Wang et al., 2002), whereas its two family members Myocardin-related transcription factor A (MRTF-A) and Myocardin-related transcription factor B (MRTF-B) are ubiquitously expressed and located in the cytosol due to the structural difference (RPEL motif) they possess from Myocardin (Guettler et al., 2008). SMCs with Myocardin knocked out can still differentiate (Pipes et al., 2005). Myocardin is dispensable for vascular development, but not visceral development. Mice with a homozygous null mutation of Myocardin

could not survive and died at embryonic day 10.5 (Li et al., 2003), and the death was caused by the loss of Myocardin in vascular SMCs.

Other than SMC contractile markers which are controlled by the Myocardin-SRF-CArG regulatory system, what is also induced by this system is a set of micro-RNAs, such as miR-1 (Chen et al., 2011) and miR-143/145 (Boettger et al., 2009; Cheng et al., 2009; Cordes et al., 2009; Xin et al., 2009), which play a role in the negative feedback loop (Jiang et al., 2010) or the positive feedback loop in the complex and integrated SMC differentiation mechanism.

Regulated Myocardin level

It has been shown that Myocardin expression in cardiac and SMCs is regulated by the Myocardin enhancer through scanning the genomic DNA for *cis*-regulatory elements capable of directing Myocardin transcription *in vivo*. As a direct target of Myocardin enhancer factor 2 (MEF2), Foxo and Tead factors, Myocardin enhancer could be activated with the combination of these factors and display increased Myocardin expression independent of the SRF-CArG regulatory system (Creemers et al., 2006) (Figure 1-3). In comparison with the SRF-CArG independent regulation, other studies showed that CArG *cis* elements were also present upstream of the Myocardin gene (Miano, 2003), and cofactors such as Nkx2.5, p49/STRAP (SRF-dependent transcription regulation associated protein) and Myocardin itself could induce the expression of Myocardin (Zhang et al., 2004).

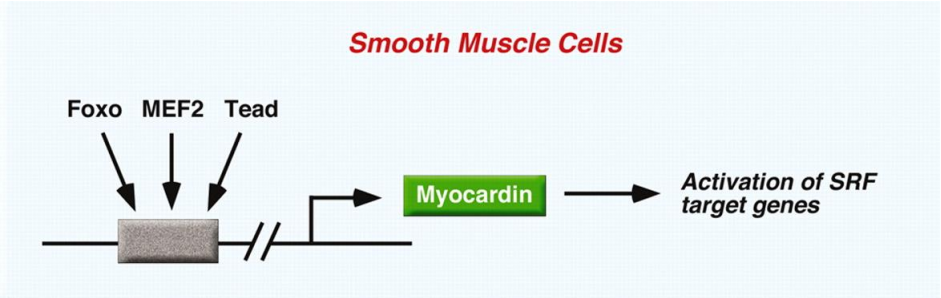

Figure 1-3 The combination of Foxo, MEF2 and Tead at Myocardin enhancer could activate Myocardin expression independent of SRF-CArG element

This figure is reproduced from (Creemers et al., 2006).

Environmental cues which can stimulate the expression of Myocardin include TGFβ1 (Shi and Chen, 2013), angiotensin II (AngII) (Yoshida et al., 2004), increased calcium influx, insulin-like growth factor (IGF) and hypoxia (Jie et al., 2010), and the modulation mainly influences the interaction of SRF cofactors (Nkx2.5 (Shi and Chen, 2013) and Prx1 (Yoshida et al., 2004)) with SRF.

PDGF-BB inhibits the expression of Myocardin and this is probably through the SRF-CArG-dependent pathway in cultured SMCs (Yoshida et al., 2007). Atorvastatin, a widely used lipid lowering drug, inhibits the expression of Myocardin *in vivo* and *in vitro* through the RhoA-Rho-associated kinases pathway (Li et al., 2012). BMP2 was shown in cardiac myocytes to inhibit the expression of Myocardin (Callis et al., 2005), but not in SMCs (Hayashi et al., 2006), reflecting a differential response governed by cell types.

Posttranslational modification including acetylation, phosphorylation, sumoylation and ubiquitination can also influence the activity of Myocardin. Chromatin-modifying enzyme p300 acetylates lysine residues at the N terminus of the Myocardin protein and promotes its interaction with SRF and the formation of Myocardin-SRF-CArG box

ternary complex (Cao et al., 2012). Phosphorylation of Myocardin by ERK1/2 at four sites (Ser812, Ser859, Ser866, and Thr893) is required for its interaction with acetyltransferase (Taurin et al., 2009). Ubiquitination of Myocardin directs its degradation, resulting in altered activity of Myocardin. Evidence suggests that degradation of ubiquitinated Myocardin by proteasomes can activate Myocardin activity and that accumulations of Myocardin due to dysfunction of ubiquitination were unable to activate its target genes, probably because of its inability to recruit RNA polymerase II to the Myocardin-SRF-CArG complex (Sandbo et al., 2005; Yin et al., 2011). *In vivo* study of a canine carotid model showed that the downregulation of ubiquitin, E2, E3 and proteasome subunits in anastomotic intimal hyperplasia indirectly supported this degradation-induced transactivation model of Myocardin (Stone et al., 2001).

Regulated Myocardin activity

Interaction of Myocardin with other proteins reduces the accessibility of Myocardin to SRF, thus inhibiting its transcriptional activity. FOXO4, which is a forkhead transcription factor, can repress the expression of SMC specific genes through interaction with Myocardin. IGF can induce SMC phenotypic switching from a synthetic and proliferative phenotype to a contractile and differentiated phenotype through phosphorylation of FOXO4 by activation of the phosphoinositide-3-kinase (PI3K)-Akt signalling pathway and translocating phosphorylated FOXO4 from the nucleus to cytoplasm, thus releasing Myocardin from the interaction and promoting the binding of Myocardin with SRF (Liu et al., 2005) (Figure 1-4).

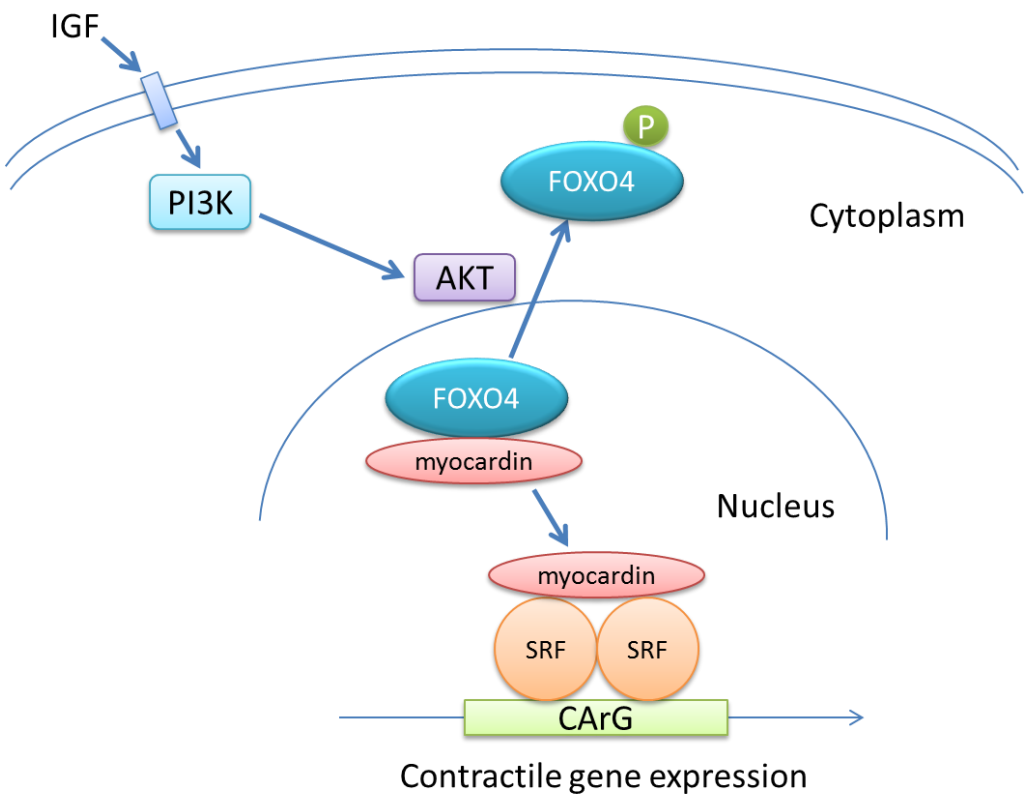

Figure 1-4 IGF induces contractile gene expression in SMCs through PI3K-Akt pathway

Phosphorylated FOXO4 is translocated from the nucleus to the cytoplasm thus releasing Myocardin. Myocardin binds to SRF and then promotes the differentiation of SMCs.

Other factors that can interact with Myocardin and inhibit Myocardin activity include SOX9 (Xu et al., 2012b), which is a master regulator of chondrogenesis, and Msx1 and Msx2 (Hayashi et al., 2006), which are induced by bone morphogenetic proteins (BMPs). Nuclear uPAR (Urokinase-type plasminogen activator receptor) has been shown to associate with Myocardin and recruit it from the promoters of serum response factor target genes, resulting in Myocardin degradation by the proteasomes (Kiyan et al., 2012). Apart from abrogating Myocardin function through disrupting its binding with SRF, high mobility group 2 like 1 (HMG2L1) abolished the SRF-Myocardin complex binding to CArG elements of SMC specific genes (Zhou et al.,

2010). (The factors that could inhibit the interaction of Myocardin and SRF are summarised in Figure 1-5.)

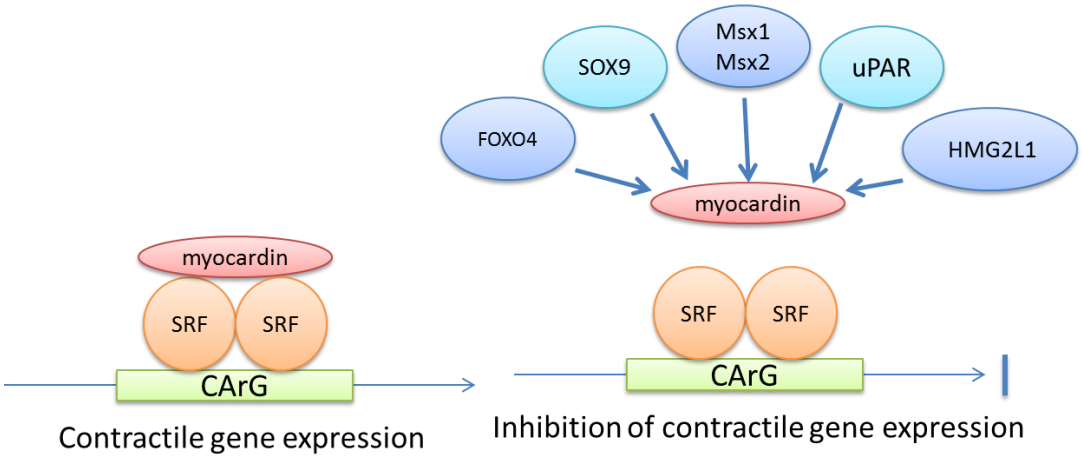

Figure 1-5 Factors that could inhibit the interaction of Myocardin and SRF

Myocardin binds to SRF dimers and forms and complex which could bind the CArG element at the promoter region of target genes. Transcription factors such as FOXO4, SOX9, Msx1, Msx2 and uPAR could interact with Myocardin and prevent it from binding to SRF dimers. HMG2L1 could prevent the Myocardin-SRF dimer complex from binding to the CArG element. In both ways, the downstream target gene expression would be inhibited.

1.3.1.3. RhoA regulated signalling pathway

It was discussed in the part of "**SRF – CArG-dependent regulation of SMC differentiation**" that SRF dimers bind to CArG elements of SMC specific genes and stimulate expression of these genes with the help of Myocardin or MRTFs, thus promoting SMC differentiation or phenotypic switching from synthetic phenotype to contractile phenotype. Due to the structural difference between Myocardin and MRTFs (MRTF-A and MRTF-B), Myocardin constitutively exists in the nucleus, while MRTFs are mainly located in the cytoplasm.

RhoA was proved to influence SMC differentiation in a variety of studies (Lu et al., 2001; Wamhoff et al., 2004), and RhoA kinases were important RhoA effectors. Various environmental cues can promote SMC differentiation through the RhoA/ROCK pathway including thrombin (Martin et al., 2009), TGFβ (Chen et al., 2006; Deaton et al., 2005), sphingosine-1-phosphate (S1P) (Lockman et al., 2004), BMP (Lagna et al., 2007) and cell stretch (Zeidan et al., 2003). These agonists activated the transmembrane G protein coupled receptors (GPCRs) and then with the facilitation of guanine exchange factors (GEFs) which exchange GDP for GTP, RhoA was activated (Heasman and Ridley, 2008). Details about the GPCRs types and GEFs that respond to each agonist are reviewed elsewhere (Mack, 2011).

Before RhoA activation, MRTFs bind to G-actin and remain in the cytoplasm. After RhoA-ROCK (RhoA kinases) pathway activation, however, G-actin in the cytoplasm forms F-actin and dissociates with MRTFs, releasing MRTFs and promoting the translocation of them from the cytoplasm to the nucleus. Increased MRTFs in the nucleus interact with SRF and enhance SMC specific gene expression (Miralles et al., 2003). Direct evidence of this nuclear translocation pattern was observed using enhanced GFP fusion protein (Hinson et al., 2007). (The RhoA regulated signalling pathway is depicted in Figure 1-6)

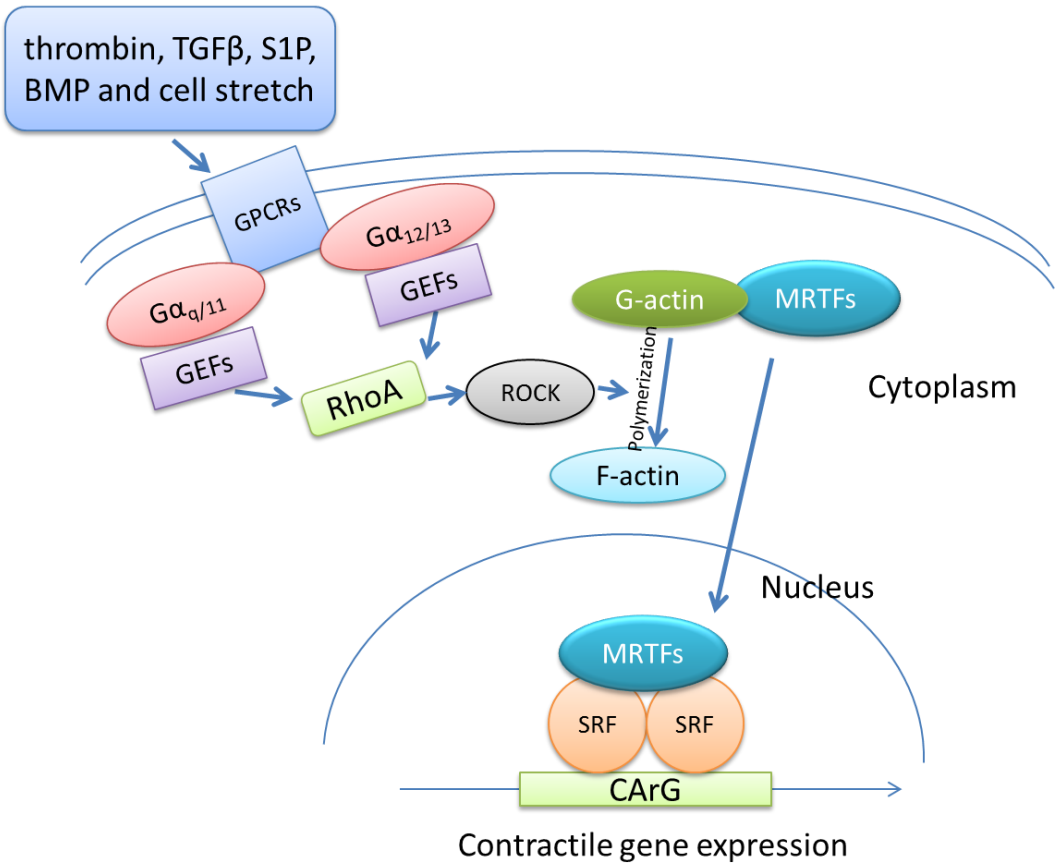

Figure 1-6 RhoA pathway regulates SMC differentiation in response to various environmental cues

Thrombin, TGFβ, S1P, and BMP bind to G protein coupled receptors (GPCRs) and signals through the RhoA-ROCK pathway, which results in polymerisation of G-actin. MRTFs then dissociate with G-actin and are translocated to the nucleus, thus activating SMC gene expression by binding the SRF-CArG elements.

1.3.2. Epigenetic modulation

1.3.2.1. Chromatin modification

Genomic DNA is wrapped in a compact structure known as chromatin, which is composed of nucleosomes and linked by a linker chromatin. Histones (2x H2A, 2x H2B, 2x H3, 2x H4) and a 146 base pair long genomic DNA form the basic unit of a

nucleosome. The linker chromatin is formed by DNA of variable lengths and histone H1. The N terminal tail of histones are freely exposed to the environment and are prone to modifications including methylation, acetylation, phosphorylation, ubiquitination and ADP-ribosylation (Cheung et al., 2000). Modification of histones or interaction of histones with other binding proteins could then change the protein conformational structure and the accessibility of DNA within the chromatin to transcription factors (Figure 1-7).

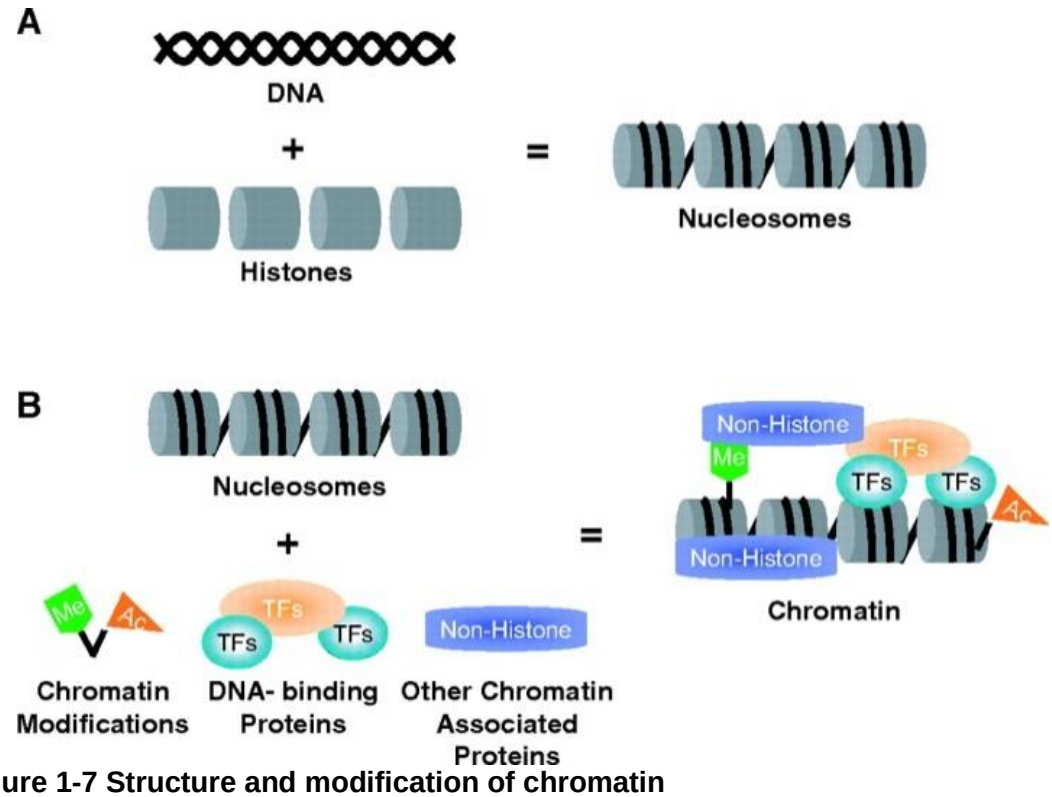

Figure 1-7 Structure and modification of chromatin

(A) Naked DNA binds to histones to form a spatial configuration. **(B)** Modification and interaction of chromatin with other proteins could regulate chromatin configuration and function.

The first evidence that certain chromatin modification promoted smooth muscle differentiation was presented by Manabe and his colleagues in 2001 (Manabe and

Owens, 2001). It was found that in the undifferentiated state of A404 cell line (derived from P19 embryonal carcinoma stem cells), although Myocardin and SRF were highly expressed, they could not bind to the CArG containing regions of the promoters of SMC specific genes. Upon retinoic acid treatment, however, binding was promoted, followed by the stimulation of SMC specific gene expression. Hyperacetylation of H3 and H4 through histone acetyltransferase (HAT) proved to be critical to this process and histone deacetylase (HDAC) inhibitors could have the same effect. Other studies later confirmed their results. Cao and colleagues showed that p300, a histone acetyltransferase associated with the Myocardin transcription activation site induced the acetylation of histones surrounding SRF binding site in the promotor region of SMC specific genes (Cao et al., 2005). HDAC7 underwent alternative splicing in collagen IV-induced SMC differentiation from embryonic stem cell through modulation of the SRF-Myocardin complex (Margariti et al., 2009). Recruitment of HDAC2 and HDAC5 by Krüppel-like factor 4 (Klf4) and pElk at the αSMA promotor region resulted in hypoacetylation of histone 4, thus inhibiting the gene expression (Yoshida et al., 2008).

Other than acetylation, methylation also proved to be of major importance in the regulation. H3K4 methylation increased the binding of SRF with CArG regions in the activation of SMC specific genes (Yoshida et al., 2008).

A specific modification pattern was identified which was termed “bivalent domains” by screening embryonic stem cells for specific histone methylation patterns (Azuara et al., 2006; Bernstein et al., 2006). H3 lysine 27 methylation and H3 lysine 4 methylation coincide with transcription factors expressed at low levels in embryonic stem cells, keeping the developmental gene/lineage specific genes silent while in the meantime, keep them poised for activation (Azuara et al., 2006; Bernstein et al., 2006). It is easy to reason that this silencing pattern should be eliminated when inducing lineage specific gene expression.

In summary, epigenetic modification plays a critical role in initiating SMC differentiation from a stem cell state and requires the integration and cooperation of other signalling pathways to promote and determine SMC fate.

1.3.2.2. MicroRNAs

MicroRNAs are necessary for the differentiation of SMCs as demonstrated by the study of Dicer deletion experiments which resulted in the failure of microRNA maturation (Albinsson et al., 2010; Pan et al., 2011). Dicer deletion in vascular SMCs caused embryonic lethality at day 16 to 17, with extensive internal haemorrhage generated by reduction of SMC proliferation and impaired contractility which could be partly rescued by overexpression of miR-145 (Albinsson et al., 2010).

1.3.2.2.1. MiR-143/145

Both *in vitro* and *in vivo* loss-of-function studies have shown that miR-143/145 is important for SMC differentiation (Boettger et al., 2009; Elia et al., 2009). Through the repression of antagonistic factor (Klf4, Klf5, Elk1, versican and angiotensin converting enzyme) gene expression in the SMC differentiation process, miR-143/145 facilitates expression of SMC specific genes (Cordes et al., 2009; Davis-Dusenbery et al., 2011; Long and Miano, 2011; Rangrez et al., 2011; Xin et al., 2009). MiR-143 and miR-145 are expressed in proximity in chromosome 5 and share the same promotor which contains CArG elements, as with most contractile SMC specific genes. Thus miR-143/145 is regulated in an SRF-CArG-dependent pathway. Briefly, for the induction of miR-143/145, TGFβ signals through the Smad2/3 pathway and Myocardin is required to promote binding of SRF to the CArG element, and BMP4 signals through RhoA pathway and MRTF-A translocation to the nucleus is required (Davis-Dusenbery et al., 2011). PDGF-BB, which is known as a synthetic SMC phenotype inducer, activates Src through PDGF receptor and as a result, p53 (Suzuki et al., 2009), which is an inducer of miR-143/145 is repressed (Quintavalle et al., 2010). In summary, miR-143/145 is critical for SMC differentiation.

1.3.2.2.2. MiR-1

MiR-1 was observed to be steadily increased in the differentiation process from embryonic stem cells to SMCs and loss-of-function study showed that miR-1 was essential to the process. MiR-1 induces SMC differentiation through the repression of Klf4 (Xie et al., 2011a) and Pim-1 (a serine/threonine kinase) (Chen et al., 2011) which also serves as a negative regulator of SMC differentiation. Upstream regulators include Myocardin, whose overexpression resulted in significant induction of miR-1 (Chen et al., 2011). However, contradictory data was also observed which demonstrated that exogenous miR-1 inhibited contractility of SMCs and repressed the expression of contractile proteins (Jiang et al., 2010). Further studies are needed for the elucidation of miR-1 function in SMC differentiation.

1.3.2.2.3. MiR-21

MiR-21 was also involved in TGFβ- and BMP4-induced SMC differentiation by downregulating programmed cell death 4 (PDCD4), which is a repressor of SMC contractile genes (Davis et al., 2008). Dedicator of cytokinesis (DOCK) protein superfamily was also identified as the targets of miR-21, whose downregulation inhibited cell migration (Kang et al., 2012). Mature miR-21 could be increased by the recruitment of TGFβ and BMP4 specific SMAD signal transducers to the DROSHA complex which facilitated the processing of pri-miR-21 to precursor miR-21 (Davis et al., 2008). However there was still evidence that miR-21 could be repressed by increased miR-143 through repression of fos-related antigen 1 (FRA-1) in SMC differentiation (Horita et al., 2011) suggesting the complex regulatory role of miR-21. MiR-21 has also been investigated in many tissues outside of the vasculature and its function is suggested to be highly context-dependent (Lin et al., 2009).

1.3.2.2.4. MiR-10a

Retinoic acid induces SMC differentiation from embryonic stem cells during which process miR-10a was increased (Huang et al., 2010). This increase is the direct result of retinoic acid-induced nuclear translocation of NF- κB. Upregulated miR-10a binds to the 3'-UTR of HDAC4 which is a negative regulator of SMC differentiation (Huang

et al., 2010). The regulatory function of microRNAs in SMC differentiation is summarised in Figure 1-8**.**

1.3.2.2.5. Others

Other microRNAs that contribute to SMC differentiation, proliferation and migration include miR-100 (Grundmann et al., 2011) and miR-125b (Goettsch et al., 2011; Mizuno et al., 2008). Furthermore, various microRNAs are involved in the promotion of a synthetic phenotype of SMCs, such as miR-24(Chan et al., 2010b), miR-26a (Leeper et al., 2011), miR-31 (Liu et al., 2011), miR-146a (Sun et al., 2011), miR-204 (Morrell et al., 2001), miR-208 (Zhang et al., 2011) and miR-221 (Liu et al., 2009).

In summary, microRNAs play a critical role in SMC differentiation, and represent an important therapeutic choice for cardiovascular diseases (Scalbert and Bril, 2008).

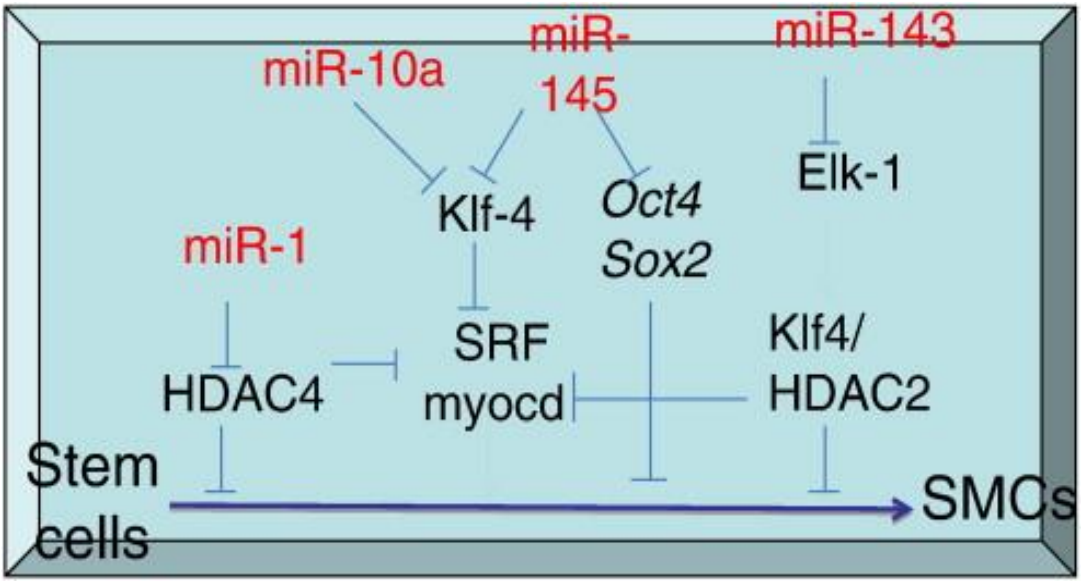

Figure 1-8 MicroRNAs that could induce SMC differentiation

MicroRNAs induce SMC differentiation by repressing the expression of proteins that inhibit SMC differentiation (Zhang L, 2011).

1.3.3. TGFβ1-induced SMC differentiation

TGFβ is a multi-functional regulator in vascular development and maintenance, by controlling the proliferation, differentiation and other properties of SMCs. It was described earlier in the report that TGFβ could induce SMC differentiation by dissociating MRTF-A from G-actin through the RhoA-ROCK pathway and translocating it to the SRF-CArG complex at the SMC specific gene promotors in the nucleus, thus inducing SMC differentiation.

Moreover, TGFβ could also induce the expression of SMC specific genes through putative Smad binding elements other than the SRF-CArG regulating system (Hu et al., 2003; Qiu et al., 2003; Qiu et al., 2005). Independent of CArG elements, Smad3 was induced by TGFβ and could bind to the Smad binding element of SMC specific gene promotor and induce SMC differentiation. In addition, this process was enhanced by Myocardin (Qiu et al., 2005).

Moreover, it is worth mentioning again that miR-143/145 is also upregulated upon TGFβ treatment through the RhoA-ROCK/MRTF-A/SRF-CArG system as stated earlier. MiR-143/145 is known as positive regulators of SMC differentiation and the detailed mechanism is explained in the last part of the report.

It was displayed earlier in the report that IGF signals through the PI3K-Akt-FOXO pathway and translocated phosphorylated FOXO from the nucleus to the cytoplasm thus inhibiting the repressive function of nuclear FOXO on the Myocardin-SRF-CArG system and SMC specific gene expression (Qureshi et al., 2007).

Moreover, TGFβ1 *in vivo* stimulates the expression of NADPH oxidase 4 (Nox4) in the media of the vessel wall (Clempus and Griendling, 2006; Clempus et al., 2007), which constitutively produces large amounts of H_2O_2. Xiao and colleagues showed that Nox4 was crucial for SMC differentiation by the generation of H_2O_2, translocation of phosphorylated SRF to the nucleus and subsequent induction of SMC differentiation (Xiao et al., 2009). It was displayed that Nox4 could also produce $O2^-$ and stimulate SMC differentiation through the p38-MAPK pathway (Su et al., 2001).

As a result, Nox4, as well as reactive oxygen species, is an important signalling pathway for TGFβ-induced SMC differentiation.

1.4. Recognition of small regulatory miRNAs

1.4.1. Recognition of small regulatory RNAs

In the human genome, only 1-2% of the genes code for proteins. However, with recent next-generation deep sequencing technologies, it is revealed that most of the genome is transcribed to RNAs. Apart from the mRNAs which would be translated to proteins, there is also a vast number of RNAs which were not thought to be functional, i.e. noncoding RNAs. Recent studies have established a significant regulatory role of these non-coding RNAs in various molecular mechanisms (Beermann et al., 2016).

Non-coding RNAs could be divided into two groups: the constitutive non-coding RNAs and regulatory ones. Like the housekeeping genes, constitutive non-coding RNAs are stably transcribed in the cells and the transcription is not generally affected by the cell state. Ribosomal RNAs, transfer RNAs, small nuclear RNAs and small nucleolar RNAs are included in the constitutive non-coding RNA category. According to the size, regulatory non-coding RNAs could be sub-grouped into short non-coding RNAs and long non-coding RNAs. Short non-coding RNAs are defined to be RNAs less than 200 nucleotides long and include endogenous short interfering RNAs (siRNAs), microRNAs (miRNAs) and others such as piwi-associated RNAs (Hombach and Kretz, 2016). Among the short non-coding RNAs, miRNAs are the most extensively studied and have been proved to play important roles in diverse regulatory pathways and numerous disease contexts. The size of long non-coding RNAs ranges from 200 nucleotides to several kilobases. The mechanism through which they function is not fully understood. Continuous efforts have been invested to develop standard characterisation methods of long non-coding RNAs such as ribosome profiling and genome engineering with clustered regularly interspaced short palindromic repeats

(CRISPR). The focus will be placed on the discovery, biogenesis, and current research trends on miRNAs in this thesis introduction.

1.4.2. Discovery and history of miRNAs

Though it seems easy for us to accept the concept of regulatory RNAs which is not included in the central dogma now, it takes the scientists several decades from the description of the first regulatory miRNA to subsequent establishment of various miRNAs along with their involvement in numerous physiological and pathophysiological processes. Reviewing the discovery of miRNA and the associated establishment of concept-changing scientific discoveries would give us some implications about future research that could push the present scientific boundaries.

The first miRNA and its inhibitory effect through binding to 3'-UTR region of target mRNA was depicted in nematode Caenorhabditis elegans (C. elegans) in which cell lineages were fully understood. In 1981, it was reported that mutation of gene lin-4 resulted in reiterative cell lineages in C. elegans (Chalfie et al., 1981). Later in 1989, lin-4 was proved to be a negative regulator of lin-14 as suggested by the almost identical defect induced by lin-4 loss-of-function mutation e912 and lin-14 gain-of-function mutation n536 and n355 (Ambros, 1989). Two years after that, two mutations in lin-14 gene that caused the deletion of its 3'-UTR region led to the inappropriate accumulation of lin-14 proteins within the nucleus and helped to identify the 3'-UTR region as a negative regulatory element (Wightman et al., 1991). With these results combined, researchers continued to examine whether the negative regulatory effect of lin-4 on lin-14 was exerted through the 3'-UTR region of lin-14.

In 1993, two studies published in Cell worked in line to further confirm and add details to the hypothesis (Lee et al., 1993; Wightman et al., 1993). Wightman et al. described the necessity and sufficiency of lin-14 3'-UTR existence in the exertion of lin-4 negative regulatory effect on lin-14 protein (Wightman et al., 1993). Conservation of lin-14 3'-UTR across several different species acted as another evidence of its participation in the regulating process. Whereas Wightman et al. invested their main

efforts in deciphering the role of lin-14 3'-UTR in mediating the inhibitory effect of lin-4 on lin-14 protein level, Lee et al. focused mainly on characterising the lin-4 gene (Lee et al., 1993). By introducing frameshift mutation as well as point mutation of the putative open reading frame of lin-4 gene, Lee and co-workers first managed to rule out the possibility that lin-4 gene could code for any proteins because the introduction of mutation did not affect the function of lin-4. Afterwards, in Northern blots and RNAase protection experiments, they detected two small RNA transcripts (lin-4S and lin-4L) with lin-4 gene probe which rescued the lin-4 loss-of-function mutation e912. Furthermore, these two small RNAs were found partially complementary to the 3'-UTR region of lin-14 gene (Lee et al., 1993).

Until then, sufficient experimental evidence was gathered about the first miRNA lin-4. Firstly, it is a non-protein-coding gene which gives rise to miRNA transcript lin-4. Secondly, miRNA lin-4 functions through partially binding to the 3'-UTR region of target lin-14 mRNA and induces translational inhibition of lin-14. This serves as the prototype of miRNA functioning mode for later research. However, before moving forward to set miRNA as a general and universal regulatory element, more miRNAs have to be described other than this isolated report of lin-4.

In the following years, more reports have been published to prove involvement of miRNA lin-4 in inhibiting the translation of lin-14 mRNA through targeting its 3'-UTR region (Ha et al., 1996; Olsen and Ambros, 1999). It was not until 2000 that the report of the second miRNA let-7 was documented. Reinhart et al. described the transcription of the 21 nucleotides long let-7 RNA and its inhibitory regulation of lin-41 and other genes by binding to their 3'-UTR region (Reinhart et al., 2000). Pasquinelli et al. in the same year analysed the conservation of let-7 RNA across various species and managed to detect it in species ranging from vertebrate, hemichordate, mollusc and others (Pasquinelli et al., 2000). Different tissues from Homo sapiens were also found to express let-7 RNA including the brain, kidney, lung, spleen and stomach (Pasquinelli et al., 2000). These two reports serve more important roles than being the second report of small RNA regulating translation through complimentary binding to 3'-UTR region of target mRNA. If these two reports

were examined more pervasively, the information suggested was that the concept of regulatory non-coding small RNAs could move beyond nematodes to invertebrates and vertebrates. This valuable piece of information, however, could not be achieved from the examination of the first miRNA lin-4, since its expression seemed to be restricted to Caenorhabditis or nematode species as shown by database search and Northern blot experiments (Pasquinelli et al., 2000).

After the recognition of the second miRNA and its existence in Homo sapiens, the concept of regulatory small non-coding RNAs started to be shaped. Extensive efforts were then invested to characterise more miRNAs in various species including C. elegans and humans. Only one year after the description of miRNA let-7, abundant miRNAs were detected in different species which unveiled the curtain of this essential regulatory RNA group that were previously shaded by the dominant central dogma (Lagos-Quintana et al., 2001; Lau et al., 2001; Lee and Ambros, 2001).

Since the genes coding from miRNA transcripts do not normally contain open reading frames and other features recognised by then, most of the miRNAs were not identified. For this reason, Lau et al. went on to directly clone RNA transcripts from total RNAs isolated from C. elegans. The standards they set for miRNAs while they were exploring miRNA pool in the cells include the following. Firstly, it should be around 22 nucleotides long. Secondly, it should contain a 5'-terminal monophosphate and a 3'-terminal hydroxyl group. Thirdly, the longer transcript from which it was processed should form a "stem-loop" structure (Lau et al., 2001). With these standards to develop a protocol to clone miRNAs, they first found 330 clones that match the genomic sequence of C. elegans; out of these clones, 300 contain the capacity to form fold-back structures and they represent 54 miRNA transcript sequences. What is assuring is that, lin-4 and let-7 were among the abundant miRNAs characterised with this approach. Northern blot analysis later confirmed the existence of some of the miRNAs identified (Lau et al., 2001). Moreover, it was found that a large fraction of these miRNAs could also be found in C. briggsae (Lau et al., 2001).

In the same year, Lee et al. published in the same issue of Science reporting similar results about the characterisation of miRNAs in C. elegans (Lee and Ambros, 2001). It is of more significant meaning that apart from the elucidation of miRNA pool in nematodes, Lagos-Quintana et al. managed to characterise and clone 21 novel miRNAs from Hela cell, a human cervical cancer cell line (Lagos-Quintana et al., 2001). The recognition of abundant miRNA existence in various species especially in human has led the research to a new era focusing on regulatory noncoding miRNAs. Till now, the miRNA-related research is still on-going and numerous challenges remain such as the involvement of miRNAs in specific diseases, miRNAs as diagnostic biomarkers and miRNAs as therapeutic targets in the clinics. Further and more extensive studies are required.

1.4.3. Biogenesis of miRNAs

MicroRNA biogenesis is a multistep process, beginning from the initial transcription of primary miRNA, which has a hairpin/stem-loop structure. After being transcribed with RNA polymerase II or RNA polymerase III, primary miRNAs were first processed in the nucleus through Drosha/DGCR8 microprocessor complex in a sequence independent but structural-dependent manner to form the precursor miRNA around 60 to 80 nucleotides long. Afterwards, precursor miRNAs were actively exported to the cytoplasm with Exportin-5 in a Ran-GTP-dependent manner. In the cytoplasm, the transition of GTP to GDP helped to release the precursor miRNAs from Exportin-5. Dicer later works cooperatively with TRBP to cleave the precursor miRNA and generate mature miRNAs which would be incorporated into the RISC complex and then bind to the 3'-untranslated region (3'-UTR) of the target sequence in a complementary manner to induce target mRNA degradation or translation inhibition. (The processes of miRNA biogenesis are summarised in Figure 1-9.)

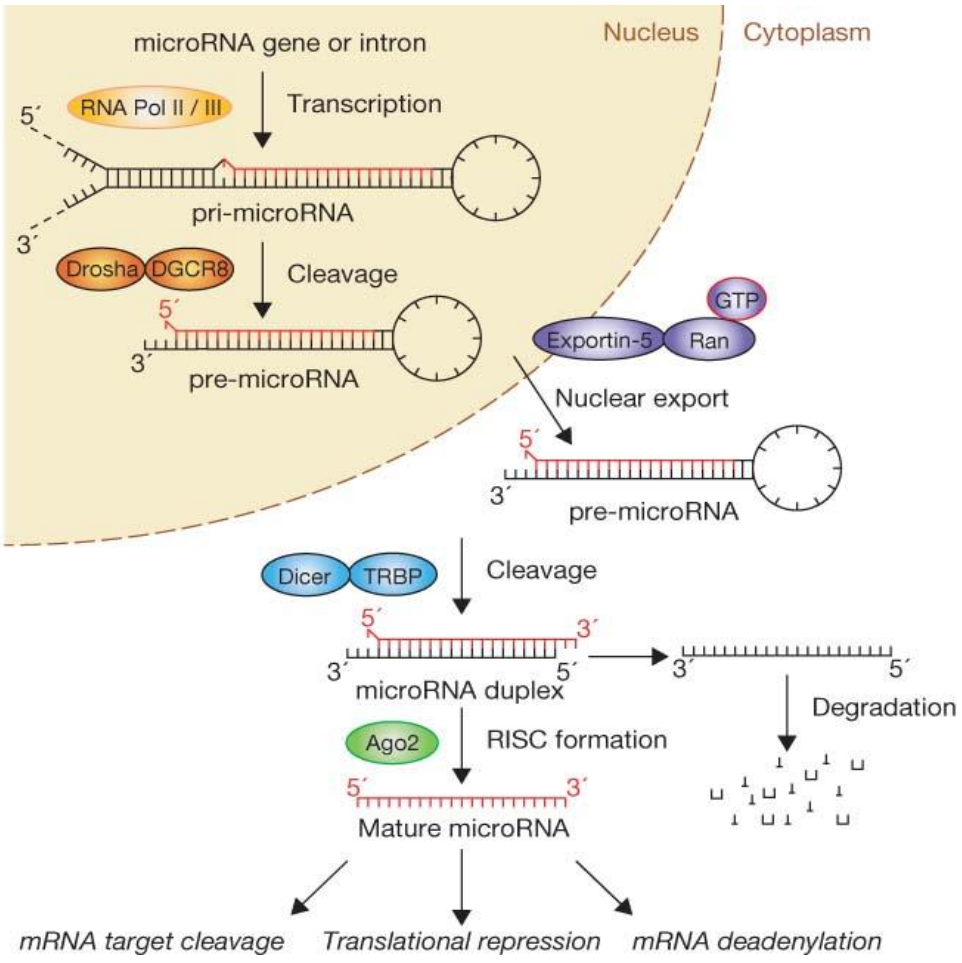

Figure 1-9 The synthesis and maturation process of microRNAs

The microRNA gene was transcribed to be pri-microRNA. With the facilitation of enzymes later, it was processed to pre-microRNA and then microRNA duplex. One strand of the duplex is later degraded and the other strand, which is the mature microRNA, binds to RISC and 3'-UTR of the target gene to inhibit the gene expression http://www.mir-nat.com/.

1.4.4. Database of miRNAs: annotation and target prediction

1.4.4.1. Criteria for miRNA annotation

After the identification and characterisation of multiple miRNAs from C. elegans, insects, mammals and human cells, regulatory miRNAs emerge to be a new focus in research and exhibit potentials to unveil a previously hidden regulatory layer of various physiological and pathophysiological processes (Lagos-Quintana et al., 2001; Lau et al., 2001; Lee and Ambros, 2001). The first challenge that had to be overcome in laying a solid foundation of miRNA research and move from single/isolated reports of one miRNA and its function to large scale miRNA-related processes was to define the features of miRNAs and standardise the annotation. As shown by previous studies on several miRNAs such as let-7 and lin-4, miRNAs exert nice conservation among different species. Consistent annotation of these miRNAs is necessary. Furthermore, there are other small RNAs in the cells, such as fragments of larger noncoding RNAs including ribosomal RNAs, small nuclear RNAs and siRNAs. Standard annotation is a pre-requisite for differentiation of miRNAs with these small RNAs.

Among these RNAs, siRNAs bear the biggest similarity to miRNAs. They were both small and shared a similar structure. They could both function in a complementary binding manner with target mRNAs and exhibit the inhibitory effect. Although siRNAs normally bind to target mRNAs with strict and complete complementarity which is different from the generally accepted partial binding mode of miRNAs to target mRNAs, there are also miRNAs that could function with a complete complementary binding mode (Hutvagner and Zamore, 2002). The more distinguishable difference between siRNAs and miRNAs may lie in their biogenesis process. SiRNAs are processed from long double-stranded RNAs and could be generated from both strands, whereas miRNAs are generated from primary and precursor hairpin/stem-loop miRNAs and the mature form originates normally from one strand.

Given the necessity for standard characterisation and annotation to ensure that it is the miRNA that we are working with and experiment results about the same miRNA

across different species and different research groups could be referred to, criteria to define and name the miRNAs were proposed by Ambros et al in 2003. It was required that the small single-stranded RNA around 22 nucleotides needed to be detected both by specific primers and in the cDNA library prepared from size fractionated RNA. Furthermore, at the biogenesis level, it was required that the precursor miRNAs from which they were processed should have a hairpin structure and Dicer should be confirmed to be the enzyme mediating that process (Ambros et al., 2003).

The database was updated every several years to include more newly annotated miRNAs and the criteria were proved to be capable of keeping a clean database of miRNAs. This database of miRNAs provided consistent annotation scheme and served as a repository of miRNAs over the years for reference of researchers (Griffiths-Jones, 2010; Griffiths-Jones et al., 2006).

Later on, with the development of new RNA sequencing technologies, deep sequencing data were integrated to the database to further facilitate the error correction of miRNA sequences and provide a whole picture of miRNA expression mode in different contexts (Kozomara and Griffiths-Jones, 2011, 2014). With data utilisation from published articles that reported novel miRNAs, the sequence reads and counts were extracted and compared against those already reserved in the miRBase. Data acquired from different tissues, species and with different methods were pooled together with the inclusion of published RNA deep sequencing data. It gradually provided an outlook for researchers about the distribution and level of various miRNAs. Furthermore, the comparison of sequence data with known sequences from the miRBase enables the error correction of the reserved database (Kozomara and Griffiths-Jones, 2011). For example, for dme-miR-317, it was revealed by the sequencing data that it was actually 21 nucleotides long whereas it was 24 nucleotides as recorded by the database before. The addition of certain miRNA isoforms suggested by the sequencing data was possible as well (Kozomara and Griffiths-Jones, 2011). Moreover, deep sequencing data could also demonstrate the level of confidence when annotating novel miRNAs (Kozomara and Griffiths-Jones, 2014).

1.4.4.2. Principles of target recognition by miRNAs and databases of miRNAs

1.4.4.2.1. Canonical sites and marginal sites

With the characterisation of a high number of miRNAs across different species, understanding the mechanism through which miRNAs exert their inhibitory functions becomes a hurdle to be crossed. The brief conclusion was drawn from the several firstly discovered miRNAs that complementary binding of miRNA and target mRNA is necessary for mediating the effect. In 2003, Lewis et al. firstly described a computational tool with algorithms to predict targets of miRNA, which was the first version of the web based TargetScan software that is still widely used now in miRNA research field. This study was a hallmark of miRNA researches as it identified the "seed site" which was the 7 nucleotides (2-8 from the 5' end of miRNA) at the 5' end of miRNA and was the major location of Watson-Crick pairing site to bind to target mRNAs (Lewis et al., 2003). Although the "seed site" was later modified by the same group to be the 6 nucleotides from the second to the seventh at the 5' end of miRNA, the basic principle remained the same (Lewis et al., 2005).

It was determined that the 5' end of miRNA was more conserved than the 3' end and this conservation significantly contributed to better target prediction. Further sequence alignment across different species showed a frequently conserved A in the target mRNA 3'-UTR immediately downstream of the sequence that was complimentary to the seed site (Lewis et al., 2005). This conserved A was named A1. Since the nucleotide A could not always bind to the first nucleotide of miRNA in a Watson-Crick base pair matched manner, it was proposed that this conserved nucleotide A could be recognised by proteins in the RISC. Conservation at the 8th nucleotide from the 5' end of the miRNA was also revealed and named m8. Thus in the article, three kinds of canonical target sites centred on the seed site was uncovered to be of great predicative value, i.e. central seed site (2-7) with A1 and m8 (8mer), central seed site with only A1 (7mer-A1) as well as central seed site with only m8 (7mer-m8) (Lewis et al., 2005). Conservation analysis showed that miRNA sequence other than the 8 nucleotides containing the seed site at the 5' end was often

not conserved. It further supported the exclusion of those sequences when predicting miRNA targets.

1.4.4.2.2. 3’ complimentary sites and 3’ supplementary sites

Krek et al. in 2005, the same year when Lewis described the seed site concept, published an article utilizing a similar computational method to identify potential target site for miRNAs (Krek et al., 2005). Apart from the conservation analysis of miRNAs across species, they also applied thermodynamic parameters in determining a fine miRNA:mRNA base pairing duplex which required a low free energy as shown by software predicted RNA secondary structures (Krek et al., 2005). Their validation of target sites also mainly emphasised the importance of seed sites at the 5’ end of miRNAs. In addition, they found that if imperfect seed site was present bearing mismatches, bulges, or G:U wobbles, compensatory base pairing at the 3’ end of miRNAs would help to strengthen the miRNA:RNA duplex formation. This could be called 3’ end compensatory site (Krek et al., 2005). If 3’ end base pairing exists even if there is perfect seed site base pairing at the 5’ end of the miRNA, this 3’ end base pairing could be called 3’ complimentary site and could literally compliment the effect of seed site binding. This formed the basis of another web based software PicTar and softwares using similar algorithms to powerfully predict miRNA targets (Krek et al., 2005). In that same year, Brennecke et al. validated consistent findings as demonstrated by Krek et al. with an *in vivo* assay (Brennecke et al., 2005). After expressing the enhanced green fluorescent protein (eGFP) ubiquitously, they transfected the cells with a miRNA in a specific region of Drosophila and examined their inhibition of eGFP with different modifications of the 3’-UTR, which yielded similar results (Brennecke et al., 2005). Furthermore, they explored the 6mer site (seed pairing at the seed site only with Watson-Crick base pairing at position 2-7 from 5’ end of miRNA) effect and revealed their minimal contribution to target inhibition (Brennecke et al., 2005).

In comparison to TargetScan, Pictar based target prediction algorithm did not include a conserved A immediately downstream the seed pairing at the 3’-UTR of target

mRNAs. Later large scale proteomic experiments checking the effect of miRNAs on a wide range of targets at the protein level showed that the 7mer-A1 target site characterised by TargetScan with the conserved A outperformed the kind of base pairing described by Pictar at the first 7 nucleotides of 5' end miRNA. This implies that perfect base pairing might not be the only determinant factor in identifying potential targets, more factors such as the structural interaction of miRNAs with mRNAs as well as proteins also need to considered (Baek et al., 2008).

Collectively, the target sites described could be separated into 2 groups according to their location on miRNAs. The first group mainly includes the seed site centred ones located at the 5' end of miRNAs: 8mer site, 7mer-A1 site, 7mer-m8 site and 7mer site, which could be called canonical sites of miRNAs for target prediction. Efforts have also been invested to identify 6mer and offset 6mer sites (Friedman et al., 2009). The second group was 3' supplementary site and 3' compensatory site, which, as suggested by the nomenclature, locates at the 3' end of miRNAs. 3' supplementary site serves a supplementary role for miRNA:mRNA binding when there is perfect base pairing at the seed site, whereas 3' compensatory site compensates for the imperfect 5' end base pairing. They are non-canonical or atypical sites.

The involvement of canonical sites has been confirmed by high throughput transcriptomic or proteomic studies (Baek et al., 2008; Grimson et al., 2007; Selbach et al., 2008). However, in these high throughput studies, canonical target site are endogenously more prevalent, with the non-canonical sites taking a smaller fraction and might not be granted sufficient data acquisition, attention or efforts in the identification (Helwak et al., 2013). Furthermore, the target prediction by different algorithms largely depends on sequence conservation across species. A presupposition of these computational methods is that the target site lies within the 3'-UTR of target mRNAs. This further restricts the view in a limited segment of the mRNA, whereas other parts of mRNA might also be targeted, even the protein coding region. False positive prediction always exists. Moreover, in some cases, even perfect pairing at the seed site or canonical site sometimes is not sufficient in

predicting the miRNA and mRNA interaction (Didiano and Hobert, 2006; Vella et al., 2004a).

1.4.4.2.3. Other target sites

Under this circumstance, to obtain an unbiased analysis of miRNA:RNA interaction, or prediction of target binding site, high throughput sequencing of RNAs isolated by crosslinked immunoprecipitation (Argonaute HITS-CLIP) method was utilised to study the miRNA/RNA and Argonaute protein interaction (Chi et al., 2009). Argonaute proteins, mainly Argonaute 2, was an indispensable composition of RISC *in vivo*, being the catalytic centre of it. However, Argonaute proteins from the same family such as Argonaute 1, 3 and 4 also exhibit cleavage activity when they are loaded with mRNAs *in vitro*, but the only Argonaute protein recognised to be active *in vivo* is Argonaute 2. Data gathered about miRNA/Argonaute interaction site as well as mRNA/Argonaute interaction site could be combined with bioinformatic methods, which could provide valuable information for site characteristics both within miRNAs and within mRNAs. The predominant advantage of this experiment based analysis about interaction sites is that all identified interaction sites would be characterised without any pre-exclusion of either the 3' end of miRNA or mRNA segments outside the 3'-UTR region (Chi et al., 2009). The importance of this unbiased view lies in the possibility it could provide for further identification of non-canonical sites. It even provides a chance to study interactions of miRNA and mRNA without any binding site. The main disadvantage, however, is that physical interaction of miRNA/mRNA with Argonaute protein does not necessarily guarantee downstream functional inhibitory effect of miRNAs.

Most studies utilising Argonaute HITS-CLIP method firstly confirmed the already established canonical sites on miRNAs, further proving their importance for miRNAs to exert effect (Easow et al., 2007; Hendrickson et al., 2008; Karginov et al., 2007; Konig et al., 2012). On top of that, more efforts have been invested in determining non-canonical sites. With Argonaute HITS-CLIP method, miR-124 interaction site with mRNA in the brain *in vivo* was analysed, and focus was mainly placed on the

non-canonical ones (Chi et al., 2012). A new class of sites were identified. This G-bulge site was described to be the existence of a G nucleotide on mRNA which rendered the skipped base pairing at miRNA position 5 or 6. Nice conservation of this G-bulge site was found to be present in almost all miRNAs and it was also widespread, compromising nearly a similar fraction as the canonical seed site (Chi et al., 2012). The concept of bulged site was already demonstrated in several isolated miRNAs before the general description in this report. It was found in 1996 in the first ever reported miRNA lin-4 that bulged site was present and sufficient in inducing the inhibitory effect of lin-4 (Ha et al., 1996). In addition, it was shown in 2008 by Didiano et al. that for miRNA lys-6 and its target mRNA cog1, perfect base pairing in the target site exerts no inhibitory regulation, whereas a bulged site was required for effective down regulation (Didiano and Hobert, 2008).

Non canonical G:U wobbles were also found to be functional. For miRNA let-7 and its target lin-41 mRNA as well as miR-196 and its target HoxB8 mRNA, wobble G:U base pairing was found and proved to display inhibitory function (Vella et al., 2004b). However, in the algorithm utilised by the computational prediction of miRNA targets software TargetScan and PicTar, G:U wobbles was not tolerated even though the established G:U wobble functional effect was already described since the tolerance would significantly decrease signal:noise ratio in the bioinformatic prediction (Brennecke et al., 2005; Lewis et al., 2005; Lewis et al., 2003). Mutation study in 2008 by Didiano et al. showed that G:U wobble in the binding site could not achieve equivalent inhibition as demonstrated by site with Watson-Crick base pairing at the same position, however, the inhibitory function was not abrogated and should not thus be eliminated in target prediction (Didiano and Hobert, 2008).

Other atypical target sites have been identified as well. Centred site, which means the 11-12 perfect base-pairing on the miRNA from position 4-15, was demonstrated in miRNAs lacking both the seed sites and 3’ compensatory sites. The method the authors used was the cleavage assay rather than previously established computation methods, which might be the reason why the authors managed to characterise this kind of site (Shin et al., 2010). They also claimed conservation to some extent about

this centred site in various miRNAs (Shin et al., 2010). They only constitute a small proportion of the predicted sites, which is similar to the fraction of 3' compensatory sites (Shin et al., 2010).

Crosslinking, ligation and sequencing of RNA-RNA interaction hybrids (CLASH) method allowed the analysis of a direct interaction between miRNAs and mRNAs, which is a significant progress after the utilisation of Argonaute HITS-CLIP method to study RNA protein interaction (Kudla et al., 2011). In addition to the sites described by other studies, they also identified the miRNA and mRNA interaction at more atypical sites. Though miRNA binds predominantly to mRNA 3'-UTRs, direct interaction between miRNA with other parts of mRNA such as the coding region and the 5'-UTRs have also been observed (Helwak et al., 2013). This is consistent with previous isolated reports (Brodersen and Voinnet, 2009; Grey et al., 2010; Ørom et al., 2008; Tay et al., 2008). More interestingly, the direct interaction between miRNAs and noncoding RNAs have also been uncovered with CLASH experiments, adding a new class of potential target types to the already complicated miRNA regulation network (Helwak et al., 2013).

Apart from all kinds of sites on miRNAs, including the canonical ones and the non-canonical ones (Illustration of different target sites are shown in Figure 1-10), "seedless" inhibition of miRNA on mRNA was also observed, implying that the whole system of miRNA regulation mechanism might be more complex than we have already described. E2F2 gene could be directly inhibited by miR-24 through seedless 3'-UTRs (Lal et al., 2009). Additionally, as introduced earlier, perfect canonical seed sites were not sufficient to predict the functional interaction between miRNA and its target mRNAs. The possible explanation behind it is that there are other factors influencing the interaction process. Argonaute 2 protein is an important component of the RISC complex. It was demonstrated by structural studies that it displayed a flexible structure which could be stabilised by miRNAs binding to it (Elkayam et al., 2012). Another element that influences the interaction process is the mRNA accessibility to binding sites (Brodersen and Voinnet, 2009). Binding of the target site on mRNAs with RNA binding protein (RBP) or the inclusion of target site within the

stem loop structures of mRNA itself would prevent the target site from being accessible to miRNAs. Whereas other factors that promote the release of RBP from binding to complimentary sequences which could form the stem loop structure with the target sites would increase the accessibility of mRNA target site. The better binding affinity of RISC with target site that could help release other translational repressors from the target site would increase the accessibility as well (Brodersen and Voinnet, 2009).

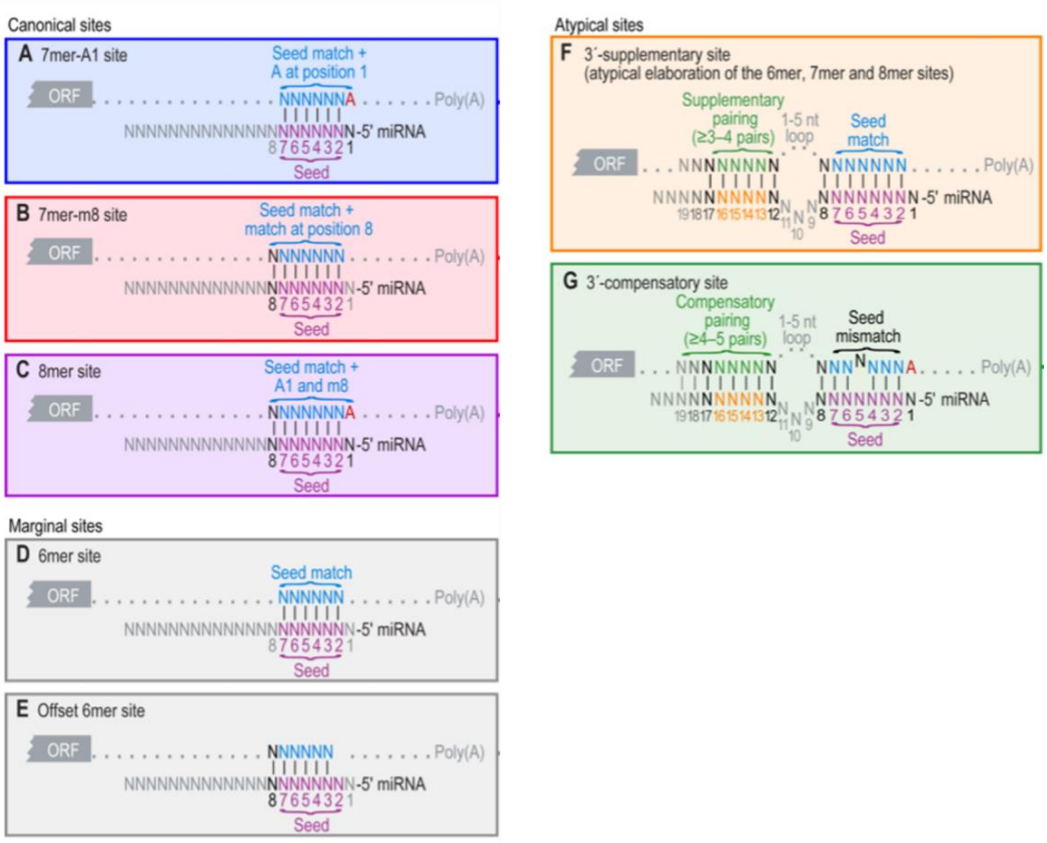

Figure 1-10 Illustration of different miRNA target sites

The different types of miRNA target sites depicting the binding mode of target mRNA and miRNA including canonical sites (A-C), marginal sites (D, E) and atypical sites (F, G) are briefly illustrated in the figure. The figure is reproduced from (Bartel, 2009).

1.5. Vascular tissue engineering

1.5.1. Introduction of tissue engineered vascular grafts

Cardiovascular diseases are the leading medical problems which often require surgical bypass intervention. Saphenous vein and internal mammary arteries as well as the radial arteries are typical vascular graft choices (Writing Group et al., 2016). The saphenous veins are the most commonly used graft choices owing to their ease of availability (Desai et al., 2004). However, compared to internal mammary arteries or radial arteries, the saphenous vein grafts display not as good long term patency rate since they are more prone to develop graft body diseases including aneurysm formation at the anastomotic site, intimal hyperplasia and atherosclerosis, which are the main causes for graft failures in the long run (Hess et al., 2014; Sabik et al., 2005; Yamasaki et al., 2016). These side effects are conceivable because of the mechanical mismatch and structural difference between veins and arteries. However, artery bypass graft harvesting sometimes may lead to severe side effects such as limb oedema. Moreover, precedent disease conditions such as atherosclerosis in the patients may involve the autologous artery bypass choices as well rendering them to be not as effective as what is expected. In patients who have undergone graft failures of previous coronary artery bypasses surgeries, the bypass choices would be more limited. Given these circumstances, it is imperative that novel choices of bypass grafts be explored. Tissue engineered vascular bypass emerge in the last 50 years as a promising alternative for the replacement of disease-involved and symptom-causing coronary arteries as well as peripheral arteries.

1.5.2. Scaffold-based vascular tissue engineering

1.5.2.1. First report of non-degradable synthetic scaffold in 1952 and later development

As early as 1952, it was reported that Vinyon “N” cloth, a synthetic fibre made from polyvinyl chloride and invented in 1939, could be constructed as a tubular mesh structure and transplanted *in vivo* as an arterial bridge. Exposure of this arterial prostheses to arterial blood flow would result in fibrin formation in the mesh holes and lead to integral prostheses wall, thus preventing the high speed arterial flow from leaking into adjacent tissue space (Voorhees et al., 1952). The thought of utilising Vinyon “N” mesh to serve as an arterial bypass originated from previous experimental observation. When Vinyon “N” was sutured in the cardiac wall, a new layer of the film could form throughout its length. The implication of this experiment was that the presentation of Vinyon “N” *in vivo* could result in an appropriate level of healing reaction without intensive foreign body immuno-rejection (Voorhees et al., 1952). Out of the 15 dogs which have undergone a segment of abdominal artery replacement with Vinyon “N” mesh, 11 got autopsy examination upon the sacrifice, and 8 arterial prostheses among these remained patent. In the remaining 4 live dogs, nice patency was also demonstrated by the pulsation of the femoral artery (Voorhees et al., 1952). Encouraged by the promising patency rate in canine experiments, the group went on with a larger scale of canine abdominal arterial replacement experiments and yielded similarly promising results (Blakemore and Voorhees, 1954). Later clinical efficacy examination of the Vinyon “N” mesh in 18 patients exhibited to some extent gratifying results with a recovery of the 10 patients previously suffering from the abdominal aneurysm. However, the other 8 patients died from direct or indirect reasons related to the difficulty of handling vascular walls that had degenerated (Blakemore and Voorhees, 1954).

It was found later that vascular grafts with synthetic materials, in general, displayed poorer patency rate when used to replace small diameter vessels (<6 mm) compared to the utilisation of them in replacing larger diameter vessels as the velocity of blood flow was significantly lower. Reduced blood flow velocity leads to higher thrombosis rate and a low degree of intimal hyperplasia might result in extensive occlusion of the vessel, and thus graft failure (Bennion et al., 1985). Indeed, the engineering of small diameter blood vessels presents as a long existing challenge since the recognition of

its importance in the clinics especially in the treatment of coronary artery diseases. Continuous and intensive efforts are invested in improving the performance of synthetic grafts as they are easily manufactured and could be tailor made according to patients' need and parameters of the diseased vessel. Many other synthetic and non-degradable materials have demonstrated potential in vascular tissue engineering such as expanded polytetrafluoroethylene (ePTFE), polyethylene terephthalate (PET), polyurethane (PU) and polyhedral oligomeric silsesquioxane poly(carbonate-urea) urethane(POSS-PCU) (G et al., 2015).

1.5.2.2. First report of degradable synthetic scaffold in 1999 and later development

In 1999, Niklason and his group firstly utilised the polyglycolic acid polymer (PGA) which was a biodegradable material to generate small vascular grafts. Combined with the mechanical stimuli provided by the bioreactor system which was also firstly used by their group, grafts with satisfactory mechanical strength was constructed with a burst pressure of more than 2000 mmHg (Niklason et al., 1999). Compared to the non-degradable scaffolds, degradable scaffolds could be gradually degraded and absorbed. The rate of degradation should be delicately designed so that it matches the rate of *in vivo* integration. Too fast degradation rate would lead to compromised mechanical feature and hence aneurysm formation or graft rupture; whereas when degradation rate is too slow, the unintended immunogenic response could persist. Degradation process of the graft may also yield PH change which could affect the proliferation and differentiation of SMCs seeded on the graft (Higgins et al., 2003). Apart from polyglycolic acid based material, other degradable materials have also been explored in vascular tissue engineering including polylactic acid (PLA), poly e-caprolactone (PCL), poly(l-lactide-co-e-caprolactone)(PLCL), and polyglycerol sebacate (PGS) (G et al., 2015).

One crucial drawback of the synthetic graft lies in their poor biocompatibility which often leads to native immune response and thrombosis within a short term of

transplantation. The mechanical strength of the synthetic grafts also needs further improvement to match the requirement and meet *in vivo* haemodynamic environment.

To overcome these drawbacks and take full advantage of the synthetic materials, numerous approaches were attempted in the last 50 years or so to achieve satisfying results. Firstly, different modifications of these synthetic grafts including molecular level modifications are examined. Various peptides have shown anti-thrombogenic potentials (Ren et al., 2015). It was shown on chitosan hydrogel/poly(ethylene glycol)-b-poly(L-lactide-co-caprolactone) (PELCL)-based scaffold that VEGF and PDGF dual delivery from the scaffold could help promote *in vivo* vessel regeneration (Zhang et al., 2013). Polyurethane (PU) conduits loaded with SDF-1 and VEGF demonstrated better tissue compatibility and promoted endothelialisation *in vivo* (Guo et al., 2017). Secondly, seeding of the synthetic grafts with cells proves to increase the biocompatibility as well as the mechanical property. Cell sources that have anti-thrombogenic capacity include ECs, endothelial progenitor cells and perhaps bone marrow mononuclear cells. Lastly, preconditioning of the grafts *in vitro* to haemodynamic environments might help to increase the chance for the grafts to match better with *in vivo* vascular haemodynamics. What's more encouraging is that the development of novel material manufacturing techniques such as electrospinning and 3D printing techniques helps revolutionise the field of vascular tissue engineering (Duan, 2017; Elliott and Gerecht, 2016; Rocco et al., 2014). For example, owing to innovative electrospinning technique, elastic polyurethane and reinforcing poly-glycolic acid could be engineered to act in a "J-shaped" mode upon cyclic strain application mimicking the *in vivo* action of elastin and collagen in response to cyclic strain in native vessels (Rapoport et al., 2012).

1.5.2.3. First report of natural scaffold in 1986

In 1986, Weinberg and his colleagues managed to generate a tubular like structure *in vitro* that resembled the *in vivo* artery structure (Weinberg and Bell, 1986). By mixing culture medium, collagen and SMCs and casting them in an annular mould, the first layer would be formed shortly consisting SMCs and collagen matrix. Later,

the fibroblast layer with a mixture of matrix and fibroblast cells was cast outside to mimic the adventitia layer. A Dacron mesh would then be placed outside the tubular structure to provide additional mechanical support. In the end, an endothelial layer was added by seeding the cells inside the lumen after peeling the tubular structure off the mandrel. The mechanical strength of the assembled vessel was then examined. It was found that without the Dacron mesh, the graft was greatly distensible and got easily dilated with a low pressure (<10 mmHg). With one layer Dacron mesh protection, however, the vessel managed to tolerate the burst pressure as high as 40 to 70 mmHg. Furthermore, the mechanical strength of the graft was proportional to the concentration of the Matrigel in the mixture (Weinberg and Bell, 1986). In 1993, L'Heureux et al. utilised a similar way to construct a vessel *in vitro* that managed to contract and reorient under periodic mechanical stimulation from the casting mandrel (L'Heureux et al., 1993).

Other natural scaffolds that have been explored in vascular tissue engineering include fibrin (Swartz et al., 2005), silk fibroin (Enomoto et al., 2010; Lovett et al., 2010) and chitosan (Zhang et al., 2006b).

1.5.3. Decellularised vascular grafts - first report and subsequent development

The first report of the vascular graft *in vivo* was the "vinyon N" mesh that was used in large diameter arteries (Voorhees et al., 1952). It not only provided enough mechanical strength, but also presented as a backbone for fibrin formation which was essential for the integrity of the vessel wall. However, their success is mainly restricted for large diameter vessel replacement. For small diameter vascular grafts which are more prone to thrombosis and long term intimal hyperplasia that can result in graft failure, the lack of biocompatibility has largely hampered the generalised application. While efforts have been invested in improving the biocompatibility of the synthetic materials, alternatives of vascular scaffolds which are more biocompatible

are explored. It is reasonable that people started from analysing the protein components of the extracellular matrix of native vessels. What was initially found out is that collagen and elastin are the two major proteins in the extracellular matrix. It was then investigated whether homogeneous collagen itself could be applied in vascular tissue engineering, which led to the first case report of natural material based scaffold for vascular graft in 1986 by Weinberg and his colleagues (Weinberg and Bell, 1986). However, it turned out that between mechanical strength and bio-compatibility, only one could be achieved with that approach. Collagen-based scaffold failed to provide sufficient mechanical strength which had to be complemented by a synthetic material reinforcement outside the engineered graft. This intrinsic limit of natural material based scaffold then resulted in numerous efforts to achieve the satisfying mechanical strength of the graft including using crosslinking agents and hybrids of other natural materials. In the meanwhile, new ideas emerged in 2001 that the extracellular matrix of the whole native vessel might be possible to be used as a scaffold for vascular grafts. What encumbered people from doing so might be the allogeneic immunologic response which might cause severe rejection of the vascular grafts followed by the graft failure. To utilise the whole vascular backbone as a scaffold and at the same time get rid of the cells, a decellularisation process of the native vessel was performed.

In 2001, Kaushal et al. were the first to use porcine iliac vessels to generate decellularised vascular grafts. Decellularisation was achieved through Triton X-100 and ammonium hydroxide. These decellularised grafts were not able to remain patent for more than 15 days after the implantation in sheep as carotid interposition grafts whereas pre-seeding of the graft with endothelial progenitors significantly improved the patency rate (Kaushal et al., 2001). The excellent biocompatibility and mechanical strength led to more attempts to engineer vascular grafts with other cell sources which would be explained in detail later. Enzyme-based, detergent-based and perfusion-based methods are all explored in decellularising the native vessel which exhibit different efficacy and would influence the features of the vessel. When optimising the decellularisation method, a balance between removal of the allogeneic cellular

fractions and the reservation of the mechanical strength as well as extracellular matrix integrity should be achieved.

1.5.4. Self-assembled scaffold free vascular grafts

When we use natural scaffolds to engineer vascular grafts, what we normally use are the purified extracellular matrix proteins in the native vessel such as collagen I and fibrin. However, one drawback of this method is that the extracellular matrix in native vessels is a complex network and contains multiple fractions. To better recapitulate the native composition of the extracellular matrix, efforts have been invested in directly utilising cells to produce them rather than use of purified extracellular matrix proteins. It has led to another method to generate vascular grafts: engineering vascular grafts with self-assembly. The concept and development of self-assembled vascular grafts was largely driven by the L'Heureux group.

To achieve the goal of constructing vascular grafts with a better extracellular matrix complex, SMCs were firstly grown on a surface for about 3 weeks to form cell sheets. After the maturation of SMCs and the production of extracellular matrix from them, the cell sheets were rolled around a mandrel to form a tubular structure, which was allowed to further mature for 1 week. Later, the fibroblasts were seeded outside to form the adventitia layer and allowed 7 weeks to mature. ECs were seeded inside the lumen after peeling the sheets from the mandrel and allowed one more week for their growth (L'Heureux et al., 1998). Vascular grafts generated in this manner contained more biological extracellular matrix and displayed mechanical strength similar to that of native vessels with the burst pressure to be over 2000 mmHg (L'Heureux et al., 1998). Also, *in vivo* evaluation of the grafts demonstrated that they were easy to handle and tough enough to be sutured with native vessels (L'Heureux et al., 1998). Further modification with glycation of the extracellular matrix was explored to strengthen the grafts produced and proved to be beneficial (Girton et al., 2000; Girton et al., 1999). Comparison of mechanical property including tensile strength and

stiffness between tissue rings formed with cell seeded collagen or fibrin gel and tissue rings assembled by cells demonstrated a significant advantage of self-assembled grafts (Adebayo et al., 2013).

Preclinical examination of the self-assembled vascular grafts was then encouraged by the experimental results and transplantation of the graft into dogs, nude rats and primates was carried out. Autologous cells were used in canine and nude rat experiments and human cells were used in primates along with immuno-suppressive treatment (L'Heureux et al., 2006). Further checking of the graft showed the existence of both collagen and elastic fibres within the extracellular matrix. *In vivo* integration of the grafts was observed with the formation of adventitial *vasa vasorum* and intact endothelial lining 90 days after the graft implantation (L'Heureux et al., 2006). These safety and efficacy results accumulated from different species paved the way of the self-assembled vascular grafts into the clinics. In 2007, 10 patients who needed alternative arteriovenous shunts for haemodialysis were grafted with the self-assembled conduits engineered with autologous cells. Results showed that these grafts were feasible to be used as a temporary arteriovenous shunt although an aneurysm was still observed in sites which were punctured frequently (L'Heureux et al., 2007). Long term follow-up of patients showed 78% patency rate after 1 month and 60% patency rate after 6 months (McAllister et al., 2009).

Although self-assembled vascular grafts are shown to be effective, the process to construct a graft is especially time-consuming which largely hinders their application in the clinics. However, people who need vascular bypass surgery could in a way be predicted according to the disease condition which may grant enough time for vascular tissue engineering. Moreover, the utilisation of self-assembled vascular grafts could be more cost-effective if less time was required for construction. Much effort has been invested in generating “off-the-shelf” self-assembled vascular grafts to achieve this goal. The “off-the-shelf” vascular grafts were constructed without the last endothelialisation step and then dehydrated and devitalised. After storage at -80 °C for more than 9 months, the mechanical strength remained. 5 days before the implantation of the grafts in patients, endothelialisation was performed on the graft

with autologous cells to prevent thrombosis. These grafts served as haemodialysis shunts in patients for up to 11 months without signs of dilation or degradation (Wystrychowski et al., 2011; Wystrychowski et al., 2014). The fibroblasts utilised to generate the grafts could be allogeneic since fibroblasts are not immunologically active and don't express major histocompatibility complex class II antigens (Wystrychowski et al., 2014). Thus, the whole process from the stored "off-the-shelf" grafts to ready-to-use grafts was minimised to less than a week. However, it still requires further exploration to determine whether the allogeneic fibroblasts could be utilised without compromising their efficacy. Decellularisation of the constructed scaffold to bypass the immuno-activity issue was also explored (Bourget et al., 2012). The fibroblast cell sheets were decellularised and then used to serve as support of SMCs (Bourget et al., 2012). Apart from saving time for vascular graft construction, another advantage of this process is that the extracellular matrix production is not anymore crucially dependent on the SMCs seeded which allowed the use of SMCs from some elder or diseased patients in tissue engineering since the capacity of the cells to secrete extracellular matrix might be compromised (Bourget et al., 2012).

Apart from mature vascular cells, stem cells have also been explored including BMMSCs and UCMSCs in generating self-assembled vascular grafts (Bourget et al., 2015; Zhao et al., 2012). It was shown that BMMSCs could act like ECs and prevent thrombolisation. Moreover, the time needed for generating the graft was shortened to 2 weeks without compromising the *in vivo* performance of the grafts (Bourget et al., 2015; Zhao et al., 2012).

1.5.5. Mechanical stimuli

The engineered vascular grafts would be under constant mechanical pressure *in vivo* imposed by dynamic blood flow *in vivo*. Therefore, when constructing the blood vessel grafts, the mechanical properties of the graft should be evaluated. Subsequently, efforts should be invested in engineering grafts with reinforced mechanical strength.

For coronary artery bypass, it was introduced earlier that the internal thoracic artery would be the golden standard for the bypass surgery with a long-term patency. However, its application sometimes is hampered by the relatively severe complication that would be caused by the harvesting process or by the precedent atherosclerotic lesion involvement. Saphenous vein was presented as a secondary choice with a relatively lower long-term patency rate. In order to achieve satisfying results when engineering blood vessels, the mechanical property of the graft comparable to the internal thoracic artery or saphenous veins should be obtained (Catto et al., 2014; Sarkar et al., 2006). Mechanical parameters that should be firstly evaluated include the burst pressure, suture retention strength and compliance. They are respectively 3072 mmHg, 1.72 N and 11.5% /100 mmHg for the internal thoracic artery and 2134 mmHg, 1.92 N, and 25.6% /100 mmHg for the saphenous vein (Konig et al., 2009). Other terms such as the tensile strength or pliability of the vessel were sometimes used as well (Yokota et al., 2008). These features provide the basic information as to whether the engineered vessel would be able the handle the pressure brought by the highly dynamic blood flow *in vivo*.

However, the mechanical behaviour of native vessels is far more complex. When examined further, it was revealed that when handling the pressure, native vessels *in vivo* normally display a J-shaped mode to deal with the cyclic strain. Under low strain pressure, compliant and elastic elastin fibres could handle it with only small cyclic stress changes, whereas under high strain pressure, the corrugated collagen could stretch and result in rapid cyclic stress changes (Pashneh-Tala et al., 2016; Rapoport et al., 2012). As the extracellular matrix proteins elastin and collagen are both crucial contributors to vessel mechanical strength, inclusion of both in vascular tissue engineering could be pertinent (Rapoport et al., 2012).

However, since we always aim at engineering vessels with the internal thoracic artery or the saphenous vein as the golden standard, the ultimate effect of the engineered grafts would not surpass those manifested by them. Mechanical properties also variate depending on the patients' gender, age and the location of the vessel (Ozolanta et al., 1998). To provide personalised medical care with tailor made

vascular grafts, these factors should be taken into consideration as well for the better performance of the graft.

1.5.6. Cells utilised in tissue engineered vascular grafts

Although in the first Vinyon “N” cloth scaffold that was transplanted *in vivo* for canine abdominal aorta replacement, the scaffold was nude without any cell seeding or modification, the relatively satisfying patency rate could not be duplicated when the nude graft with only the synthetic material was utilised to engineer small diameter vascular grafts (Seifu et al., 2013). The lack of biocompatibility as well as mechanical compliance contributes significantly to the high thrombosis rate in small diameter vascular grafts since the velocity of the blood flow is much lower. To increase the biocompatibility, numerous cell types are explored for their potential to improve the graft performance *in vivo*.

1.5.6.1. Mature cells

Efforts in engineering vascular grafts first took advantage of mature vascular cells for biomimicry of the *in vivo* vascular structures. ECs were utilised for its anti-thrombogenic effect and SMCs were used due to its capacity to produce extracellular matrix and mechanical support for the vessel. Sometimes fibroblasts were applied to the outer layer of the engineered graft to further provide an “adventitial” like layer (Niklason et al., 1999; Shinoka et al., 1998; Weinberg and Bell, 1986). This approach was successful in animal models and later encouraged the first clinical case to utilise *in vitro* cultured vascular cells from the peripheral vein to construct pulmonary artery (Shin'oka et al., 2001). After seeding the *in vitro* cultured SMCs and ECs onto the polycaprolactone-polylactic acid copolymer reinforced with woven polyglycolic acid, the graft was transplanted in a child patient and no graft occlusion or aneurysm was observed after 7 months.

However, the intrinsic limit for utilising mature vascular cells lies in their finite life span and proliferation capacity. It takes relatively a long time (around 8 weeks) to get enough cells and these autologous cells might be in a compromised state due to the disease condition of the host (Shin'oka et al., 2001). To overcome this disadvantage, hTERT, a reverse transcriptase constituting human telomerase, was ectopically expressed in human SMCs and the proliferative ability was retained which shortened the time needed to culture enough cells to generate vascular grafts (McKee et al., 2003; Poh et al., 2005).

Apart from this, more attention was gradually placed on a large variety of stem cells which are proliferative *in vitro* and display the differentiation capacity towards vascular lineages. These include the embryonic stem cells, induced pluripotent stem cells and adult stem cells such as bone marrow mononuclear cells, mesenchymal stem cells, endothelial progenitor cells and muscle-derived stem cells.

1.5.6.2. Embryonic stem cells

Embryonic stem cells are the first to come in sight while alternative sources for vascular tissue engineering were being searched due to their highly proliferative potential and totipotency. Regarding vascular graft engineering, it is shown that embryonic stem cells can differentiate towards vascular lineages including ECs and SMCs (Levenberg et al., 2002; Odorico et al., 2001; Xiao et al., 2009; Yamashita et al., 2000). Harnessing the endothelial differentiation potential, the vascular graft was generated with mouse embryonic stem cell-derived ECs together with mature SMCs isolated from artery (Shen et al., 2003). Histological analysis demonstrated the integral endothelial lining on the luminal side of the polyglycolic acid scaffold (Shen et al., 2003). The differentiation capacity of embryonic stem cells towards SMCs was also explored and harnessed in vascular graft engineering. When SMCs differentiated from the embryonic stem cells were seeded onto polyglycolic acid polymer mesh scaffold and cultured under pulsatile conditions for 8 weeks, vascular graft resembling the native vessels with regard to smooth muscle marker expression in the media layer was obtained (Sundaram et al., 2014a). Isolation of c-kit^{+} cells from

embryonic stem cells was carried out, and these cells displayed vascular lineage potential towards both ECs and SMCs, both of which were utilised to generate vascular grafts with decellularised mouse aorta as the scaffold. The survival rate was higher when grafts seeded with both ECs and SMCs were transplanted *in vivo* as a vein graft compared to decellularised scaffold only (Campagnolo et al., 2015b). Although the attempts to generate vascular grafts from embryonic stem cells are rather gratifying, drawbacks remain as well. First, it is ethically controversial to use embryonic stem cells in the clinics. Secondly, embryonic stem cells are totipotent. Apart from vascular lineage differentiation capacity, they could also differentiate towards various other cell lineages. They might generate teratoma or cancer when transplanted *in vivo*. Additionally, their differentiation potential towards osteogenic lineages and chondrogenic lineages might contribute to the vessel wall calcification in engineered vascular grafts which would hamper their efficacy (Sundaram et al., 2014a).

1.5.6.3. Induced pluripotent stem cells

Since the discovery of Yamanaka factors that could drive the terminally differentiated adult cells back to the pluripotent stage, numerous attempts have emerged elucidating the underlying mechanism as well as harnessing the pluripotency for tissue regeneration. The discovery was also encouraging since it might help realise the popular concept of personalised medicine in the clinics. These adult cells derived pluripotent stem cells could bypass embryonic stem cells and the associated ethical concerns when stemness was required in tissue regeneration. It was demonstrated that the pluripotent stem cells could differentiate towards vascular lineages. In 2012, researchers from the Shinoka group differentiated the human induced pluripotent cell line towards both SMCs and ECs with the hanging drop method. The biodegradable scaffold seeded with the differentiated cells was then transplanted to mice as an interposition graft, with no development of graft rupture, thrombosis, aneurysm or calcification formation (Hibino et al., 2012). In the same year, Margariti et al. utilised lung fibroblasts and directly reprogrammed them towards ECs which successfully endothelialised the vascular scaffold decellularised from mouse aorta (Margariti et al.,

2012). Later, people from the same group managed to reprogram embryonic lung fibroblasts and differentiate them towards the smooth muscle lineage. These SMCs derived from reprogrammed lung fibroblasts were then combined with previously derived ECs to engineer functional vascular grafts with both smooth muscle and endothelial layers (Karamariti et al., 2013a). Furthermore, it was demonstrated by the Niklason group, who are the first to utilise the bioreactor system in vascular tissue engineering for mechanical preconditioning, that mechanical stimuli provided by the bioreactor system also contributed significantly in engineering vascular grafts with induced pluripotent stem cells by increasing the mechanical strength or potentiating the arterial specification of derived ECs (Sivarapatna et al., 2015; Sundaram et al., 2014b). All in all, exploration of vascular tissue engineering with induced pluripotent stem cell might help bring the concept of personalised treatment in cardiovascular disease one step further.

1.5.6.4. Bone marrow mononuclear cells

Bone marrow mononuclear cells are among the most extensively studied adult stem cells. Their potential in engineering small diameter vascular grafts was first explored in 2003 on biodegradable scaffolds. It was found that scaffolds seeded with bone marrow mononuclear cells displayed significantly higher patency rate compared to the non-seeded scaffolds when transplanted in dogs in the inferior vena cava (Matsumura et al., 2003). The seeded cells were labelled with green fluorescence that enabled the *in vivo* tracking of the cells. Further examination of the explanted graft after 4 and 8 weeks revealed co-staining of both endothelial and smooth muscle markers with the green fluorescence, demonstrating the *in vivo* differentiation of seeded bone marrow mononuclear cells and their participation in the *in vivo* regeneration of the graft (Matsumura et al., 2003). The application of bone marrow mononuclear cells does not necessarily require *in vitro* differentiation towards vascular lineages, largely shortening the time needed for vascular graft engineering (Hibino et al., 2005). It is also implicated that bone marrow cells might exhibit other features apart from differentiating towards vascular lineages. SDF-1 is a potent cell mobilisation factor and could be secreted by bone marrow nuclear cells which might

attract other progenitors from the circulation to regenerate the implanted graft. The success of bone marrow mononuclear cells in generating vascular graft led to clinical trials with engineered grafts that could serve as extra-cardiac cavopulmonary conduits to treat patients with single ventricle (Hibino et al., 2010; Shin'oka et al., 2005). Long term follow-up after an average of 5.8 years of the clinical trial showed no graft-related mortality. Aneurysm formation, conduit wall calcification, or graft rupture was not observed. Graft stenosis was seen in 4 patients out of 42 and was successfully intervened with percutaneous angioplasty (Hibino et al., 2010). However, it is noteworthy that the satisfying result of the clinical trial has to be partially attributed to the relatively large diameter of the conduit which renders the graft less prone to thrombosis and stenosis.

Other than directly seeding the bone marrow nuclear cells onto biodegradable scaffolds, the bone marrow cells were also differentiated *in vitro* first to generate vascular SMCs and ECs. The differentiated cells were then seeded on the decellularised vessel scaffold. Grafts seeded with cells displayed better patency rate (Cho et al., 2005). A similar approach was utilised in 2012 to generate vascular grafts by seeding bone marrow-derived SMCs and ECs onto decellularised allogenic iliac vein to serve as a bypass branch for the hepatic vein. Patient follow-up after 9 months was normal. Although graft narrowing was observed in 1 year, it was not caused by the graft itself but the pressuring adjacent tissues, which was successfully taken care of by removing the pressing tissue (Olausson et al., 2012). Overall, bone marrow mononuclear cells prove to be a promising cell source for vascular tissue engineering.

1.5.6.5. Mesenchymal stem cells

Vascular tissue engineering with mesenchymal stem cells would be discussed later in detail in the thesis.

1.5.6.6. Other adult stem cells

Potential of other adult stem cells to generate small diameter vascular grafts has also been explored including the muscle-derived stem cells (Nieponice et al., 2008), bone

marrow-derived muscle progenitors (Liu et al., 2007) and hair follicle stem cells (Peng et al., 2011).

1.5.6.7. Revival of acellular vascular grafts

In recent years, more efforts have been invested in exploration of novel material manufacturing methods which could in the end provide comparable results with those biocompatible cell-seeded scaffolds (Wu et al., 2012; Zhang et al., 2013). Indeed, cell seeding onto the scaffolds provides exceptional advantages. But the cell seeding process is time consuming and brings with them immunogenic problems if allogeneic cells were used. With the emergence of novel biomaterials (Wu et al., 2012), novel manufacturing methods (Rapoport et al., 2012) as well as further understanding of the mechanism how cells provide their benefits, acellular scaffold might have the potential to bring revolutionary changes in the field of vascular graft engineering.

1.5.7. Vascular graft engineering with mesenchymal stem cells

After the initial exploration of vascular tissue engineering with mature vascular SMCs and ECs as well as adult fibroblasts, stem cells emerge as alternative cell sources for vascular tissue engineering to overcome the inherent *in vitro* limited proliferation capacity and compromised function of the mature cells. All kinds of stem cell sources have been examined for their potential for engineering functional and patent small diameter vascular grafts, such as embryonic stem cells, induced pluripotent stem cells, bone marrow mononuclear cells, endothelial progenitor cells and mesenchymal stem cells from various origins as introduced earlier. The application of embryonic stem cells is hampered by the ethical issues they bring with them as well as the totipotent differentiation capacity which might cause cancer or unintended/uncontrolled cell lineage differentiation. Induced pluripotent stem cells prove to promising as they bear the potential to personalize the engineering of vascular grafts with completely autologous adult cells which are easily available and abundant. Researches are still ongoing to improve their performance in *in vivo*

implantation experiments. (Dash et al., 2016; Gui et al., 2016) Stem cells from the bone marrow are the earliest recognized and well-established adult stem cells. Numerous efforts have been invested which have demonstrated their potential in vascular graft engineering. However, the harvesting procedure from the bone marrow is invasive and it is difficult to get an adequate number of cells. Thus, it is necessary to look for new stem cell sources to engineer vascular grafts.

Mesenchymal stem cells could be isolated from almost all tissues around the body, such as the bone marrow, adipose tissue, umbilical cord, cord blood and hair follicle. As introduced earlier, they not only exhibit multiple differentiation capacities towards adipocytes, osteocytes and chondrocytes, they are also capable to differentiate towards vascular lineages such as SMCs (Gong and Niklason, 2008b) and ECs (Oswald et al., 2004). The vascular lineage differentiation capacities are crucial in generating vascular grafts which resemble the structure of native vessels. In addition, the immuno-modulation function of the mesenchymal stem cell presents a possibility to engineer vascular grafts with allogeneic cells which significantly expands the cell sources available that could be utilised in the clinics as autologous cell might not be of a sufficient amount or might be of compromised function caused by the disease status in patients (Aggarwal and Pittenger, 2005; Uccelli et al., 2008). It has also been reported that mesenchymal stem cells might display anti-thrombogenic ability (Hashi et al., 2007).

1.5.7.1. Bone marrow-derived mesenchymal stem cells

In 2007, Hashi et al. firstly seeded BMMSCs onto nanofibrous scaffolds and implanted the cell seeded scaffolds *in vivo* to examine the long-term patency. It was found that BMMSCs could inhibit the platelet adhesion to the scaffolds and thrombus formation in the short term, thus increasing the long term patency rate and inducing excellent *in vivo* vascular regeneration (Hashi et al., 2007). Promotion of scaffold endothelialisation might be another reason for the improved performance of grafts seeded with BMMSCs (Alexandre et al., 2017). To determine whether BMMSCs could directly take part in vascular regeneration *in vivo*, Mirza et al. implanted a

polyurethane vascular prosthesis scaffold seeded with undifferentiated and green fluorescent protein labelled BMMSCs in rats. After 2 weeks *in vivo*, cells co-expressing smooth muscle markers and green fluorescent proteins were observed indicating the smooth muscle differentiation of the seeded BMMSCs (Mirza et al., 2008).

Furthermore, it was shown that the cells could promote the endothelialisation of the prostheses when seeded on the grafts (Mirza et al., 2008). 6-month long term *in vivo* performance of bone marrow-derived mesenchymal cells seeded on the vascular grafts was examined. After seeding undifferentiated BMMSCs onto a novel biodegradable tubular scaffold, the scaffold was *in vitro* cultured for 7 days before implantation *in vivo* as a canine abdominal aorta. Excellent patency rate and satisfying *in vivo* vascular remodelling such as formation of an integral endothelial layer, multiple smooth muscle layers and accumulation of the extracellular matrix collagen, were observed (Zhang et al., 2008). It was also explored whether *in vitro* differentiated SMCs from BMMSCs could contribute to vascular graft engineering (Gong and Niklason, 2008b). Combined with mature ECs, SMCs differentiated from BMMSCs were seeded onto polyglycolic acid scaffold and cultivated in the bioreactor system. Grafts bearing histological similarity with native vessels were constructed (Gong and Niklason, 2008b). Moreover, the excellent performance of BMMSCs in vascular graft engineering is not restricted to grafts constructed with synthetic materials. Cell sheets containing BMMSCs could be assembled to form completely biological vascular grafts and the cells could also be seeded onto scaffolds decellularised from arteries. Grafts constructed with both methods above could also exhibit satisfying long-term patency rate when implanted *in vivo* (Zhao et al., 2012; Zhao et al., 2010).

However, though endothelial differentiation capacity was shown *in vitro* in BMMSCs, the differentiation capacity *in vivo* was still controversial and was not observed in some reports both *in vitro* and *in vivo* (Au et al., 2008). After establishing the beneficial effect of BMMSCs in vascular graft engineering, efforts were then invested in further improving the performance of vascular grafts to bring it even closer to that of native

arteries. Modification of endothelial nitric oxide synthase (eNOS) expression could help increase the graft performance (Zhang et al., 2006a). Fibronectin coating of the synthetic materials could promote the smooth muscle differentiation of BMMSCs while preserving its proliferation rate which might contribute to better graft performance as well (Shudo et al., 2016).

1.5.7.2. Adipose tissue-derived mesenchymal stem cells

Mesenchymal stem cells could also be derived from adipose tissues that could be easily harvested from the body. In fact, ADSCs are under extensive investigations for tissue regeneration and emerge to be a promising adult stem cell source (Krawiec and Vorp, 2012; Ramakrishnan and Boyd, 2017). However, they are not as widely investigated as BMMSCs. Most attempts examining the potential for vascular graft engineering are limited to *in vitro* studies with *in vivo* efficacy of the cells in vascular tissue engineering not that well established. In 2008, ADSCs were *in vitro* expanded and cultured for one passage before being seeded onto electrospun collagen and elastin hybrid scaffolds. The cell seeded scaffolds were cultured in the bioreactor system for 2-4 weeks. The cells could attach well to the scaffold and depending on the cell culture medium, the seeded cells either exhibited smooth muscle features or endothelial features (Heydarkhan-Hagvall et al., 2008). This study implicated the potential to use ADSCs to generate vascular grafts. Apart from the *in vitro* cultured undifferentiated ADSCs, partially differentiated cells in response to specific growth factors were also investigated. It was shown that under TGFβ1 stimulation, ADSCs could be differentiated towards SMCs, and these partially differentiated cells could also attach to scaffolds such as the polyglycolic acid mesh (Wang et al., 2010a) and the decellularised saphenous vein (Harris et al., 2011) which resulted in reinforced mechanical property of the vascular grafts. Endothelial differentiation capacity of the cells contributed to the endothelial layer formation of the decellularised grafts (Bertanha et al., 2014). Furthermore, it was demonstrated that ADSCs displayed dual differentiation capacities towards both vascular SMCs and ECs which could be seeded then to the biodegradable polycaprolactone (PCL)-gelatin mesh to construct a two layered vascular graft (Zhou et al., 2016a). Overall, differentiation capacity of

adipose tissue derived stem cells towards vascular lineages could be utilised in vascular tissue engineering. Like BMMSCs, ADSCs could also form cell sheets *in vitro* and then be assembled to generate completely biological vascular grafts (Costa et al., 2017).

To speed up the process of vascular tissue engineering, stromal vascular fraction which was the primarily digested adipose tissue without *in vitro* culturing, was compared with *in vitro* expanded ADSCs (Krawiec et al., 2016). Not as good but comparable performance was observed in terms of *in vivo* patency at 8 weeks (Krawiec et al., 2016). This implies that *in vitro* culture of ADSCs might be omitted to save time given some further improvement of the stromal vascular fraction seeded grafts such as growth factor incorporation. Proteomic profile of the adipose tissue derived stem cells seeded onto synthetic scaffolds was compared with cells from native vessels as an investigation of the mechanism through which to improve the vascular graft performance (Wang et al., 2013). Differentially expressed proteins include enzymes, anchored proteins and those that are involved in cell apoptosis, cellular organisation, energy metabolism and so on. However, it requires further experiments to pinpoint those that are related to the functional differences and could, in the end, contribute to improved vascular graft function (Wang et al., 2013).

1.5.7.3. Mesenchymal stem cells from other origins

Other mesenchymal stem cell (MSC) sources explored in vascular tissue engineering include umbilical cord blood derived mesenchymal stem cells, amniotic fluid derived mesenchymal stem cells, hair follicle-derived mesenchymal stem cells and pericytes. Although it is still controversial whether pericytes are included in the classification of mesenchymal stem cells, they bear so many similarities that pericyte utilisation in vascular tissue engineering would be explained here as well.

Through self-assembling, cell sheets formed by umbilical cord blood derived mesenchymal stem cells could be rolled around a mandrel and give rise to a vascular conduit with a higher mechanical burst pressure and better contractile response

compared to grafts formed by cell sheets of SMCs or fibroblasts (Bourget et al., 2015). Mesenchymal stem cells could be isolated from amniotic fluid and display the potential to differentiate towards SMCs which lays the foundation for their use in vascular tissue engineering (Weber et al., 2016).

Similarly, smooth muscle differentiation capacity was demonstrated in hair follicle derived mesenchymal stem cells and the expression of the induced smooth muscle markers could be maintained when they were seeded on decellularised scaffolds (Gao et al., 2014a; Liu et al., 2010). The investigation of hair follicle derived mesenchymal stem cells is mainly limited to *in vitro* studies. Synthetic scaffolds incorporated with pericytes demonstrated 100% patency rate compared to unseeded controls. Examination of the explants after 8 weeks showed nice *in vivo* integration as displayed by the functional smooth muscle layers and integral endothelial layer (He et al., 2010). Furthermore, pericytes could work synergistically with peptides contained by the synthetic scaffolds to promote endothelialisation and growth factor preservation (Campagnolo et al., 2016).

1.5.8. TGFβ1 in vascular graft engineering

As introduced earlier, TGFβ1 is a potent growth factor and could induce smooth muscle differentiation from multiple stem cells as well as SMC phenotypic switching from the secretory phenotype to the contractile phenotype (Goldsmith et al., 2006; Goumans et al., 2009). For the native vessel, the extracellular matrix, the cellular components and the haemodynamic environment work synergistically to maintain its normal function. In the process of vascular graft engineering, factors, which could influence these basic elements of vessel function, have the potential to improve the performance of the graft. Growth factors including TGFβ1, mechanical flow exposure, and extracellular matrix production have all been elucidated to contribute to smooth muscle phenotypic change to the contractile phenotype and the resultant enhanced vascular graft function (Beamish et al., 2010). When stem cells are employed in

vascular graft engineering, it could be concluded from the part “Cells utilised in tissue engineered vascular grafts” that they are either allowed to differentiate *in vitro* towards vascular lineages including SMCs and ECs, or they are seeded on the graft in the undifferentiated state and allowed to differentiate and participate in vascular regeneration *in vivo*.

When stimulating stem cell differentiation *in vitro*, TGFβ1 is a widely used growth factor. It has been applied in various vascular graft engineering systems involving different origins of stem cells such as smooth muscle progenitors, BMMSCs (Gong and Niklason, 2008a; Hahn et al., 2007), hair follicle derived mesenchymal stem cells (Gao et al., 2014b; Liu et al., 2008), adipose tissue derived stem cells (Parvizi et al., 2016; Zhou et al., 2016a), and embryonic stem cells (Sundaram et al., 2014a). However, TGFβ1 alone sometimes is not potent enough to drive gratifying smooth muscle differentiation (Au et al., 2008). As a result, among these studies, several combined the application of TGFβ1 with bone morphogenetic protein 4 (BMP4) to give rise to SMCs with satisfactory function (Wang et al., 2010a; Wang et al., 2013; Zhou et al., 2016a). Other factors that could be utilised in inducing smooth muscle differentiation include AngII and sphingosylphosphorylcholine (SPC) (Harris et al., 2011).

Furthermore, since the recognition of the significance of mechanical stimuli in vascular tissue engineering, most studies have included the bioreactor system in their vessel manufacturing process. It has also been implicated that the mechanical stimulation could help drive the differentiation of stem cells towards the smooth muscle lineage (Bulick et al., 2009). And when combined with endothelial presence, mechanical stimulus could drive more differentiated SMCs than TGFβ1 as evidenced by the higher increase of smooth muscle markers (Au et al., 2008; Bulick et al., 2009). Differentiated SMCs have been proved to maintain the differentiated state after being seeded to the vascular graft. Addition of TGFβ1 in the culture medium when mechanical stimuli was applied to the vessel could further reinforce the differentiation (Riha et al., 2005). Apart from smooth muscle differentiation, TGFβ1 has also been shown in one study to drive the embryonic stem cells to form embryonic bodies which

was later further driven towards the endothelial lineage and employed in generating vascular grafts (Shen et al., 2003).

Also, TGFβ1 has long been shown to upregulate the production of elastin in the extracellular matrix which could in turn lead to stronger mechanical strength of the graft (Long and Tranquillo, 2003; Neidert et al., 2002). Although another study did not observe significant mechanical feature improvement with TGFβ1 incorporation within the scaffold, it was found that the bio-compatibility of the graft was greatly increased (Yao et al., 2005). Notably, it was shown that miR-29 inhibition performs better in inducing elastin production than TGFβ1 treatment in fibroblasts and vascular SMCs (Rothuizen et al., 2016). This might be due to the potent but various function of TGFβ1 which might result in the activation of too many signalling pathways. In the end, along with the development of numerous scaffold modification methods, TGFβ1 was also found feasible to be conjugated with scaffold materials containing functionalised poly(ester amide)s (Knight et al., 2014). However, further studies should be done to examine its potential to activate downstream signalling pathways (Knight et al., 2014).

1.6. Hypothesis and aim of the study

MSCs are characterised by their certain phenotypic marker profile and multi-lineage differentiation potentials which present them as a promising cell type for tissue engineering. Compared to other stem cells, human umbilical cord derived mesenchymal stem cells (hUCMSCs) have superior proliferation capacity which facilitates their application in tissue engineering.

In our program, we explored the differentiation potential of hUCMSCs into vascular SMC lineages and the application of SMCs derived from hUCMSCs to vascular graft engineering. The main aims of the project are summarised in the figure 1-11.

The protocols of differentiating hUCMSCs into SMCs are firstly established before proceeding to engineer vascular grafts. TGFβ1, which is a recognised growth factor

to drive stem cell to SMC lineage, is applied to stimulate the differentiation of hUCMSCs towards SMCs.

MicroRNA array analysis is subsequently performed on undifferentiated MSCs and differentiated cells to identify microRNA candidates regulating the differentiation process. Bioinformatics prediction and literature review were combined to pinpoint possible microRNA targets after which microRNA loss and gain-of-function experiments are utilised to confirm the role of specific microRNAs as well as their targets in the regulation of the SMC differentiation. Afterwards, the miRNA oriented mechanism was explored including the upstream regulation of miRNA level and the downstream 3'-UTRs of target genes.

Vascular grafts will be subsequently generated with decellularised vessel scaffold followed by histologic evaluation.

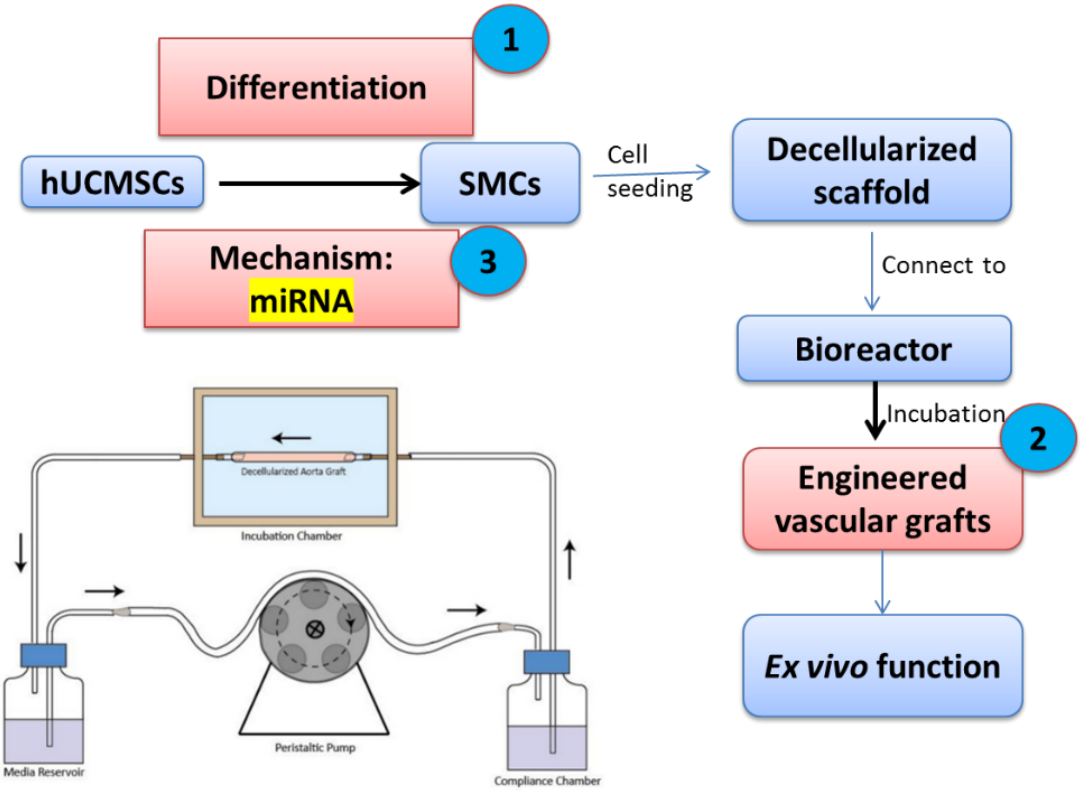

Figure 1-11 Schematic graph of the hypothesis and aims in the project

Firstly, SMC differentiation potential from hUCMSCs would be explored (aim 1). After that, the differentiation mechanism (aim 3) would be checked as to uncover novel miRNAs in MSC-SMC differentiation process as well as their upstream and downstream regulation components. In the end, the hUCMSC-derived SMCs would be applied in the bioreactor system to explore their potential in generating vascular grafts (aim 2). The graph of the bioreactor system is reproduced from (Wong et al., 2015).

2. Materials and Methods

2.1 Materials

hUCMSCs were purchased from ATCC and cultured in manufacturer's recommended medium. TGFβ1 was from Peprotech, and aliquoted into stock solution (10 ng/μl) in 10 mM citric acid with 0.5% BSA. Total RNAs were extracted with the RNesay mini kit and microRNAs were extracted with miRNeasy mini kit from Qiagen. TaqMan microRNA Reverse Transcription kit, human TaqMan microRNA assay primers, and TaqMan universal master mix were purchased from Applied Biosystems. Matrigel for *in vivo* subcutaneous Matrigel assay was from Corning. All the materials including the reagents, chemicals and kits are listed in the table (Table 2-1). Primers and antibodies used in each experiment were listed in the Methods part.

Table 2-1 Materials

Reagents or kits	Company	Cat. No.
U6 snRNA	Life Tech	4427975 001973
TaqMan® MicroRNA Assays; hsa-miR-503-5p	Life Tech	4427975 001048
TaqMan® MicroRNA Assays; hsa-miR-222-5p	Life Tech	4427975 002097
TaqMan® MicroRNA Assays; hsa-miR-503-3p	Life Tech	4440885 476380_mat
TaqMan® MicroRNA Assays; hsa-miR-424-5p	Life Tech	4427975 000604
TaqMan® MicroRNA Assays hsa-miR-145	Life Tech	4427975
miRNeasy Mini Kit (50)	QIAGEN	217004
TaqMan® MicroRNA Reverse Transcription Kit,	Life Tech	4366597
TaqMan® Universal Master Mix II, no UNG	Life Tech	4440040
miRNA Mimic, Negative Control #1	Life Tech	4464058
hsa-miR-503-5p mimic	Life Tech	4464066 MC10378
hsa-miR-222-5p mimic	Life Tech	4464066 MC12656
Negative control A miRCURY LNA™ microRNA inhibitor control,	Exiqon	199006-001
hsa-miR-503-5p miRCURY LNA™ microRNA inhibitor	Exiqon	4100899-001
hsa-miR-222-5p miRCURY LNA™ microRNA inhibitor	Exiqon	4101567-001
RNAiMax	Life Tech	13778-075
opti-MEM	Life Tech	31985062

miRNA Target clone control vector for pEZX-MT06	Genecopoeia	CmiT000001-MT06
miRNA 3´UTR target expression clone for Human A NM_001141945.1	Genecopoeia	HmiT054221-MT06
miRNA 3' UTR target clone for human NM_001190 SMAD family member 7,	Genecopoeia	HmiT055200-MT06
custom 3'UTR target clone for human ROCK2 with 2026bp Sequence (NM_001321643.1, 3'UTR positions: 165 3676), in pEZX-MT06 vector	Genecopoeia	CS-HmiT088447-MT06-0
QuikChange Lightning Site-Directed Mutagenesis K Rxn	Agilent Tech	210518
Detection of Firefly Luciferase Activity	Promega	E1501
Detection of *Renilla* Luciferase Activity	Promega	E2810
SiRNA negative control	Life Tech	AM4611
Human Smad7 siRNA	Life Tech	AM16708 155241
Human ROCK2 siRNA	Life Tech	Cat AM51331 110867
Umbilical Cord-Derived Mesenchymal Stem Cells; H Human	ATCC	ATCC® PCS-500-010™
Mesenchymal Stem Cell Basal Medium for Adipose Umbilical and Bone Marrow-derived MSCs	ATCC	ATCC® PCS-500-030™
Mesenchymal Stem Cell Growth Kit for Adipose and Umbilical-derived MSCs - Low Serum	ATCC	ATCC® PCS-500-040™
Human recombinant TGFβ1	Peprotech	100-21
Cultrex Rat Collagen I, 100 mg	R&D systems	3440-100-01
Smad4 Antibody(H-552) X	Santa Cruz	sc-7154 X
Chromatin Immunoprecipitation (ChIP) Assay Kit	Millipore	17-295

2.2 Methods

2.2.1 Cell culture of umbilical cord-derived stem cells

HUCMSCs were purchased from ATCC (Cat No: PCS-500-010) and cultured on gelatin coated flasks (0.04% diluted from 2% Solution Type B from Bovine Skin, Sigma G1393) in ATCC Mesenchymal Stem Cell Basal Medium (PCS-500-030) supplemented with 1 kit of Mesenchymal Stem Cell Growth Kit–Low serum (PCS-500-040), (see Table 2-2) and 100 U/ml penicillin and streptomycin in a humidified incubator supplemented with 5% CO_2. Cells were passaged every second day at the ratio of 1:2. Cells below passage 15 were used for all experiments.

Table 2-2 Mesenchymal Stem Cell Growth Kit for Adipose and Umbilical-derived MSCs Low Serum Components

Component	Volume	Final Concentration
MSC Supplement	10 mL	2% FBS 5 ng/mL rh FGF basic 5 ng/mL rh FGF acidic 5 ng/mL rh EGF
L-Alanyl-L-Glutamine	6 mL	2.4 mM

hUCMSCs were ensured by the manufacturer to have more than 98% of the cells expressing CD73, CD90, CD105, CD44, CD29, CD166 and less than 2% of the cells expressing CD14, CD31, CD34 and CD45. Furthermore, trilineage differentiation potential into adipocyte, chondrocyte and osteocyte was also guaranteed (Figure 2-1).

A

Characterization	Percentage
CD29	99.98% positive
CD44	98.35% positive
CD73	99.58% positive
CD90	99.86% positive
CD105	99.77% positive
CD166	99.43% positive
CD14	0.34% positive
CD31	0.20% positive
CD34	0.54% positive
CD45	0.05% positive

B

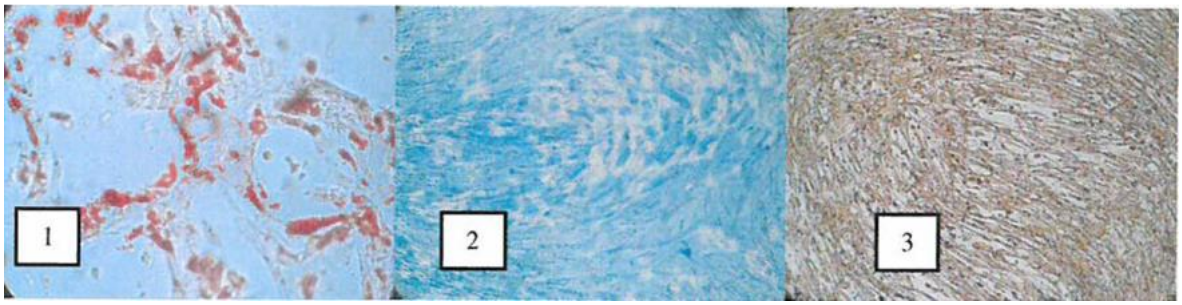

Figure 2-1 Characterisation of hUCMSCs

(A) hUCMSC were characterised by surface marker panel and trilineage differentiation capacity. More than 98% of hUCMSC were positive for CD29, CD44, CD73, CD90, CD105 and CD166, but less than 2% were positive for CD14, CD31, CD34 and CD45. **(B)** Additionally, hUCMSCs were shown to have adipogenic (1), chondrogenic (2) and osteogenic (3) differentiation capacity. The figure is copied from the datasheet.

2.2.2 Smooth muscle differentiation

hUCMSCs were seeded on gelatin coated flasks and maintained in differentiation medium for several time points. For SMC differentiation, the differentiation medium was αMEM (minimum essential medium) with 1% or 10% FBS and 0 or 5 ng/ml TGFβ1 as specified in each experiment. The culture time and seeding density varied as mentioned in the text. To prevent the cells from being too dense, the seeding density is carefully controlled to ensure that the cell density is around 80% upon harvesting. Before establishing the final SMC differentiation protocol, the experiment

conditions are optimised including serum concentration, differentiation time and the effect of TGFβ1.

2.2.3 Flow cytometry analysis

hUCMSCs were detached from the flasks by trypsin, after which cells were counted. Cells were then fixed with 4% paraformaldehyde (PFA) for 15 minutes at room temperature. After washing with PBS, cells were re-suspended in 5% swine serum and blocked with Fc Receptor Blocking Solution (Human TruStain FcX™, BioLegend, Cat No: 422301; TruStain fcX™ (anti-mouse CD16/32) Antibody, BioLegend, Cat No: 101319) for 5 minutes. Aliquots of about $2x10^5$ cells were then incubated with specific antibodies (human CD44 antibody: PerCP anti-mouse/human CD44 antibody, Cat No. BioLegend 103035; IgG control: PerCP IgG2b, κ Isotype Ctrl Antibody, Cat No. BioLegend 400629) at manufacturer suggested concentration for 1 hour at 4 °C. Three additional washes were conducted before the cells were taken to be analysed at the flow cytometer (BD FACS Canto™ II system). Further analysis was done with Flow Jo. Gating was set as less than 1% of marker expression in IgG control group.

2.2.4 RNA extraction

Total RNA from cells was extracted using the RNeasy mini kit (Qiagen Cat. No: 74106). It was performed according to the manufacturer's protocol with a centrifugation speed of more than 10000rpm/8000g. Cells were lysed in 350 µl RLT lysis buffer and then homogenised with QIAshredder spin column to shear high molecular weight genomic DNA and other cellular components. After an equal volume of 70% ethanol was added to the homogenised lysate, a total volume of 700 µl of the sample was added to the RNeasy spin column. The column was centrifuged for 30 sec and the flow-through was discarded. 700 µl of RW1 buffer was then added to the column followed by centrifugation for 15 seconds. Another two washes were carried out by adding 500 µl RPE washing buffer. The flow-through was again discarded. The washing buffer was applied to remove the salts in the lysis buffer which could later interfere with the reactions of reverse transcription of mRNA and polymerase chain

reaction of cDNA. An additional centrifugation without additional buffer was carried out to further remove any remaining solution before 30-50 µl of RNase free water was added to the spin column membrane. After spinning for 1 minute, the flow-through was the sample containing total RNA. The RNA concentration was measured with a Nanodrop Spectrophotometer and RNA quality was controlled with 260/280 ratio and 260/230 ratio to rule out possible contamination of the sample by protein and other reagents such as phenol and guanidine.

2.2.5 Reverse transcription (RT) of RNA

Reverse transcription of RNA was performed with the QuantiTect Reverse Transcription Kit (QIAGEN, Cat No: 205314). 1000 ng of total RNA was used for each reaction of reverse transcription. After adding a corresponding volume of DEPC water to the calculated volume of RNA to reach a total volume of 12 µl of the sample, 2 µl of gDNA wipeout buffer was added to the sample. The final volume of mix A was 14 µl. Mix A was briefly vortexed and centrifuged before being taken to the reverse transcription system (prime thermal cycler) in which the samples were kept at 42 °C for 2 minutes. Meanwhile mix B was prepared with the composition of 1 µl Quantiscrpt Reverse Transcriptase, 4 µl 5x Quantiscrpt RT buffer and 1 µl RT primer included in the kit. (The composition of master mix A and B is listed in Table 2-3) At the end of the 2-minute incubation at 42 °C, mix B was added to the sample and incubation at 42 °C for 15 minutes in the system was followed. Finally, a temperature of 95 °C for 3 minutes was applied to inactivate the Quantiscript Reverse Transcriptase. cDNA obtained was diluted with 80 µl DEPC treated water to reach a final concentration of 10 ng/µl.

Table 2-3 Composition of master mix A and B for RNA reverse transcription

Component		Volume (µl)/reaction	Final concentration
Mix A	RNA	x (1000 ng)	

	DEPC water	12-1000 /x	
	gDNA Wipeout Buffer,7x	2	1x
Mix B Reverse-transcription master mix	Quantiscript Reverse Transcriptase	1	
	Quantiscript RT Buffer, 5x	4	1x
	RT Primer Mix	1	
Total volume		20	

2.2.6 Quantitative polymerase chain reaction (Q-PCR)

Gene expression level in cells was detected by Q-PCR using Eppendorf Mastercycler ep realplex. Each Q-PCR reaction was a 20 µl reaction composed of 10 µl 2x qPCRBIO SyGreen Mix (qPCRBIO SyGreen Mix Hi-ROX, PCRBIOSYSTEMS, Cat No: PB20.12-20), 0.8 µl forward primer, 0.8 µl reverse primer, 2 µl cDNA and 6.4 µl RNase free water. Before putting the 96 well plates (Eppendorf, twin. tec real time PCR plates) in Eppendorf Mastercycler ep realplex, samples were loaded in the plates and the plates underwent a brief centrifugation. The Q-PCR program was 2 minutes at 95 °C followed by 40 cycles of 95 °C for 5 seconds (denaturation) and 60 °C for 30 seconds (annealing and extension) as suggested in the manufacturer's protocol. Every sample had duplicates. Wells loaded with water rather than samples were utilised to serve as a blank control. The primers used for Q-PCR were designed using software provided by DNA integrated Technologies and are listed below. The specificity of each primer was ensured with post-amplification melting curve. The threshold cycle (Ct) value was automatically obtained in excel format and the Ct value of GAPDH was used to serve as internal control. Fold change of gene of interest induced by specific treatment was calculated by the Ct value difference against internal control GAPDH with the following algorithm. (Primer sequences used in Q-PCR are listed in Table 2-4**.**)

ΔCt (Treatment) = Ct (Gene of interest) - Ct (GAPDH)

ΔCt (Control) = Ct (Gene of interest) - Ct (GAPDH)

ΔΔCt = ΔCt (Treatment) - ΔCt (Control)

Fold change = $2^{(-\Delta\Delta Ct)}$

Table 2-4 Primer sequence used in Q-PCR

Gene Symbol	Sequence (5’→3’)	Ct value range
Human GAPDH	F: 5-CAT GTT CGT CAT GGG TGT GAA CCA-3 R: 5-ATG GCA TGG ACT GTG GTC ATG AGT-3	17-19
Human Calponin	F: 5-TTG AGG CCA ACG ACC TGT TTG AGA-3 R: 5-TCG AAT TTC CGC TCC TGC TTC TCT-3	20-25
Human SM22	F: 5-TTG AAG GCA AAG ACA TGG CAG CAG-3 R: 5-TCC ACG GTA GTG CCC ATC ATT CTT-3	18-22
Human α SMA	F: 5-TGA CAA TGG CTC TGG GCT CTG TAA-3 R: 5-TTC GTC ACC CAC GTA GCT GTC TTT-3	20-23
Human Collagen I	F: 5-CTG CAA AGG CAG CCA AAT AC-3 R: 5-ACA CCA AAG CCG GGA AA-3	29-32
Human SRF	F: 5-TGA GTG CCA CTG GCT TTG AAG AGA-3 R: 5-AGA GGT GCT AGG TGC TGT TTG GAT-3	20-23
Human Myocardin	F: 5-TTG AAA GCG GAG AAA TGC CAG CAG-3 R: 5-ACT GTC GGT GGC ATA GGG ATC AAA-3	20-23
Human SMMHC	F: 5-ATC CAT CCT CAC TCC TCG TAT C-3 R: 5-CCA AAG CCT CTA CAG CAA AGT-3	27-31
Human Elastin	F: 5-TGT TCC TGG ACT TGG AGT TG-3 R: 5- GCT CCA TAT TTG GCT GCT TTA G-3	29-32

2.2.7 MicroRNA extraction

Extraction of RNA including microRNA was performed with miRNeasy mini kit (Qiagen, Cat No: 217004) at room temperature unless otherwise specified. Briefly, trypsinised cells were lysed with 700 µl Qiazol lysis buffer provided in the kit, and then homogenised by intensive vortexing for 60 seconds. After the homogenate was kept at room temperature for 5 minutes, 140 µl chloroform (VWR, Cat No: BDH1109-4LG) was added to the sample, followed by intensive vortexing for 30 seconds. Before the samples were centrifuged at 4 °C for 15 minutes at 12000 g, they were left at room temperature for 3 minutes. After centrifugation, the homogenate was separated into three phases: an upper aqueous phase, a white interphase and a lower red organic

phase. The aqueous phase, approximately 350 µl, was then transferred to a new tube, and 1.5 volumes (525 µl) of absolute ethanol were added. Up to 700 µl of the mix was pipetted into the RNeasy mini spin column, followed by centrifugation at 8000 g for 15 seconds. This step was repeated for the rest of the mix with the same column. The flow-through was discarded. 700 µl RWT buffer was then added to the column followed by centrifugation at 8000 g for 15 seconds, after which, two additional washes were performed with 500 µl RPE buffer, with centrifugation time of the second wash to be 2 minutes. Before pipetting 30-50 µl RNase free water directly to the membrane of the RNeasy spin column, another empty centrifugation without any buffer was performed. Finally, a RNeasy spin column with RNase free water was centrifuged and the flow-through was the RNA (including microRNA) containing sample. RNA concentration was measured with Nanodrop Spectrophotometer.

2.2.8 Reverse transcription and pre-amplification of RNA (including microRNA)

After measuring the RNA concentration, samples were diluted to 10 ng/µl with RNase free water. 2 µl of RNA was used as input in each reverse transcription reaction. RNA was transcribed with primers from Applied Biosystems (Human Pool A and human pool B). Reverse transcription reaction was performed according to manufacturer's recommendations. Briefly, a master mix was first prepared as listed in Table 2-5 and then 5.5 µl master mix was mixed with 2 µl of the diluted RNA. Then, the program for reverse transcription was 16 °C for 2 min, 42 °C for 1 min and 50 °C for 1 s for 40 cycles and then incubation at 85 °C for 5 min using a Veriti thermocycler (Applied Biosystems).

1 µl of the reverse transcription product was then mixed with 9 µl of master mix B (Components are listed in Table 2-6) prepared as follows. Then pre-amplification was performed by heating samples to 95 °C for 10 min, followed by 12 cycles of 95 °C for 15 s and 60 °C for 4 min. Finally, samples were heated to 95 °C for 10 min to ensure enzyme inactivation. Pre-amplification products were diluted to a final volume of 40 µl and stored at -20 °C. Pre-amplification was performed to enable detection of

microRNAs at very low levels, enabling the generation of a comprehensive expression profile using as little as 1 ng of input total RNA.

Table 2-5 Reagents and their volume used in reverse transcription of RNA (including microRNA)

Reagent	Volume (µl)
Primer pool A/B	0.8
dNTPs	0.2
10 x RT buffer	0.8
MgCl2	0.9
RT	1.5
RNase inhibitor	0.1
Rnase free water/DEPC treated water	1.2
Final volume	5.5

Table 2-6 Reagents and their volume used in pre-amplification of RNA (including microRNA)

Reagent	Volume (µl)
Preamp mastermix 2x	5
Megaplex preamp primers pool A/B	1
RNase free water	3
Final volume	9

2.2.9 TaqMan Q-PCR assay

TaqMan microRNA assay was used to assess the expression of individual microRNAs. 1 µl of the pre-amplification product was combined with 5 µl TaqMan master mix 2X, 0.5 µl primer (TaqMan assay 20X), and 3.5 µl distilled water and then loaded to a 96 well plate. Q-PCR was performed on an Applied Biosystems 7900 HT thermocycler at 95 °C for 10 min followed by 40 cycles of 95 °C for 15 s and 60 °C for 1 min. All samples were run in duplicates and standardised to U6.

2.2.10 Protein extraction

30-50 µl RIPA buffer (RIPA Lysis and Extraction Buffer, Life Tech, Cat No: 89901) with phosphatase inhibitor tablets and protease inhibitor tablets resolved in

(Phosphatase Inhibitor Tablets, Roche, Cat No: 04906845001, 1 tablet/10 ml RIPA buffer; Protease Inhibitor Tablets, Roche, Cat No: 04693159001, 1 tablet/10 ml RIPA buffer) was added to harvested cell pellets and sonicated with Branson Sonifier 150 at the lowest setting for 12 s. After incubation at 4 °C for 45 minutes, the lysate was centrifuged at highest speed (more than 10000 g) for 10 minutes at 4 °C. The supernatant containing protein was then transferred to a new tube and protein concentration was measured with Biorad Protein Assay. Briefly, 2 µl of the supernatant of the protein lysate was added to 998 µl 1x Bio-Rad Protein Assay Dye Reagent (Bio-Rad Protein Assay Dye Reagent Concentrate, 5x, BIO-RAD, Cat No: 5000006). The sample was well mixed and incubated at room temperature for 5 minutes. Each measurement was measured with duplicates and the concentration was measured with Bio-Rad Spectrophotometer 3000. An equal volume of lysis buffer was measured to serve as a blank control.

2.2.11 Western blot

10-50 µg of the protein was mixed with a ¼ volume of the boiled 5x SDS loading buffer and then adjusted to the same volume with 1x SDS loading buffer. The mix was then boiled at 95 °C for 10 minutes before being loaded to the NuPage 4-12% Bis Tris gel immersed in NuPage MOPS SDS running buffer in a XCell SureLock Mini-Cell (Life Technologies, Cat No: NP0335BOX). Protein ladder (Precision Plus Protein Ladder, Bio-rad, Cat No: 161-0374) was loaded into a separate well together with the samples and the gel was run at 160 V for about 75 minutes until the marker with lowest molecular weight was at the bottom of the gel. Protein was then transferred from the gel to the membrane (Transfer membranes, BioTrace™ NT, VWR, Cat No: 732-3031) in 1X transfer buffer (Thermo Fisher Scientific, NuPAGE® Transfer Buffer (20X), Cat No: NP-0006-1) for 45 minutes. The membrane was then blocked with 5% milk in PBS-Tween and incubated with primary antibody diluted in 5% milk at room temperature for 2 hours or at 4 °C overnight. After being washed with PBS-Tween for three times with 10 minutes each, the membrane was incubated with secondary antibody for 1 hour at room temperature. Secondary antibodies were HRP-conjugated and purchased from Dako (Polyclonal Rabbit anti-goat, Cat No:

P0449; Polyclonal Rabbit anti-mouse, Cat No: P0260; Polyclonal Swine anti-rabbit, Cat No: P0217). Further 3 washes were performed before addition of ECL detection solutions (ECL Western Blotting Detection Reagents, Fisher Scientific, Cat No: RPN2106). After incubation with the detection solution for 2 minutes, exposure of the films (Amersham Hyperfilm ECL, Fisher Scientific, Cat No: 28-9068-37) was carried out with the Compact X4 (Xograph Imaging System) in the dark room. Primary antibodies and their corresponding concentration are listed in Table 2-7.

Table 2-7 Primary antibodies and their dilution used in Western blot

Primary Antibody	Company and Catalogue Number	Dilution (in 5% milk in PBS-Tween)
Human Calponin	Abcam ab46794	1:1000
Human SM22	Abcam ab14106	1:3000
Human α SMA	Sigma A2547-100	1:3000
Human SMMHC	Abcam ab53219	1:500
Human Myocardin	Santa Cruz sc34238	1:2000
Human SRF	Abcam ab33147	1:2000
Human Smad7	R&D systems MAB2029	1:1000
Human ROCK2	Abcam ab71598	1:1000

2.2.12 Immunofluorescence

Cells were trypsinised and resuspended in medium and were then seeded on 8-well chamber slides (Millicell EZ SLIDE 8-well, Merck Millipore, Cat No: PEZGS0816) coated with gelatin. After the cells were cultured on the slides for an intended time in differentiation medium with medium change every second day, the slides were taken out of the 5% CO2 humidified incubator and washed with PBS followed by fixation of the cells with 4% paraformaldehyde (PFA) for 15 minutes at room temperature. Permeabilisation was then performed with 0.1 Triton-X-100 in PBS for 10 minutes at room temperature. An additional wash in PBS was carried out before continuing. For the frozen sections of vessels harvested from *ex vivo* experiments, the samples were fixed with 100% cold acetone for 10 minutes and then washed with PBS for three times. After fixation and permeabilisation, all slides were blocked with 5% swine serum in PBS for 30 minutes at room temperature. The primary antibodies used and

their corresponding concentration were listed in Table 2-8. Incubation was carried out at 37 °C for 1 hour. The slides were then again washed with PBS (3 times, 5 minutes each) followed by incubation with secondary antibody (secondary antibodies were Alexa Fluor conjugates purchased from Life Technologies) at 37 °C for 45 minutes. Slides were washed 3 times with 5 minutes each before staining with DAPI (1:1000) for 5 minutes at room temperature. Another 3 washes with PBS were carried out before mounting the slides with fluorescent mounting media (Dako, Fluorescent Mounting Media, Cat No: S3023). Images were taken with Axio Imager M2 microscope and Volocity software.

Table 2-8 Primary antibodies and their dilution used in immunofluorescence

Primary Antibody	Company and Cat No.	Dilution (in 5% swine serum in PBS-Tween)
Calponin	Abcam ab46794	1:200
SM22	Abcam ab14106	1:200
α SMA	Sigma C6198-2ML	1:200
α SMA	Abcam ab184675	1:400
SMMHC	Abcam ab53219	1:100
CD31	Santa Cruz sc1506	1:50

2.2.13 Transient transfection of miRNA mimics, miRNA inhibitors and siRNAs

MicroRNA mimics, siRNAs, transfection reagent RNAiMax and transfection media opti-MEM were from Life Technologies. MicroRNA inhibitors were purchased from Exiqon. HUCMSCs were seeded at $1x10^4$ /cm^2 one day before transfection on gelatin coated plates to reach 60%-70% density the next day. For one well of 6 well plate, medium was changed to 1 ml empty αMEM without antibiotics or FBS approximately 20 minutes before the transfection. In final experiments, mix A (50 µl opti-MEM/well + 0.5 µl siRNA or miRNA mimic/well) and mix B (50 µl opti-MEM/well + 2 µl RNAiMax/well) was prepared. For miRNA inhibitors, the amount of each component in mix A and B was as follows: mix A, 50 µl opti-MEM/well + 2 µl miRNA inhibitors; mix B, 50 µl opti-MEM/well + 3 µl RNAiMax/well. The final concentration of siRNA and miRNA mimic was 12.5 nM and for miRNA inhibitor, the final concentration was

60 nM. In protocol optimisation experiments, a series of different amounts of reagent were used. After being mixed separately by pipetting up and down, mix A and mix B were then mixed together and let stand for 10 minutes at room temperature. 95 µl of the final mixture was then added to the each well. After 5 hours, 1 ml of αMEM with antibiotics and 2% FBS with or without 10 ng/ml TGFβ1 was added to each well. Cells were harvested after 1-3 days for gene expression detection experiments. For protein level analysis with cells grown and harvested in T-75 flasks, amount of all transfection reagents was scaled up accordingly. SiRNA negative control (Cat No. AM4611, Life Tech) and Smad7 siRNA (Cat No. AM16708 155241, Life Tech) was purchased from Life Technologies. Transfection reagent RNAiMax (Cat No. 13778-075, Life Tech) and transfection media opti-MEM (Cat No. 31985062, Life Tech) were also from Life Technologies.

2.2.14 Luciferase reporter assays

MiRNA target specificity was examined by luciferase reporter assays. Plasmids utilised in miRNA target validation experiment were purchased from Genecopoeia. A plasmid containing the 3'-UTR of target genes was cloned downstream of humanised Firefly luciferase and Synthetic *Renilla* luciferase gene was included in the plasmid for indication of plasmid transfection efficiency. A backbone of the plasmid was shown in the figure (Figure 2-2).

$1.5x10^4$ HEK293 cells were seeded in each well of 24 well plates and transfected next day upon the density of 60% to 70%. Medium was first changed to 200 µL αMEM medium without either antibiotics or FBS. Mix A and mix B was prepared separately according to the table (Table 2-9) and then mixed, and let stand for 10 minutes before being added to the well. The final concentration of miRNA was 37.5 nM. 200 µl αMEM medium with double the concentration of antibiotics and 20% FBS was added to each well after a 5-hour incubation. Firefly and *Renilla* luciferase activity was detected with luciferase assay kit (Promega) 24 hours after the transfection.

Table 2-9 Mixture components for dual transfection of miRNA and plasmid

Mix A	Mix B
50 µl opti-MEM	50 µl opti-MEM
0.375 µl miRNA negative control or mimic	0.5 µl Lipofectamine 3000
50 ng plasmid	
0.5 µl p3000	

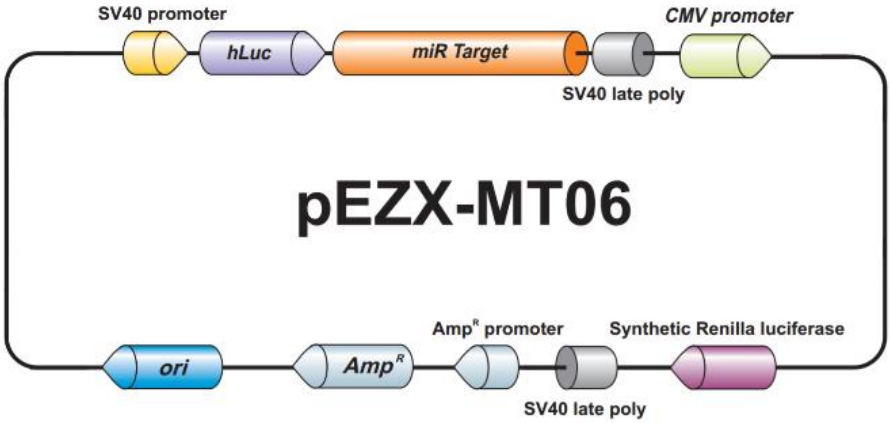

Figure 2-2 Schematic graph of miRNA target reporter plasmids

The graph is reproduced from the datasheet of the plasmid. 3'-UTR of a specific gene was cloned into the plasmid downstream of humanised firefly luciferase gene. Moreover, synthetic *Renilla* luciferase was utilised as an indication of the plasmid concentration transfected into the cells. For control plasmid, there is no gene segment cloned to the miR Target site.

2.2.15 Site mutation of plasmids

Mutation of the target site in plasmids was performed with QuikChange Lightning Site-Directed Mutagenesis Kit from Agilent Tech following the manual. Briefly, primers for mutation of the target site was first designed with the website www.agilent.com/genomics/qcpd based on the intended mutation. Primers used for each 3'-UTR mutation were listed as follows (Table 2-10). Secondly, mutation and amplification of the DNA template of plasmids bearing 3'-UTR of the target gene were

mutated with the following reaction. The reaction mix contains 5 µl 10x reaction buffer, 50ng dsDNA template, 125 ng mutation primer 1, 125 ng mutation primer 2, 1 µl dNTP mix, and 1.5 µl QuickSolution reagent. Water was added at the end to reach the total volume of 50 µl. After the following mix was prepared, 1 µl of QuickChange Lightning Enzyme was added. Program of the reaction has 3 stages, with the first to be one cycle of 2 mins at 95 ˚C, the second to be 18 cycles of 20 seconds at 95 ˚C, 10 seconds at 60 ˚C and varied time at 68 ˚C and the third stage to be one cycle of 5 mins at 68 ˚C. The varied time at the second stage is decided by the length of plasmid, with the time to be 30 seconds for every kilobase of the plasmid. Upon completion of the reaction, 2 µl of Dpn I restriction enzyme was added to the final solution and mixed thoroughly by pipetting up and down. After incubation for 5 minutes, the parental or nonmutated dsDNA template was digested. Transformation of mutated dsDNA and amplification of single colony was then carried out. Amplified plasmids were extracted with Qiagen mini prep kit (Qiagen, cat: 27104).

Table 2-10 Mutation primer of the plasmids containing 3'-UTR segments of specific gene

3'-UTR	Mutation primer
hSmad7 m1	1: 5'-AGCACTCAGGAGGAAAATATTACGTGCAAAGTAGTTTGAAGTGTGGC-3' 2: 5'-GCCACACTTCAAACTACTTTGCACGTAATATTTTCCTCCTGAGTGCT-3'
hSmad7 m2	1: 5'-GCAAGCACTCAGGAGGAAAATATGATCTCCAAAGTAGTTTGAAGTGTGGCCT-3' 2: 5'-AGGCCACACTTCAAACTACTTTGGAGATCATATTTTCCTCCTGAGTGCTTGC-3'
hROCK2 m1	1: 5'-CAAAACCAGTTTCAGTCTATCTGCACGCCAGTAGCTACTCTTCAGTT-3' 2: 5'-AACTGAAGAGTAGCTACTGGCGTGCAGATAGACTGAAACTGGTTTTG-3'
hROCK2 m2	1: 5'-GGGAAGGAGAGGTGAGTCTGCACCAGTGTCAATGCAGACTC-3' 2: 5'-GAGTCTGCATTGACACTGGTGCAGACTCACCTCTCCTTCCC-3'
h α SMA m	1: 5'-CTGCTCGAACTAGTCTCGAGACCACTCCCCTATTTCAGATTTATTAAAAAAC-3' 2: 5'-GTTTTTTAATAAATCTGAAATAGGGGAGTGGTCTCGAGACTAGTTCGAGCAG-3'

2.2.16 Chromatin immunoprecipitation

Chromatin Immunoprecipitation experiments were performed with a kit from Millipore (Cat No. 17-295, Millipore) and immunoprecipitation was performed following the kit manual. Briefly, $1x10^6$ hUCMSCs that were treated with or without 5 ng/mL TGFβ1 for 4 hours were crosslinked with 1% formaldehyde for 10 minutes by adding 270 µL 37% formaldehyde into 10 mL of growth medium in the flask. Cells washed and harvested were lysed with SDS lysis buffer (1% SDS, 10 mM EDTA, 50 mM Tris, pH 8.1 1X protease inhibitors). DNA was sheared by sonication (15 cycles of 15 seconds sonication and 15 seconds pause). Sonicated lysate was centrifuged and 180 µl supernatant was diluted 10 times with ChIP Dilution Buffer. 20 µl of the sonication lysate supernatant was saved to serve as input. Diluted cell supernatant was blocked with 75 µl of Protein A Agarose/Salmon Sperm DNA (50% Slurry) for 30 minutes at 4˚C. 10 µl of immunoprecipitating antibody (anti-Smad4 antibody: sc-7154 X, Santa Cruz; IgG control: Cat No. ab37415, Abcam) was then added to the supernatant after pelleting and was incubated overnight at 4˚C with rotation. 60 µl Protein A Agarose/Salmon Sperm DNA (50% Slurry) was added next day for 1 hour at 4 ˚C to collect the antibody/histone complex. Agarose was pelleted by gentle centrifugation at 1000 rpm at 4 ˚C for 1 min. Pelleted protein A agarose/antibody/histone complex was then washed with Low Salt Immune Complex Wash Buffer, High Salt Immune Complex Wash Buffer, LiCl Immune Complex Wash Buffer, and TE buffer. Histone complex was then eluted from the antibody by adding 250 µl freshly prepared elution buffer (1% SDS, 0.1 M $NaHCO_3$) to the pelleted complex. Elution was repeated once and eluates were combined. Histone-DNA crosslinks were reversed with 20 µl 5 M NaCl by heating at 65 ˚C for 4 hours. Crosslinks of input material was also reversed. 10 µl of 0.5 M EDTA, 20 µl 1 M Tris-HCl and 2 µl of 10 mg/ml Proteinase K was then added to the combined eluates and incubated for 1 hour at 4 ˚C.

DNA was then recovered by phenol/chloroform extraction and ethanol precipitation. An equal volume of phenol was added to the tube and then vigorous vortex was performed. Different phases were then separated by centrifugation at top speed.

The aqueous phase was transferred to another tube and remnant phenol was removed by adding an equal volume of chloroform:isoamyl alcohol. 1/10 volume 3 M sodium acetate, 1/2 volume 5 M ammonium acetate and 2 volumes of 100% ethanol were added in the order they were mentioned and the sample was then frozen in -80 ˚C for 1 hour. The centrifugation at full speed was performed for 30 minutes and the supernatant was discarded. The pellet was washed with 70% ethanol and air dried at room temperature. Afterwards, 50 µl of buffer TE was added.

Q-PCR was performed to examine the enrichment of Smad4 at the promoter region of miR-503. Fold change of enrichment was calculated against input material and IgG control. The promoter of GAPDH was used to serve as negative control. Primers used were listed in the following table (Table 2-11).

Table 2-11 Primers for GAPDH and miR-503 promoter

Gene promoter	primer
GAPDH	F: 5'-GGC CTC CAA GGA GTA AGA CC-3' R: 5'-AGG GGT CTA CAT GGC AAC TG-3'
miR-503 primer 1	F: 5'-GAG AGA AGG TAC ATC GTG TGT T-3' R: 5'-CAC TTC AGG AGA GGG TCA TTC-3'
miR-503 primer 2	F: 5'-AAA CAG GAA GGA GCG ACT TG-3' R: 5'-TCT TAC ACT ATC GTT GCG ACA TAT AC-3'
miR-503 primer 3	F: 5'-GAG TGA AGT GGC CTA GTC ATA AG-3' R: 5'-CCT GGT GGC AGG AAC AC-3'

2.2.17 Collagen gel contraction assay

hUCMSCs cultured in medium (αMEM with 1% FBS) with or without 5 ng/ml TGFβ1) were detached and then mixed with collagen gel. After detachment, cells were resuspended in medium (5x αMEM with 5% FBS) at the concentration of $2x10^5$/ml. 100 µl of the cell suspension was later mixed with 200 µl empty αMEM medium and 200 µl collagen gel reagent (R&D systems, 3440-100-01). The mixture was later neutralised with 5 µl of 1M NaOH. The final concentration of the collagen gel was 2 mg/ml. 500 µl final mixture was placed in one well of 24 well plates for 24 hours before the gel was formed and then detached with the pipette tips. The contraction of the collagen gel was observed every 2 hours and pictures were taken 5 hours after the

gel detachment. Triplicates were included for both undifferentiated cells and differentiated ones. The surface area of the gel was measured with Image J. Mean value was obtained between triplicates and then subjected to calculation of surface area ratio between cells treated without and with TGFβ1.

2.2.18 Subcutaneous Matrigel plug assay

hUCMSCs were differentiated with αMEM with 1%FBS and 5 ng/ml TGFβ1 for 5 days. After that, 0.5 million differentiated cells were harvested and mixed with 0.5 million HUVECs in 100 µl Matrigel and injected subcutaneously into nude mice. The same number of undifferentiated cells mixed with the same number of HUVECs was used as a control. The Matrigel plug was harvested 2 weeks after the injection and subjected to cryostat sectioning. H&E staining as well as immunofluorescent staining of the slide for SMC marker and EC marker was subsequently carried out to examine the vasculogenesis capacity of the cell mixture. Four Matrigel plugs were obtained in each experiment group. Animal-related experiments were all approved by the Institutional Committee for Use and Care of Laboratory Animal according to standard protocols.

2.2.19 Cell seeding and vascular graft engineering with the bioreactor system

Cells seeding and bioreactor establishment was conducted following standard protocol with minor modifications (Wong et al., 2015). Differentiated hUCMSCs were seeded on aortic scaffold which was previously decellularised (with 0.075% SDS and washed with PBS), in a specially constructed bioreactor with shear stress applied. Briefly, a roller pump (Masterflex: Standar Drive, mode 7520, Standard pump head, mode 7018-20, Tubing, Core-Parmer UK) was utilised to apply shear stress on the decellularised scaffold. The graft was fixed between two 25 G needles after connecting them on plastic tubes fixed by 8-0 silk sutures (8-0 black virgin silk, Ethicon Inc., Johnson and Johnson, Norderstedt, Germany). The complete set up was put in a 5% CO_2 incubator at 37 °C and the scaffold was connected to a self-

constructed chamber. The scaffold was preconditioned in culture media for 2 hours and then 1.5 million of differentiated hUCMSCs (differentiated with αMEM with 1% FBS and 5 ng/ml TGFβ1) were resuspended in 100 µl Matrigel which was liquified at 4 °C overnight beforehand. Resuspended cells were seeded onto the outer side of the scaffold and the chamber was maintained at room temperature until the Matrigel was solidified. Media in the chamber consists of αMEM with 10% FBS and 5 ng/ml TGFβ1. Circulating medium consists of 30 ml αMEM with 10% FBS. After establishing the bioreactor system, shear stress was applied to the bioreactor by applying 3 ml/min fluid speed to the system which would be increased gradually to 5 ml/min over a 24-hour period. The system was kept in the incubator for at least 5 days for the cells to migrate into the vessel wall. After 5 days, the graft was harvested, and cryostat sectioned to get frozen sections which were later subjected to H&E staining and immunofluorescent staining of SMC markers.

2.2.20 Statistical analysis

The data analysis was carried out with GraphPad Prism 6 software (GraphPad Software Inc.). All data were tested for normal distribution first with D'Agostino & Pearson omnibus normality test. Data between two groups with normal distribution were analysed with unpaired and ungrouped t-test, and data that were not normally distributed between two groups were analysed with unpaired and nonparametric Mann-Whitney test. Data across multiple groups were analysed with one-way ANOVA test, followed by Bonferroni post-hoc analysis if the P value was less than 0.05. Data were shown as the Mean ± SEM (standard error of mean) and graphs were generated using GraphPad Prism 6 software. P value <0.05 was considered statistically significant. (*P < 0.05; **P < 0.01 and ***P < 0.001.)

3. Results

3.1 Characterisation of human umbilical cord-derived mesenchymal stem cells (hUCMSCs)

3.1.1 Surface marker expression of hUCMSCs

hUCMSCs were characterised by their marker profile, as suggested by the minimal criteria proposed by the ISCT (Dominici et al., 2006). The cells are characterised by the manufacturer and more than 98% of the cells are positive for CD29, CD44, CD73, CD90, CD105 and CD166, while at the same time less than 2% of the cells are positive for CD14, CD31, CD34 and CD45. Their trilineage differentiation potential into adipocytes, osteocytes and chondrocytes was also ensured. Furthermore, FACS analysis showed that more than 98% of the cells still express CD44 at passage 10 (Figure 3-1).

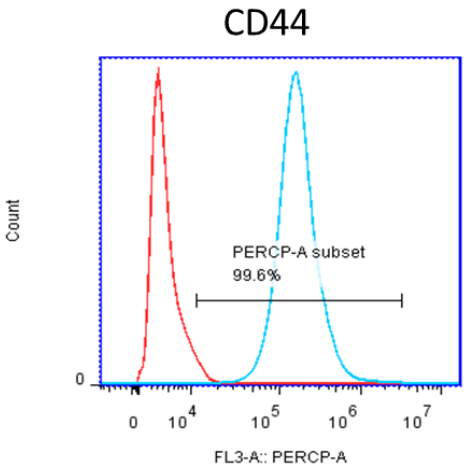

Figure 3-1 More than 98% of the cells still express CD44 after 10 passages

Human UCMSCs were cultured in mesenchymal stem cell basal medium supplied by the manufacturer. Cells were passaged at 1:2 ratios at 60%-80% confluence. CD44 expression was examined at passage 10.

3.1.2 Analysis of SMC markers in hUCMSCs

hUCMSCs were maintained in a basal medium as suggested and supplied by the manufacturer. The basal expression of contractile SMC markers was examined by Western blot. Compared to human umbilical artery-derived SMCs, hUCMSCs (P10) did not express Calponin, αSMA or SMMHC, but expressed a certain level of SM22 (Figure 3-2). This is consistent with the published study (Rodriguez et al., 2006) showing that some early markers for smooth muscle differentiation were found to be spontaneously transcribed in undifferentiated mesenchymal stem cells.

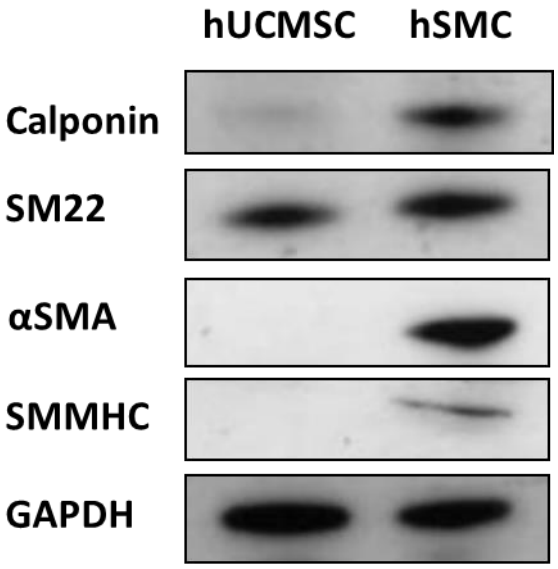

Figure 3-2 Basal expression of SMC specific markers in hUCMSCs

Compared to human umbilical artery-derived SMCs (hSMCs), hUCMSC expressed a low fraction of SM22, but did not express Calponin, αSMA or SMMHC at the protein level. Representative picture of 3 individual experiments was shown.

3.2 TGFβ1 induces differentiation of hUCMSCs towards SMC lineage

3.2.1 Establishment and optimisation of the differentiation protocol

3.2.1.1 hUCMSCs were induced to differentiate into SMCs with TGFβ1

TGFβ1 is a multifunctional regulator of vascular development and is widely utilised for promoting SMC differentiation (Hu et al., 2003; Qiu et al., 2003; Qiu et al., 2005). Firstly, in order to identify the optimal conditions to induce SMC differentiation from hUCMSCs, cells were cultured in differentiation medium (αMEM with 1% FBS) with or without TGFβ1. Quantitative gene expression analysis showed an upregulation of Calponin, SM22, αSMA and SMMHC when cells were cultured in αMEM with 1% FBS (Figure 3-3 A, B). This upregulation of SMC markers was further significantly enhanced by adding 5 ng/ml TGFβ1 in the differentiation medium (Figure 3-3 A, B). It is worth noting that the expression of specific SMC marker SMMHC was induced from less than 10 folds to more than 20 folds by the addition of 5 ng/ml TGFβ1 (Figure 3-3 B). Furthermore, genes related to extracellular matrix synthesis (collagen I and elastin) were also induced by TGFβ1 at the gene expression level (Figure 3-3 C).

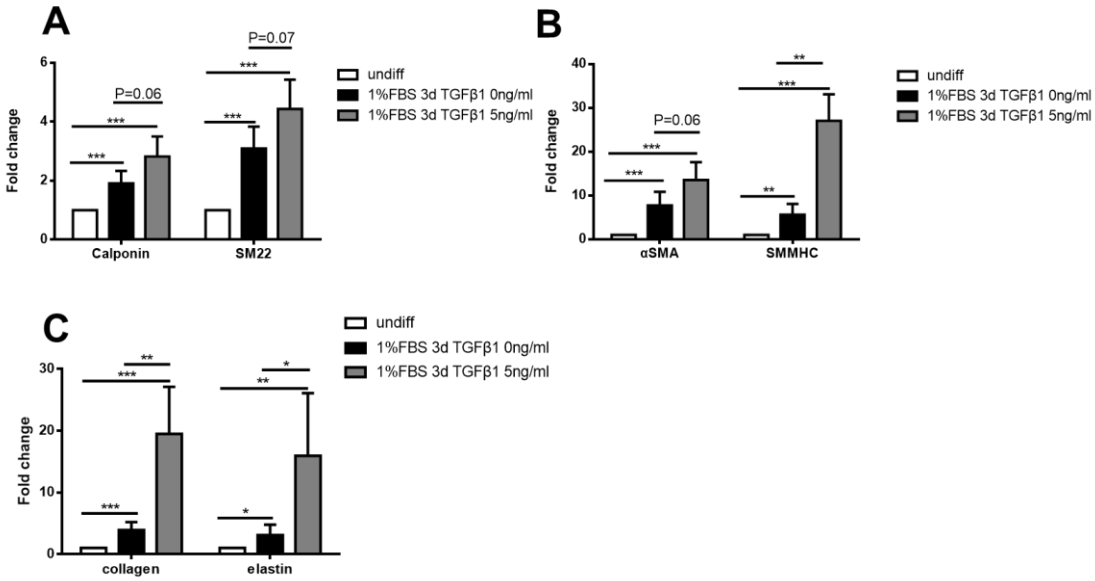

Figure 3-3 Induction of hUCMSCs differentiation into SMCs by TGFβ1

hUCMSCs displayed an increase in the expression of SMC specific markers including Calponin, SM22, αSMA and SMMHC at the mRNA level in differentiation medium for 3 days. Differentiation medium is composed of αMEM with 1% FBS. The seeding density is $3x10^5$ cells/ T25 flask. Negative control consists of cells at the same passage before cells were plated in differentiation medium. **(A, B)** 5 ng/ml TGFβ1 could enhance the expression of SMC markers. Moreover, TGFβ1 significantly enhanced the expression of SMMHC. **(C)** Human UCMSCs displayed an increase in the expression of extracellular proteins collagen I and elastin at the mRNA level in differentiation medium for 3 days. Differentiation medium is composed of αMEM with 1% FBS. 5 ng/ml TGFβ1 could also enhance this significantly. Data are shown as mean ± SEM. Statistics are obtained with one-way ANOVA test, followed by Bonferroni post-hoc analysis. *P < 0.05; **P < 0.01 and ***P < 0.001.

3.2.1.2 Low concentration of serum promotes SMC differentiation

The optimal serum concentration was subsequently tested. To elucidate the effect of serum concentration, we compared cells cultured in 1% FBS and 10% FBS with or without TGFβ1. Results showed an increase of SMC contractile markers in cells cultured in both 1% FBS or 10% FBS for 3 days. However, the increase induced by 1% FBS is significantly higher than that induced by 10% FBS (Figure 3-4 A, B). The same trend was observed when cells were cultured in medium with 5 ng/ml TGFβ1 with 1% or 10% FBS. These results led us to conclude that low serum concentration yielded better efficiency in the induction of SMC differentiation.

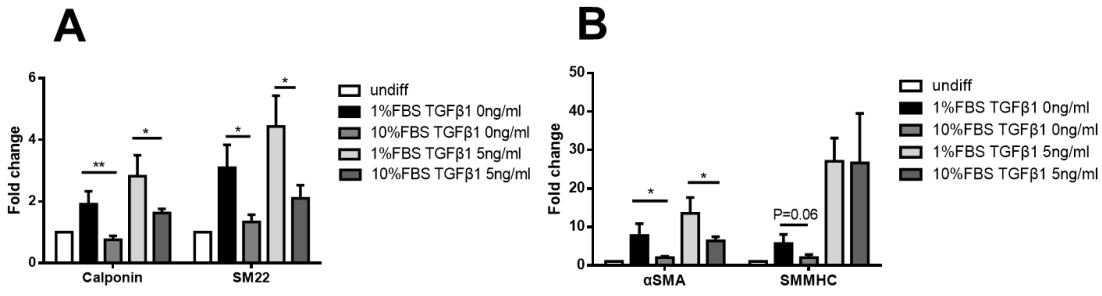

Figure 3-4 Effect of serum concentration in SMC differentiation

Compared to medium with 10% FBS, medium with 1% FBS has the better efficiency to induce the increase of SMC contractile genes, with or without 5 ng/ml TGFβ1. **(A and B)** At the 3-day time point, cells in αMEM medium with 1% FBS displayed a higher increase of Calponin, SM22, αSMA and SMMHC. The same was observed in medium with 5 ng/ml TGFβ1. Data are shown as mean ± SEM. Statistics are obtained with one-way ANOVA test, followed by Bonferroni post-hoc analysis. *P < 0.05 and **P < 0.01.

3.2.1.3 TGFβ1 stimulates SMC differentiation in a time-dependent manner

We have established that differentiation medium containing 1% FBS and 5 ng/ml TGFβ1 showed optimal ability to induce hUCMSCs differentiation towards SMCs. Therefore, this medium was applied in following experiments. The time course of differentiation from 6 hours to 5 days was studied. The quantitative gene expression was analysed at all the time points. Results demonstrated that all SMC markers started to increase at a low level from 6 hours of differentiation and continued to increase until 5 days. The increase was time-dependent (Figure 3-5).

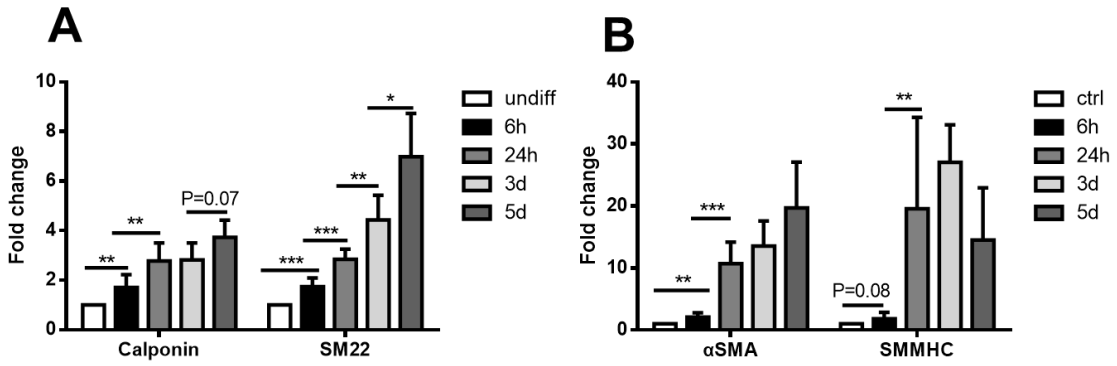

Figure 3-5 Time course study of SMC marker expression in hUCMSCs treated with TGFβ1

(A and B) Human UCMSCs were induced to differentiate into SMCs in a time-dependent manner at the mRNA level. Differentiation medium consists of αMEM with 1% FBS and 5ng/ml TGFβ1. Each time point was compared to the time point next to each other. Data are shown as mean ± SEM. Statistics are obtained with one-way ANOVA test, followed by Bonferroni post-hoc analysis. *P < 0.05; **P < 0.01 and ***P < 0.001.

3.2.2 Morphology of hUCMSC-derived SMCs

We observed a different morphology of hUCMSC-derived SMCs (differentiated in αMEM with 1% FBS and 5 ng/ml TGFβ1 for 3 days), as compared to the undifferentiated MSCs. While undifferentiated MSCs displayed a stellate, fibroblastic morphology, differentiated cells displayed more of a spindle shape morphology typically observed in SMCs (Figure 3-6).

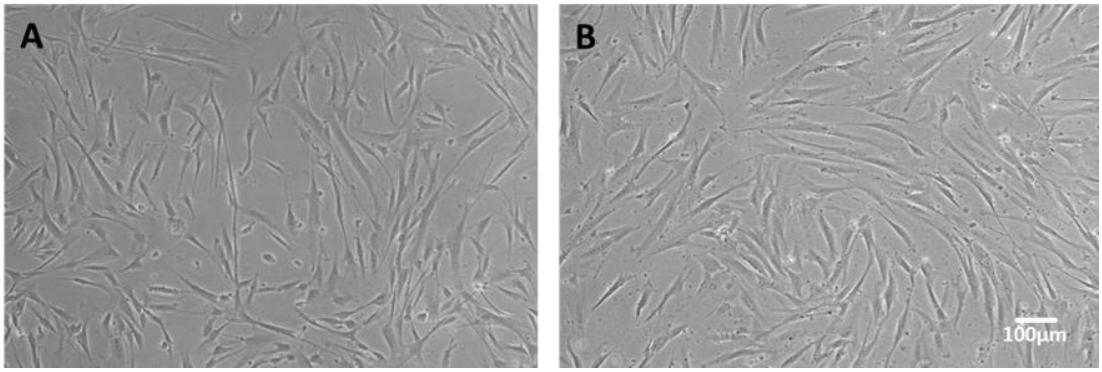

Figure 3-6 Morphology of hUCMSCs-derived SMCs and undifferentiated hUCMSCs

hUCMSCs displayed a spindle shaped morphology after 3 days in differentiation medium (αMEM with 1% FBS and 5 ng/ml TGFβ1). Light microscope images displayed that MSC-derived SMCs exhibited a SMC like morphology **(B)** compared to control cells **(A)**. Images

were taken with Nikon Eclipse TS100 at 10X magnification. Images were representative of 3 independent experiments.

3.2.3 Expression of SMC specific markers in hUCMSC-derived SMCs at the protein level

To confirm the expression of SMC markers at the protein level, Western blot analysis was performed on hUCMSC-derived SMCs at different time points. Differentiation medium consists of αMEM with 1% FBS and 5 ng/ml TGFβ1. SMC contractile markers significantly increased during the differentiation at the protein level (Figure 3-7).

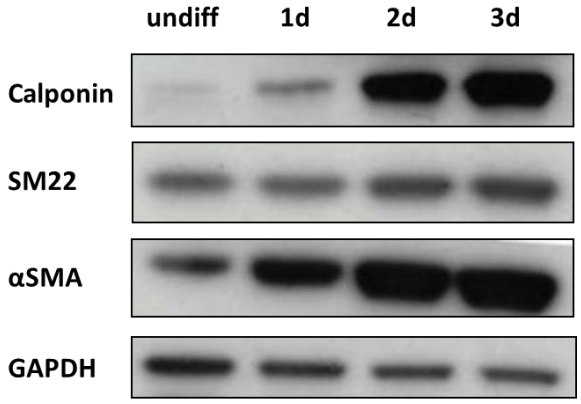

Figure 3-7 Typical SMC marker changes of hUCMSCs-derived SMCs at the protein level

hUCMSC differentiation medium consists of αMEM with 1% FBS and 5 ng/ml TGFβ1 and cells were differentiated for 1 day, 2 days and 3 days before being harvested. Seeding density for different time points are $1.8x10^6$ /T75 flask, $1.5x10^6$ /T75 flask, and $1.2x10^6$ /T75 flask for 1 day, 2 days and 3 days respectively. The result is representative of at least three experiments.

Furthermore, expression of SMC markers at day 1 and 3 was examined by immunofluorescent staining. Cells were cultured in αMEM with 1% FBS and 5 ng/ml TGFβ1 for 1 day and 3 days followed by staining of Calponin, SM22, and αSMA. Cells cultured in mesenchymal stem cell basal medium for 3 days were used as undifferentiated control. In accordance with previous results, it was demonstrated that increased time of differentiation led to a stronger expression of SMC markers (Figure 3-8).

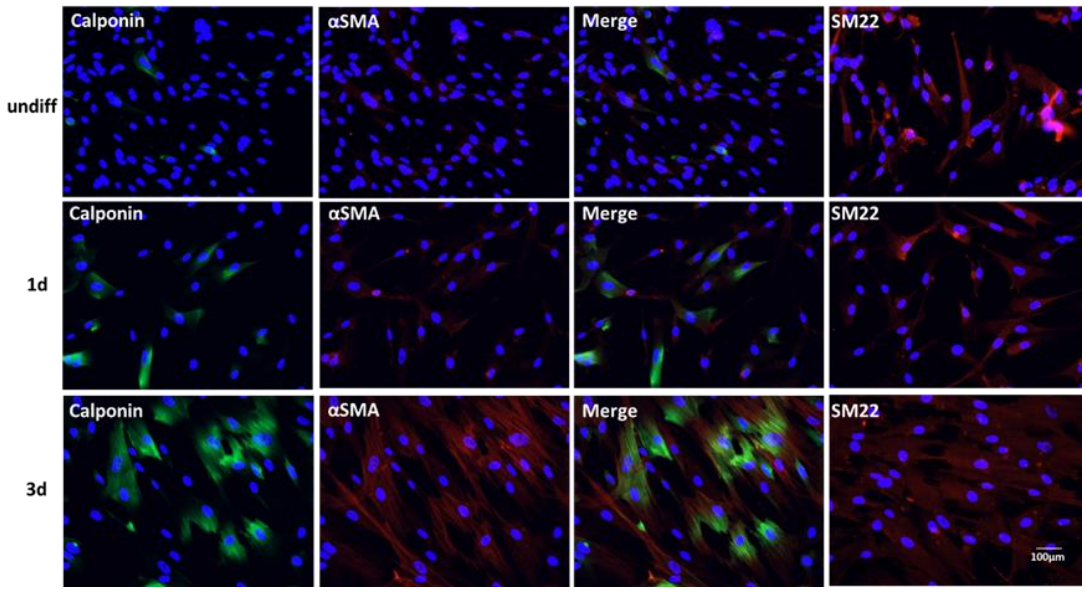

Figure 3-8 Immunofluorescent staining of hUCMSCs-derived SMCs for SMC markers

Cells were cultured in αMEM with 1% FBS and 5 ng/ml TGFβ1 for 1 day and 3 days before being fixed and stained. Control undifferentiated cells were cultured in the mesenchymal stem cell basal medium until they reached 80% confluence. The seeding density was $2x10^4$ cells/well and $1.2x10^4$ cells/well in 8 well chamber slides for 1 day and 3 days respectively. It was shown that SMC markers (αSMA, Calponin and SM22) significantly increased at day 3 compared to control undifferentiated cells cultured in the basal medium. Representative picture of at least 3 experiments is shown.

3.3 Functional characterisation of differentiated SMCs derived from hUCMSCs

To functionally characterise the SMCs differentiated from hUCMSCs, the cells were subjected to collagen gel contraction assay and subcutaneous Matrigel assay. SMCs differentiated from hUCMSCs displayed better contracting capacity as displayed by the collagen gel contraction assay compared to cells cultured without TGFβ1 (Figure 3-9). Furthermore, the differentiated cells and control undifferentiated cells were separately mixed with human umbilical vein endothelial cells (HUVECs) into Matrigel and injected subcutaneously into the mouse. H&E staining showed finer tubular structures in Matrigel plug with differentiated cells and HUVECs, which was not observed in Matrigel plugs containing undifferentiated hUCMSCs and HUVECs (Figure 3-10 A). Immunofluorescent staining of Matrigel plug frozen sections with SMC marker αSMA and endothelial marker CD31 demonstrated close proximity of both markers which indicated the formation of vessel-like structures (Figure 3-10 B).

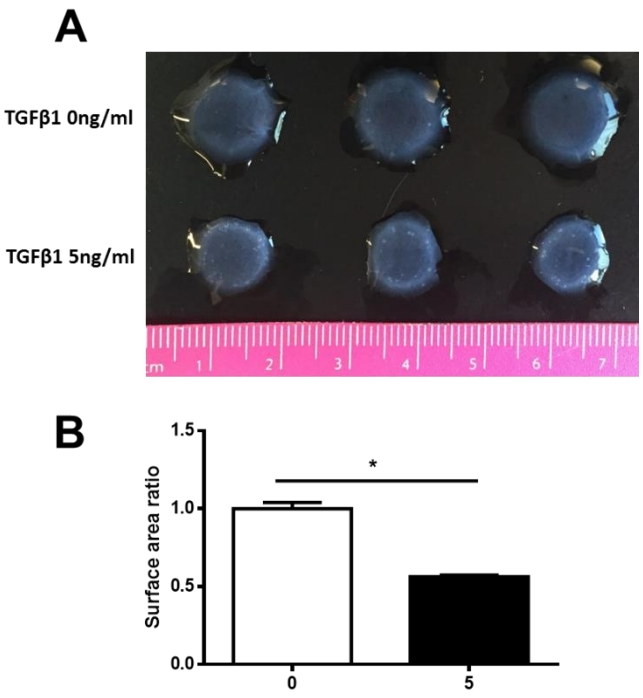

Figure 3-9 Collagen gel contraction assay showed better contractility of SMCs differentiated from hUCMSCs compared to cells cultured without TGFβ1

hUCMSCs cultured in medium (αMEM with 1% FBS with or without 5 ng/ml TGFβ1) were both detached and then mixed with collagen gel. The final concentration of the cells was $2x10^5$ /500 µl, and the final concentration of the collagen gel was 2 mg/ml. Neutralisation of the mixture was with the addition of 5 µl of 1 M NaOH. 500 µl of the neutralised mixture was added to one well of 24 well plates in triplicates for 24 hours before the gelled cell-collagen mixture was detached by pipette tips. **(A)** Pictures were taken 5 hours after the detachment. **(B)** The ratio of the surface area was calculated with the mean value of the surface area analysed with ImageJ between triplicates. Data are obtained from at least three independent experiments and shown as mean ± SEM. Statistics are obtained with student t-test. *P < 0.05.

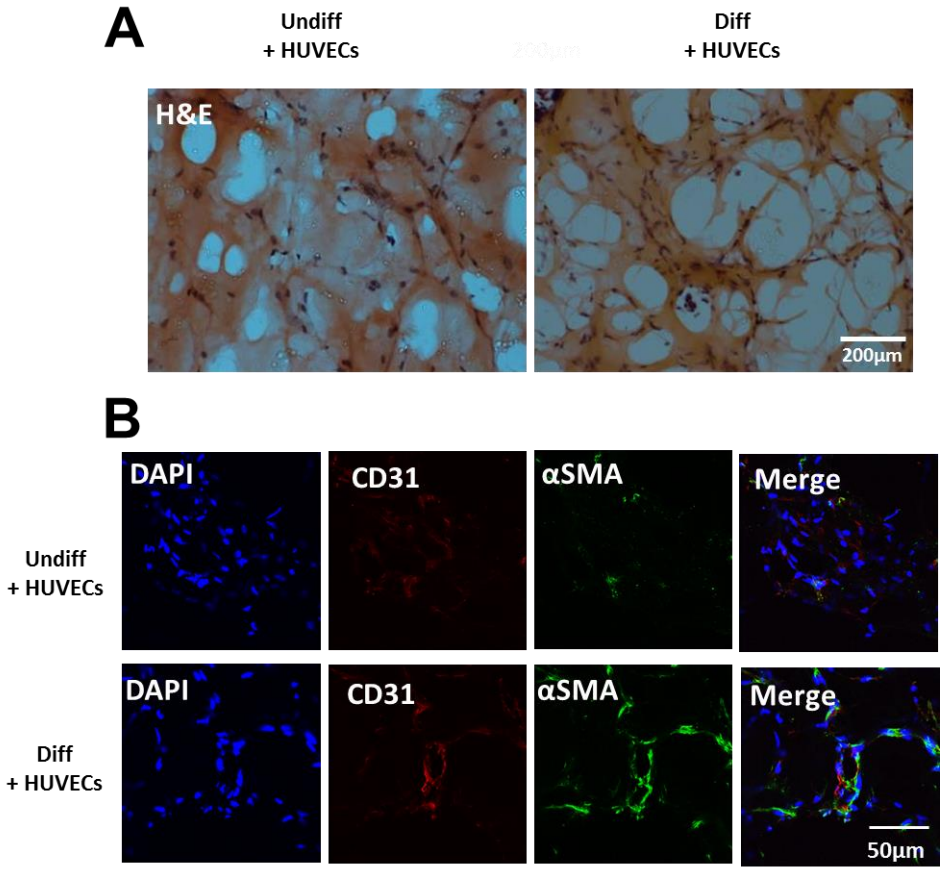

Figure 3-10 Subcutaneous Matrigel plug assay demonstrated the potential of hUCMSCs-derived SMCs to form vessel-like structures

hUCMSCs were differentiated with αMEM with 1% FBS and 5 ng/ml TGFβ1 for 5 days. After that 0.5 million differentiated cells were harvested and mixed with 0.5 million HUVECs in 100 µl Matrigel and injected subcutaneously into nude mice. The same number of undifferentiated cells mixed with the same number of HUVECs was used as a control. The Matrigel plugs were harvested 2 weeks after the injection and subjected to cryostat sectioning. H&E staining and immunofluorescent staining of the slide were subsequently carried out. **(A)** H&E staining showed tubular structure formation with finer walls in the group containing hUCMSC-derived SMCs and HUVECs compared to control. **(B)** Immunofluorescent staining demonstrated the proximity of EC marker CD31 and SMC marker αSMA as well as an upregulation of SMC marker αSMA in the group with hUCMSC-derived SMCs and HUVECs compared to control. Four Matrigel plugs were obtained in each experiment group. Undiff + HUVECs means the mixture of undifferentiated hUCMSCs with HUVECs and diff + HUVECs means the mixture of differentiated hUCMSCs with HUVECs.

3.4 Mechanism involved in hUCMSC towards SMC differentiation: confirmation of established mechanism

As discussed earlier, Myocardin and SRF are potent regulators of SMC differentiation. Therefore, we evaluated their expression along the process of MSC to SMC differentiation. The result demonstrated that Myocardin and SRF expression had a transient upregulation at 6 hours and lasted for 24 hours (Figure 3-11). Therefore we hypothesised that this increase contributed to the induction of SMC specific markers (Calponin, SM22, αSMA, and SMMHC) which also started to express at the time as early as 6 hours and lasted for 5 days. There is evidence that the increase of Myocardin and SRF levels could promote their interaction, and then drive the gene expression at the CArG element of the controlled genes, including almost all SMC markers. Therefore, the increase of Myocardin and SRF levels at the early time point

of the differentiation process might play an important role in initiating and further enhancing the SMC contractile gene expression.

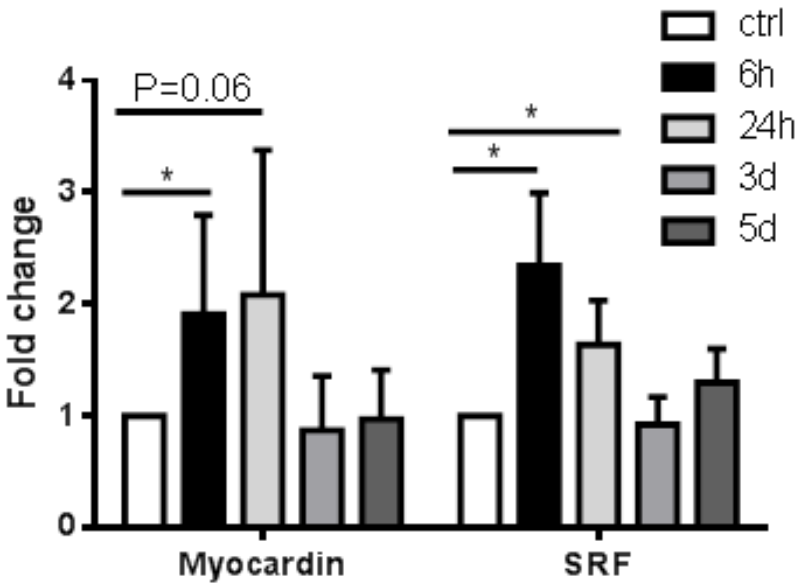

Figure 3-11 Time course study of Myocardin and SRF expression

Myocardin and SRF, two important regulators for SMC differentiation, were induced at early time point (6 hours and 24 hours). The increase peaked at 6 hours and then decreased. Data are obtained from at least three experiments and shown as mean ± SEM. Statistics are obtained with one-way ANOVA test, followed by Bonferroni post-hoc analysis. *P < 0.05.

MicroRNAs are of vital importance in regulating SMC differentiation process by regulating the expression of proteins that play important roles in SMC differentiation. Among these microRNAs, miR-145 is well established to induce the expression of SMC contractile proteins by repressing the expression of Klf4 and Elk1. As both Klf4 and Elk1 are SMC differentiation repressors, working by recruiting HDAC2 and HDAC5 to the Myocardin-SRF-CArG complex (Yoshida et al., 2008). HDAC2 and HDAC5 subsequently decrease acetylated histones (Yoshida et al., 2008). As a result,

decreased KLF4 and ELK1 promote acetylation of the histone within CArG elements, which respectively increases the expression of SMC contractile markers. During hUCMSC differentiation towards SMCs, miR-145 level was detected and found to increase steadily over the first 24 hours (Figure 3-12). Besides, microRNA array analysis was performed for undifferentiated MSCs, cells differentiated towards SMCs for 6 hours and 24 hours. Novel microRNAs and their target genes regulating the differentiation would be further explored, which could shed new light on SMC differentiation mechanism.

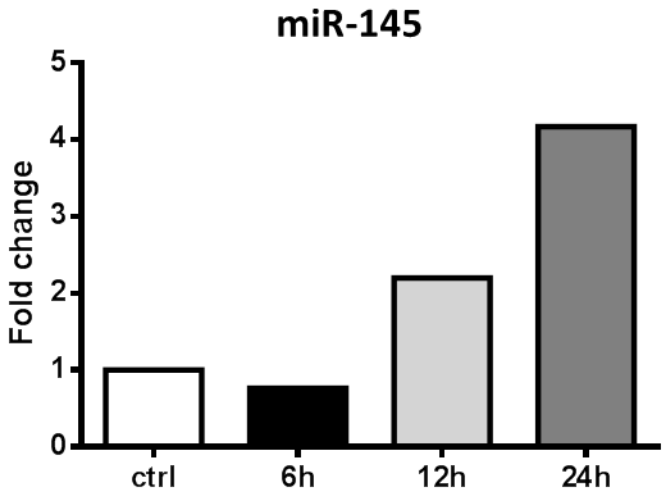

Figure 3-12 Time course study of miR-145 expression in hUCMSCs differentiated with TGFβ1

The level of miR-145 was increased at early time points of SMC differentiation. Differentiation medium (αMEM with 1% FBS and 5 ng/ml TGFβ1) led to the increase of miR-145 during the process. Data are from one experiment.

3.5 Mechanism involved in hUCMSC towards SMC differentiation: miRNA-oriented mechanism

3.5.1 Identification of potential miRNAs that might be important in SMC differentiation

To search for novel miRNAs involved in SMC differentiation, hUCMSCs differentiated for 6 hours and 24 hours were harvested and subjected to miRNA array analysis with undifferentiated hUCMSCs as control. The miRNAs upregulated more than 1.5-fold or downregulated more than 0.5-fold in comparison with the level in undifferentiated samples at either 6-hour time point or 24 hour time point were selected as shown in the tables (Table 3-1 and Table 3-2). P value indicates the statistical significance of the fold change. The cutoff value of the fold change was selected according to several published studies which also utilised miRNA array to provide valuable information about miRNAs involved in diseases or pathological processes (He et al., 2005; Kung et al., 2017). It has been established that miR-143 and miR-145 are important regulators in determining smooth muscle cell fate (Cordes et al., 2009). Consistent with what has been reported in the literature, miR-143-5p and miR-145-5p were upregulated in the differentiated hUCMSCs at 24-hour time point in the microRNA array analysis when compared to undifferentiated cells, although the level of miR-143-5p and miR-145-5p was not altered after 6 hours of differentiation (Table 3-1). Notably, this pattern of miR-145 expression is in accordance with what has been confirmed by the TaqMan miRNA assay (Figure 3-12). These collectively served as evidence that results obtained from the microRNA array are robust and of predicative value.

Among all the miRNAs that were upregulated, apart from the established miR-143/145 family of miRNAs, miRNAs among the upregulated group are from the miR-15 family, including the miR-503 mature strand miR-503-5p and the miR-503 star strand miR-503-3p. Furthermore, stem loop forms or precursor forms of miR-503 and miR-424 are both upregulated. There were several studies published demonstrating the importance of miR-424 and miR-503 in pulmonary hypertension (Kim et al., 2013) and diabetes mellitus-related vascular dysfunction (Caporali et al., 2015). In both studies, the effect of miR-503 or miR-424 has in part attributed to their roles in regulating pericyte or smooth muscle cell function. In addition, miR-424/322 (miR-322 is the ortholog of miR-424 in rats) displayed protective role in neointimal formation in the rat by inhibiting smooth muscle proliferation and preventing the phenotypic

switching to secretory phenotype (Merlet et al., 2013). Collectively, these studies implied the probable involvement of miR-503 and miR-424 in the smooth muscle-related pathological processes, but it merits further examination whether they play any regulatory role in smooth muscle differentiation from stem cells, which is the main issue being explored in the present study. Other upregulated miRNAs including hsa-miR-6890-5p, hsa-miR-6780b-5p, hsa-miR-7106-5p, hsa-miR-6730-5p, hsa-miR-6813-5p and hsa-miR-670-5p are not reported to be related to any physiological or pathophysiological conditions yet. Hsa-miR-3651 was found to be a promising biomarker of oral squamous cell carcinoma and oesophageal squamous cell carcinoma (Ries et al., 2014; Wang et al., 2015). More importantly, none of these miRNAs were reported to be related to cardiovascular diseases in any studies. Therefore, we excluded these miRNAs for further investigation.

In addition to the upregulated miRNAs, the list of downregulated miRNAs was also examined (Table 3-2). After reviewing the literature with all the miRNAs in the list, we found that most of them are more related to diverse types of cancers rather than cardiovascular diseases. The exception was miR-222. Thus, miR-222-5p was selected as a further candidate. Even though miR-222-5p is the star strand of miR-222, which was conventionally interpreted as the non-functional miRNA strand, this concept is gradually changed with star strand of various miRNAs getting recognised as functional participants in physiological or pathophysiological processes (Yang et al., 2011).

Before moving on to check the involvement of these selected miRNAs in the regulation of smooth muscle differentiation process, the expression of these miRNAs in differentiated cells at the chosen time points as well as upon the treatment with TGFβ1 were first confirmed with TaqMan miRNA assay (Figure 3-13). Consistent with microRNA array results, the level of miR-503-5p and miR-424-5p was both significantly increased after 24-hours of differentiation, and miR-222-5p was significantly downregulated both at both 6-hour and 24-hour time points (Figure 3-13 A). Moreover, the changes in expression of these miRNAs are all in a time-dependent manner. Additionally, the expression of these miRNAs was also compared between

samples treated with or without TGFβ1, with the intention to determine the attribution of TGFβ1 in the change of miRNA level (Figure 3-13 B). It was revealed that TGFβ1 was the indeed the major contributor to the miRNA level changes, which suggests the possible involvement of these miRNAs in TGFβ1 signalling pathways, although further investigations are needed to decide the specific signalling pathways.

Although miR-503-3p was significantly upregulated after being cultured in differentiation medium for 6 hours in miRNA array, this was not replicated with TaqMan miRNA assay. The expression level of miR-503-3p fluctuated too much which compromised the stability of the expression. For this reason, miR-503-3p was not included in further experiments and miR-503 would be used to refer to miR-503-5p in the remaining part of the thesis.

Table 3-1 List of miRNAs that are upregulated during the differentiation process

miRNAs	6 h vs undiff fold change	6 h vs undiff p value	24 h vs undiff fold change	24 h vs undiff p value
Stem loop hsa-mir-424	**1.90669**	**0.02065172**	**2.03778**	**0.064650457**
Stem loop hsa-mir-503	**1.88365**	**0.004096631**	**1.26284**	**0.113026727**
hsa-miR-503-3p	**8.54808**	**0.006320632**	**1.42198**	**0.309534797**
hsa-miR-503-5p	**1.57691**	**0.087578228**	**2.40261**	**0.007192791**
hsa-miR-145-5p	**0.942784**	**0.09197638**	**1.52203**	**0.005327755**
hsa-miR-145-3p	**1.43283**	**0.258517561**	**1.74432**	**0.092687102**
hsa-miR-143-5p	**1.35169**	**0.260788654**	**3.6681**	**0.03070377**
hsa-miR-6890-5p	1.46115	0.108594122	2.47409	0.041962345
hsa-miR-6780b-5p	0.739608	0.242151849	2.15985	0.014754481
hsa-miR-3651	1.87207	0.026502945	1.97064	0.152838709
hsa-miR-7106-5p	1.83961	0.016278885	1.73873	0.164114267
hsa-miR-6730-5p	1.33398	0.164746662	1.49796	0.031673769
hsa-miR-6813-5p	2.1279	0.007201024	1.21515	0.468215359
hsa-miR-670-5p	2.08522	0.007720557	1.65937	0.175163019

Table 3-2 List of miRNAs that are downregulated during the differentiation process

miRNAs	6 h vs undiff fold change	6 h vs undiff p value	24 h vs undiff fold change	24 h vs undiff p value
hsa-miR-222-5p	**0.290659**	**0.001763729**	**0.0931996**	**0.005217518**
hsa-let-7a-2-3p	0.331328	0.004959387	0.365227	0.030661528
hsa-miR-4443	0.398348	0.020406356	0.34834	0.048534934
hsa-miR-3617-5p	0.487689	0.00411999	0.427699	0.002948294
hsa-miR-5100	0.506476	0.003142387	0.470805	0.017901315
hsa-miR-92a-1-5p	0.356325	0.053660566	0.227752	0.030589371
hsa-miR-3617-5p	0.487689	0.00411999	0.427699	0.002948294
hsa-miR-378f	0.864318	0.204306421	0.437807	0.049394981
hsa-miR-758-5p	0.424597	0.060956051	0.451407	0.004627807
hsa-miR-1303	0.701947	0.235036451	0.468029	0.043837473
hsa-miR-1260b	0.716034	0.090153928	0.484455	0.000412866
hsa-miR-4286	0.477653	0.011969736	0.484873	0.027230141
hsa-miR-548ae	0.634694	0.097476613	0.483964	0.045450639

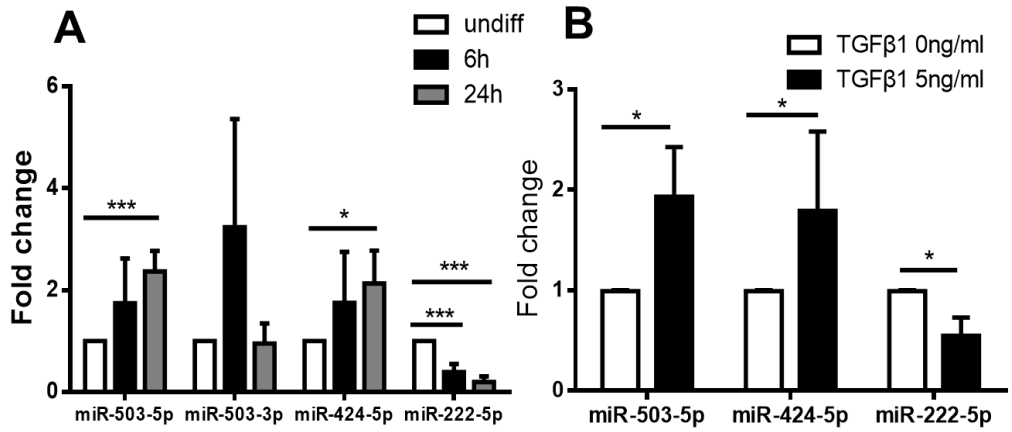

Figure 3-13 Change of miRNA expression during the differentiation process confirmed by TaqMan miRNA assay

(A) MiR-503-5p and miR-424-5p were confirmed to be significantly upregulated 24 h after being seeded in differentiation medium, while miR-222-5p was significantly downregulated. **(B)** The upregulation of miR-503-5p and miR-424-5p as well as the downregulation of miR-222-5p was mediated by TGFβ1. hUCMSCs were cultured in basal medium for one day before the medium was changed αMEM with 1% FBS with or without TGFβ1. Cells were harvested 24 hours after the medium change. Data are shown as mean ± SEM and are analysed from at least three experiments. Statistics are obtained with one-way ANOVA test, followed by Bonferroni post-hoc analysis. *P < 0.05 and ***P < 0.001.

3.5.2 MiR-503 is transcriptionally upregulated through Smad4-dependent pathway and promotes SMC differentiation through directly targeting Smad7

As established earlier, miR-503 and miR-424 were among the upregulated miRNAs and therefore were further studied to determine their role in MSC-SMC differentiation. To achieve this goal, miRNA mimics and inhibitors were utilised to examine the gain-of-function and loss-of-function effects of miR-503. The transfection efficiency was

first confirmed 24 hours after transfection as shown by the more than 100-fold increase in miR-503 expression in cells transfected with the miR-503 mimics when compared to those transfected with miRNA control mimics (Figure 3-14 A). Transfection of miR-503 mimics in hUCMSCs promotes SMC differentiation with increased expression of SMC markers including Calponin, SM22, αSMA and SMMHC at the mRNA level after 3 days as confirmed by Q-PCR (Figure 3-14 B). Upregulation of Calponin, SM22 and αSMA was further confirmed by their increased protein level using Western blot analysis (Figure 3-14 C and D).

Loss-of-function effects of miR-503 were demonstrated by the transfection of miR-503 inhibitors in the cells. One day after transfecting the cells with inhibitors, the level of miR-503 was significantly decreased (Figure 3-15 A). SMC markers including Calponin, SM22, and αSMA were not altered at the gene expression level as shown by Q-PCR (Figure 3-15 B). But moderate reduction in expression of these SMC markers could be observed at the protein level (Figure 3-15 C and D). This suggested that some other post-transcriptional regulation processes influencing mRNA translation and protein stability might exist (Filipowicz et al., 2008).

MiR-424 belongs to the same miRNA family as miR-503. The level of miR-424 was upregulated during the differentiation process. The gain-of-function study with miRNA mimic transfection experiments showed the potential of miR-424 to promote SMC differentiation as demonstrated by the upregulation of SMC markers Calponin and SM22 3 days after transfection (Figure 3-16). However, the degree of expression changes in both markers at the gene expression level by miR-424 overexpression was not as great as that induced by miR-503 mimics. Furthermore, αSMA and SMMHC was not significantly altered (Figure 3-16), which implied the limited capacity of miR-424 in inducing SMC differentiation. In the view of the greater capacity of miR-503 in promoting MSC-SMC differentiation, miR-503 was therefore chosen to be further explored for more extensive mechanistic study.

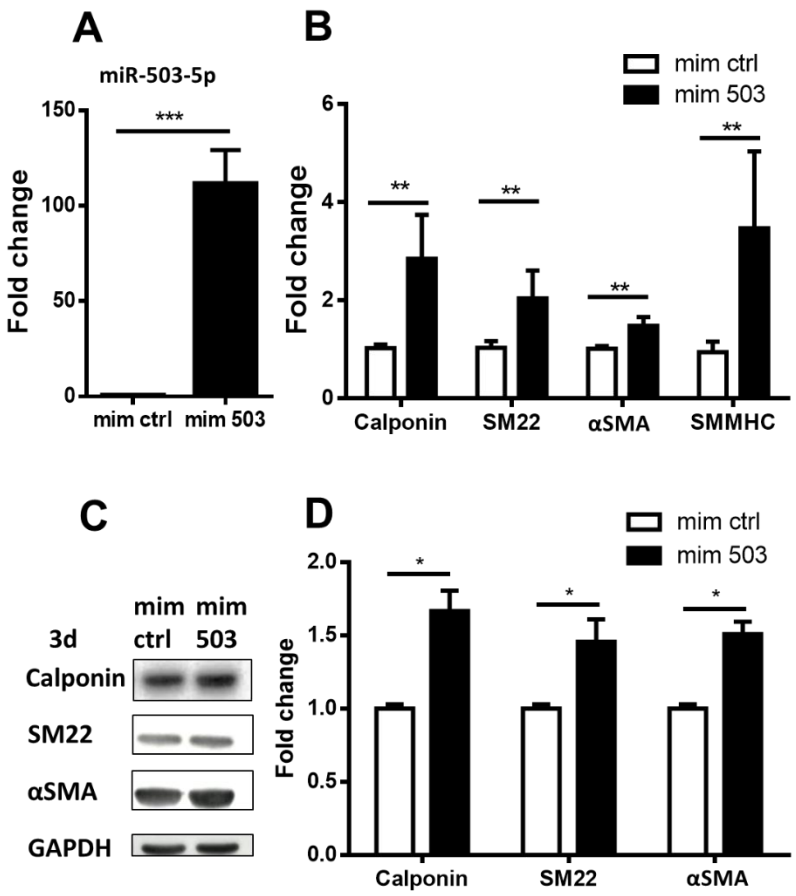

Figure 3-14 miR-503 mimic promotes SMC differentiation from hUCMSCs

HUCMSCs were seeded in culture flask at $1x10^4$ /cm^2 and allowed to grow for one day before transfection with either miR-503 mimics or control mimics using lipofectamine RNAiMax with the final concentration of 12.5 nM. The medium was changed every second day. **(A)** miR-503-5p is significantly upregulated 24 hours after transfection. Transfection of miR-503 promoted the differentiation of SMCs as shown by the change of SMC markers including Calponin, SM22, αSMA and SMMHC, both at the gene expression level **(B)** and at the protein level **(C)** as demonstrated with q-PCR and Western blot 3 days after transfection. Statistical analysis of protein level change from three in dependent experiments was also shown **(D)**. Mim ctrl indicates miRNA mimic negative control, and mim 503 indicates the treatment of cells with miR-503 mimics. Data are obtained from at least three independent experiments and shown as mean ± SEM. Statistics are obtained with student t-test. *P < 0.05; **P < 0.01 and ***P < 0.001.

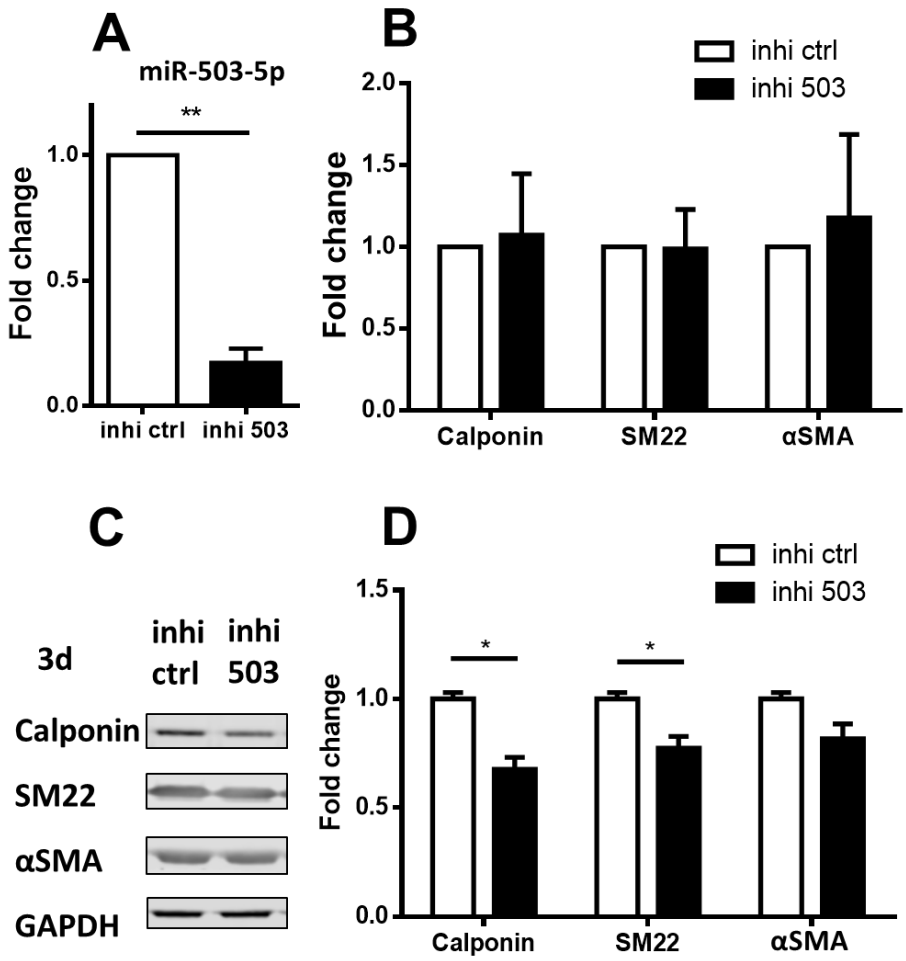

Figure 3-15 miR-503 inhibitor downregulates SMC differentiation from hUCMSCs

HUCMSCs were seeded in culture flask at $1x10^4$ /cm^2 and allowed to grow for one day before transfection with miR-503 inhibitor or control inhibitor using lipofectamine RNAiMAX, with final concentration of 62.5 nM. The medium was changed every second day. **(A)** MiR-503-5p is significantly downregulated 24 hours after transfection of miR-503 inhibitor. **(B)** Inhibition of miR-503-5p did not inhibit the SMC marker expression at the gene expression level. **(C and D)** Treatment of miR-503-5p inhibitor in the cells downregulated SMC markers at the protein level, however, the inhibition was only statistically significant in Calponin and SM22. Inhi ctrl indicates the negative control of miR-503, and inhi 503 indicates the miR-503 inhibitors. Data are obtained from at least three independent experiments and shown as mean ± SEM. Statistics are obtained with student t-test. *P < 0.05 and **P < 0.01.

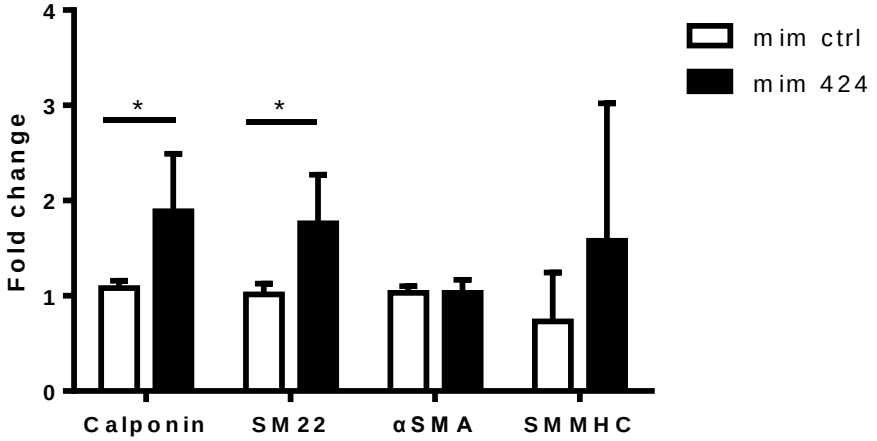

Figure 3-16 miR-424 promotes SMC differentiation, but at a lesser degree compared to miR-503

HUCMSCs were seeded in culture flask at 10000/cm^2 and allowed to grow for one day, before transfection with either miR-424 mimic or control mimic using lipofectamine RNAiMax, with final concentration of 12.5 nM. SMC markers Calponin and SM22 were significantly upregulated 3 days after transfection, whereas no statistically meaningful change was observed for αSMA and SMMHC. Mim ctrl indicates miRNA mimic negative control, and mim 424 indicates the treatment of cells with miR-424 mimics. Data are obtained from at least three independent experiments and shown as mean ± SEM. Statistics are obtained with student t-test. *P < 0.05.

3.5.2.1 Exploration of potential targets of miR-503

In the exploration of potential targets of miR-503, algorithm based bioinformatic prediction, literature review and *in vitro* examination of gene expression were conducted.

As introduced earlier, miRNAs functions by binding to the 3'-UTR region of target mRNA and induce mRNA degradation or translation inhibition. Prediction of miRNA targets could be based on the mainstream seed site rule. It was explained earlier in the introduction that the most prominent miRNA targets bind with miRNAs in a complimentary mode to the 2nd to 7th nucleotides at the 5' end. Binding of the 8th nucleotide to the mRNA and the presence of an A at 3' end of the target sites on the mRNA further increases the reliability of target prediction. However, these target prediction algorithms will need further experimental validation.

To predict targets of miR-503, TargetScan and miRbase were mainly used for algorithm based target prediction. After obtaining the list of predicted targets, further screening for those related to TGFβ1 signalling pathway was carried out, given the importance of TGFβ1 in SMC differentiation and the involvement of it in promoting miR-503 expression. Among these, mothers against decapentaplegic homolog 7 (Smad7), SMAD specific E3 ubiquitin protein ligase 2 (Smurf2), Ski, ADP ribosylation factor like GTPase 2 (Arl2) and E2F transcription factor 3 (E2F3) were selected for further analysis. Smad7, Smurf2 and Ski are potent negative regulators of the TGFβ1 signalling pathway (Deheuninck and Luo, 2009; Kavsak et al., 2000; Nakao et al., 1997). E2F3 is a transcription factor implied in other pathological processes to be indirectly involved in TGFβ1 signalling (Hu et al., 2000). Arl2 is a GTPase that might be indirectly involved in ROCK/GTPase pathway which could affect SMC differentiation and it has been validated to be a direct target of miR-424 (Nishi et al., 2010). Genome browsing in the UCSC genome sequence database confirmed that the 3'-UTR segments of these selected genes all contain at least one site of "GCUGCUA" sequence.

One day after transfecting the cells with miR-503 mimics, which would give rise to miR-503-5p strand within the cells, the samples were harvested and subjected to gene expression analysis with Q-PCR. Although the best way to experimentally screen for miRNA targets is to examine the expression changes at the protein level since miRNA may target that mRNA by translation inhibition rather than mRNA degradation, it requires much more efforts to validate all possible targets with Western

blot. Therefore, we started the screening process with gene level detection. It was shown in samples transfected with miR-503 mimics for one day that only Arl2 level was clearly downregulated (Figure 3-17 A). This is reasonable since 3 sites of "GCUGCUA" were found in the 3'-UTR segment of Arl2 mRNA which might allow a stronger target recognition and subsequent inhibition by miR-503. Although Smad7 and Smurf2 level was not downregulated, given their importance to negatively regulate Smad-dependent TGFβ1 signalling pathways, their level was examined further after a longer exposure time of cells to miR-503 mimics. Three days after transfection with miR-503 mimics, mRNA expression of Smad7 was significantly downregulated, whereas Smurf2 is instead upregulated after three days (Figure 3-17 B). These indicated that the downregulated SMAD7 could potentially be a target of miR-503, while the upregulated SMURF2 is not likely the target since this is not consistent with the inhibitory effect of miRNA. Thus, Smurf2 was excluded as a direct target of miR-503 and not checked further in future experiments. Arl2 was still greatly suppressed at the three-day time point by miR-503 mimics which makes it a promising direct target of miR-503, but a further functional study of it was required to establish its role in SMC differentiation system in which it was not demonstrated before in literature to be involved (Figure 3-17 B). Validation of the protein level change for Smad7 and Arl2 showed significant downregulation after 3 days of treatment in miR-503 mimics (Figure 3-18 A and B).

The time-dependent and TGFβ1-dependent changes of these two markers were also examined. Smad7 was upregulated with increased time of differentiation and by TGFβ1 at the gene expression level, whereas Arl2 was downregulated with time and by TGFβ1 at the gene expression level (Figure 3-19). Collectively, these results strongly imply that Smad7 and Arl2 might be targets of miR-503, and as expression of both genes change upon TGFβ1 stimulation, they both might be involved in TGFβ1 signalling pathway. But further experiments were required for validation.

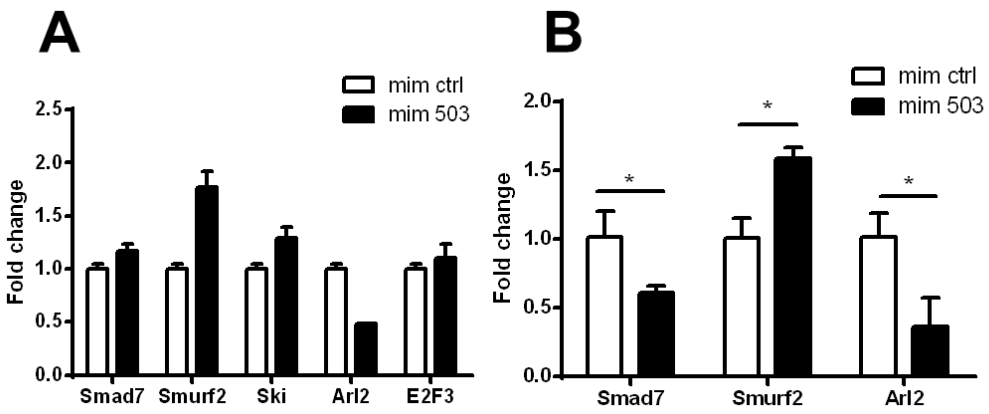

Figure 3-17 Expression of potential targets after miR-503 mimic treatment

HUCMSCs were treated with miR-503 mimics and then harvested for after one day for gene expression analysis. **(A)** Potential targets including Smad7, Smurf2, Ski, Arl2 and E2F3 were examined with q-PCR. Arl2 was the only gene found to be downregulated with miR-503 treatment one day after mimic transfection. Results were from 2 independent experiments. **(B)** The effect of miR-503 mimic on Smad7 and Arl2 3 days after transfection was also explored and a statistically significant decrease of these two genes at the gene expression level was observed. Mim ctrl indicates miRNA mimic negative control, and mim 503 indicates the treatment of cells with miR-503 mimics. Data are obtained from at least three independent experiments and shown as mean ± SEM. Statistics are obtained with student t-test. *P < 0.05.

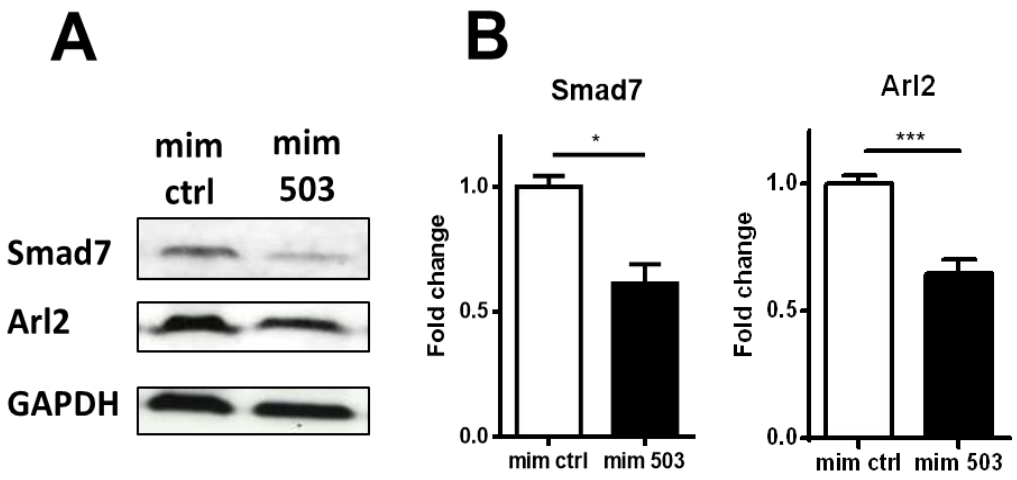

Figure 3-18 Change at the protein level after miR-503 mimic treatment

HUCMSCs were treated with miR-503 mimics and then harvested 3 days after transfection. (**A**) Both Smad7 and Arl2 were significantly downregulated at the protein level as demonstrated by Western blot. (**B**) Statistical analysis of the Western blot results showed consistent results. Mim ctrl indicates miRNA mimic negative control, and mim 503 indicates the treatment of cells with miR-503 mimics. Image is representative of at least three experiments. Statistics are obtained with student t-test. *P < 0.05 and ***P < 0.001.

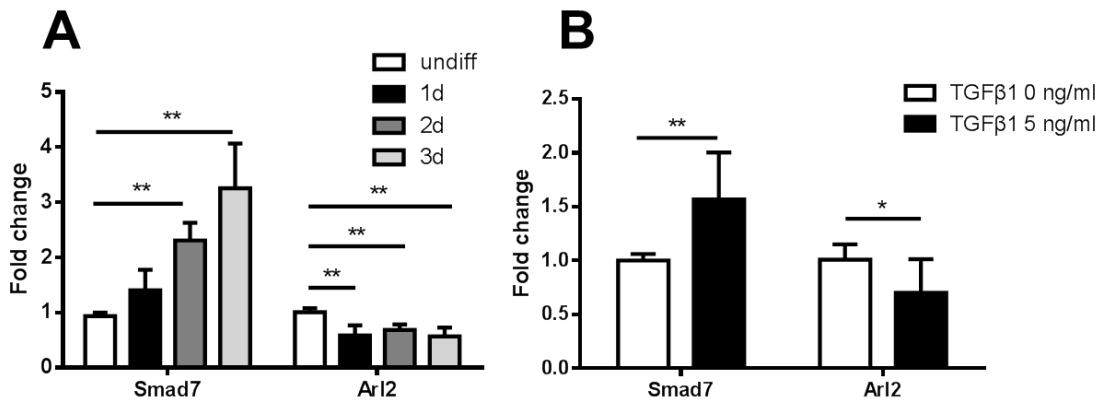

Figure 3-19 Time-dependent and TGFβ1-dependent changes of Smad7 and Arl2 expression

(A) HUCMSCs were differentiated in differentiation medium (αMEM with 1% FBS and 5 ng/ml TGFβ1) for 1, 2 and 3 days and then harvested for gene expression analysis for Smad7 and Arl2 with q-PCR. Undifferentiated cells were used as a control. **(B)** The change of Smad7 and Arl2 at the gene expression level after 2 days in culture was also examined between TGFβ1 treated and untreated group to confirm the relationship of the change with TGFβ1. Undiff indicates undifferentiated cells that were kept in basal medium. 0 indicates that the cells were cultured in medium (αMEM with 1% FBS) without TGFβ1, and 5 indicates that the cells were cultured in medium (αMEM with 1% FBS) with 5 ng/ml TGFβ1. Data are obtained from at least three independent experiments and shown as mean ± SEM. Statistics are obtained with student t-test. *P < 0.05 and **P < 0.01.

3.5.2.2 Promotion of SMC differentiation by miR-503 is not through Arl2 inhibition

As displayed in previous experiments, Arl2 and Smad7 were the two main potential targets for miR-503. Arl2 was subjected to further examination first. It was shown in cardiac myocytes that miR-15b family could directly target Arl2 and modulate cellular ATP levels through mitochondrial degeneration (Nishi et al., 2010). Although it was miR-424 but not miR-503 that was included in the study, miR-503 and miR-424 belong to the same miRNA family and share similar seed sequence. It was reasonable to postulate that miR-503 could also directly target Arl2 3'-UTR sequence. Furthermore, no published study has yet established Arl2 in relation to SMC differentiation process. To examine the function of Arl2, loss-of-function study by siRNA knockdown was carried out. Arl2 gene knockdown was firstly confirmed with Q-PCR with the decrease of Arl2 at the gene expression level 2 days after treating the cells with Arl2 siRNA. However, a further check on SMC markers including Calponin, SM22 and αSMA did not reveal any change at the gene expression level (Figure 3-20). Further examination at the protein level was not carried out later as the experimental evidence suggests that Arl2 was not functionally involved in the SMC

differentiation process. Downregulation of Arl2 and subsequent incidents are not likely to be the driving factors for SMC differentiation. Although Arl2 could be a direct target of miR-503, and it was evident that Arl2 expression decreases during the differentiation process, after treatment with TGFβ1 and after transfection with miR-503 mimics, Arl2 involved change might only be an unrelated subsequence of miR-503 upregulation without a functional role in SMC differentiation.

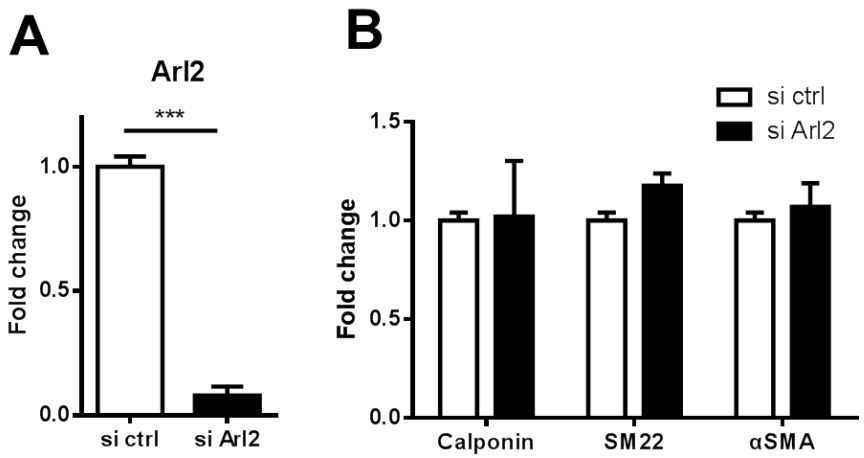

Figure 3-20 Arl2 gene knockdown by siRNA does not alter SMC differentiation

HUCMSCs were seeded at $1x10^4/cm^2$ for one day before getting transfected with Arl2 siRNA (Life Tech). Arl2 siRNA was transfected with RNAiMax in differentiation medium at a final concentration of 10 nM. Cells were harvested 2 days after transfection. **(A)** Gene expression level of Arl2 detection showed successful knockdown of Arl2 gene. **(B)** Examination of SMC markers including Calponin, SM22 and αSMA at the gene expression level did not demonstrate a statistically significant change of these markers. Si ctrl indicates siRNA negative control and si Arl2 indicates the knockdown of Arl2 by siRNA. Data are obtained from at least three independent experiments and shown as mean ± SEM. Statistics are obtained with student t-test. ***P < 0.001.

3.5.2.3 MiR-503 promotes SMC differentiation through directly targeting Smad7

Smad7 was an established negative regulator in the Smad-dependent TGFβ1 signalling pathway (Kavsak et al., 2000). It works through binding to the activated type I receptor of TGFβ1 that blocks the binding of R-Smads to the receptor, or through recruiting ubiquitin E3 ligase Smurf1/2 and could result in the degradation of the receptor (Yan et al., 2009). Furthermore, Smad7 could be upregulated by TGFβ1 which suggests a mode of negative feedback loop regulation. Consistent with what has been established in the literature, Smad7 upregulation in the differentiation process and upon treatment of TGFβ1 was also examined in my study.

To further demonstrate whether miR-503 could participate in TGFβ1 signalling pathway through inhibition of Smad7, thereby promoting SMC differentiation, we first cloned Smad7 3'-UTR to a miRNA target reporter clone with firefly luciferase gene lying upstream of the Smad7 3'-UTR and *Renilla* luciferase as an internal control of the plasmid transfection efficiency. Target sites at Smad7 3'-UTR was pinpointed by miRNA target prediction algorithms and the target site was then mutated (Figure 3-21 A). It was revealed that miR-503 could inhibit the relative luciferase activity compared to miRNA control, whereas the inhibition would be recovered if the target site on the 3'-UTR segment was mutated (Figure 3-21 B).

After building up the direct inhibition relationship of miR-503 on Smad7, experiments to check the role of Smad7 in the present SMC differentiation system were carried out. Loss-of-function study by siRNA knock down experiments showed that loss of Smad7 could result in a moderate but statistically significant upregulation of SMC marker SM22 and αSMA at the mRNA level (Figure 3-22 A and B). At the protein level, Calponin was significantly upregulated (Figure 3-22 C and D).

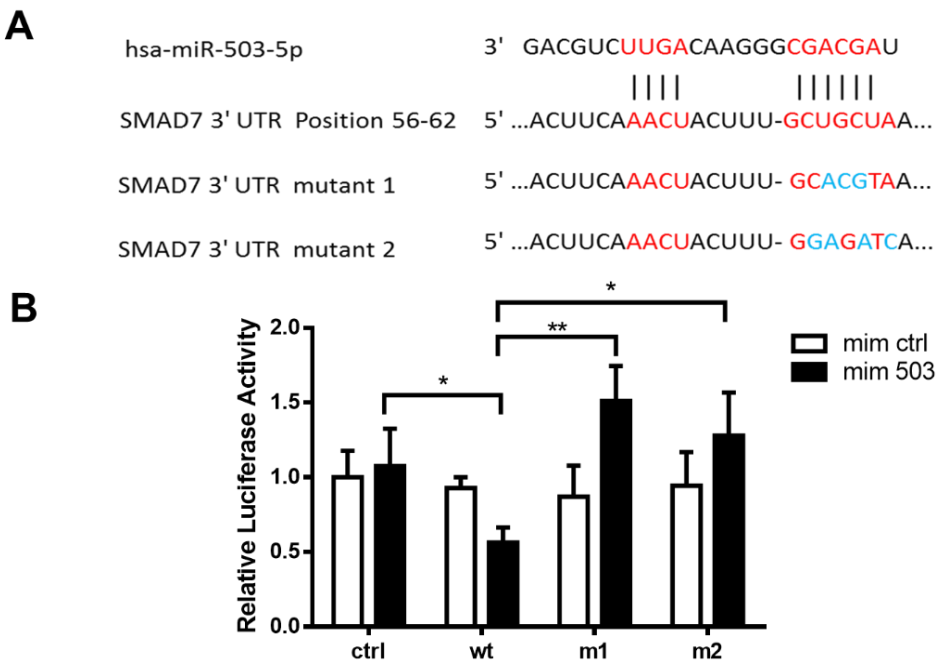

Figure 3-21 Smad7 is a direct target of miR-503

(A) Alignment of miR-503 and the 3'-UTR of smad7 gene showed the postulated target binding sites (marked in red) and induced mutations (marked in blue). 3'-UTR of Smad7 was cloned into a miRNA target reporter (Genecopoeia). **(B)** Co-transfection of miR-503 mimics and reporter with wild type Smad7 3'-UTR segment showed reduced relative luciferase activity as compared to vector with empty plasmid, while mutation of target binding sites recovered the reduction. Relative luciferase activity was calculated with firefly luciferase activity/*Renilla* luciferase activity. Mim ctrl indicates miRNA mimic negative control, and mim 503 indicates the treatment of cells with miR-503 mimics. Data are obtained from at least three independent experiments and shown as mean ± SEM. Statistics are obtained from two-way ANOVA test followed by Bonferroni post-hoc analysis. *P < 0.05 and **P < 0.01.

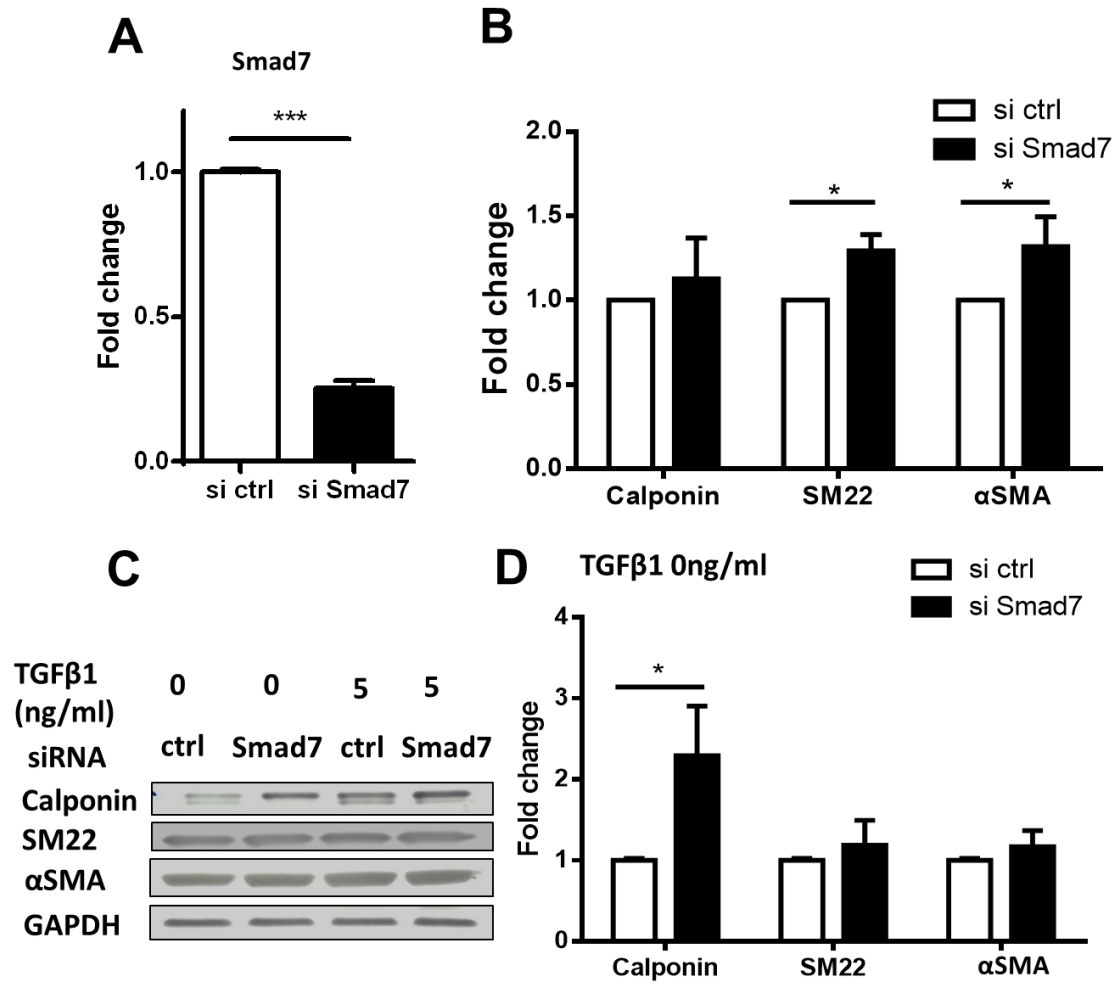

Figure 3-22 Knockdown of Smad7 augmented SMC differentiation

(A) Transfection of Smad7 siRNA resulted in a significantly lower level of Smad7 at the gene expression level after 1 day. **(B)** Cells were harvested 2 days after siRNA transfection for mRNA and protein analysis. Knockdown of Smad7 by siRNA upregulated the level of smooth muscle markers SM22 and αSMA at the mRNA level. **(C and D)** Knockdown of Smad7 by siRNA prompted a notable increase of Calponin at the protein level whereas the changes in SM22 and αSMA were not significant, as assessed by Western blot. Si ctrl indicates siRNA negative control and si Smad7 indicates the knockdown of Smad7 by siRNA. Q-PCR data are obtained from at least three independent experiments and shown as mean ± SEM. Western blot images are representative of at least three experiments. Statistics are obtained from unpaired student t-test. *P < 0.05 and ***P < 0.001.

3.5.2.4 TGFβ1 transcriptionally upregulates miR-503 through Smad4-dependent pathway

After establishing Smad7 as a direct target of miR-503, miR-503 was implied to be a new component of TGFβ1 signalling pathway. As demonstrated earlier, Smad7 and miR-503 are both transcriptionally upregulated by TGFβ1. A possible explanation of this is that the miR-503 upregulation could serve as a limiting factor to prevent the uncontrolled upregulation of Smad7. Smad7 is mainly involved in Smad-dependent TGFβ1 signalling pathway: its upregulation is activated through Smad4-dependent pathway and it exerts its inhibitory effect through inhibiting R-Smads from binding to TGFβ1 type I receptor. In addition, there is a direct relationship between miR-503 and Smad7. Thus, it is reasonable to postulate that the upregulation of miR-503, similar to Smad7, might be regulated by Smad-dependent TGFβ1 signalling pathway.

To explore whether the hypothesis is valid, knockdown experiments of Smad4 was carried out since Smad4 is the co-Smad which is necessary for all R-Smads to function. Confirmation of Smad4 knockdown was shown by the significant decrease in expression of Smad4 and downstream SMC markers including Calponin, SM22 and αSMA (Figure 3-23 A and B). Next, the level of miR-503 was examined after the Smad4 knockdown. The level of miR-503 was significantly downregulated when Smad4 is depleted in medium with TGFβ1, whereas its level is not affected if the medium does not contain TGFβ1 (Figure 3-23 C and D). These results imply that Smad4 might play a key role in TGFβ1 mediated upregulation of miR-503.

To further explore the direct involvement of Smad4 in promoting miR-503 upregulation, the physical interaction of Smad4 with the promoter region of miR-503 was checked with ChIP experiments. Enrichment of Smad4 at the promoter region of miR-503 was confirmed. At the same time, Smad4 was not enriched at the promoter region of GAPDH, which served as a negative control and ensured the robustness of fold enrichment at the miR-503 promoter region (Figure 3-24).

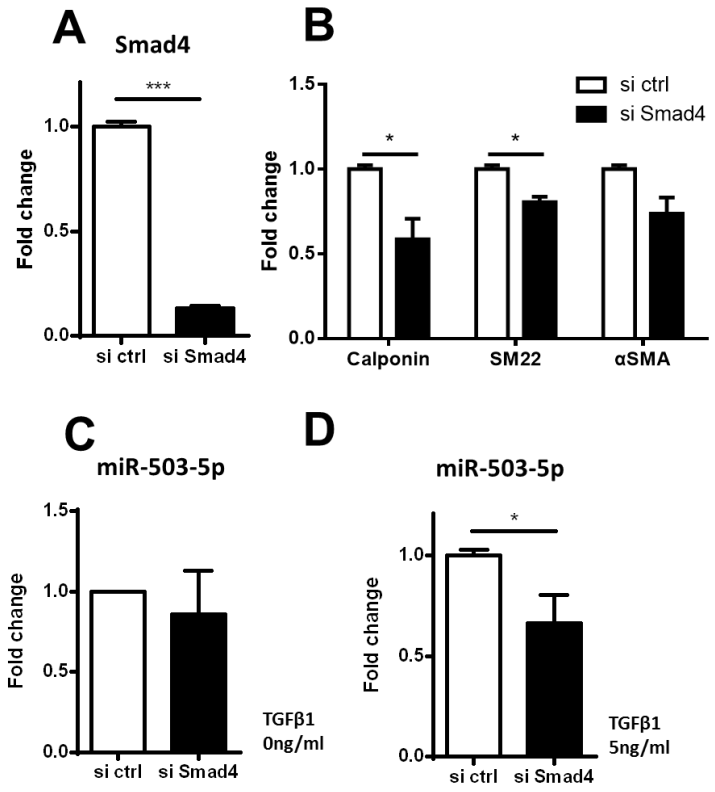

Figure 3-23 Upregulation of miR-503 by TGFβ1 is Smad4-dependent

HUCMSCs were seeded in the culture flask at $1x10^4$ /cm^2 the day before Smad4 siRNA transfection. The final concentration of the siRNA was 5 nM. **(A)** Knockdown of Smad4 gene was confirmed with q-PCR 48 hours after transfection. **(B)** Smad4 knockdown also resulted in statistically significant downregulation of SMC markers including Calponin and SM22 at the gene expression level 2 days after transfection of Smad4 siRNA. Gene expression of αSMA also displayed a trend to be decreased, but it was not statistically significant. In the knockdown experiments cells were cultured in medium with 5 ng/ml TGFβ1. The level of miR-503 was also checked after 48 hours. **(C and D)** It was found that Smad4 siRNA could downregulate miR-503 level in medium with TGFβ1 but not in medium without TGFβ1. Si ctrl indicates siRNA negative control and si Smad4 indicates the knockdown of Smad4 by siRNA. Data are obtained from at least three independent experiments and shown as mean ± SEM. Statistics are obtained from unpaired student t-test. *P < 0.05 and ***P < 0.001.

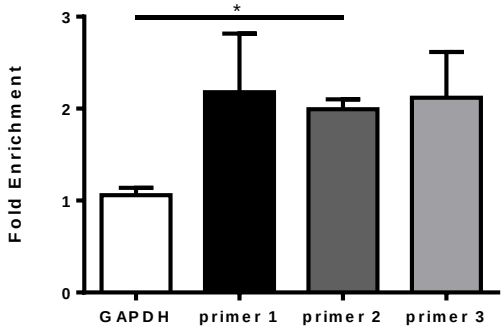

Figure 3-24 Smad4 directly binds to the promoter region of miR-503

HUCMSCs were cultured in medium (αMEM with 1% FBS) at $1x10^4$ /cm^2 for 24 hours before the medium is changed to serum free αMEM with antibiotics. After 5 hours starvation of the cells, TGFβ1 is added and cells are harvested 4 hours later for ChIP experiments. Cells cultured in the same condition but without TGFβ1 addition is used as a control. Different primers specific to the promoter region of the miR-503 promoter are used to detect the enrichment of Smad4 at the promoter region. A primer specific to GAPDH promoter region was used as a negative control. It was demonstrated that at the promoter region of miR-503 that is detected by primer 2, the Smad4 was enriched. For GAPDH, Smad4 was not enriched in its promoter region. Data are obtained from at least three independent experiments and shown as mean ± SEM. Statistics are obtained with one-way ANOVA test, followed by Bonferroni post-hoc analysis. *P < 0.05.

3.5.2.5 Schematic representation of miR-503-related differentiation mechanism

Taken together, it could be concluded that miR-503 is transcriptionally upregulated upon TGFβ1 treatment through a Smad4-dependent pathway and subsequently targets Smad7 which is a negative regulator of Smad-dependent signalling pathway. (Figure 3-25) This adds another layer of regulation into the already complex network of TGFβ1 signalling pathway with miRNAs being significantly involved in the fine

tuning of various pathways, which could be crucial to obtain the balance of signalling pathways in physiological and pathophysiological conditions.

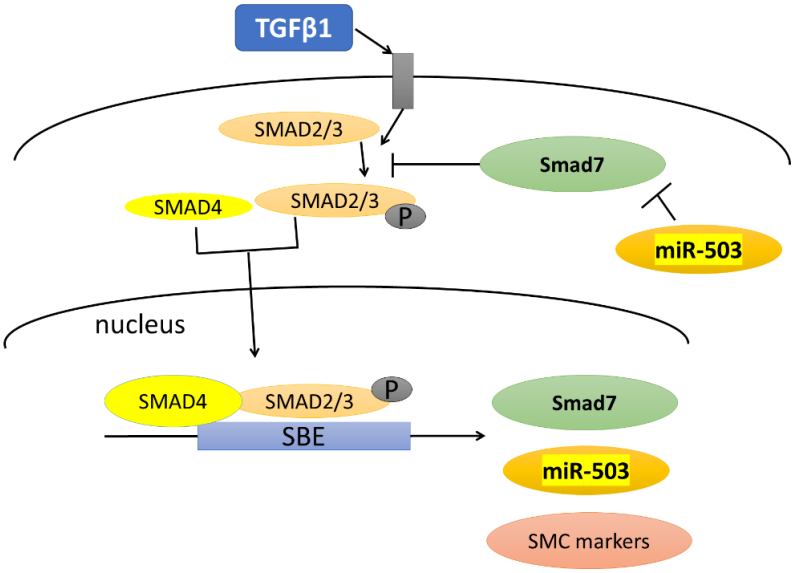

Figure 3-25 Schematic representation of miR-503 in SMC differentiation

Upon TGFβ1 treatment, Smad2/3 get phosphorylated by the activated receptors and binds to co-Smad Smad4. This complex would then be translocated into the nucleus and bind to the Smad binding element (SBE) of target gene promoters including SMC marker, Smad7 and miR-503. Interestingly, Smad7 and miR-503 both display regulatory role in the TGFβ1 signalling pathway, and their effects are contrary to each other. Smad7 takes its inhibitory effect in TGFβ1 Smad-dependent signalling pathway through blocking the direct binding of Smad to the receptor or phosphorylation of it. MiR-503 exerts further regulatory significance in TGFβ1 signalling pathway through imposing another layer by inhibiting Smad7.

3.5.3 Downregulation of miR-222-5p in differentiation process is important for de-repression of SMC markers

3.5.3.1 MiR-222-5p inhibits SMC differentiation from hUCMSCs

MiR-222-5p is the most prominent miRNA that was downregulated in the differentiation process as revealed by miRNA array and subsequent confirmation with TaqMan miRNA assay. The role of the miR-222 mature strand miR-222-3p has been established to have a crucial role in inhibiting SMC proliferation both *in vitro* and *in vivo* (Liu et al., 2009). Moreover, miR-222, which belongs to the same miRNA family as miR-221, was identified as an important modulator in platelet-derived growth factor (PDGF)-induced SMC phenotypic change (Davis et al., 2009). However, it is the mature strand that was studied in both studies, whereas the downregulated miR-222-5p during MSC-SMC differentiation is the passenger strand, whose role has not been established. Although the passenger or star strand of miR-222 (i.e. miR-222-5p) was widely accepted to be destined for degradation without any function after maturation, numerous studies have recently emerged to depict the pathological importance of passenger strands of miRNAs (Bang et al., 2014; Matsushita et al., 2016).

For the reasons mentioned above, even though miR-222-5p is the passenger strand, it was worth being examined for its role in SMC differentiation process. The influence of miR-222-5p on the differentiation process first was checked by transfecting miR-222-5p mimics into hUCMSCs. The success of miRNA mimic transfection was confirmed by the significant increase of miRNA mimics inside the cells (Figure 3-26). Increased level of miR-222-5p prompts the downregulation of SMC markers including Calponin and αSMA both at the gene expression level as exhibited by Q-PCR (Figure 3-27 A) and the protein level as exhibited by Western blot and immunofluorescent staining (Figure 3-27 B and C, Figure 3-28), thus demonstrated the capacity of miR-222-5p mimics in inhibiting SMC differentiation. However, the influence of miR-222-5p mimics on SM22 was limited which could be observed in the unchanged level of it both at the gene expression level and the protein level (Figure 3-27 and Figure 3-28). SMMHC level was not altered at the gene expression level but was downregulated at the protein level as displayed in the Western blot (Figure 3-27). Inhibitors of miR-222-5p, which are single stranded RNAs that complimentary bind to miR-222-5p, were also used to treat the cells to provide information about the loss-of-function effect. MiR-222-5p level was significantly downregulated after treatment with miR-222-5p

inhibitor (Figure 3-29 A). MiR-222-5p inhibitors resulted in only limited upregulation of SMC markers including Calponin, SM22 and αSMA, with the fold change to be less than 1.5-fold (Figure 3-29 B). As revealed by the miRNA array and TaqMan miRNA assay, miR-222-5p level was significantly downregulated at 24-hour time point to around one tenth of its level in cells cultured in basal medium. Thus, on top of this downregulation, further inhibition of miR-222-5p might only have minimal effect. This might explain the asymmetry of the function between miR-222-5p mimics and inhibitors.

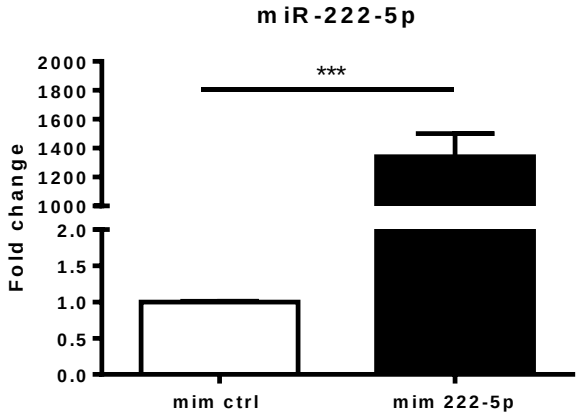

Figure 3-26 miR-222-5p level is significantly upregulated after miR-222-5p mimic transfection

HUCMSCs were cultured at the density of $1x10^4$ /cm^2 for 1 day in medium (αMEM with 1% FBS) before they were transfected with miR-222-5p mimics. The final concentration of the mimics was 12.5 nM. Cells were harvested 1 day after transfection. The success of miRNA mimic transfection was confirmed by the level of miR-222-5p inside the cells. Data are obtained from at least three independent experiments and shown as mean ± SEM. Statistics are obtained from unpaired student t-test. ***P < 0.001.

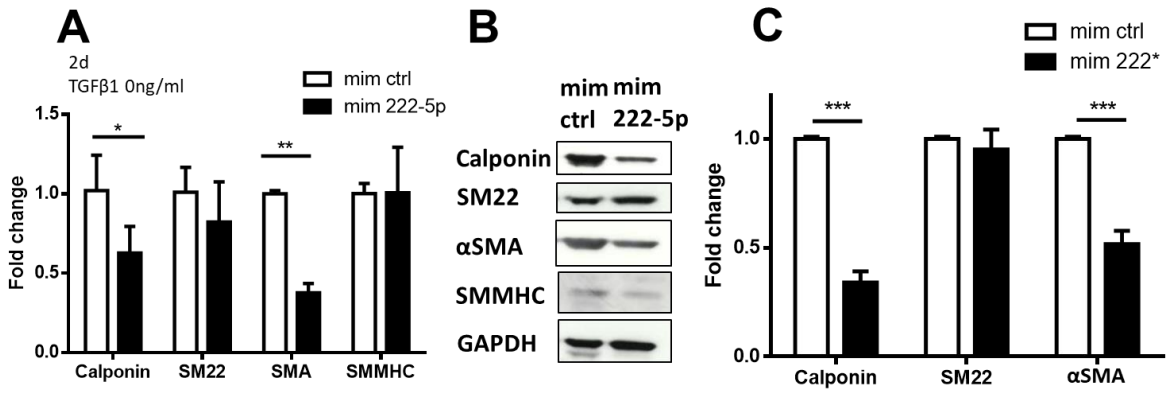

Figure 3-27 miR-222-5p mimic inhibits SMC differentiation as shown by Q-PCR and Western blot

HUCMSCs were cultured at the density of $1x10^4$ /cm^2 for 1 day in medium (αMEM with 1% FBS) before they were transfected with miR-222-5p mimics. The final concentration of the mimics was 12.5 nM. Cells were harvested 2 days after transfection. Cells cultured in the same condition but transfected with miRNA mimic negative control was used as a control. TGFβ1 was not added to the medium in the entire process. **(A)** It was shown that miR-222-5p mimics could downregulate the level of Calponin and αSMA at the gene expression level as demonstrated by q-PCR, but the effect on the SM22 and SMMHC expression was limited. **(B)** Examination of SMC markers at the protein level displayed downregulation of Calponin, αSMA and SMMHC, but there was no effect on SM22 level. **(C)** Statistical analysis of Western blot results showed significant inhibition of Calponin and αSMA. Mim ctrl indicates miRNA mimic negative control, and mim 222-5p indicates the treatment of cells with miR-222-5p mimics. Q-PCR data are obtained from at least three independent experiments and shown as mean ± SEM. Western blot images are representative of at least three independent experiments. Statistics are obtained from unpaired student t-test. *P < 0.05, **P < 0.01 and ***P < 0.001.

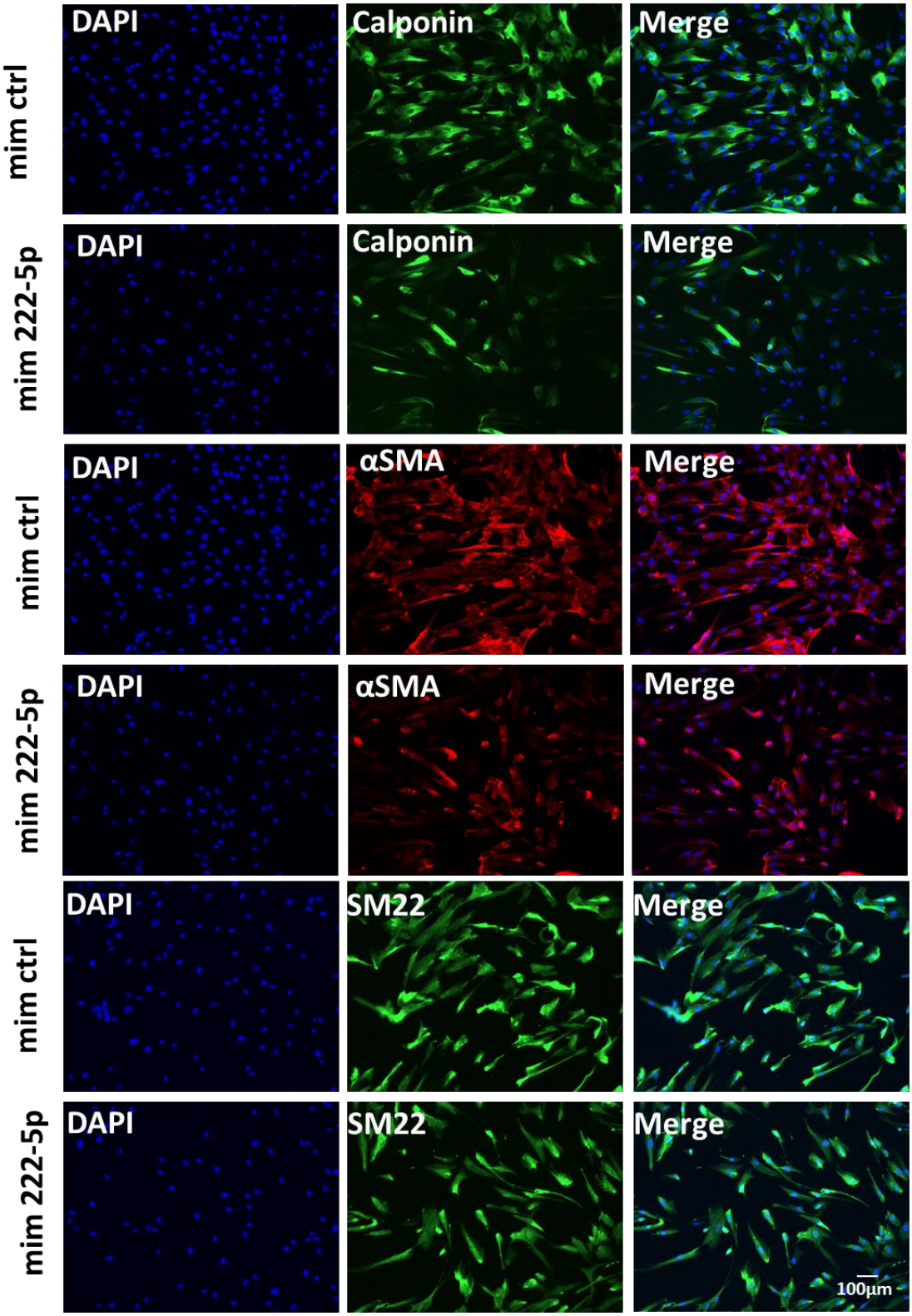
mim ctrl
DAPI
Calponin
Merge
mim 222-5p
DAPI
Calponin
Merge
mim ctrl
DAPI
αSMA
Merge
mim 222-5p
DAPI
αSMA
Merge
mim ctrl
DAPI
SM22
Merge
mim 222-5p
DAPI
SM22
Merge
100μm

Figure 3-28 miR-222-5p mimic inhibits SMC differentiation as shown by immunofluorescent staining

HUCMSCs were cultured at the density of $1x10^4$ /cm^2 for 1 day in medium (αMEM with 1% FBS) before they were transfected with miR-222-5p mimics. The final concentration of the mimics was 12.5 nM. Cells cultured in the same condition but transfected with miRNA mimic negative control was used as a control. TGFβ1 was not added to the medium in the entire process. Cells were fixed and stained 2 days after transfection and visualised with confocal microscope. Effect of miR-222-5p mimics on SMC markers at the protein level was also checked with immunofluorescence. The downregulation of Calponin and αSMA was evident by miR-222-5p mimics whereas no obvious effect of the mimics on SM22 at the protein level was observed. Mim ctrl indicates miRNA mimic negative control, and mim 222-5p indicates the treatment of cells with miR-222-5p mimics. Image shown here is representative of at least three independent experiments.

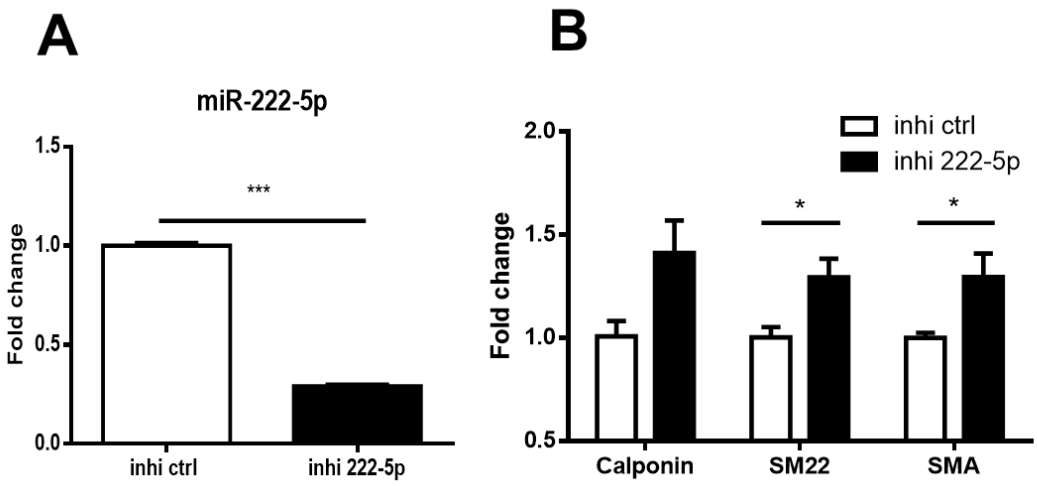

Figure 3-29 miR-222-5p inhibitor promotes SMC differentiation

HUCMSCs were cultured at the density of $1x10^4$ /cm^2 for 1 day in medium (αMEM with 1% FBS) before they were transfected with miR-222-5p inhibitors. The final concentration of the inhibitors was 62.5 nM. Cells were harvested 2 days after transfection. Cells cultured in the

same condition but transfected with miRNA inhibitor negative control was used as a control. TGFβ1 was not added to the medium in the entire process. **(A)** Successful inhibition of miR-222-5p level was confirmed by the significant downregulation of miR-222-5p level inside the cells. **(B)** It was shown that miR-222-5p inhibitor could to some extent promote SMC differentiation as demonstrated by the upregulation of SMC markers Calponin, SM22 and αSMA, but the promotion ability is limited since the fold change of the SMC markers are minimal and are less than 1.5. Data are obtained from at least three independent experiments and shown as mean ± SEM. Statistics are obtained from unpaired student t-test. *P < 0.05 and ***P < 0.001.

3.5.3.2 3'-UTR of αSMA is a direct target of miR-222-5p

Given the prominent inhibitory effect of miR-222-5p mimics on αSMA expression both at the gene expression and the protein levels, it was postulated that αSMA 3'-UTR might be directly targeted by miR-222-5p which that results in the degradation of αSMA mRNA and subsequent decreased expression of αSMA at the protein level. To test this hypothesis, the sequence of miR-222-5p was aligned with αSMA mRNA and complementarity was found at both the 5' and 3' end of miR-222-5p with the 3'-UTR of αSMA mRNA (Figure 3-30 A). Luciferase reporter gene assays with inserts of either αSMA 3'UTR sequence or mutated sequence at predicted complementary sites were then utilised to validate whether 3'-UTR of αSMA mRNA could be directly targeted by miR-222-5p. Dual transfection of the plasmid encoding αSMA 3'-UTR sequence and miR-222-5p mimics into HEK293 cells revealed that miR-222-5p mimics inhibited αSMA 3'-UTR and mutation of the target site on the 3'-UTR rescued the inhibition (Figure 3-30 B). However, the rescue of the inhibition was not statistically significant (Figure 3-30 B). Collectively, this evidence implies that miR-222-5p might directly target αSMA 3'-UTR and lead to downregulation of αSMA both at the gene expression and the protein level.

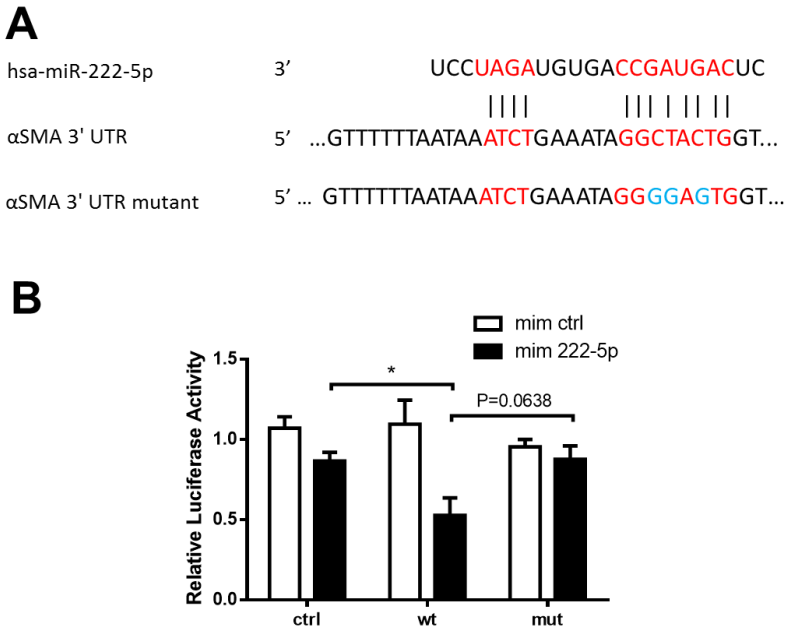

Figure 3-30 3’-UTR of αSMA is a direct target of miR-222-5p

(A) Alignment of miR-222-5p sequence and partial sequence of αSMA 3’-UTR was shown in the figure. The possible complimentary binding between the two sequences are marked in red. Mutation of the predicted binding site was mutated which was marked in blue. **(B)** The 3’-UTR of αSMA was constructed into miRNA target reporter plasmids with humanised firefly luciferase as a reporter of the inhibition of target 3’-UTR and the *Renilla* luciferase as the internal control of plasmid transfection efficiency (Genecopoeia). Dual transfection of plasmids and miR-222-5p into HEK293 cells demonstrated the inhibition of the miRNA on the 3’-UTR of αSMA, and mutation of the predicted target site recovered the inhibition. No significant influence of miR-222-5p on empty plasmid or miRNA mimic negative control on the plasmid with 3’-UTR of αSMA was observed. Data are obtained from at least three independent experiments and shown as mean ± SEM. Statistics are obtained with two-way ANOVA test, followed by Bonferroni post-hoc analysis. *P < 0.05.

3.5.3.3 ROCK2 is a potential target of miR-222-5p

Although αSMA was demonstrated as a direct target of miR-222-5p, it was not sufficient to explain the potent inhibition of Calponin upon treatment of cells with miR-222-5p mimics. Probable explanation was that miR-222-5p in the meanwhile had other targets that could affect SMC differentiation. As introduced earlier, SMC differentiation could also be promoted through RhoA/ROCK pathway. Thus, proteins in this pathway along with proteins involved in Smad-dependent TGFβ1 signalling pathway was checked to see whether there were any potential miR-222-5p targets. 3'-UTR sequences of selected genes were subjected to screening to search for the putative seed site of miR-222-5p "CTACTGA". It was revealed that ROCK2 contained two putative seed sites which strongly implied that it might be targeted by miR-222-5p.

Before moving on to examine the gain- and loss-of-function effect of ROCK2 in the differentiation process and the direct interaction between miR-222-5p and ROCK2, the expression of ROCK2 during MSC-SMC differentiation was firstly explored. Q-PCR analysis demonstrated an upregulation of ROCK2 at the gene expression level in a time-dependent manner (Figure 3-31 A). However, no definite influence of TGFβ1 on the ROCK2 level was demonstrated (Figure 3-31 B). Next, the ROCK2 level was investigated after miR-222-5p mimic treatment. Q-PCR analysis showed the downregulation of ROCK2 at the gene expression level 1 day after miR-222-5p mimic treatment (Figure 3-32 A). Protein level inhibition was also demonstrated by Western blot analysis and immunofluorescent staining (Figure 3-32 B and Figure 3-33). To conclude, ROCK2 expression changes in a time-dependent manner during differentiation and can be remarkably inhibited by miR-222-5p mimics.

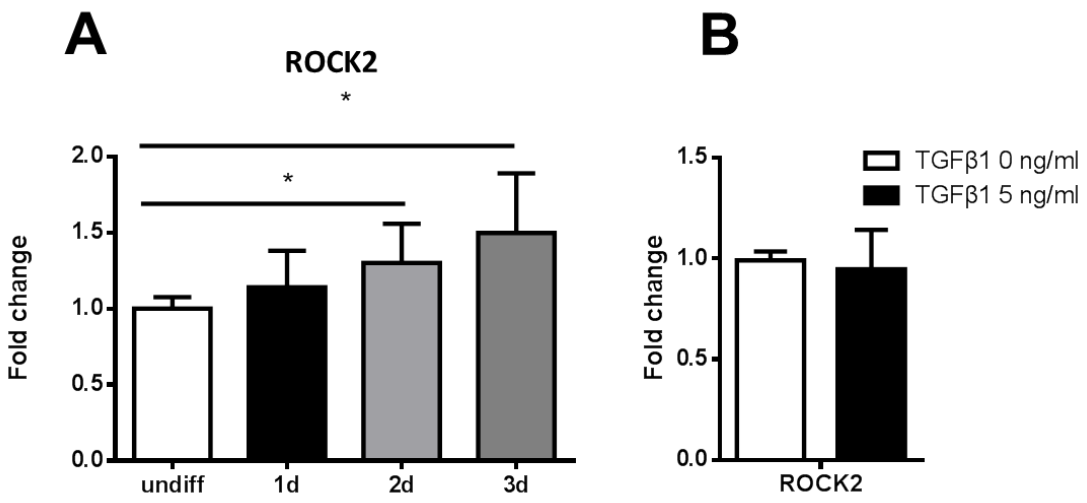

Figure 3-31 ROCK2 level is upregulated in a time-dependent manner but not TGFβ1-dependent manner

HUCMSCs were differentiated in differentiation medium (αMEM with 1% FBS and 5 ng/ml TGFβ1) at $1x10^4$ /cm^2 for 1 to 3 days before being harvested. ROCK2 level was detected with primer at the gene expression level with q-PCR. **(A)** It was shown that ROCK2 level increased in a time-dependent manner along with the differentiation process. **(B)** In comparison with cells cultured in the same condition but without TGFβ1, it was found that ROCK2 level was not altered in cells cultured with TGFβ1. Data are obtained from at least three independent experiments and shown as mean ± SEM. Statistics are obtained with one-way ANOVA test, followed by Bonferroni post-hoc analysis. *$P < 0.05$.

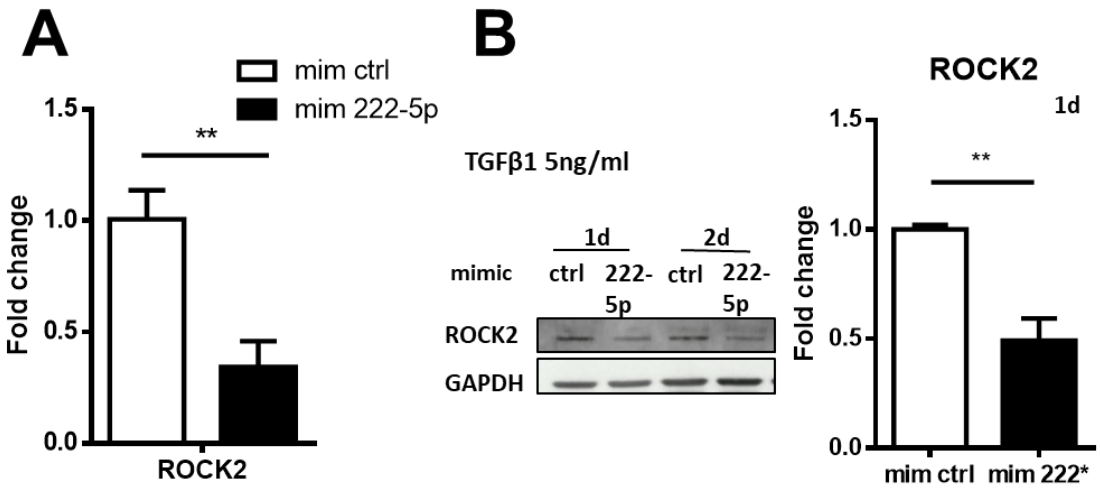

Figure 3-32 ROCK2 is inhibited by miR-222-5p

HUCMSCs were cultured in medium (αMEM with 1% FBS) for 1 day at the density of $1x10^4$ /cm^2 before being transfected with miR-222-5p mimics. Final concentration of miR-222-5p mimics was 12.5 nM. TGFβ1 was not added in the entire process. Cells were harvested 1 day after transfection for q-PCR analysis. **(A)** It was shown that miR-222-5p mimics could potently inhibit the level of ROCK2 at the gene expression level. **(B)** Further protein level examination of ROCK2 1 and 2 days after miR-222-5p mimic treatment was conducted with Western blot analysis. It was demonstrated that ROCK2 could be greatly inhibited at the protein level as early as 1 day after mimic treatment and this inhibition persisted until 2 days after the treatment. Q-PCR data are obtained from at least three independent experiments and shown as mean ± SEM. Western blot images are representative of at least three independent experiments. Statistics are obtained with unpaired student t-test. **P < 0.01.

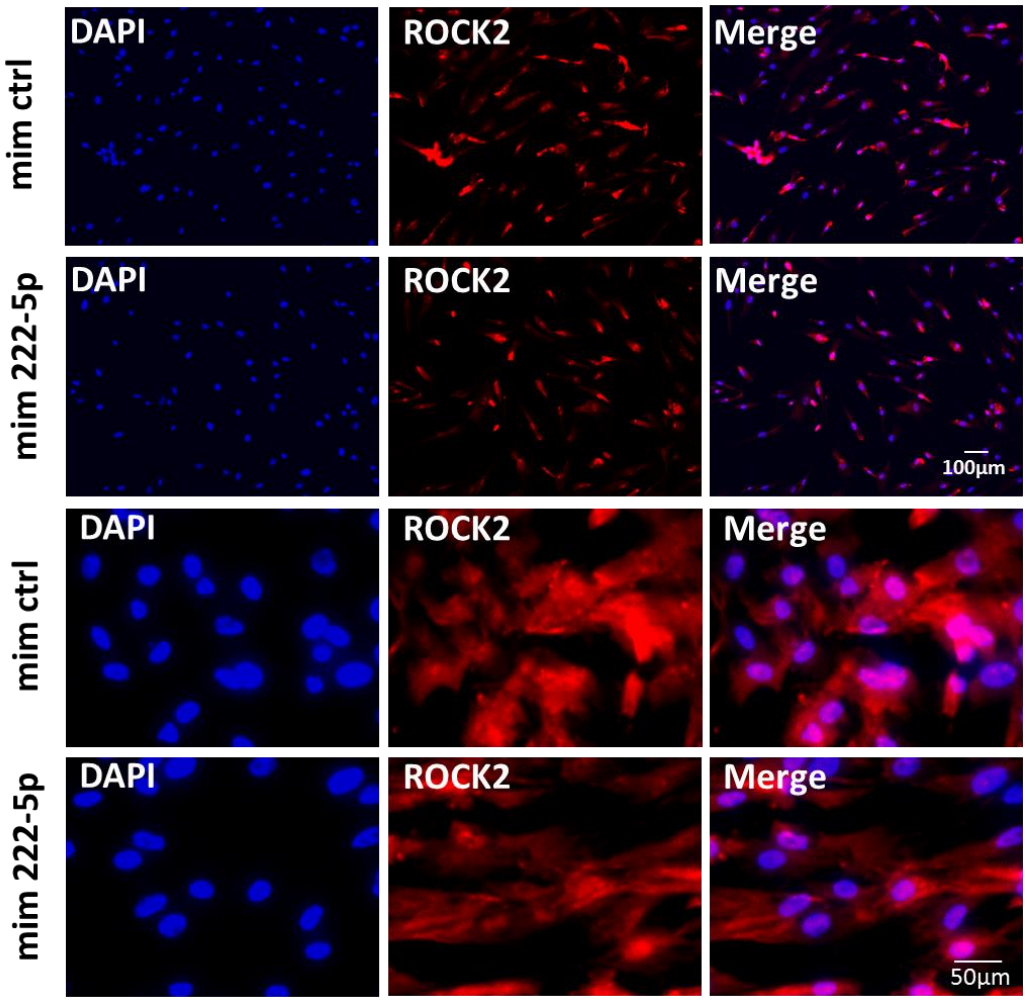

Figure 3-33 ROCK2 is inhibited at the protein level by miR-222-5p mimics

HUCMSCs were cultured in medium (αMEM with 1% FBS) for 1 day at the density of $1x10^4$ /cm^2 before being transfected with miR-222-5p mimics. Final concentration of miR-222-5p mimics was 12.5 nM. TGFβ1 was not added in the entire process. Cells were harvested 2 days after transfection for Immunofluorescent staining of ROCK2. It was shown in the figure that miR-222-5p mimic could downregulate the expression of ROCK2 at the protein level as observed by immunofluorescent staining. Images shown here are representative of at least three independent experiments.

3.5.3.4 ROCK2 knockdown by siRNA inhibits SMC differentiation

Two requirements are elemental for ROCK2 to be a direct functional target of miR-222-5p. First, ROCK2 needs to be functionally involved in the differentiation process. Secondly, miR-222-5p should directly target the 3'-UTR segment of ROCK2.

Knockdown of ROCK2 with siRNA was first examined to check the importance of ROCK2 in SMC differentiation. Confirmation of ROCK2 knockdown was first demonstrated at both the gene expression and protein level (Figure 3-34 A, C and Figure 3-35). Subsequent examination of SMC markers displayed significant inhibition of SMC markers including Calponin and αSMA both at the gene expression level and protein level (Figure 3-34 B and D, Figure 3-35). Even so, the effect of ROCK2 on SMC differentiation was evident. A possible explanation of the limited influence with the presence of TGFβ1 was that TGFβ1 was a very potent growth factor and could activate other signalling pathways to compensate ROCK2 downregulation.

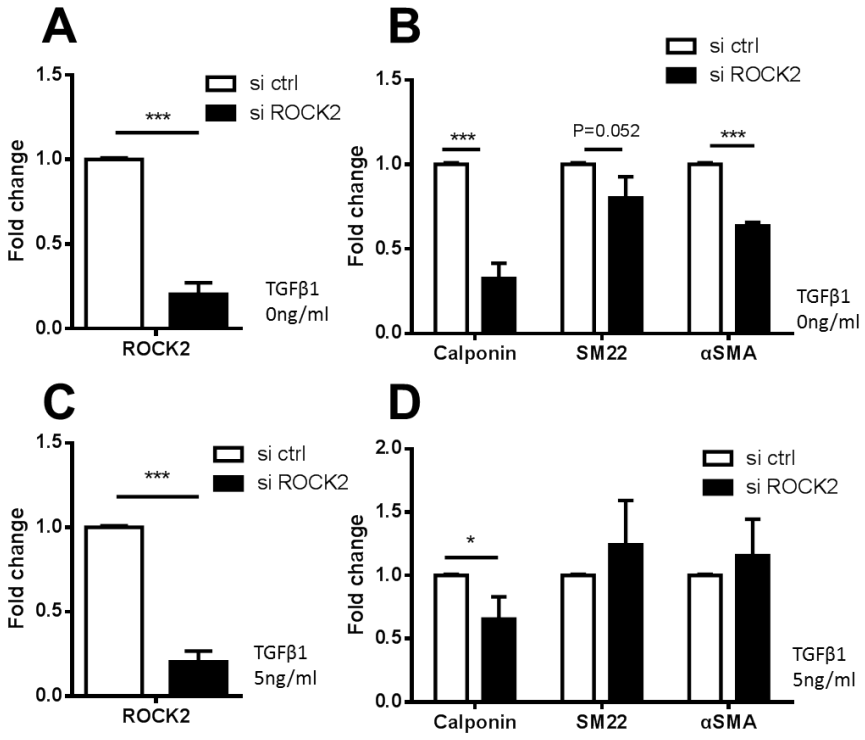

Figure 3-34 Knockdown of ROCK2 with siRNA inhibits the expression of SMC markers at the gene expression level

HUCMSCs were cultured in medium (αMEM with 1% FBS) for 1 day at the density of $1x10^4$ /cm^2 before being transfected with ROCK2 siRNA. The final concentration of ROCK2 siRNA was 5 nM. TGFβ1 addition was as mentioned in the figure. The effects of ROCK2 siRNA knockdown were checked in culture conditions with and without TGFβ1. Cells were harvested 2 days after transfection. **(A and C)** ROCK2 decrease at the gene expression level was confirmed by q-PCR. **(B)** In culture condition without TGFβ1, the effect of ROCK2 knockdown was potent with the downregulation of Calponin, SM22 and αSMA at the gene expression level. **(D)** In culture condition with TGFβ1, the effect of ROCK2 knockdown was less prominent with the only significant decrease of Calponin at the gene expression level. Data are obtained from at least three independent experiments and shown as mean ± SEM. Statistics are obtained from unpaired student t-test. *P < 0.05 and ***P < 0.001.

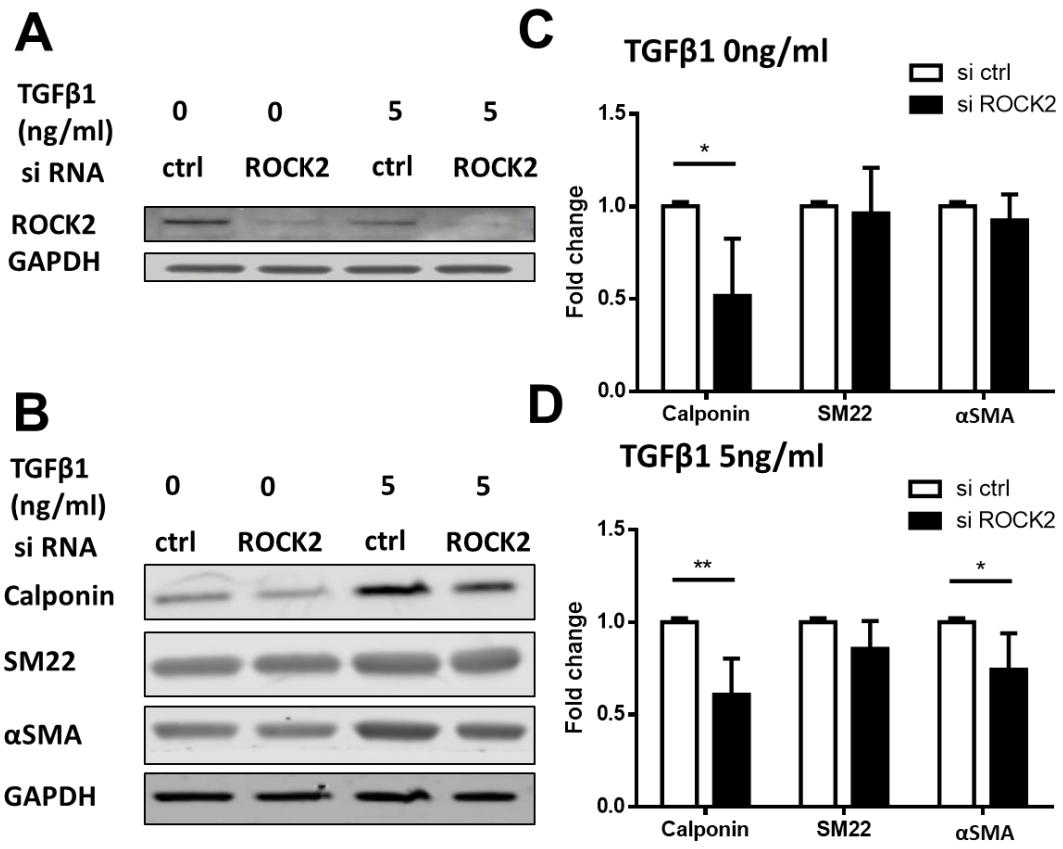

Figure 3-35 Knockdown of ROCK2 with siRNA inhibits the expression of SMC markers at the protein level

HUCMSCs were cultured in medium (αMEM with 1% FBS) for 1 day at the density of $1x10^4$ /cm^2 before being transfected with ROCK2 siRNA. The final concentration of ROCK2 siRNA was 5 nM. TGFβ1 addition was as mentioned in the figure. The effects of ROCK2 siRNA knockdown were both checked in culture conditions with and without TGFβ1. Cells were harvested 2 days after transfection. **(A)** ROCK2 decrease at the protein level was firstly confirmed. **(B)** Moreover, in culture condition without TGFβ1, the effect of ROCK2 knockdown was potent with the downregulation of Calponin and αSMA at the protein level. **(C and D)** Statistical analysis of Western blot results showed signification downregulation of Calponin and αSMA in culture condition with TGFβ1. Result shown is representative of three independent experiments and shown as mean ± SEM. Statistics are obtained from unpaired student t-test. *P < 0.05 and **P < 0.01.

3.5.3.5 ROCK2 3'-UTR is a direct target of miR-222-5p

After establishing that miR-222-5p mimics decreases ROCK2 expression and the functional role of ROCK2 in promoting SMC differentiation, it is essential to explore whether miR-222-5p inhibits ROCK2 through directly targeting ROCK2 3'-UTR or through other mediators. To examine whether ROCK2 3'-UTR was directly targeted by miR-222-5p, the 3'-UTR segment was cloned into miRNA target reporter plasmids. Mutation of the two putative target sites within the 3'-UTR segment was carried out separately or together to check whether the inhibition was through the complimentary binding to either or both putative target sites. Results showed that compared to the empty plasmid, the plasmid containing the wild type ROCK 3'-UTR demonstrated lower relative luciferase activity when co-transfected with miR-222-5p mimics and this effect was not observed when the plasmids were co-transfected with miRNA mimic negative control. Mutation of both target sites, but not a single target site, could rescue the inhibited relative luciferase activity and mutation (Figure 3-36). Taken all into consideration, it could be concluded that ROCK2 3'-UTR is a direct target of miR-222-5p and the inhibitory effect requires the presence of both putative target sites on the 3'-UTR segment.

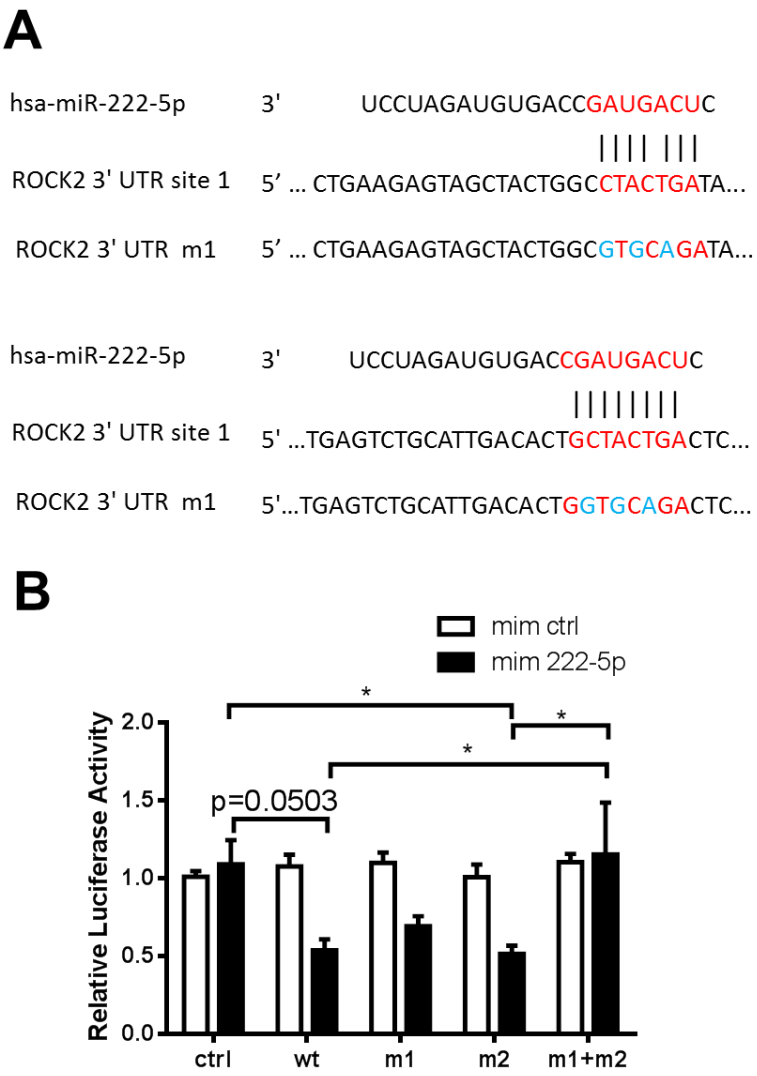

Figure 3-36 3'-UTR of ROCK2 is directly targeted by miR-222-5p

(A) Sequence alignment of miR-222-5p and ROCK2 3'-UTR showed two separate putative target sites (site 1 and site 2) which was marked in red. Mutated nucleotides within the target site were marked in blue. Site 1 and site 2 was first separately mutated to obtain plasmid m1 and m2 respectively. Next, site 2 was mutated in plasmid m1 to obtain a plasmid containing the ROCK2 3'-UTR with both target sites mutated, which was annotated m1 + m2 in later luciferase experiments. **(B)** Empty miRNA target luciferase reporter plasmid (ctrl), plasmid

containing wild type ROCK2 3'-UTR (wt), plasmid with target site 1 mutated (m1), plasmid with target site 2 mutated (m2) and plasmid with both target sites mutated (m1+m2) were transfected into HEK293 cells together with miRNA mimic negative control or miR-222-5p mimics one day after the cells were seeded onto the 24 well culture flask. Lipofectamine 3000 was used as the transfection reagent. 50 ng of plasmid and 25 nM of miRNA plasmids were used in each well of 24 well plate. Cells were harvested 24 hours after transfection for luciferase detection. Ratio of firefly luciferase activity and *Renilla* luciferase activity (relative luciferase activity) was utilised as the parameter for 3'-UTR activity. It was demonstrated that miR-222-5p mimics could result in inhibition of relative luciferase activity in wt plasmids compared with that in empty plasmids. This inhibition was not observed in cells transfected with miRNA mimic negative control. De-repression was only achieved when both target sites were at the same time mutated and mutation of the single target site (target site 1 or target site 2) was not adequate to recover the inhibition. Data are obtained from at least three independent experiments and shown as mean ± SEM. Statistics are obtained with two-way ANOVA test, followed by Bonferroni post-hoc analysis. *$P < 0.05$.

3.5.3.6 Summary of miR-222-5p-involved differentiation mechanism

In the SMC differentiation process, miR-222-5p was downregulated which de-repressed αSMA and ROCK2. ROCK2 was established in other studies to facilitate the polymerisation of glomerular actin (G-actin) to filamentous actin (F-actin), which helped the release of MRTFs from G-actin and free MRTFs were subsequently translocated to the nucleus to work together with SRF and activate the downstream SMC markers. The de-repression of ROCK2 from miR-222-5p could augment SMC differentiation possibly through this depicted pathway (Figure 3-37).

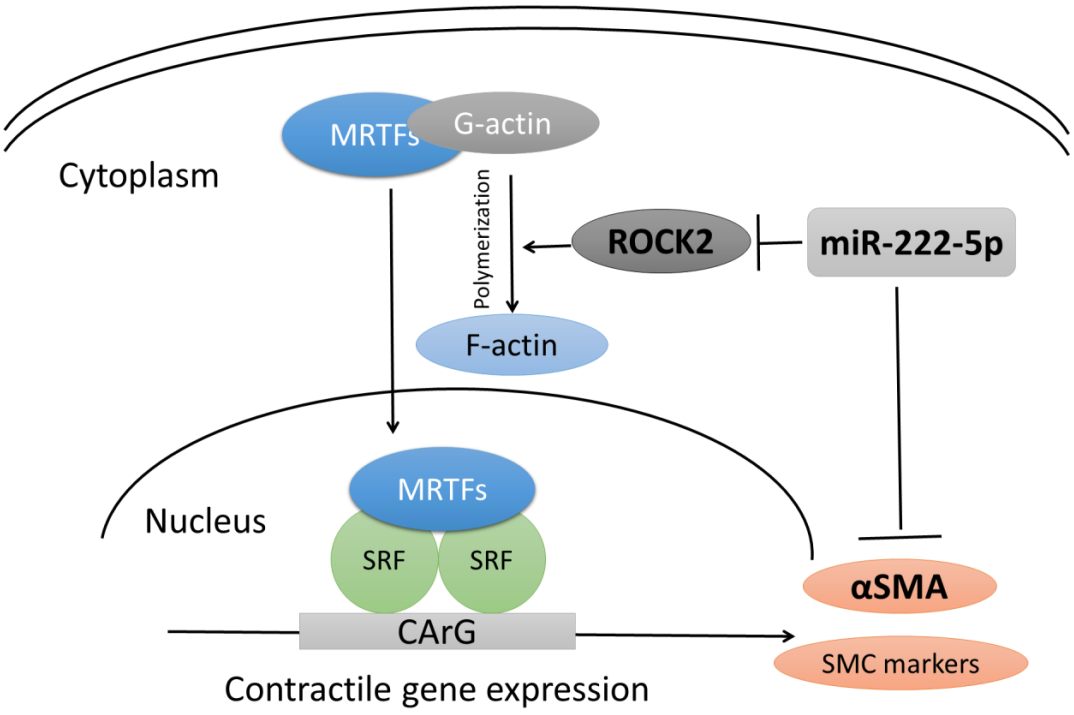

Figure 3-37 Schematic representation of miR-222-5p involved signalling pathway

MiR-222-5p was downregulated in the differentiation system. It directly targeted αSMA and ROCK2. Thus, the downregulation of miR-222-5p further potentiated the upregulation of αSMA and ROCK2. ROCK2 was confirmed to augment SMC differentiation with knockdown experiments. Downstream ROCK2 involved signalling was not further explored in our differentiation system, but it was established in other studies that ROCK2 activation signals through MRTF-dependent pathway to activate SMC markers.

3.6 Vascular graft engineering with hUCMSC-derived SMCs

Tissue engineered vascular grafts emerge to be a promising surgical alternative for cardiovascular diseases. Exploration of novel cell choices and methods for vascular graft engineering continues to be a great research interest which bears significant

clinical importance. Our lab has previously established an *ex vivo* bioreactor system-based method to generate cell seeded vascular grafts with scaffold decellularised from mouse aorta. The constructed vascular grafts displayed comparable structure with native vessels and demonstrated improved patency and function in comparison with decellularised grafts that were not seeded with cells (Campagnolo et al., 2015a; Margariti et al., 2012; Wong et al., 2015).

3.6.1 Confirmation of decellularisation efficiency

Mouse aorta was harvested and decellularised with detergents as described in the Method section. The efficiency of the decellularisation was shown by DAPI staining of the graft in *en face* samples. Decellularised vascular graft demonstrated weak staining of destructed nucleus fraction, whereas the nucleus was intact and in an undamaged shape in the cells within the normal aorta (Figure 3-38). Further inspection of the SMC marker reminiscence on the cross-sections of decellularised aorta displayed minimal SMC marker staining including Calponin and αSMA, and in comparison, the staining of these markers on the normal aorta demonstrated much stronger signal (Figure 3-39). Collectively, successful decellularisation of the mouse aorta was achieved.

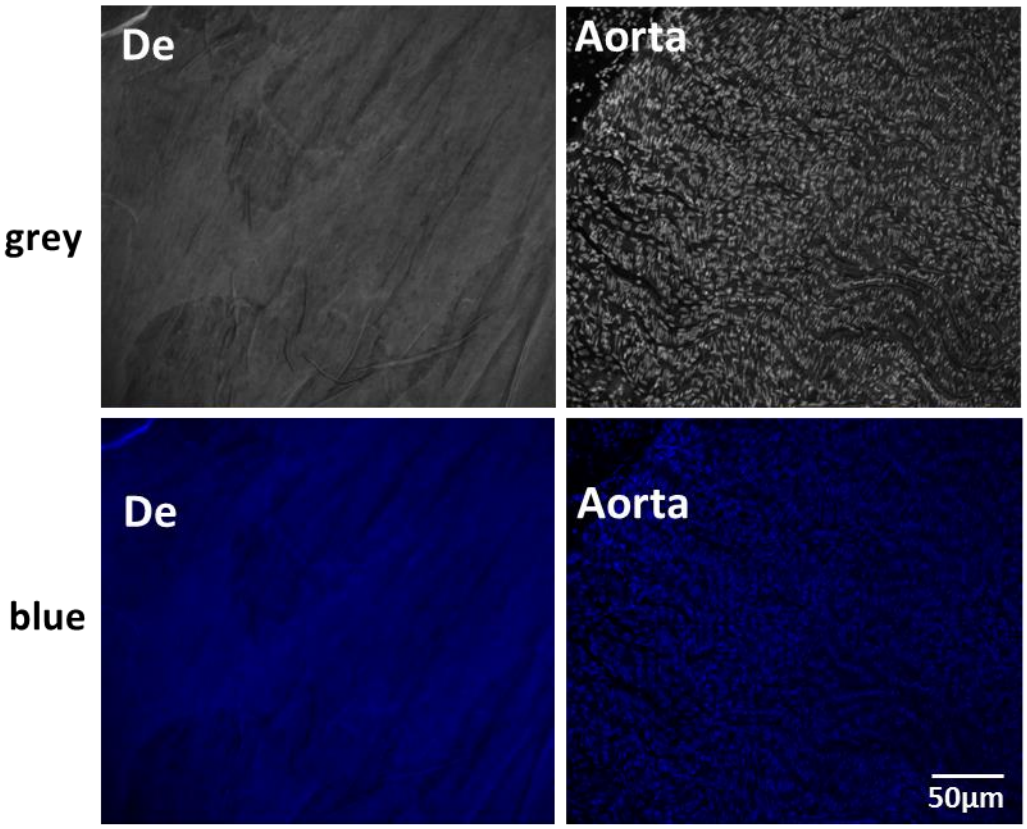

Figure 3-38 Decellularisation of mouse aorta

Mouse aorta was harvested and decellularised with detergents as depicted in method part. Decellularised aorta was subjected to *en face* staining with DAPI. DAPI staining showed that cell nucleus on the decellularised vascular graft were destructed with minimal reminiscent nucleus fraction stained, and the nuclei in the cells on the normal aorta displayed their characteristic shape. De indicates decellularised aorta, and Aorta indicates normal mouse aorta. Presented images are representatives of three independent experiments.

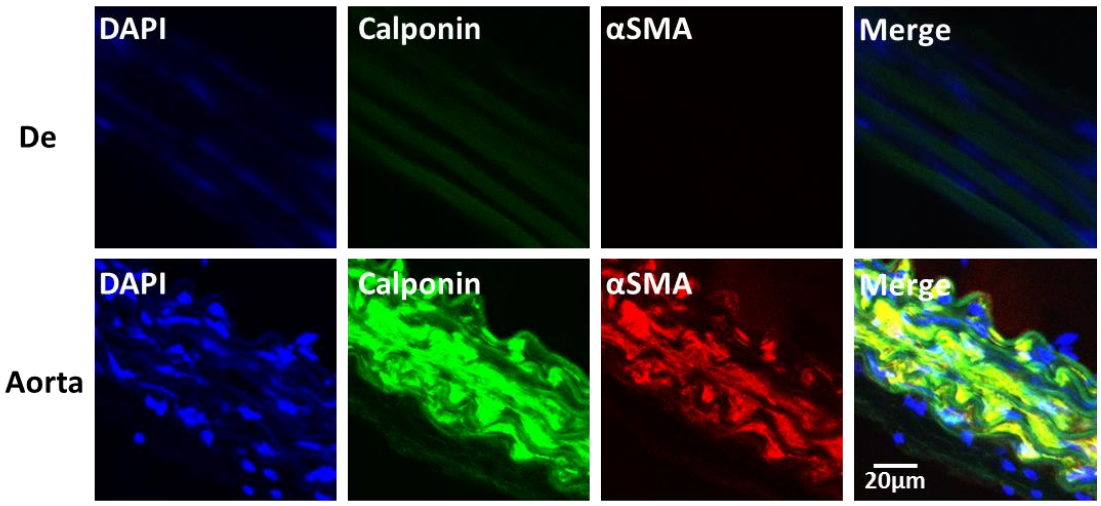

Figure 3-39 SMC markers were not stained in decellularised vascular graft

Decellularised aorta grafts as well as normal aortas were cut into sections in 30 μm thickness and then stained with DAPI and SMC markers. Consistent with the previous figure, decellularised graft only displayed minimal reminiscent nuclear fraction staining, whereas the DAPI staining in the normal aorta demonstrated the normal shape of cell nuclei. Moreover, compared with the normal aorta, decellularised grafts were not staining with SMC markers Calponin and αSMA, which displayed the efficiency of decellularisation. De indicates decellularised aorta, and Aorta indicates normal mouse aorta. Images shown are representative of two independent experiments.

3.6.2 Engineering of vascular graft with hUCMSC-derived SMCs

After confirmation of the decellularisation efficiency, cell seeding was then performed for the construction of vascular grafts. SMCs differentiated from hUCMSCs were mixed in Matrigel and then wrapped outside the decellularised scaffold that was connected to the bioreactor system. The medium was then added to the culture chamber and inside the system after the solidification of the Matrigel. The graft was harvested 5 days after it was kept in the bioreactor system with medium flowing inside. Staining of the graft with DAPI showed the colonisation of seeded cells in the decellularised scaffold compared to the scaffold that was not seeded with cells (Figure 3-40). Further examination of the generated graft with SMC marker staining, including Calponin, SM22, αSMA and SMMHC, demonstrated that the seeded cells retained SMC marker expression after they migrated inside the decellularised scaffold (Figure 3-41).

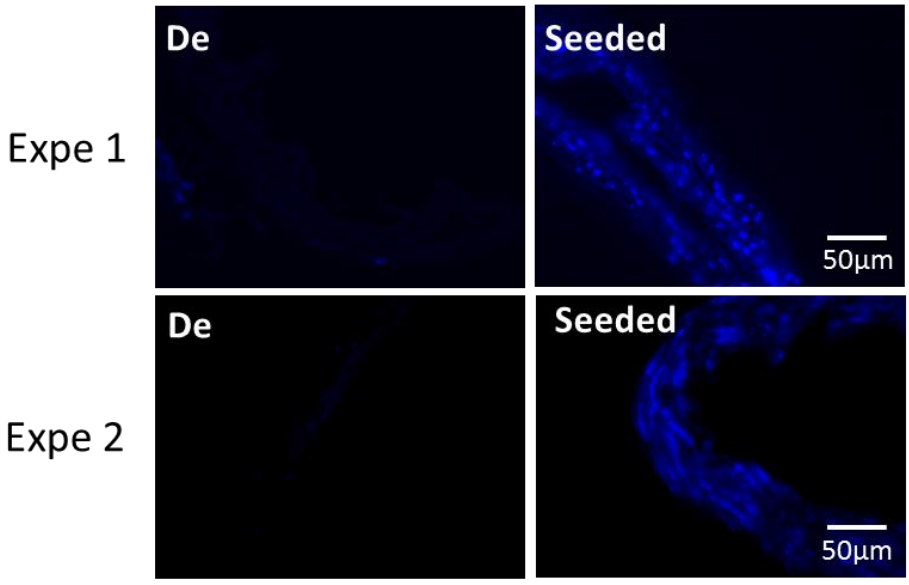

Figure 3-40 Cell seeding onto the decellularised vascular grafts

HUCMSCs were cultured in differentiated medium (αMEM with 1% FBS and 5 ng/ml TGFβ1) for 5 days and then mixed in Matrigel which was then wrapped outside the decellularised vascular graft and connected to the bioreactor system. Medium in the chamber and flowing

inside the bioreactor system was αMEM with 10% FBS and 5 ng/ml TGFβ1. After being kept in the bioreactor system for 5 days, the graft was harvested and subjected to frozen sectioning with the thickness of 30 μm. DAPI staining demonstrated the colonisation of seeded cells in the decellularised vascular graft, whereas decellularised vascular graft was not stained with DAPI. Images from two representative experiments are shown and three independent experiments in total were conducted.

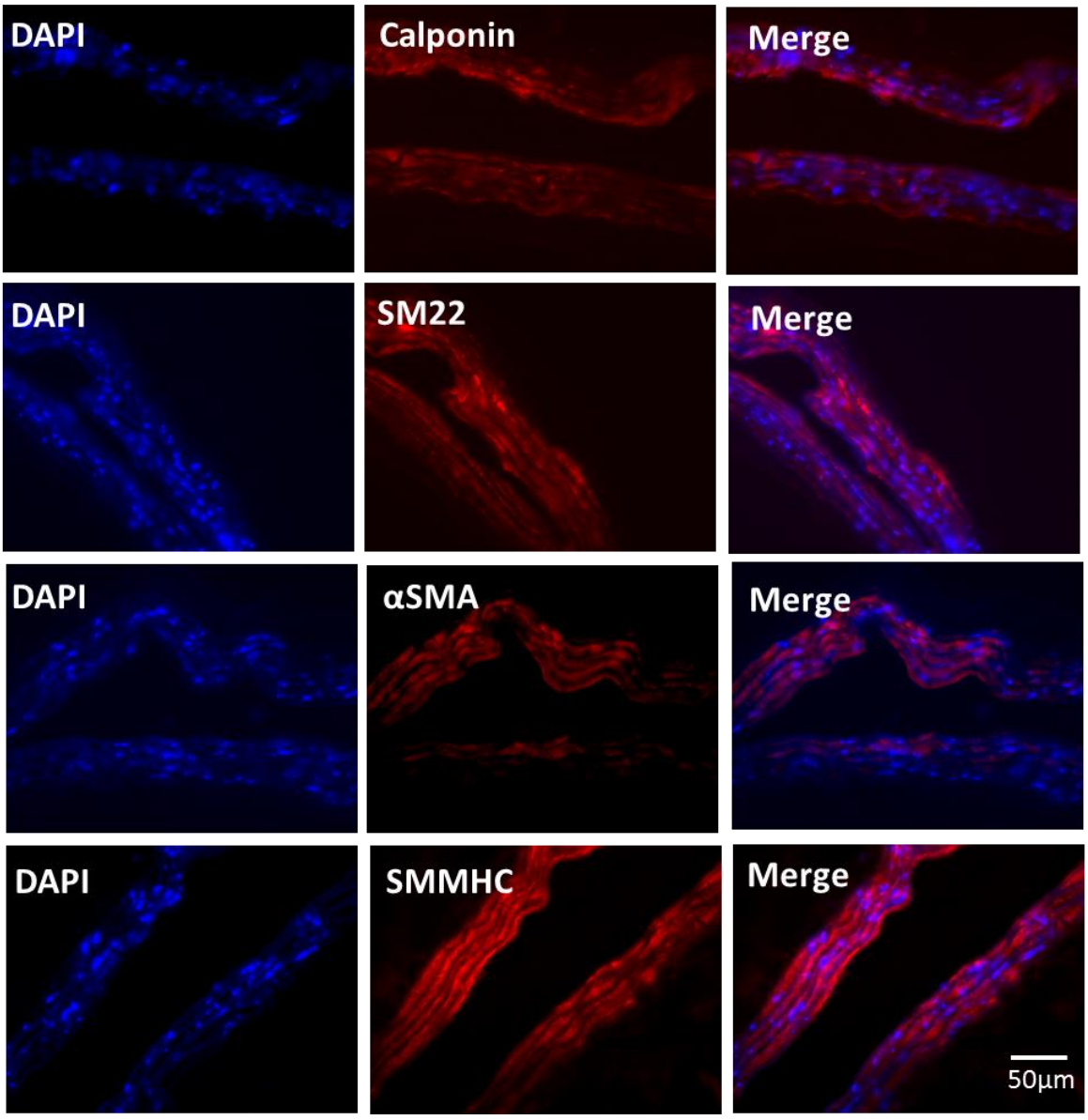

Figure 3-41 Differentiated cells migrated into the decellularised vascular graft and expressed SMC markers

HUCMSCs were cultured in differentiation medium (αMEM with 1% FBS and 5 ng/ml TGFβ1) for 5 days and then mixed in Matrigel to be wrapped outside the decellularised vascular graft which was then connected to the bioreactor system. The medium in the chamber and flowing inside the bioreactor system was αMEM with 10% FBS and 5 ng/ml TGFβ1. After being kept in the bioreactor system for 5 days, the graft was harvested and subjected to frozen sectioning with the thickness of 30 μm. Staining of the vascular grafts for SMC markers including Calponin, SM22, αSMA and SMMHC showed that the differentiated cells seeded outside the graft managed to migrate inside and retain the SMC marker expression. Demonstrated images are representative of at least three independent experiments.

4. Discussion

In this study, I have successfully established an efficient protocol to differentiate hUCMSCs towards the SMC lineage and have explored the underlying miRNA-related mechanisms. Furthermore, I have tested the potential of these differentiated SMCs for vascular graft engineering. The SMC differentiation was achieved through culturing the cells in low serum medium with the addition of TGFβ1, an established and potent stimulator for SMC differentiation. Notably, these differentiated cells exhibited typical functional SMC properties, including increased contractility and vasculogenesis capacity. Subsequently, the miRNA centred mechanism involved in this differentiation process was elucidated with the identification of novel regulatory miRNAs (miR-503-5p and miR-222-5p). Moreover, these miRNAs participate in SMC differentiation through targeting known components of established TGFβ1 signalling pathways, including the Smad-dependent pathway and ROCK-dependent pathway. Finally, vascular grafts could be generated utilising the differentiated SMCs from hUCMSCs, indicating the potential application of the cells in vascular tissue engineering.

4.1 Establishment of the differentiation protocol from hUCMSCs towards the SMC lineage

The differentiation of stem cells towards SMCs is usually achieved through the manipulation of the cell culture condition including the addition of various biochemicals, the concentration of serum and duration of differentiation. Numerous growth factors like TGFβ1, bone morphogenetic protein 4 (BMP4), angiotensin II (Kim et al., 2008), sphingosine 1- phosphate (Lockman et al., 2004) and thromboxane A2 (Kim et al., 2009) could all be utilised to stimulate SMC differentiation (Elcin et al., 2017). Among these reagents, TGFβ1 is a potent stimulator for SMC differentiation from stem cells both *in vitro* and *in vivo* (Grainger et al., 1998; Guo et al., 2013;

Yamazaki et al., 2017). It promotes the induction of SMC contractile markers including Calponin, SM22, αSMA and SMMHC in cultured SMCs (Bjorkerud, 1991; Deaton et al., 2005). Furthermore, these factors could cooperate or interact with each other. The promotion of SMC differentiation from human mesenchymal stem cells by sphingosine-1-phosphate was dependent on TGFβ1 signalling pathway (Jeon et al., 2006). Studies also showed that only when TGFβ1 was combined with BMP4 could contractile SMCs be obtained (Elcin et al., 2017; Wang et al., 2010b).

Due to the potency and widespread use of TGFβ1 in inducing SMC differentiation, it was tested in this study. It demonstrated a concentration-dependent and time-dependent enhancement of SMC marker level both at the gene expression and the protein level, together with augmented contractility and vasculogenesis potential, which are functions typically displayed by SMCs. For this reason, further addition of BMP4 was not necessary. Apart from the induction of contractile SMC markers during the differentiation process, induction of extracellular matrix proteins such as collagen I and elastin by TGFβ1 demonstrates the potential of these differentiated cells to be utilised in vascular graft engineering as production of extracellular matrix proteins would help increase the mechanical strength and bio-compatibility of the graft. This is consistent with published results showing elastin matrix enhancement in vascular SMCs upon stimulation of TGFβ1 and hyaluronan (Kothapalli et al., 2009).

Another culture condition that was optimised in the experimental system was the serum concentration. *In vitro* culture condition with high serum concentration induces the smooth muscle cells to enter the proliferative synthetic phenotype which is similar to the smooth muscle cell phenotypic switching during vascular injuries (Poliseno et al., 2006; Shankman et al., 2015). The synthetic phenotype can be switched back to contractile phenotype upon serum deprivation as indicated by the increases in contractile markers (Poliseno et al., 2006). In SMC differentiation from stem cell sources such as pluripotent stem cells, BMMSCs and skin-derived precursors, contractile SMCs were acquired with lower serum concentration (Steinbach et al., 2011; Tamama et al., 2008; Wanjare et al., 2013). Although contradictory studies exist demonstrating that serum concentration in the culture medium does not affect

SMC marker expression, these reports are few and isolated (Gong et al., 2009). Thus, it could be concluded overall that serum concentration reduction or deprivation are in favour of functional SMC differentiation.

As to whether lower serum concentration could enhance SMC differentiation, experimental evidence was gathered in the present differentiation process from hUCMSCs to SMC lineage. Compared to differentiation medium containing 10% FBS, hUCMSCs differentiated in medium containing 1% FBS displayed at least two-fold higher expression of almost all SMC contractile markers including Calponin, SM22, and αSMA either with or without TGFβ1 except for SMMHC. The unaffected level of SMMHC in conditions with different serum concentrations in TGFβ1 containing medium might be explained by the potent effect of TGFβ1 that masked the effect of serum concentration. This result is reasonable considering that the serum concentration of the basal culture medium for hUCMSCs is 2% which is already quite low. Therefore, differentiation medium with 1% FBS and TGFβ1 was utilised in subsequent experiments as established differentiation condition unless otherwise specified.

Furthermore, it is noteworthy that the basal culture medium of hUCMSCs contains 2% FBS as well as growth factors including basic fibroblast growth factor (bFGF), acidic fibroblast growth factor (aFGF) and epidermal growth factor (EGF). It was shown by several studies that bFGF helps promote the proliferation capacity of mesenchymal stem cells and retain the multi-potent differentiation capacity which justifies its utilisation in MSC culture (Eom et al., 2014; Hori et al., 2004; Solchaga et al., 2005; Sotiropoulou et al., 2006; Tsutsumi et al., 2001). In the meantime, it was found in vascular SMCs that FGF signalling inhibits TGFβ-induced SMC phenotypic switching from synthetic phenotype to contractile phenotype, which suggests that FGF signalling pathway inhibits the low basal expression of SMC markers present in MSCs (Chen et al., 2016; Schuliga et al., 2013).

Under this postulation, the switch of the culture medium of hUCMSCs from basal medium with bFGF to differentiation medium without bFGF might retract the

suppression of bFGF on SMC marker expression and manifest the spontaneous differentiation capacity of hUCMSCs. This is proved to be crucial as shown by the significant increase of contractile SMC markers expression both at the mRNA and protein level in hUCMSCs cultured with medium deprived of bFGF and containing only 1% FBS compared to undifferentiated hUCMSCs. The lineage specific differentiation of hUCMSCs to SMCs was further enhanced by TGFβ1 addition.

4.2 Functional characterisation of differentiated SMCs

Physiologically, SMCs reside in the media layer of the vessel and display the contractile capacity to maintain the vascular tone. In vascular tissue engineering, it is essential to construct vascular grafts which have contractile SMCs in the media layer to achieve satisfying vascular tone and sufficient mechanical strength. At present, there are several approaches to examine the contractile function of SMCs *in vitro*. First, contractility of SMCs could be checked at the single cell level with calcium sensitising reagent such as KCl. Subsequent change of contractility could be measured with the change of force produced by the cells (Ratz et al., 2005). Karamariti et al. visualised the migration of SMCs derived from reprogrammed pluripotent stem cells with time lapse microscopy after stimulating the cells with KCl which provides indirect evidence of the cell function (Karamariti et al., 2013b). Furthermore, the contractile function of the SMCs could be detected at the cell population level with collagen gel contraction assay in which the cells were mixed with collagen I to form polymerised gel lattice (Jiang et al., 2010; Lenga et al., 2008). Cells with better contractility would yield collagen gel with a smaller diameter when the gel is freed from the culture flask (Jiang et al., 2010; Lenga et al., 2008).

In this study, *in vitro* examination of the contractility was explored with collagen gel contraction assay given that in the established differentiation protocol from hUCMSCs to SMCs, more than 90% of the cells expressed contractile markers after 5 days of differentiation. Therefore, population level examination of the cells would be sufficient

to represent the contractile function improvement after differentiation. Consistent with the strong differentiation capacity demonstrated by the high level of contractile SMC marker expression, increases of in their contractile potential after differentiation further confirmed the efficiency of differentiation. Furthermore, SMCs are a major component of vessels that are with larger diameters. The hUCMSCs-derived SMCs, when mixed with endothelial cells in subcutaneous Matrigel plugs, exhibited the capacity to form finer vascular structures with αSMA-expressing media layer. This is evidence that differentiated cells display a better vasculogenesis function when mixed with endothelial cells.

4.3 Exploration of SMC differentiation mechanism

The SMC differentiation mechanism is a complex regulatory network. Exploration of novel miRNAs involved in the differentiation network could provide new therapeutic choices. In vascular tissue engineering, miRNAs that could improve SMC differentiation and contractile function bear great potential in improving graft performance. Since TGFβ1 was added to the differentiation medium and directed the lineage commitment of hUCMSC to SMC lineage, further exploration of the mechanism underlying SMC differentiation was mainly focused on merging novel miRNAs uncovered by the miRNA array with well-established TGFβ1-related signalling pathways.

Successful differentiation protocol was confirmed first by the detected increase of Myocardin and SRF in the differentiation process in addition to contractile SMC markers. It was also confirmed that miR-145, a well-established contractile SMC differentiation enhancer, was also upregulated in a time-dependent manner in the differentiation system (Boucher et al., 2011; Cordes et al., 2009). Exploration of miR-145-related SMC differentiation mechanism has mainly involved candidates lying upstream and downstream in the pathways. Apart from Myocardin and SRF, it was revealed that miR-145 could also be upregulated by TGFβ1 (Cordes et al., 2009;

Gays et al., 2017; Long and Miano, 2011). Smad binding elements were characterised in an enhancer region of miR-145 and the binding of Smad4 on this region was confirmed by chromatin immunoprecipitation experiments (Long and Miano, 2011). Jagged 1/Notch signalling pathway could also control the expression of miR-145. Downstream targets of miR-145 include Klf4 (Kruppel-like factor 4), Elk-1 (ELK1, a member of ETS oncogene family) and Myocardin (Cordes et al., 2009). There are also reports in cancer cells showing that miR-145 could target Smad3 to inhibit TGFβ1-induced epithelial-mesenchymal transition and cancer invasion and target ROCK1 to inhibit proliferation and invasion of osteosarcoma cells (Hu et al., 2016; Li et al., 2014). As Smad3 and ROCK1 are both components of TGFβ signalling pathways, these imply a complex interaction between miR-145 and TGFβ signalling pathways.

After uncovering novel miRNAs whose expression is changed during MSC-SMC differentiation using miRNA array, miR-503, which is upregulated during the differentiation process and promotes MSC-SMC differentiation, as well as miR-222-5p, which is downregulated in the differentiation process and de-represses MSC-SMC differentiation, emerge to be two promising candidates. To further establish their roles in SMC differentiation, similar approaches to the study of miR-145 involvement were employed placing the exploration focuses on the upstream control of miRNA level and the downstream targets. More importantly, both upstream upregulation of miRNAs and downstream target explorations were tightly oriented within well-established TGFβ1 signalling pathways. Detailed exploration of the mechanism will be discussed below.

4.3.1 Mechanism of SMC differentiation – miR-503-related mechanism

4.3.1.1 Targets of miR-503 during MSC-SMC differentiation

MiR-503 participates in numerous pathophysiological conditions. In cancer cells, it can target L1CAM (L1 cell adhesion molecule), thus inhibiting the proliferation and invasion of glioma cells and target oncogene DDHD2, thus inhibiting the proliferation

of human glioma cells (Liu et al., 2015; Polioudakis et al., 2015). In pulmonary arterial hypertension, miR-503 can be regulated by endothelial apelin and target FGF in pulmonary SMCs, thereby disrupting the apelin-FGF link and mediating pulmonary arterial hypertension disease progression (Kim et al., 2013). Interestingly, apelin could be targeted by miR-503 in cardiac fibrosis, which suggests that in miRNA regulation of pathological conditions, at least for miR-503, feedback control exists and might be widespread (Zhou et al., 2016b).

Other downstream targets of miR-503 include Cdc25A, CCND1 and Cyclin D3 which promote cell cycle quiescence and inhibit proliferation (Long et al., 2015; Sarkar et al., 2010; Xiao et al., 2013). Particularly, it was shown that miR-424, which belongs to the same family of miR-503, can target Cyclin D1, decrease SMC proliferation and ultimately attenuate neointimal formation after vascular injury (Merlet et al., 2013). Moreover, important components of TGFβ1 signalling pathways are also shown to be targets of miR-503. These include Smurf1 (SMAD specific E3 ubiquitin protein ligase 1), Smurf2 (SMAD specific E3 ubiquitin protein ligase 2) and Smad7, among which the latter three are negative regulators of the TGFβ1 Smad-dependent signalling pathway (Cao et al., 2014; Llobet-Navas et al., 2014; Sun et al., 2017; Zhao et al., 2017b).

In this study, miR-503 has been confirmed to directly target Smad7 by binding onto its 3'-UTR, leading to RNA degradation. This is the first time that miR-503 has been shown to target Smad7, thereby influencing SMC differentiation process. In Smad-dependent signalling, TGFβ1 binds to and activates the TGFβ receptors on the cell membrane, and subsequently mediates the phosphorylation of R-Smad/Co-Smad complex. The phosphorylated complex is then translocated to the nucleus, and binds to the Smad binding element at the promoter region of target genes, thereby upregulating the gene transcription (Derynck and Zhang, 2003). Smad7 exhibits an inhibitory effect on Smad-dependent signalling pathway by binding to the TGFβ type I receptor on the cell membrane, thus blocking the binding of R-Smad/Co-Smad complex to the receptor or the phosphorylation of the complex. Interestingly, although Smad7 is a well-known negative regulator of TGFβ1 Smad-dependent signalling

pathway, it could be transcriptionally upregulated by TGFβ1, suggesting a negative feedback loop control for TGFβ1 signalling (Nakao et al., 1997; Zhu et al., 2004). Upregulation of Smad7 during the MSC-SMC differentiation process and the increased SMC differentiation when Smad7 is knocked down in this study are consistent with those published in the literature. However, the augmented SMC differentiation after siRNA-mediated Smad7 knockdown was mainly exhibited on Calponin at the protein level, suggesting that other mechanisms mediating SMC differentiation might also be at play.

In addition to Smad7, there are other potential targets of miR-503 which might participate in the SMC differentiation system, such as targets involved in cell cycle control as mentioned above. These targets are not examined in the current study since they might not fit into the complex network of TGFβ1 signalling pathway. However, the inhibition of proliferation resulted from the downregulation of these targets might help potentiate the upregulation of contractile SMC markers, which is consistent with the role of miR-503 in promoting SMC differentiation (Merlet et al., 2013). However, the regulation of miR-503 and its specific targets are delicate and context-dependent, and it cannot be simply denoted here that these proliferation-related targets are involved in this MSC-SMC differentiation system without experimental evidence.

4.3.1.2 Transcriptional regulation of miR-503

As to the upstream regulation of miR-503 transcription, peroxisome proliferator-activated receptor γ (PPARγ) was demonstrated to be a direct regulator (Lee et al., 2017). Under inflammatory conditions, PPARγ level and activity were both downregulated in endothelial cells, which led to downregulation of miR-503 and the upregulation of miR-503 target CD40 (Lee et al., 2017). NF-κB (nuclear factor κ-light-chain-enhancer of activated B cells) was also proved to be a major regulator of miR-503 expression. Upon stimulation with LPS (lipopolysaccharides), epithelial cells exhibited increased recruitment of NF-κB p50 and HDACs at the promoter region of miR-503 and subsequent downregulation of miR-503 level (Zhou et al., 2013). In

diabetic conditions, hyperglycemia triggered the upregulation of miR-503 through NF-κB p75-dependent manner in vascular endothelial cells and the produced miR-503 could exert effects on adjacent pericytes and influence vascular pericyte coverage (Caporali et al., 2015). MiR-503 could also be upregulated through Smad-dependent pathway as shown in the epithelial remodelling of the mammary gland (Llobet-Navas et al., 2014).

In the current study, as suggested by the close relationship between TGFβ1 stimulation and increased miR-503 expression, it was postulated that TGFβ1 signalling pathway might be the dominant pathway regulating miR-503 transcription. This was later confirmed with the downregulation of miR-503 level after Smad4 knockdown and the enrichment of Smad4 at the promoter region of miR-503 after TGFβ1 treatment as demonstrated by ChIP experiments. Consistent downregulation of miR-503 after Smad4 knockdown was not achieved in culture conditions without TGFβ1 as miR-503 is upregulated through TGFβ1 activation via Smad4. Furthermore, even though other potential upstream signalling pathways are not examined and excluded here, sufficient evidences have been obtained to conclude the definite role of Smad4 in miR-503 transcriptional upregulation during MSC-SMC differentiation.

4.3.1.3 Lineage specification effect of miR-503

Different from what is validated in our system demonstrating the vital role of miR-503 in SMC lineage differentiation, other published reports have shown the importance of miR-503 in determining cardiac progenitor cell fate commitment to cardiomyocytes, as well as promoting monocyte differentiation from THP-1 cells (an M5-acute myeloid leukemia cell line containing the MLL-MLLT3 fusion) when combined with other miRNAs (Forrest et al., 2010; Shen et al., 2016). There are two possible explanations for this. First, the lineage specification of miR-503 to cardiomyocytes or monocytes is attributed to the anti-proliferative effects rather than lineage specification effects. In the promotion of monocytic differentiation, the effect of miR-503 lies in their inhibition of targets involved in cell proliferation and it needs to be combined with other miRNAs such as miR-155 and miR-222 to ultimately drive the cell differentiation towards

monocytes. Another explanation is that miR-503 might be a lineage-determining miRNA towards muscle cell lineage that encompasses cardiomyocytes, skeletal muscle cells and the smooth muscle cell lineage which is studied here. Furthermore, the context-dependent regulation should always be taken into consideration while the results are being interpreted. Different stem cell lines as well as different stimulators have been utilised in this study compared to those published studies. MiR-503 might play different roles in these different contexts.

What is also noteworthy is that miR-503 gene locates within the X chromosome. Notably, the promotion of SMC differentiation by miR-503 might be one attributable factor for the different morbidity of pulmonary hypertension in subjects with different genders (Dempsie and MacLean, 2013; Swift et al., 2014). This is an avenue for future investigations on elucidating the possible relationship of this miRNA with other sex-linked diseases such as coronary artery disease (Yahagi et al., 2015).

4.3.2 Mechanism of SMC differentiation – miR-222-5p-related mechanism

MiR-222 participates in numerous physiological and pathophysiological conditions including cancer progression, skeletal muscle regeneration and vascular remodelling. It was reported that miR-222 targets cyclin-dependent kinase inhibitor 1B (CDKN1B/$p27^{kip1}$) in hepatocellular carcinoma HepG2 cells and breast cancer cells, promoting cell proliferation and mediating tumour growth (Wang et al., 2016; Yang et al., 2014). In breast cancers, miR-222 starts to get recognised as a biomarker since it could target estrogen receptor α (ERα) (Chen et al., 2013). Inhibitory effect of miR-222 on tumour cell proliferation was also observed. In lung cancer cells, miR-222 induces S phase arrest in the cell cycle, thus inhibiting tumour growth (Yamashita et al., 2015). Apart from cancers, miR-222 also could target cyclin-dependent kinase inhibitor 1C (CDKN1C/$p57^{kip2}$) and regenerate skeletal muscle after hindlimb ischemia (Togliatto et al., 2013). In vascular diseases, miR-222 was shown to exert a pro-proliferative and pro-migratory effect by targeting CDKN1B/$p27^{kip1}$ and CDKN1C/$p57^{kip2}$ which results in promotion of smooth muscle cell proliferation and

neointimal hyperplasia (Liu et al., 2009; Urbich et al., 2008). In endothelial cells, however, they display contrary anti-proliferative and anti-migratory effect which causes inhibition of re-endothelialisation after vascular injury, possibly through targeting c-kit (Liu et al., 2012). Different effects of miR-222 in different cell types imply the importance of the contexts for miRNAs to exert their functions. Furthermore, miR-222 was demonstrated to be crucial in vascular calcification and vascular remodelling upon inflammatory stimuli (Dentelli et al., 2010; Mackenzie et al., 2014). In one study, miR-222 was shown to repress the TGFβ1-induced growth inhibition in breast cancer cells (Rao et al., 2011). However, there has been no report in the literature demonstrating the direct relation of miR-222 with TGFβ1 signalling pathway.

As to the upstream upregulation of miR-222, only isolated reports exist. MiR-222-3p was shown to be upregulated in a p53-dependent manner, but chromatin immunoprecipitation experiments did not demonstrate its direct binding to the promoter region of miR-222 (Rihani et al., 2015). In the promoter region of miR-222, binding sites for NF-κB p65 and c-jun were characterised and found to cooperate with each other to control the miR-222 transcription, which subsequently exerts oncogenic effect in prostate carcinoma and glioblastoma cell lines (Galardi et al., 2011).

However, these studies have limited significance in providing information for the study of miR-222-5p in the current experimental system, as it was the mature strand miR-222-3p that was examined in most publications. In the MSC-SMC differentiation system here, miR-222-5p, which is the passenger strand of miR-222, was examined. Despite the general recognition that miRNA star strand or passenger strand goes through degradation rapidly and does not exert any regulatory function, this consensus was challenged in recent years. Abundant reports have emerged and depicted the fate of miRNA passenger strand as well as their regulatory role in human diseases such as cancers, inflammatory diseases and cardiovascular diseases (Bhayani et al., 2012; Guo and Lu, 2010; Mah et al., 2010; Yang et al., 2011). Furthermore, genomic analyses revealed that more than 40% of the miRNA star strands displayed conservation across species and conservative targets were preferred when they exert effects (Okamura et al., 2008). In addition, in some miRNAs,

both strands would cooperate with each other to participate in the regulation of the same disease condition or pathological circumstance. MiR-200b-3p and miR-200b-5p function together to inhibit the epithelial to mesenchymal transition in breast cancer cells (Rhodes et al., 2015). MiR-126 and miR-126* work together in regulating leukocyte adhesion to endothelium (Cerutti et al., 2017). What is more interesting is that miR-17-5p and miR-17-3p regulate the same target tissue inhibitor of metalloproteinase 3 (TIMP3) and modulate prostate tumour growth (Yang et al., 2013).

In this study, miR-222-5p is the star strand of miR-222. It was found to be important in regulating SMC differentiation from hUCMSCs to SMCs. Its level was significantly downregulated in a time-dependent manner in the differentiation process. The gain-of-function assessment with miRNA mimics demonstrated their prominent role in inhibiting SMC differentiation. Moreover, its downregulation serves as a prerequisite for the upregulation of contractile SMC markers in differentiation. As shown in the Results section, however, miR-222-5p mimics did not inhibit all contractile SMC markers, with minimal effect on SM22 both at the gene expression and the protein level. This suggests that the downregulation of miR-222-5p is not sufficient in de-repressing all contractile SMC marker expression and may only participate in the differentiation process as a complimentary regulation pathway.

While exploring the underlying miR-222-5p-related mechanism, important components of TGFβ1 signalling pathway were screened first since the miR-222-5p level was found to be related to the treatment of exogenous TGFβ1. The complex TGFβ1 signalling network may interact with each other through miRNAs and requires fine tuning to reach a balance. I postulate that miR-222-5p might target other TGFβ1-related signalling pathways other than the Smad-dependent pathway. However, there is no study reported to date that directly relates miR-222-3p and its targets to TGFβ1 signalling pathway or any physiological or pathophysiological conditions. Thus, I set out to look for their targets with computational miRNA target prediction approaches like TargetScan. Among the list of predicted targets provided, ROCK2 was selected as the candidate target to be examined further.

RhoA/ROCK pathways are important regulators of cardiovascular diseases (Hartmann et al., 2015; Shimokawa et al., 2016). Numerous cellular events could be under the control of RhoA/ROCK pathway including cell proliferation, cytoskeletal remodelling, migration and apoptosis (Shimokawa et al., 2016). Specific to SMC phenotypic switching or differentiation, activation of RhoA/ROCK pathway leads to the glomerular actin (G-actin) to form filamentous actin (F-actin), which results in the release of MRTF-A/B from the glomerular actin and translocation of it to the nucleus to activate downstream genes (Parmacek, 2007).

In this study, ROCK2 contained 2 target sites for miR-222-5p at the 3'-UTR region and its level was upregulated in a time-dependent manner which was consistent with the downregulation of miR-222-5p level during differentiation. Furthermore, ROCK2 was inhibited both at the gene expression level and at the protein level after treatment of miR-222-5p mimics. Knockdown of ROCK2 prompted downregulation of the SMC markers Calponin and αSMA, which is also consistent with the effect of miR-222-5p mimics on these markers in its inhibition of SMC differentiation. Although TGFβ1 did not exert significant effect in regulating the level of ROCK2, ROCK2 was still confirmed to be a direct target as shown by the site mutation experiments.

Furthermore, although αSMA 3'-UTR was not a predicted target with the computational prediction method, the complementarity of it with miR-222-5p was still examined given its predominant downregulation both at the gene expression level and at the protein level after miR-222-5p mimic treatment in the cells. Alignment of αSMA 3'-UTR sequence with miR-222-5p sequence revealed complementarity of 8 nucleotides at the 5'-end of the miRNA and complementarity of another 4 nucleotides at the 3'-end of the miRNA. Subsequent target site mutation experiments confirmed that αSMA 3'-UTR is a direct target of miR-222-5p. However, the mutation of the target site complementary to the 5'-end of the miRNA did not consistently recover the inhibition of the miR-222-5p on plasmids containing αSMA 3'-UTR, implying that the site complementary to the 3'-end might also have some effect in inducing the complementary binding of miR-222-5p to αSMA 3'-UTR and promoting the inhibitory effect.

4.4 Interaction of miR-503-related and miR-222-5p-related mechanisms

Multiple TGFβ1-related signalling pathways could interact with each other and work synergistically. Apart from the well-known Smad-dependent pathway, RhoA/ROCK pathway was also established to be important in TGFβ1-induced SMC differentiation (Bhowmick et al., 2001; Chen et al., 2006). As to the cooperation of RhoA/ROCK signalling pathway and Smad-dependent signalling pathway, it was found that they could exert effects in regulating each other. ROCK could modulate the activity of Smad signalling pathway possibly through phosphorylation of the Smad linker region (Chen et al., 2006; Kamato et al., 2013). Smad-dependent pathway could upregulate miR-155 which targets RhoA and modulates epithelial plasticity (Kong et al., 2008). The mutual regulation of these two pathways was also confirmed in one study with loss-of-function experiments with either ROCK pathway or Smad-dependent pathway and observation of the activity change of the other pathway (Ji et al., 2014). In embryonic stem cell self-renewal and differentiation, it was found that Smad2 and ROCK could be both regulated by Zonula Occludens-1 (ZO-1) (Xu et al., 2012a). However, reports also exist showing that early activation of RhoA upon TGFβ1 treatment was independent of Smad2/3 (Papadimitriou et al., 2011). Moreover, in some studies, two parallel pathways may exert similar effects on the same pathological setting without interaction with each other. Expression of tetraspanin 2 (TSPAN2) was independently regulated by Smad signalling pathway and Myocardin/SRF (Zhao et al., 2017a).

As to the miRNA interactions with each other, since miRNAs are generated in pairs endogenously, these miRNA pairs exhibit complementarity with each other. Although it was originally established that one strand of the miRNA pair goes through degradation directly, this concept starts to change. It has been shown that these miRNAs might form a duplex *in vivo* and mutually regulate each other (Guo et al., 2012). Some miRNAs are formed from the same cluster, regulated in similar patterns in pathological conditions and share high similarity in seed sequences, which

demonstrate their potential collaborative ways of functioning (Guo et al., 2014; Xu et al., 2013). Furthermore, some miRNAs could indirectly control the transcription of some other miRNAs. Upon co-inhibition of miR-21 and miR-221 in laryngeal squamous cells carcinoma, a set of pro-apoptotic miRNAs were upregulated, providing insights on the highly complex miRNA regulation network (Kan et al., 2016). With the large-scale data analysis of the expression level of miRNAs and the primary miRNA-like characteristics (mlRNA) which encodes miRNAs, it was demonstrated that miRNA level in specific tissue corresponds with the reduced level of mlRNAs, implying potential control of some miRNAs on the transcription of other miRNAs (Zhao et al., 2008). Based on experimental evidence, further interactive network of miRNAs was obtained with the integration of data from different diseases with computational method (Xu et al., 2011; Xu et al., 2016). Furthermore, miRNAs interacting in various types of cancers could be seen visually online (Nalluri et al., 2017). These miRNAs were further merged into established functional modules (Song et al., 2015; Zhao et al., 2013). Although miRNA interaction network has been gradually recognised, it requires large scale data pool and subsequent bioinformatic analysis, which was not realistic to be achieved in the experimental system in this study and it may not be required anyway. For miRNA interaction in one specific condition like what it is in the current experimental system, it was interesting that in oesophageal squamous cell carcinoma cells, the combination of increases in miR-31 and decreases in miR-338-3p correlates with the survival time, implicating the precedence of this type of cooperation of multiple miRNAs in a single experimental setting (Wu et al., 2013).

In this study, miR-503 upregulation and miR-222-5p downregulation correspond with each other and work synergistically to promote MSC-SMC differentiation. However, apart from the parallel analysis of both miRNAs, it was rather difficult to study the additive effect of both miRNAs. The reason is that the miRNA gain-of-function and loss-of-function studies are mainly achieved through the transfection of miRNA mimics and inhibitors. After co-transfection of miRNA mimics or inhibitors, the relative concentration of the two miRNAs would be difficult to recapitulate their level within

cells in the differentiation process, which will make it complicated and biased for subsequent interpretation of results. For this reason, co-transfection experiments of miRNA mimics or inhibitors were not conducted. However, future work might include the detection of miR-503 level after miR-222-5p mimics treatment or ROCK2 knockdown, and the detection of miR-222-5p level after miR-503 mimics treatment or Smad4 knockdown, which might provide further information whether the two miRNA-involved SMC differentiation pathways studied here work independently or entangle with each other to exert a more complex tuning of the differentiation system. Possible regulatory interactions of the pathways are highlighted in the green lines in the figure (Figure 4-1).

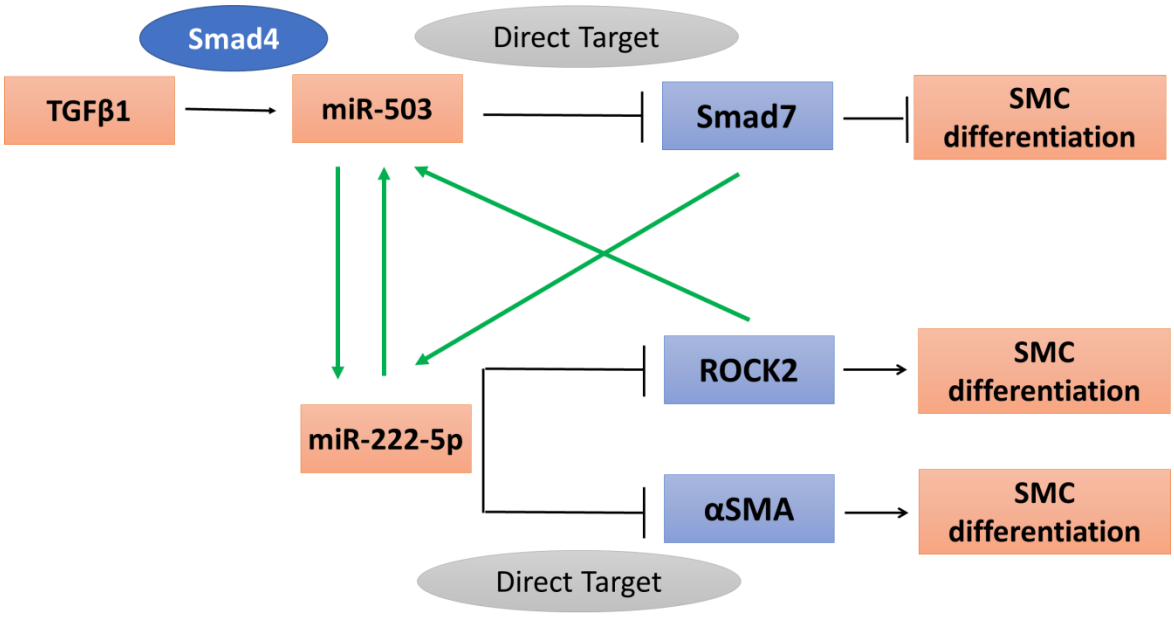

Figure 4-1 Possible interaction of the two established miRNA-related signalling pathways

Upon treatment of TGFβ1, miR-503 is upregulated in a Smad4 dependent pathway and directly targets Smad7, which is a negative regulator of TGFβ1 Smad-dependent signalling pathway, to promote SMC differentiation. The level of miR-222-5p was downregulated in the differentiation process, which results in de-repression of ROCK2 and αSMA and further promotion of SMC differentiation. Based on these established miRNA-related mechanisms in

our experimental system, it would be interesting to examine the interaction of these two miRNAs, their mutual regulation on each other and interaction of the two signalling pathways. The possible interaction points that might exist in the regulation network are highlighted in green lines in the figure.

4.5 Potential application of differentiated cells in vascular graft engineering

Vascular graft engineering is an important research field given that the morbidity and mortality of cardiovascular diseases are among the highest. Vascular bypass or replacement surgery is crucial for the treatment of these diseases involving coronary arteries. Peripheral artery diseases, which are the manifestation of major end stage metabolic syndrome, also often require vascular replacement surgery. Vascular grafts, however, are not always in sufficient needs, mostly because of the disease involvement or previous harvesting. Engineering of vascular grafts with synthetic materials, bio-compatible materials, or decellularised scaffolds is of significant value in matching the clinical need of vascular grafts. In constructing vascular grafts, numerous types of stem cells have been explored.

In our lab, c-kit positive cells from mouse embryonic stem cells and reprogrammed pluripotent stem cells derived from fibroblasts have been explored in engineering functional small diameter blood vessels, which upon transplantation *in vivo* demonstrated improvement in patency and increases of mouse mortality rate compared to transplantation of the grafts that have not been seeded with cells (Campagnolo et al., 2015a; Karamariti et al., 2013a). Mesenchymal stem cells have emerged to be a potential promising choice in vascular tissue engineering since they are multipotent and display immune modulation characteristics, which make it possible to engineer vascular grafts seeded with allogeneic cells (Uccelli et al., 2006). Moreover, mesenchymal stem cells are a large source of numerous trophic factors which might facilitate the vascular regeneration and integration *in vivo* after

transplantation. Among all the mesenchymal stem cell sources, BMMSCs and ADSCs are the most extensively explored, which exhibited satisfying results both in the lab and in the clinics.

Therefore, in this study, mesenchymal stem cell has been utilised as cell source for SMC generation. Specifically, MSCs from human umbilical cord, rather than those from bone marrow or adipose cells, were chosen to further explore in my experiments, as hUCMSCs demonstrate better proliferative capacity and higher multi-potent differentiation potential (Kern et al., 2006). In addition, hUCMSCs displayed strong SMC differentiation potential *in vitro* in differentiation conditions with low serum and addition of TGFβ1. Importantly, these differentiated cells exhibited the capacity to migrate inside the decellularised vessel wall while maintaining the expression of SMC markers after the seeded vessel was connected back to the bioreactor system.

In addition to directly differentiating the stem cells towards SMCs and seeding them onto vascular scaffolds, much effort has also been invested into the improvement of graft performance. Extracellular matrix protein coating has been explored in the capacity to induce SMC differentiation, with fibronectin showing the ability to increase SMC marker expression of BMMSCs, which implies the potential of fibronectin coating in improving SMC differentiation in vascular grafts (Shudo et al., 2016). Pre-treatment of SMCs utilised for vascular tissue engineering with miR-29a inhibitors performed better than TGFβ1 in promoting the production of elastin, which is a prominent component of extracellular matrix and contributes significantly to the mechanical strength of engineered vessel (Rothuizen et al., 2016).

Mechanistic study of the differentiation process showed the importance of miR-503 and miR-222-5p in SMC differentiation. Implication from the *in vitro* study was that miR-503 mimics and miR-222-5p inhibitors might have the potential in augmenting the performance of vascular grafts by promoting the differentiation of hUCMSCs towards SMCs. In the induction of SMC markers with TGFβ1, unintended signalling pathways and effects might be induced since TGFβ1 was well-known to be a potent growth factor with activation of diverse signalling pathways and potentiation of diverse

downstream effects. Future efforts might include the exploration of miR-503 mimic or miR-222-5p inhibitor treatment in other types of mesenchymal stem cells or even other types of stem cells to promote or augment the SMC differentiation.

Efforts in differentiating the hUCMSCs towards the endothelial lineage have not been successful *in vitro* (Data was not shown). For this reason, the endothelial layer was not included in the vascular grafts. However, in our lab, methods to engineer vascular grafts with both the smooth muscle layer and endothelial layer have been successful thus far (Campagnolo et al., 2015a; Karamariti et al., 2013a). Feasibility of endothelial adhesion to the grafts would be further achieved with mature endothelial cells such as HUVECs. When examining engineered vascular grafts *in vivo*, those grafts seeded with both the smooth muscle layer and the endothelial layer should be utilised to increase the patency rate for further inspection of the vascular mechanical property and *in vivo* integration.

In conclusion, hUCMSCs prove to be a promising choice of cell source for providing functional SMCs for engineering vascular grafts, which display extensive clinical potential to serve as vessel replacements in treating coronary artery diseases and peripheral artery diseases. MiR-503 mimics or miR-222-5p inhibitors carry the potential to improve the performance of these vascular grafts.

4.6 Summary and perspective

In summary, this is the first study to utilise hUCMSCs to generate functional SMCs with TGFβ1 and to engineer small diameter vascular grafts. Furthermore, we illustrated the differentiation mechanism involving miRNAs. It was established *in vitro* that miR-503 could target Smad7 to promote MSC-SMC differentiation and miR-222-5p could target ROCK2 to inhibit the differentiation process. However, there are several limitations about this project and future works might need to be conducted.

First, the interaction of the two miRNAs that was shown to affect SMC differentiation should be further studied to provide additional information about the collaborative control of differentiation to uncover another miRNA-related layer of the complex SMC differentiation regulation network. In addition to the approaches to study the miRNA interaction as depicted in the discussion part by checking the level of one miRNA after the mimic or inhibitor transfection of the other one in my specific experimental system, broader overlook of the miRNA interaction might be explored by putting the miRNAs to already established signalling pathways, checking the interaction of these signalling pathways and studying the possibilities of miRNA interaction as well as pathway interaction in pathological conditions. For example, a study has previously shown the interaction of PDGF-BB signalling pathway and TGFβ1-Smad signalling pathway with the connection point of miR-24 (Chan et al., 2010a). Furthermore, it was shown that miR-222 could be induced by PDGF-BB to modulate SMC phenotypic switching (Davis et al., 2009; Liu et al., 2009). Although the miR-222 explored in both studies were the mature strand miR-222-3p, it is reasonable to postulate that upon transcription of miR-222, both strands including miR-222-3p and miR-222-5p would be upregulated at least temporarily. As miR-222-5p was shown in this study to be targeting ROCK2, it would be interesting to study the possible interaction of PDGF-BB and ROCK2 given the potent function of both in a broad range of pathological conditions.

Secondly, miR-503 was demonstrated here to target Smad7 which is an important negative regulator of TGFβ1-Smad signalling pathway. Through the promotion of SMC contractile marker expression, theoretically vascular grafts with better functions would be expected if cells treated with miR-503 mimics were seeded onto the scaffold compared to cells treated with miRNA mimic control. However, further experiments need to be performed to test this hypothesis and elucidate the ultimate effect of miR-503 in further improvement of vascular graft performance.

As to vascular graft construction, apart from examining the potential of miR-503 in replacing or augmenting the effect of TGFβ1, it is also essential that the vascular grafts need to be properly endothelialised before being transplanted *in vivo*. Due to

the unsuccessful differentiation of hUCMSCs towards ECs, future work includes short term HUVEC seeding in the inner side of the decellularised vascular graft after culturing the hUCMSC-derived SMCs seeded graft in the bioreactor. Subsequently, the performance of engineered vascular graft could be investigated by the patency rate and vascular integration in *in vivo* transplantation experiments. The effect of TGFβ1 and miR-503 on the production of the extracellular cellular matrix also requires further exploration.

Lastly, miR-503 was shown to be involved in various pathological conditions. It has been shown to be secreted by ECs and could be transferred to adjacent SMCs to mediate the EC–SMC crosstalk. In pulmonary hypertension, decreased secretion of miR-503 from ECs leads to the downregulation of miR-503 in vascular SMCs that prompts the de-repression of targets related to the cell proliferation and therefore promotes subsequent SMC proliferation (Kim et al., 2013). In diabetic conditions, hyperglycemia induces upregulation of miR-503 in endothelial cells. It could be transported in exosomes to pericytes and exert inhibitory effect on αSMA expression, subsequently affecting the pericyte coverage in micro-vessels (Caporali et al., 2011). Thus, the effect of miR-503 on SMCs in different pathological conditions was different. To achieve a balance is crucial in maintaining normal vascular function. Further examination of miR-503 function in different cell types might be pertinent in unraveling the cell-specific function of miR-503. Apart from the *in vivo* examination of miR-503, exploration of miR-503 function in different pathological models might also be informative. In this study, further work might include the inspection of miR-503 in improving the vascular graft performance given its role in promoting SMC differentiation *in vitro*. In addition, its therapeutic potential could also be explored. Other pathological models such as hindlimb ischemia could also be used to provide clues about the vascular regeneration potential of miR-503 as a novel therapeutic choice.

In conclusion, although future experiments are in need to further elucidate the therapeutic potential of miRNAs in addition to exploring the interaction of multiple signalling pathways, the present study has achieved the initial aims in establishing

the differentiation of SMCs from hUCMSCs and in elucidating the underlying mechanisms. Briefly, hUCMSCs were demonstrated to have the potential to differentiate towards SMCs and hUCMSC-derived SMCs can be utilised to generate vascular grafts. Furthermore, the SMC differentiation mechanism involving miRNAs was explored and illustrated. In future, miRNAs can be utilised to enhance SMC differentiation from MSCs while avoiding possible off-target effects from the use of TGFβ1 and the resultant cells seeded on decellularised scaffold have the potential in generating therapeutically useful vascular grafts with better patency to replace damaged vessels in patients with major vascular abnormalities like coronary artery disease and peripheral artery disease.

5. Publications

5.1 Review Articles and Manuscripts

- **Gu, W.,** Hong, X., Potter, C., Qu, A., & Xu, Q. Mesenchymal stem cells and vascular regeneration. Microcirculation, (2017). 24(1). (Review)
- **Gu, W.,** Xie, Y. and Xu, Q., 2017. Animal models to study pathophysiology of the vasculature. *The ESC Textbook of Vascular Biology*, 2017 Feb, p.53. (Book Chapter)
- Xie, Y., Potter, C., Le Bras, A., Bhaloo, S. I., Nowak, W., **Gu, W.,** Zhang, Z., Hu, Y., Zhang, L., Xu. Q., Leptin Induces Sca-1+ Progenitor Cell Migration Enhancing Neointimal Lesions in Vessel-Injury Mouse Models, ATVB.
- **Gu W.,** Hong X., Nowak, W., Zhang Z., Hu, Y. and Xu Q., Smooth Muscle Cells Differentiated from Human Umbilical Cord Mesenchymal Stem Cells Regulated by miR-503 Are Potent for Vascular Tissue Engineering. In preparation.
- **Gu, W.,** Nowak, W., Yao, X., Le Bras, A., Bhaloo, S. I., Hong, X., Zhang, Z., Hu, Y., Xu, Q. Smooth muscle cells differentiate from perivascular adipose tissue-derived stem cells, through Apelin inhibition and metabolic profile change. In preparation.
- Xie Y., Nowak W., **Gu W.,** Hu Y, and Xu Q. Adipose tissue influences vascular remodelling of injured arteries via adipokine release and cell migration. In preparation.

5.2 Meeting Abstracts

- **Gu W.,** Hong X., Nowak, W., Zhang Z., Hu, Y. and Xu Q., Smooth Muscle Cells Differentiated from Human Umbilical Cord Mesenchymal Stem Cells Regulated by miR-503 Are Potent for Vascular Tissue Engineering, 2nd Joint Meeting of the European Society for Microcirculation (ESM) and European Vascular Biology Organisation (EVBO), 29 May to 1 June 2017, Geneva, Switzerland. (Oral Presentation)
- **Gu W.,** Hong X., Nowak, W., Zhang Z., Hu, Y. and Xu Q., Smooth Muscle Cells Differentiated from Human Umbilical Cord Mesenchymal Stem Cells Regulated by miR-503 Are Potent for Vascular Tissue Engineering, Small Artery Remodelling (SmArteR) 2016 Symposium on Vascular remodelling: Novel developments in progenitor cell biology and gene regulation, University of Fribourg, Switzerland, 7-9 November, 2016 (Poster Presentation)
- Nowak, W., **Gu, W.,** Yao, X., Le Bras, A., Bhaloo, S. I., Smooth muscle cells differentiation from perivascular adipose tissue-derived stem cells, through Apelin inhibition and metabolic profile change, EMBO Symposia, Heidelberg, Germany, 21-23 May 2017 (Poster presentation)
- Xie Y., Potter C., Le Bras A., Nowak W., **Gu W.,** Hu Y., Zhang L., Xu Q. Leptin Induces Sca-1^{+} Progenitor Cell Migration Enhancing Neointimal Lesions in Vessel-Injury Mouse Models. The Annual Conference of the British Cardiovascular Society, Jun 5-7, 2017, Manchester, UK.

6. References

Abu Kasim, N.H., Govindasamy, V., Gnanasegaran, N., Musa, S., Pradeep, P.J., Srijaya, T.C., and Aziz, Z.A. (2012). Unique molecular signatures influencing the biological function and fate of post-natal stem cells isolated from different sources. Journal of tissue engineering and regenerative medicine.

Adebayo, O., Hookway, T.A., Hu, J.Z., Billiar, K.L., and Rolle, M.W. (2013). Self-assembled smooth muscle cell tissue rings exhibit greater tensile strength than cell-seeded fibrin or collagen gel rings. J Biomed Mater Res A 101, 428-437.

Aggarwal, S., and Pittenger, M.F. (2005). Human mesenchymal stem cells modulate allogeneic immune cell responses. Blood 105, 1815-1822.

Albinsson, S., Suarez, Y., Skoura, A., Offermanns, S., Miano, J.M., and Sessa, W.C. (2010). MicroRNAs are necessary for vascular smooth muscle growth, differentiation, and function. Arteriosclerosis, thrombosis, and vascular biology 30, 1118-1126.

Alexandre, N., Amorim, I., Caseiro, A.R., Pereira, T., Alvites, R., Rema, A., Goncalves, A., Valadares, G., Costa, E., Santos-Silva, A., et al. (2017). Long term performance evaluation of small-diameter vascular grafts based on polyvinyl alcohol hydrogel and dextran and MSCs-based therapies using the ovine pre-clinical animal model. Int J Pharm 523, 515-530.

Alsalameh, S., Amin, R., Gemba, T., and Lotz, M. (2004). Identification of mesenchymal progenitor cells in normal and osteoarthritic human articular cartilage. Arthritis and rheumatism 50, 1522-1532.

Ambros, V. (1989). A Hierarchy of Regulatory Genes Controls a Larva-to-Adult Developmental Switch in C-Elegans. Cell 57, 49-57.

Ambros, V., Bartel, B., Bartel, D.P., Burge, C.B., Carrington, J.C., Chen, X., Dreyfuss, G., Eddy, S.R., Griffiths-Jones, S., Marshall, M., et al. (2003). A uniform system for microRNA annotation. RNA 9, 277-279.

Ammit, A.J., and Panettieri, R.A., Jr. (2001). Invited review: the circle of life: cell cycle regulation in airway smooth muscle. Journal of applied physiology 91, 1431-1437.

Anjos-Afonso, F., Siapati, E.K., and Bonnet, D. (2004). In vivo contribution of murine mesenchymal stem cells into multiple cell-types under minimal damage conditions. Journal of cell science 117, 5655-5664.

Arciniegas, E., Ponce, L., Hartt, Y., Graterol, A., and Carlini, R.G. (2000). Intimal thickening involves transdifferentiation of embryonic endothelial cells. The Anatomical record 258, 47-57.

Au, P., Tam, J., Fukumura, D., and Jain, R.K. (2008). Bone marrow-derived mesenchymal stem cells facilitate engineering of long-lasting functional vasculature. Blood 111, 4551-4558.

Azuara, V., Perry, P., Sauer, S., Spivakov, M., Jorgensen, H.F., John, R.M., Gouti, M., Casanova, M., Warnes, G., Merkenschlager, M., et al. (2006). Chromatin signatures of pluripotent cell lines. Nature cell biology 8, 532-538.

Bab, I., Ashton, B.A., Gazit, D., Marx, G., Williamson, M.C., and Owen, M.E. (1986). Kinetics and differentiation of marrow stromal cells in diffusion chambers in vivo. Journal of cell science 84, 139-151.

Baek, D., Villen, J., Shin, C., Camargo, F.D., Gygi, S.P., and Bartel, D.P. (2008). The impact of microRNAs on protein output. Nature 455, 64-U38.

Bang, C., Batkai, S., Dangwal, S., Gupta, S.K., Foinquinos, A., Holzmann, A., Just, A., Remke, J., Zimmer, K., Zeug, A., et al. (2014). Cardiac fibroblast-derived microRNA passenger strand-enriched exosomes mediate cardiomyocyte hypertrophy. J Clin Invest 124, 2136-2146.

Bartel, D.P. (2009). MicroRNAs: Target Recognition and Regulatory Functions. Cell 136, 215-233.

Beamish, J.A., He, P., Kottke-Marchant, K., and Marchant, R.E. (2010). Molecular Regulation of Contractile Smooth Muscle Cell Phenotype: Implications for Vascular Tissue Engineering. Tissue Eng Part B-Re 16, 467-491.

Beermann, J., Piccoli, M.T., Viereck, J., and Thum, T. (2016). Non-coding RNAs in Development and Disease: Background, Mechanisms, and Therapeutic Approaches. Physiological reviews 96, 1297-1325.

Belaguli, N.S., Schildmeyer, L.A., and Schwartz, R.J. (1997). Organization and myogenic restricted expression of the murine serum response factor gene. A role for autoregulation. The Journal of biological chemistry 272, 18222-18231.

Bennett, J.H., Joyner, C.J., Triffitt, J.T., and Owen, M.E. (1991). Adipocytic cells cultured from marrow have osteogenic potential. Journal of cell science 99 (Pt 1), 131-139.

Bennion, R.S., Williams, R.A., Stabile, B.E., Fox, M.A., Owens, M.L., and Wilson, S.E. (1985). Patency of autogenous saphenous vein versus polytetrafluoroethylene grafts in femoropopliteal bypass for advanced ischemia of the extremity. Surg Gynecol Obstet 160, 239-242.

Beresford, J.N., Bennett, J.H., Devlin, C., Leboy, P.S., and Owen, M.E. (1992). Evidence for an inverse relationship between the differentiation of adipocytic and osteogenic cells in rat marrow stromal cell cultures. Journal of cell science 102 (Pt 2), 341-351.

Bernstein, B.E., Mikkelsen, T.S., Xie, X., Kamal, M., Huebert, D.J., Cuff, J., Fry, B., Meissner, A., Wernig, M., Plath, K., et al. (2006). A bivalent chromatin structure marks key developmental genes in embryonic stem cells. Cell 125, 315-326.

Bertanha, M., Moroz, A., Almeida, R., Alves, F.C., Acorci Valerio, M.J., Moura, R., Domingues, M.A., Sobreira, M.L., and Deffune, E. (2014). Tissue-engineered blood vessel substitute by reconstruction of endothelium using mesenchymal stem cells induced by platelet growth factors. J Vasc Surg 59, 1677-1685.

Bhayani, M.K., Calin, G.A., and Lai, S.Y. (2012). Functional relevance of miRNA sequences in human disease. Mutat Res 731, 14-19.

Bhowmick, N.A., Ghiassi, M., Bakin, A., Aakre, M., Lundquist, C.A., Engel, M.E., Arteaga, C.L., and Moses, H.L. (2001). Transforming growth factor-beta 1 mediates epithelial to mesenchymal transdifferentiation through a RhoA-dependent mechanism. Molecular Biology of the Cell 12, 27-36.

Bi, Y., Ehirchiou, D., Kilts, T.M., Inkson, C.A., Embree, M.C., Sonoyama, W., Li, L., Leet, A.I., Seo, B.M., Zhang, L., et al. (2007). Identification of tendon stem/progenitor cells and the role of the extracellular matrix in their niche. Nature medicine 13, 1219-1227.

Bianco, P., Riminucci, M., Gronthos, S., and Robey, P.G. (2001). Bone marrow stromal stem cells: nature, biology, and potential applications. Stem cells 19, 180-192.

Bjorkerud, S. (1991). Effects of transforming growth factor-beta 1 on human arterial smooth muscle cells in vitro. Arterioscler Thromb 11, 892-902.

Blakemore, A.H., and Voorhees, A.B., Jr. (1954). The use of tubes constructed from vinyon N cloth in bridging arterial defects; experimental and clinical. Ann Surg 140, 324-334.

Blaker, A.L., Taylor, J.M., and Mack, C.P. (2009). PKA-dependent phosphorylation of serum response factor inhibits smooth muscle-specific gene expression. Arteriosclerosis, thrombosis, and vascular biology 29, 2153-2160.

Boettger, T., Beetz, N., Kostin, S., Schneider, J., Kruger, M., Hein, L., and Braun, T. (2009). Acquisition of the contractile phenotype by murine arterial smooth muscle cells depends on the Mir143/145 gene cluster. The Journal of clinical investigation 119, 2634-2647.

Boucher, J.M., Peterson, S.M., Urs, S., Zhang, C., and Liaw, L. (2011). The miR-143/145 cluster is a novel transcriptional target of Jagged-1/Notch signaling in vascular smooth muscle cells. J Biol Chem 286, 28312-28321.

Bourget, J.M., Gauvin, R., Duchesneau, D., Remy, M., Auger, F.A., and Germain, L. (2015). Potential of Newborn and Adult Stem Cells for the Production of Vascular Constructs Using the Living Tissue Sheet Approach. BioMed research international 2015, 168294.

Bourget, J.M., Gauvin, R., Larouche, D., Lavoie, A., Labbe, R., Auger, F.A., and Germain, L. (2012). Human fibroblast-derived ECM as a scaffold for vascular tissue engineering. Biomaterials 33, 9205-9213.

Brennecke, J., Stark, A., Russell, R.B., and Cohen, S.M. (2005). Principles of MicroRNA-target recognition. Plos Biol 3, 404-418.

Brodersen, P., and Voinnet, O. (2009). Revisiting the principles of microRNA target recognition and mode of action. Nat Rev Mol Cell Bio 10, 141-148.

Bulick, A.S., Muñoz-Pinto, D.J., Qu, X., Mani, M., Cristancho, D., Urban, M., and Hahn, M.S. (2009). Impact of endothelial cells and mechanical conditioning on smooth muscle cell extracellular matrix production and differentiation. Tissue Engineering - Part A 15, 815-825.

Callis, T.E., Cao, D., and Wang, D.Z. (2005). Bone morphogenetic protein signaling modulates myocardin transactivation of cardiac genes. Circulation research 97, 992-1000.

Campagnoli, C., Roberts, I.A., Kumar, S., Bennett, P.R., Bellantuono, I., and Fisk, N.M. (2001). Identification of mesenchymal stem/progenitor cells in human first-trimester fetal blood, liver, and bone marrow. Blood 98, 2396-2402.

Campagnolo, P., Gormley, A.J., Chow, L.W., Guex, A.G., Parmar, P.A., Puetzer, J.L., Steele, J.A., Breant, A., Madeddu, P., and Stevens, M.M. (2016). Pericyte Seeded Dual Peptide Scaffold with Improved Endothelialization for Vascular Graft Tissue Engineering. Adv Healthc Mater 5, 3046-3055.

Campagnolo, P., Tsai, T.N., Hong, X., Kirton, J.P., So, P.W., Margariti, A., Di Bernardini, E., Wong, M.M., Hu, Y., Stevens, M.M., et al. (2015a). c-Kit+ progenitors generate vascular cells for tissue-engineered grafts through modulation of the Wnt/Klf4 pathway. Biomaterials 60, 53-61.

Campagnolo, P., Tsai, T.N., Hong, X.C., Kirton, J.P., So, P.W., Margariti, A., Di Bernardini, E., Wong, M.M., Hu, Y.H., Stevens, M.M., et al. (2015b). c-Kit plus progenitors generate vascular cells for tissue-engineered grafts through modulation of the Wnt/Klf4 pathway. Biomaterials 60, 53-61.

Cao, D., Wang, C., Tang, R., Chen, H., Zhang, Z., Tatsuguchi, M., and Wang, D.Z. (2012). Acetylation of myocardin is required for the activation of cardiac and smooth muscle genes. The Journal of biological chemistry 287, 38495-38504.

Cao, D., Wang, Z., Zhang, C.L., Oh, J., Xing, W., Li, S., Richardson, J.A., Wang, D.Z., and Olson, E.N. (2005). Modulation of smooth muscle gene expression by association of histone acetyltransferases and deacetylases with myocardin. Molecular and cellular biology 25, 364-376.

Cao, S., Xiao, L., Rao, J.N., Zou, T., Liu, L., Zhang, D., Turner, D.J., Gorospe, M., and Wang, J.Y. (2014). Inhibition of Smurf2 translation by miR-322/503 modulates TGF-beta/Smad2 signaling and intestinal epithelial homeostasis. Mol Biol Cell 25, 1234-1243.

Caplan, A.I. (1991). Mesenchymal stem cells. Journal of orthopaedic research : official publication of the Orthopaedic Research Society 9, 641-650.

Caporali, A., Meloni, M., Nailor, A., Mitic, T., Shantikumar, S., Riu, F., Sala-Newby, G.B., Rose, L., Besnier, M., Katare, R., et al. (2015). p75(NTR)-dependent activation of NF-kappaB regulates microRNA-503 transcription and pericyte-endothelial crosstalk in diabetes after limb ischaemia. Nat Commun 6, 8024.

Caporali, A., Meloni, M., Vollenkle, C., Bonci, D., Sala-Newby, G.B., Addis, R., Spinetti, G., Losa, S., Masson, R., Baker, A.H., et al. (2011). Deregulation of microRNA-503 contributes to diabetes mellitus-induced impairment of endothelial function and reparative angiogenesis after limb ischemia. Circulation 123, 282-291.

Catto, V., Farè, S., Freddi, G., and Tanzi, M.C. (2014). Vascular Tissue Engineering: Recent Advances in Small Diameter Blood Vessel Regeneration. ISRN Vascular Medicine 2014, 1-27.

Cawthorn, W.P., Scheller, E.L., and MacDougald, O.A. (2012). Adipose tissue stem cells: the great WAT hope. Trends in endocrinology and metabolism: TEM 23, 270-277.

Cerutti, C., Edwards, L.J., de Vries, H.E., Sharrack, B., Male, D.K., and Romero, I.A. (2017). MiR-126 and miR-126* regulate shear-resistant firm leukocyte adhesion to human brain endothelium. Sci Rep 7, 45284.

Chalfie, M., Horvitz, H.R., and Sulston, J.E. (1981). Mutations That Lead to Reiterations in the Cell Lineages of C-Elegans. Cell 24, 59-69.

Chan, M.C., Hilyard, A.C., Wu, C., Davis, B.N., Hill, N.S., Lal, A., Lieberman, J., Lagna, G., and Hata, A. (2010a). Molecular basis for antagonism between PDGF and the TGF beta family of signalling pathways by control of miR-24 expression. Embo Journal 29, 559-573.

Chan, M.C., Hilyard, A.C., Wu, C., Davis, B.N., Hill, N.S., Lal, A., Lieberman, J., Lagna, G., and Hata, A. (2010b). Molecular basis for antagonism between PDGF and the TGFbeta family of signalling pathways by control of miR-24 expression. The EMBO journal 29, 559-573.

Chen, J., Kitchen, C.M., Streb, J.W., and Miano, J.M. (2002). Myocardin: a component of a molecular switch for smooth muscle differentiation. Journal of molecular and cellular cardiology 34, 1345-1356.

Chen, J., Yin, H., Jiang, Y., Radhakrishnan, S.K., Huang, Z.P., Li, J., Shi, Z., Kilsdonk, E.P., Gui, Y., Wang, D.Z., et al. (2011). Induction of microRNA-1 by myocardin in smooth muscle cells inhibits cell proliferation. Arteriosclerosis, thrombosis, and vascular biology 31, 368-375.

Chen, P.Y., Qin, L., Li, G., Tellides, G., and Simons, M. (2016). Fibroblast growth factor (FGF) signaling regulates transforming growth factor beta (TGFbeta)-dependent smooth muscle cell phenotype modulation. Sci Rep 6, 33407.

Chen, S., Crawford, M., Day, R.M., Briones, V.R., Leader, J.E., Jose, P.A., and Lechleider, R.J. (2006). RhoA modulates Smad signaling during transforming growth factor-beta-induced smooth muscle differentiation. J Biol Chem 281, 1765-1770.

Chen, W.X., Hu, Q., Qiu, M.T., Zhong, S.L., Xu, J.J., Tang, J.H., and Zhao, J.H. (2013). miR-221/222: promising biomarkers for breast cancer. Tumour Biol 34, 1361-1370.

Cheng, Y., Liu, X., Yang, J., Lin, Y., Xu, D.Z., Lu, Q., Deitch, E.A., Huo, Y., Delphin, E.S., and Zhang, C. (2009). MicroRNA-145, a novel smooth muscle cell phenotypic marker and modulator, controls vascular neointimal lesion formation. Circulation research 105, 158-166.

Cheung, P., Allis, C.D., and Sassone-Corsi, P. (2000). Signaling to chromatin through histone modifications. Cell 103, 263-271.

Chi, S.W., Hannon, G.J., and Darnell, R.B. (2012). An alternative mode of microRNA target recognition. Nature Structural & Molecular Biology 19, 321-U380.

Chi, S.W., Zang, J.B., Mele, A., and Darnell, R.B. (2009). Argonaute HITS-CLIP decodes microRNA-mRNA interaction maps. Nature 460, 479-486.

Cho, S.W., Lim, S.H., Kim, I.K., Hong, Y.S., Kim, S.S., Yoo, K.J., Park, H.Y., Jang, Y., Chang, B.C., Choi, C.Y., et al. (2005). Small-diameter blood vessels engineered with bone marrow-derived cells. Ann Surg 241, 506-515.

Clempus, R.E., and Griendling, K.K. (2006). Reactive oxygen species signaling in vascular smooth muscle cells. Cardiovascular research 71, 216-225.

Clempus, R.E., Sorescu, D., Dikalova, A.E., Pounkova, L., Jo, P., Sorescu, G.P., Schmidt, H.H., Lassegue, B., and Griendling, K.K. (2007). Nox4 is required for maintenance of the differentiated vascular smooth muscle cell phenotype. Arteriosclerosis, thrombosis, and vascular biology 27, 42-48.

Clowes, A.W., Reidy, M.A., and Clowes, M.M. (1983). Mechanisms of stenosis after arterial injury. Laboratory investigation; a journal of technical methods and pathology 49, 208-215.

Cordes, K.R., Sheehy, N.T., White, M.P., Berry, E.C., Morton, S.U., Muth, A.N., Lee, T.H., Miano, J.M., Ivey, K.N., and Srivastava, D. (2009). miR-145 and miR-143 regulate smooth muscle cell fate and plasticity. Nature 460, 705-710.

Costa, M., Cerqueira, M.T., Santos, T.C., Sampaio-Marques, B., Ludovico, P., Marques, A.P., Pirraco, R.P., and Reis, R.L. (2017). Cell sheet engineering using the stromal vascular fraction of adipose tissue as a vascularization strategy. Acta Biomater 55, 131-143.

Creemers, E.E., Sutherland, L.B., McAnally, J., Richardson, J.A., and Olson, E.N. (2006). Myocardin is a direct transcriptional target of Mef2, Tead and Foxo proteins during cardiovascular development. Development 133, 4245-4256.

Crisan, M., Yap, S., Casteilla, L., Chen, C.W., Corselli, M., Park, T.S., Andriolo, G., Sun, B., Zheng, B., Zhang, L., et al. (2008). A perivascular origin for mesenchymal stem cells in multiple human organs. Cell stem cell 3, 301-313.

Croissant, J.D., Kim, J.H., Eichele, G., Goering, L., Lough, J., Prywes, R., and Schwartz, R.J. (1996). Avian serum response factor expression restricted primarily to muscle cell lineages is required for alpha-actin gene transcription. Developmental biology 177, 250-264.

da Silva Meirelles, L., Chagastelles, P.C., and Nardi, N.B. (2006). Mesenchymal stem cells reside in virtually all post-natal organs and tissues. Journal of cell science 119, 2204-2213.

Dash, B.C., Levi, K., Schwan, J., Luo, J., Bartulos, O., Wu, H., Qiu, C., Yi, T., Ren, Y., Campbell, S., et al. (2016). Tissue-Engineered Vascular Rings from Human iPSC-Derived Smooth Muscle Cells. Stem Cell Reports 7, 19-28.

Davis-Dusenbery, B.N., Chan, M.C., Reno, K.E., Weisman, A.S., Layne, M.D., Lagna, G., and Hata, A. (2011). down-regulation of Kruppel-like factor-4 (KLF4) by microRNA-143/145 is critical for modulation of vascular smooth muscle cell phenotype by transforming growth factor-beta and bone morphogenetic protein 4. The Journal of biological chemistry 286, 28097-28110.

Davis, B.N., Hilyard, A.C., Lagna, G., and Hata, A. (2008). SMAD proteins control DROSHA-mediated microRNA maturation. Nature 454, 56-61.

Davis, B.N., Hilyard, A.C., Nguyen, P.H., Lagna, G., and Hata, A. (2009). Induction of microRNA-221 by platelet-derived growth factor signaling is critical for modulation of vascular smooth muscle phenotype. J Biol Chem 284, 3728-3738.

De Bari, C., Dell'Accio, F., Tylzanowski, P., and Luyten, F.P. (2001). Multipotent mesenchymal stem cells from adult human synovial membrane. Arthritis and rheumatism 44, 1928-1942.

Deaton, R.A., Su, C., Valencia, T.G., and Grant, S.R. (2005). Transforming growth factor-beta1-induced expression of smooth muscle marker genes involves activation of PKN and p38 MAPK. J Biol Chem 280, 31172-31181.

Deheuninck, J., and Luo, K. (2009). Ski and SnoN, potent negative regulators of TGF-beta signaling. Cell Res 19, 47-57.

Dempsie, Y., and MacLean, M.R. (2013). The influence of gender on the development of pulmonary arterial hypertension. Exp Physiol 98, 1257-1261.

Dentelli, P., Rosso, A., Orso, F., Olgasi, C., Taverna, D., and Brizzi, M.F. (2010). microRNA-222 controls neovascularization by regulating signal transducer and activator of transcription 5A expression. Arterioscler Thromb Vasc Biol 30, 1562-1568.

DeRuiter, M.C., Poelmann, R.E., VanMunsteren, J.C., Mironov, V., Markwald, R.R., and Gittenberger-de Groot, A.C. (1997). Embryonic endothelial cells transdifferentiate into mesenchymal cells expressing smooth muscle actins in vivo and in vitro. Circulation research 80, 444-451.

Derynck, R., and Zhang, Y.E. (2003). Smad-dependent and Smad-independent pathways in TGF-beta family signalling. Nature 425, 577-584.

Desai, N.D., Cohen, E.A., Naylor, C.D., Fremes, S.E., and Radial Artery Patency Study, I. (2004). A randomized comparison of radial-artery and saphenous-vein coronary bypass grafts. N Engl J Med 351, 2302-2309.

Didiano, D., and Hobert, O. (2006). Perfect seed pairing is not a generally reliable predictor for miRNA-target interactions. Nat Struct Mol Biol 13, 849-851.

Didiano, D., and Hobert, O. (2008). Molecular architecture of a miRNA-regulated 3′ UTR. RNA 14, 1297-1317.

Doi, H., Iso, T., Yamazaki, M., Akiyama, H., Kanai, H., Sato, H., Kawai-Kowase, K., Tanaka, T., Maeno, T., Okamoto, E., et al. (2005). HERP1 inhibits myocardin-induced vascular smooth muscle cell differentiation by interfering with SRF binding to CArG box. Arteriosclerosis, thrombosis, and vascular biology 25, 2328-2334.

Dominici, M., Le Blanc, K., Mueller, I., Slaper-Cortenbach, I., Marini, F., Krause, D., Deans, R., Keating, A., Prockop, D., and Horwitz, E. (2006). Minimal criteria for defining multipotent mesenchymal stromal cells. The International Society for Cellular Therapy position statement. Cytotherapy 8, 315-317.

Duan, B. (2017). State-of-the-Art Review of 3D Bioprinting for Cardiovascular Tissue Engineering. Ann Biomed Eng 45, 195-209.

Easow, G., Teleman, A.A., and Cohen, S.M. (2007). Isolation of microRNA targets by miRNP immunopurification. Rna-a Publication of the Rna Society 13, 1198-1204.

Eggenhofer, E., Benseler, V., Kroemer, A., Popp, F.C., Geissler, E.K., Schlitt, H.J., Baan, C.C., Dahlke, M.H., and Hoogduijn, M.J. (2012). Mesenchymal stem cells are short-lived and do not migrate beyond the lungs after intravenous infusion. Frontiers in immunology 3, 297.

El Omar, R., Beroud, J., Stoltz, J.F., Menu, P., Velot, E., and Decot, V. (2014). Umbilical cord mesenchymal stem cells: the new gold standard for mesenchymal stem cell-based therapies? Tissue engineering Part B, Reviews 20, 523-544.

Elcin, A.E., Parmaksiz, M., Dogan, A., Seker, S., Durkut, S., Dalva, K., and Elcin, Y.M. (2017). Differential gene expression profiling of human adipose stem cells differentiating into smooth muscle-like cells by TGFbeta1/BMP4. Exp Cell Res 352, 207-217.

Elia, L., Quintavalle, M., Zhang, J., Contu, R., Cossu, L., Latronico, M.V., Peterson, K.L., Indolfi, C., Catalucci, D., Chen, J., et al. (2009). The knockout of miR-143 and -145 alters smooth muscle cell maintenance and vascular homeostasis in mice: correlates with human disease. Cell death and differentiation 16, 1590-1598.

Elkayam, E., Kuhn, C.D., Tocilj, A., Haase, A.D., Greene, E.M., Hannon, G.J., and Joshua-Tor, L. (2012). The Structure of Human Argonaute-2 in Complex with miR-20a. Cell 150, 100-110.

Elliott, M.B., and Gerecht, S. (2016). Three-dimensional culture of small-diameter vascular grafts. J Mater Chem B 4, 3443-3453.

Enomoto, S., Sumi, M., Kajimoto, K., Nakazawa, Y., Takahashi, R., Takabayashi, C., Asakura, T., and Sata, M. (2010). Long-term patency of small-diameter vascular graft made from fibroin, a silk-based biodegradable material. J Vasc Surg 51, 155-164.

Eom, Y.W., Oh, J.E., Lee, J.I., Baik, S.K., Rhee, K.J., Shin, H.C., Kim, Y.M., Ahn, C.M., Kong, J.H., Kim, H.S., et al. (2014). The role of growth factors in maintenance of stemness in bone marrow-derived mesenchymal stem cells. Biochem Biophys Res Commun 445, 16-22.

Farrington-Rock, C., Crofts, N.J., Doherty, M.J., Ashton, B.A., Griffin-Jones, C., and Canfield, A.E. (2004). Chondrogenic and adipogenic potential of microvascular pericytes. Circulation 110, 2226-2232.

Filipowicz, W., Bhattacharyya, S.N., and Sonenberg, N. (2008). Mechanisms of post-transcriptional regulation by microRNAs: are the answers in sight? Nature reviews Genetics 9, 102-114.

Forrest, A.R., Kanamori-Katayama, M., Tomaru, Y., Lassmann, T., Ninomiya, N., Takahashi, Y., de Hoon, M.J., Kubosaki, A., Kaiho, A., Suzuki, M., et al. (2010). Induction of microRNAs, mir-155, mir-222, mir-424 and mir-503, promotes monocytic differentiation through combinatorial regulation. Leukemia 24, 460-466.

Friedenstein, A., and Kuralesova, A.I. (1971). Osteogenic precursor cells of bone marrow in radiation chimeras. Transplantation 12, 99-108.

Friedenstein, A.J. (1980). Stromal mechanisms of bone marrow: cloning in vitro and retransplantation in vivo. Haematology and blood transfusion 25, 19-29.

Friedenstein, A.J. (1995). Marrow stromal fibroblasts. Calcified tissue international 56 Suppl 1, S17.

Friedenstein, A.J., Chailakhjan, R.K., and Lalykina, K.S. (1970). The development of fibroblast colonies in monolayer cultures of guinea-pig bone marrow and spleen cells. Cell and tissue kinetics 3, 393-403.

Friedenstein, A.J., Chailakhyan, R.K., and Gerasimov, U.V. (1987). Bone marrow osteogenic stem cells: in vitro cultivation and transplantation in diffusion chambers. Cell and tissue kinetics 20, 263-272.

Friedenstein, A.J., Deriglasova, U.F., Kulagina, N.N., Panasuk, A.F., Rudakowa, S.F., Luria, E.A., and Ruadkow, I.A. (1974). Precursors for fibroblasts in different populations of hematopoietic cells as detected by the in vitro colony assay method. Experimental hematology 2, 83-92.

Friedenstein, A.J., Gorskaja, J.F., and Kulagina, N.N. (1976). Fibroblast precursors in normal and irradiated mouse hematopoietic organs. Experimental hematology 4, 267-274.

Friedenstein, A.J., Ivanov-Smolenski, A.A., Chajlakjan, R.K., Gorskaya, U.F., Kuralesova, A.I., Latzinik, N.W., and Gerasimow, U.W. (1978). Origin of bone marrow stromal mechanocytes in radiochimeras and heterotopic transplants. Experimental hematology 6, 440-444.

Friedenstein, A.J., Latzinik, N.W., Grosheva, A.G., and Gorskaya, U.F. (1982). Marrow microenvironment transfer by heterotopic transplantation of freshly isolated and cultured cells in porous sponges. Experimental hematology 10, 217-227.

Friedenstein, A.J., Petrakova, K.V., Kurolesova, A.I., and Frolova, G.P. (1968). Heterotopic of bone marrow. Analysis of precursor cells for osteogenic and hematopoietic tissues. Transplantation 6, 230-247.

Friedman, R.C., Farh, K.K.H., Burge, C.B., and Bartel, D.P. (2009). Most mammalian mRNAs are conserved targets of microRNAs. Genome Res 19, 92-105.

G, N., Tan, A., Gundogan, B., Farhatnia, Y., Nayyer, L., Mahdibeiraghdar, S., Rajadas, J., De Coppi, P., Davies, A.H., and Seifalian, A.M. (2015). Tissue engineering vascular grafts a fortiori: looking back and going forward. Expert Opin Biol Ther 15, 231-244.

Galardi, S., Mercatelli, N., Farace, M.G., and Ciafre, S.A. (2011). NF-kB and c-Jun induce the expression of the oncogenic miR-221 and miR-222 in prostate carcinoma and glioblastoma cells. Nucleic Acids Res 39, 3892-3902.

Gao, Y., Liu, F., Zhang, L., Su, X., Liu, J.Y., and Li, Y. (2014a). Acellular blood vessels combined human hair follicle mesenchymal stem cells for engineering of functional arterial grafts. Ann Biomed Eng 42, 2177-2189.

Gao, Y.H., Liu, F.L., Zhang, L.H., Su, X.J., Liu, J.Y., and Li, Y.L. (2014b). Acellular Blood Vessels Combined Human Hair Follicle Mesenchymal Stem Cells for Engineering of Functional Arterial Grafts. Annals of Biomedical Engineering 42, 2177-2189.

Garat, C., Van Putten, V., Refaat, Z.A., Dessev, C., Han, S.Y., and Nemenoff, R.A. (2000). Induction of smooth muscle alpha-actin in vascular smooth muscle cells by arginine vasopressin is mediated by c-Jun amino-terminal kinases and p38 mitogen-activated protein kinase. The Journal of biological chemistry 275, 22537-22543.

Gays, D., Hess, C., Camporeale, A., Ala, U., Provero, P., Mosimann, C., and Santoro, M.M. (2017). An exclusive cellular and molecular network governs intestinal smooth muscle cell differentiation in vertebrates. Development 144, 464-478.

Girton, T.S., Oegema, T.R., Grassl, E.D., Isenberg, B.C., and Tranquillo, R.T. (2000). Mechanisms of stiffening and strengthening in media-equivalents fabricated using glycation. J Biomech Eng 122, 216-223.

Girton, T.S., Oegema, T.R., and Tranquillo, R.T. (1999). Exploiting glycation to stiffen and strengthen tissue equivalents for tissue engineering. J Biomed Mater Res 46, 87-92.

Goettsch, C., Rauner, M., Pacyna, N., Hempel, U., Bornstein, S.R., and Hofbauer, L.C. (2011). miR-125b regulates calcification of vascular smooth muscle cells. The American journal of pathology 179, 1594-1600.

Goldsmith, A.M., Bentley, J.K., Zhou, L., Jia, Y., Bitar, K.N., Fingar, D.C., and Hershenson, M.B. (2006). Transforming growth factor-beta induces airway smooth muscle hypertrophy. Am J Respir Cell Mol Biol 34, 247-254.

Gong, Z., Calkins, G., Cheng, E.C., Krause, D., and Niklason, L.E. (2009). Influence of culture medium on smooth muscle cell differentiation from human bone marrow-derived mesenchymal stem cells. Tissue Eng Part A 15, 319-330.

Gong, Z., and Niklason, L.E. (2008a). Small-diameter human vessel wall engineered from bone marrow-derived mesenchymal stem cells (hMSCs). Faseb J 22, 1635-1648.

Gong, Z., and Niklason, L.E. (2008b). Small-diameter human vessel wall engineered from bone marrow-derived mesenchymal stem cells (hMSCs). Faseb J 22, 1635-1648.

Goumans, M.J., Liu, Z., and ten Dijke, P. (2009). TGF-beta signaling in vascular biology and dysfunction. Cell Research 19, 116-127.

Grainger, D.J., Metcalfe, J.C., Grace, A.A., and Mosedale, D.E. (1998). Transforming growth factor-beta dynamically regulates vascular smooth muscle differentiation in vivo. J Cell Sci 111 (Pt 19), 2977-2988.

Grey, F., Tirabassi, R., Meyers, H., Wu, G.M., McWeeney, S., Hook, L., and Nelson, J.A. (2010). A Viral microRNA Down-Regulates Multiple Cell Cycle Genes through mRNA 5 ' UTRs. Plos Pathog 6.

Griffiths-Jones, S. (2010). miRBase: microRNA sequences and annotation. Curr Protoc Bioinformatics Chapter 12, Unit 12 19 11-10.

Griffiths-Jones, S., Grocock, R.J., van Dongen, S., Bateman, A., and Enright, A.J. (2006). miRBase: microRNA sequences, targets and gene nomenclature. Nucleic Acids Res 34, D140-144.

Grimson, A., Farh, K.K.H., Johnston, W.K., Garrett-Engele, P., Lim, L.P., and Bartel, D.P. (2007). MicroRNA targeting specificity in mammals: Determinants beyond seed pairing. Molecular Cell 27, 91-105.

Gronthos, S., Brahim, J., Li, W., Fisher, L.W., Cherman, N., Boyde, A., DenBesten, P., Robey, P.G., and Shi, S. (2002). Stem cell properties of human dental pulp stem cells. Journal of dental research 81, 531-535.

Gronthos, S., Graves, S.E., Ohta, S., and Simmons, P.J. (1994). The STRO-1+ fraction of adult human bone marrow contains the osteogenic precursors. Blood 84, 4164-4173.

Grundmann, S., Hans, F.P., Kinniry, S., Heinke, J., Helbing, T., Bluhm, F., Sluijter, J.P., Hoefer, I., Pasterkamp, G., Bode, C., et al. (2011). MicroRNA-100 regulates neovascularization by

suppression of mammalian target of rapamycin in endothelial and vascular smooth muscle cells. Circulation 123, 999-1009.

Guettler, S., Vartiainen, M.K., Miralles, F., Larijani, B., and Treisman, R. (2008). RPEL motifs link the serum response factor cofactor MAL but not myocardin to Rho signaling via actin binding. Molecular and cellular biology 28, 732-742.

Gui, L., Dash, B.C., Luo, J., Qin, L., Zhao, L., Yamamoto, K., Hashimoto, T., Wu, H., Dardik, A., Tellides, G., et al. (2016). Implantable tissue-engineered blood vessels from human induced pluripotent stem cells. Biomaterials 102, 120-129.

Guo, H.F., Dai, W.W., Qian, D.H., Qin, Z.X., Lei, Y., Hou, X.Y., and Wen, C. (2017). A simply prepared small-diameter artificial blood vessel that promotes in situ endothelialization. Acta Biomaterialia 54, 107-116.

Guo, L., and Lu, Z. (2010). The fate of miRNA* strand through evolutionary analysis: implication for degradation as merely carrier strand or potential regulatory molecule? PLoS One 5, e11387.

Guo, L., Sun, B., Wu, Q., Yang, S., and Chen, F. (2012). miRNA-miRNA interaction implicates for potential mutual regulatory pattern. Gene 511, 187-194.

Guo, L., Zhao, Y., Yang, S., Zhang, H., and Chen, F. (2014). Integrative analysis of miRNA-mRNA and miRNA-miRNA interactions. BioMed research international 2014, 907420.

Guo, X., Stice, S.L., Boyd, N.L., and Chen, S.Y. (2013). A novel in vitro model system for smooth muscle differentiation from human embryonic stem cell-derived mesenchymal cells. Am J Physiol Cell Physiol 304, C289-298.

Ha, I., Wightman, B., and Ruvkun, G. (1996). A bulged lin-4/lin-14 RNA duplex is sufficient for Caenorhabditis elegans lin-14 temporal gradient formation. Gene Dev 10, 3041-3050.

Hahn, M.S., McHale, M.K., Wang, E., Schmedlen, R.H., and West, J.L. (2007). Physiologic pulsatile flow bioreactor conditioning of poly(ethylene glycol)-based tissue engineered vascular grafts. Ann Biomed Eng 35, 190-200.

Han, C.I., Campbell, G.R., and Campbell, J.H. (2001). Circulating bone marrow cells can contribute to neointimal formation. Journal of vascular research 38, 113-119.

Harris, L.J., Abdollahi, H., Zhang, P., McIlhenny, S., Tulenko, T.N., and DiMuzio, P.J. (2011). Differentiation of adult stem cells into smooth muscle for vascular tissue engineering. The Journal of surgical research 168, 306-314.

Hartmann, S., Ridley, A.J., and Lutz, S. (2015). The Function of Rho-Associated Kinases ROCK1 and ROCK2 in the Pathogenesis of Cardiovascular Disease. Front Pharmacol 6, 276.

Hashi, C.K., Zhu, Y., Yang, G.Y., Young, W.L., Hsiao, B.S., Wang, K., Chu, B., and Li, S. (2007). Antithrombogenic property of bone marrow mesenchymal stem cells in nanofibrous vascular grafts. Proc Natl Acad Sci U S A 104, 11915-11920.

Hautmann, M.B., Thompson, M.M., Swartz, E.A., Olson, E.N., and Owens, G.K. (1997). Angiotensin II-induced stimulation of smooth muscle alpha-actin expression by serum response factor and the homeodomain transcription factor MHox. Circulation research 81, 600-610.

Hayashi, K., Nakamura, S., Nishida, W., and Sobue, K. (2006). Bone morphogenetic protein-induced MSX1 and MSX2 inhibit myocardin-dependent smooth muscle gene transcription. Molecular and cellular biology 26, 9456-9470.

He, H., Jazdzewski, K., Li, W., Liyanarachchi, S., Nagy, R., Volinia, S., Calin, G.A., Liu, C.G., Franssila, K., Suster, S., et al. (2005). The role of microRNA genes in papillary thyroid carcinoma. Proc Natl Acad Sci U S A 102, 19075-19080.

He, W., Nieponice, A., Soletti, L., Hong, Y., Gharaibeh, B., Crisan, M., Usas, A., Peault, B., Huard, J., Wagner, W.R., et al. (2010). Pericyte-based human tissue engineered vascular grafts. Biomaterials 31, 8235-8244.

Heasman, S.J., and Ridley, A.J. (2008). Mammalian Rho GTPases: new insights into their functions from in vivo studies. Nature reviews Molecular cell biology 9, 690-701.

Helwak, A., Kudla, G., Dudnakova, T., and Tollervey, D. (2013). Mapping the human miRNA interactome by CLASH reveals frequent noncanonical binding. Cell 153, 654-665.

Hendrickson, D.G., Hogan, D.J., Herschlag, D., Ferrell, J.E., and Brown, P.O. (2008). Systematic identification of mrNAs recruited to argonaute 2 by specific microRNAs and corresponding changes in transcript abundance. PLoS ONE 3.

Herring, B.P., Kriegel, A.M., and Hoggatt, A.M. (2001). Identification of Barx2b, a serum response factor-associated homeodomain protein. The Journal of biological chemistry 276, 14482-14489.

Hess, C.N., Lopes, R.D., Gibson, C.M., Hager, R., Wojdyla, D.M., Englum, B.R., Mack, M.J., Califf, R.M., Kouchoukos, N.T., Peterson, E.D., et al. (2014). Saphenous vein graft failure after coronary artery bypass surgery: insights from PREVENT IV. Circulation 130, 1445-1451.

Heydarkhan-Hagvall, S., Schenke-Layland, K., Yang, J.Q., Heydarkhan, S., Xu, Y., Zuk, P.A., MacLellan, W.R., and Beygui, R.E. (2008). Human adipose stem cells: a potential cell source for cardiovascular tissue engineering. Cells Tissues Organs 187, 263-274.

Hibino, N., Duncan, D.R., Nalbandian, A., Yi, T., Qyang, Y., Shinoka, T., and Breuer, C.K. (2012). Evaluation of the use of an induced puripotent stem cell sheet for the construction of tissue-engineered vascular grafts. J Thorac Cardiovasc Surg 143, 696-703.

Hibino, N., McGillicuddy, E., Matsumura, G., Ichihara, Y., Naito, Y., Breuer, C., and Shinoka, T. (2010). Late-term results of tissue-engineered vascular grafts in humans. J Thorac Cardiovasc Surg 139, 431-436, 436 e431-432.

Hibino, N., Shin'oka, T., Matsumura, G., Ikada, Y., and Kurosawa, H. (2005). The tissue-engineered vascular graft using bone marrow without culture. J Thorac Cardiovasc Surg 129, 1064-1070.

Higgins, S.P., Solan, A.K., and Niklason, L.E. (2003). Effects of polyglycolic acid on porcine smooth muscle cell growth and differentiation. J Biomed Mater Res A 67, 295-302.

Hinson, J.S., Medlin, M.D., Lockman, K., Taylor, J.M., and Mack, C.P. (2007). Smooth muscle cell-specific transcription is regulated by nuclear localization of the myocardin-related transcription factors. American journal of physiology Heart and circulatory physiology 292, H1170-1180.

Hombach, S., and Kretz, M. (2016). Non-coding RNAs: Classification, Biology and Functioning. Adv Exp Med Biol 937, 3-17.

Hori, Y., Inoue, S., Hirano, Y., and Tabata, Y. (2004). Effect of culture substrates and fibroblast growth factor addition on the proliferation and differentiation of rat bone marrow stromal cells. Tissue Eng 10, 995-1005.

Horita, H.N., Simpson, P.A., Ostriker, A., Furgeson, S., Van Putten, V., Weiser-Evans, M.C., and Nemenoff, R.A. (2011). Serum response factor regulates expression of phosphatase and tensin homolog through a microRNA network in vascular smooth muscle cells. Arteriosclerosis, thrombosis, and vascular biology 31, 2909-2919.

Hsieh, J.Y., Fu, Y.S., Chang, S.J., Tsuang, Y.H., and Wang, H.W. (2010). Functional module analysis reveals differential osteogenic and stemness potentials in human mesenchymal stem cells from bone marrow and Wharton's jelly of umbilical cord. Stem cells and development 19, 1895-1910.

Hu, B., Wu, Z., and Phan, S.H. (2003). Smad3 mediates transforming growth factor-beta-induced alpha-smooth muscle actin expression. American journal of respiratory cell and molecular biology 29, 397-404.

Hu, H., Xu, Z., Li, C., Xu, C., Lei, Z., Zhang, H.T., and Zhao, J. (2016). MiR-145 and miR-203 represses TGF-beta-induced epithelial-mesenchymal transition and invasion by inhibiting SMAD3 in non-small cell lung cancer cells. Lung Cancer 97, 87-94.

Hu, X., Cress, W.D., Zhong, Q., and Zuckerman, K.S. (2000). Transforming growth factor beta inhibits the phosphorylation of pRB at multiple serine/threonine sites and differentially regulates the formation of pRB family-E2F complexes in human myeloid leukemia cells. Biochem Biophys Res Commun 276, 930-939.

Hu, Y., Davison, F., Ludewig, B., Erdel, M., Mayr, M., Url, M., Dietrich, H., and Xu, Q. (2002). Smooth muscle cells in transplant atherosclerotic lesions are originated from recipients, but not bone marrow progenitor cells. Circulation 106, 1834-1839.

Hu, Y., Zhang, Z., Torsney, E., Afzal, A.R., Davison, F., Metzler, B., and Xu, Q. (2004). Abundant progenitor cells in the adventitia contribute to atherosclerosis of vein grafts in ApoE-deficient mice. The Journal of clinical investigation 113, 1258-1265.

Huang, H., Xie, C., Sun, X., Ritchie, R.P., Zhang, J., and Chen, Y.E. (2010). miR-10a contributes to retinoid acid-induced smooth muscle cell differentiation. The Journal of biological chemistry 285, 9383-9389.

Hutvagner, G., and Zamore, P.D. (2002). A microRNA in a multiple-turnover RNAi enzyme complex. Science 297, 2056-2060.

Iyer, D., Chang, D., Marx, J., Wei, L., Olson, E.N., Parmacek, M.S., Balasubramanyam, A., and Schwartz, R.J. (2006). Serum response factor MADS box serine-162 phosphorylation switches proliferation and myogenic gene programs. Proceedings of the National Academy of Sciences of the United States of America 103, 4516-4521.

Jeon, E.S., Moon, H.J., Lee, M.J., Song, H.Y., Kim, Y.M., Bae, Y.C., Jung, J.S., and Kim, J.H. (2006). Sphingosylphosphorylcholine induces differentiation of human mesenchymal stem cells into smooth-muscle-like cells through a TGF-beta-dependent mechanism. J Cell Sci 119, 4994-5005.

Ji, H., Tang, H., Lin, H., Mao, J., Gao, L., Liu, J., and Wu, T. (2014). Rho/Rock cross-talks with transforming growth factor-beta/Smad pathway participates in lung fibroblast-myofibroblast differentiation. Biomed Rep 2, 787-792.

Jiang, Y., Yin, H., and Zheng, X.L. (2010). MicroRNA-1 inhibits myocardin-induced contractility of human vascular smooth muscle cells. J Cell Physiol 225, 506-511.

Jie, W., Guo, J., Shen, Z., Wang, X., Zheng, S., Wang, G., and Ao, Q. (2010). Contribution of myocardin in the hypoxia-induced phenotypic switching of rat pulmonary arterial smooth muscle cells. Experimental and molecular pathology 89, 301-306.

Kamato, D., Burch, M.L., Piva, T.J., Rezaei, H.B., Rostam, M.A., Xu, S., Zheng, W., Little, P.J., and Osman, N. (2013). Transforming growth factor-beta signalling: role and consequences of Smad linker region phosphorylation. Cell Signal 25, 2017-2024.

Kan, X., Sun, Y., Lu, J., Li, M., Wang, Y., Li, Q., Liu, Y., Liu, M., and Tian, L. (2016). Coinhibition of miRNA21 and miRNA221 induces apoptosis by enhancing the p53mediated expression of proapoptotic miRNAs in laryngeal squamous cell carcinoma. Mol Med Rep 13, 4315-4320.

Kang, H., Davis-Dusenbery, B.N., Nguyen, P.H., Lal, A., Lieberman, J., Van Aelst, L., Lagna, G., and Hata, A. (2012). Bone morphogenetic protein 4 promotes vascular smooth muscle contractility by activating microRNA-21 (miR-21), which down-regulates expression of family of dedicator of cytokinesis (DOCK) proteins. The Journal of biological chemistry 287, 3976-3986.

Karamariti, E., Margariti, A., Winkler, B., Wang, X., Hong, X., Baban, D., Ragoussis, J., Huang, Y., Han, J.D., Wong, M.M., et al. (2013a). Smooth muscle cells differentiated from reprogrammed embryonic lung fibroblasts through DKK3 signaling are potent for tissue engineering of vascular grafts. Circ Res 112, 1433-1443.

Karamariti, E., Margariti, A., Winkler, B., Wang, X.C., Hong, X.C., Baban, D., Ragoussis, J., Huang, Y., Han, J.D.J., Wong, M.M., et al. (2013b). Smooth Muscle Cells Differentiated From Reprogrammed Embryonic Lung Fibroblasts Through DKK3 Signaling Are Potent for Tissue Engineering of Vascular Grafts. Circulation Research 112, 1433-+.

Karginov, F.V., Conaco, C., Xuan, Z., Schmidt, B.H., Parker, J.S., Mandel, G., and Hannon, G.J. (2007). A biochemical approach to identifying microRNA targets. P Natl Acad Sci USA 104, 19291-19296.

Kaushal, S., Amiel, G.E., Guleserian, K.J., Shapira, O.M., Perry, T., Sutherland, F.W., Rabkin, E., Moran, A.M., Schoen, F.J., Atala, A., et al. (2001). Functional small-diameter neovessels created using endothelial progenitor cells expanded ex vivo. Nature Medicine 7, 1035-1040.

Kavsak, P., Rasmussen, R.K., Causing, C.G., Bonni, S., Zhu, H., Thomsen, G.H., and Wrana, J.L. (2000). Smad7 binds to Smurf2 to form an E3 ubiquitin ligase that targets the TGF beta receptor for degradation. Mol Cell 6, 1365-1375.

Kern, S., Eichler, H., Stoeve, J., Kluter, H., and Bieback, K. (2006). Comparative analysis of mesenchymal stem cells from bone marrow, umbilical cord blood, or adipose tissue. Stem Cells 24, 1294-1301.

Kim, J., Kang, Y., Kojima, Y., Lighthouse, J.K., Hu, X., Aldred, M.A., McLean, D.L., Park, H., Comhair, S.A., Greif, D.M., et al. (2013). An endothelial apelin-FGF link mediated by miR-424 and miR-503 is disrupted in pulmonary arterial hypertension. Nat Med 19, 74-82.

Kim, M.R., Jeon, E.S., Kim, Y.M., Lee, J.S., and Kim, J.H. (2009). Thromboxane a(2) induces differentiation of human mesenchymal stem cells to smooth muscle-like cells. Stem Cells 27, 191-199.

Kim, Y.M., Jeon, E.S., Kim, M.R., Jho, S.K., Ryu, S.W., and Kim, J.H. (2008). Angiotensin II-induced differentiation of adipose tissue-derived mesenchymal stem cells to smooth muscle-like cells. Int J Biochem Cell Biol 40, 2482-2491.

Kiyan, Y., Limbourg, A., Kiyan, R., Tkachuk, S., Limbourg, F.P., Ovsianikov, A., Chichkov, B.N., Haller, H., and Dumler, I. (2012). Urokinase receptor associates with myocardin to control vascular smooth muscle cells phenotype in vascular disease. Arteriosclerosis, thrombosis, and vascular biology 32, 110-122.

Knight, D.K., Gillies, E.R., and Mequanint, K. (2014). Biomimetic L-aspartic acid-derived functional poly(ester amide)s for vascular tissue engineering. Acta Biomater 10, 3484-3496.

Kong, W., Yang, H., He, L., Zhao, J.J., Coppola, D., Dalton, W.S., and Cheng, J.Q. (2008). MicroRNA-155 Is Regulated by the Transforming Growth Factor beta/Smad Pathway and Contributes to Epithelial Cell Plasticity by Targeting RhoA. Molecular and Cellular Biology 28, 6773-6784.

Konig, G., McAllister, T.N., Dusserre, N., Garrido, S.A., Iyican, C., Marini, A., Fiorillo, A., Avila, H., Wystrychowski, W., Zagalski, K., et al. (2009). Mechanical properties of completely autologous human tissue engineered blood vessels compared to human saphenous vein and mammary artery. Biomaterials 30, 1542-1550.

Konig, J., Zarnack, K., Luscombe, N.M., and Ule, J. (2012). Protein-RNA interactions: new genomic technologies and perspectives. Nature Reviews Genetics 13, 77-83.

Kothapalli, C.R., Taylor, P.M., Smolenski, R.T., Yacoub, M.H., and Ramamurthi, A. (2009). Transforming growth factor beta 1 and hyaluronan oligomers synergistically enhance elastin matrix regeneration by vascular smooth muscle cells. Tissue Eng Part A 15, 501-511.

Kozomara, A., and Griffiths-Jones, S. (2011). miRBase: integrating microRNA annotation and deep-sequencing data. Nucleic Acids Res 39, D152-157.

Kozomara, A., and Griffiths-Jones, S. (2014). miRBase: annotating high confidence microRNAs using deep sequencing data. Nucleic Acids Research 42, D68-D73.

Krawiec, J.T., Liao, H.T., Kwan, L.L., D'Amore, A., Weinbaum, J.S., Rubin, J.P., Wagner, W.R., and Vorp, D.A. (2016). Evaluation of the stromal vascular fraction of adipose tissue as the basis for a stem cell-based tissue-engineered vascular graft. J Vasc Surg.

Krawiec, J.T., and Vorp, D.A. (2012). Adult stem cell-based tissue engineered blood vessels: a review. Biomaterials 33, 3388-3400.

Krek, A., Grun, D., Poy, M.N., Wolf, R., Rosenberg, L., Epstein, E.J., MacMenamin, P., da Piedade, I., Gunsalus, K.C., Stoffel, M., et al. (2005). Combinatorial microRNA target predictions. Nat Genet 37, 495-500.

Kudla, G., Granneman, S., Hahn, D., Beggs, J.D., and Tollervey, D. (2011). Cross-linking, ligation, and sequencing of hybrids reveals RNA-RNA interactions in yeast. P Natl Acad Sci USA 108, 10010-10015.

Kumar, M.S., Hendrix, J.A., Johnson, A.D., and Owens, G.K. (2003). Smooth muscle alpha-actin gene requires two E-boxes for proper expression in vivo and is a target of class I basic helix-loop-helix proteins. Circulation research 92, 840-847.

Kung, L.H., Zaki, S., Ravi, V., Rowley, L., Smith, M.M., Bell, K.M., Bateman, J.F., and Little, C.B. (2017). Utility of circulating serum miRNAs as biomarkers of early cartilage degeneration in animal models of post-traumatic osteoarthritis and inflammatory arthritis. Osteoarthritis and cartilage 25, 426-434.

L'Heureux, N., Dusserre, N., Konig, G., Victor, B., Keire, P., Wight, T.N., Chronos, N.A., Kyles, A.E., Gregory, C.R., Hoyt, G., et al. (2006). Human tissue-engineered blood vessels for adult arterial revascularization. Nat Med 12, 361-365.

L'Heureux, N., Germain, L., Labbe, R., and Auger, F.A. (1993). In vitro construction of a human blood vessel from cultured vascular cells: a morphologic study. J Vasc Surg 17, 499-509.

L'Heureux, N., McAllister, T.N., and de la Fuente, L.M. (2007). Tissue-engineered blood vessel for adult arterial revascularization. N Engl J Med 357, 1451-1453.

L'Heureux, N., Paquet, S., Labbe, R., Germain, L., and Auger, F.A. (1998). A completely biological tissue-engineered human blood vessel. Faseb J 12, 47-56.

Lagna, G., Ku, M.M., Nguyen, P.H., Neuman, N.A., Davis, B.N., and Hata, A. (2007). Control of phenotypic plasticity of smooth muscle cells by bone morphogenetic protein signaling through

the myocardin-related transcription factors. The Journal of biological chemistry 282, 37244-37255.

Lagos-Quintana, M., Rauhut, R., Lendeckel, W., and Tuschl, T. (2001). Identification of novel genes coding for small expressed RNAs. Science 294, 853-858.

Lal, A., Navarro, F., Maher, C.A., Maliszewski, L.E., Yan, N., O'Day, E., Chowdhury, D., Dykxhoorn, D.M., Tsai, P., Hofmann, O., et al. (2009). miR-24 Inhibits Cell Proliferation by Targeting E2F2, MYC, and Other Cell-Cycle Genes via Binding to "Seedless" 3 ' UTR MicroRNA Recognition Elements. Molecular Cell 35, 610-625.

Latsinik, N.V., Luria, E.A., Friedenstein, A.J., Samoylina, N.L., and Chertkov, I.L. (1970). Colony-forming cells in organ cultures of embryonal liver. Journal of cellular physiology 75, 163-165.

Lau, N.C., Lim, L.P., Weinstein, E.G., and Bartel, D.P. (2001). An abundant class of tiny RNAs with probable regulatory roles in Caenorhabditis elegans. Science 294, 858-862.

Lee, A., Papangeli, I., Park, Y., Jeong, H.N., Choi, J., Kang, H., Jo, H.N., Kim, J., and Chun, H.J. (2017). A PPARgamma-dependent miR-424/503-CD40 axis regulates inflammation mediated angiogenesis. Sci Rep 7, 2528.

Lee, R.C., and Ambros, V. (2001). An extensive class of small RNAs in Caenorhabditis elegans. Science 294, 862-864.

Lee, R.C., Feinbaum, R.L., and Ambros, V. (1993). The C-Elegans Heterochronic Gene Lin-4 Encodes Small Rnas with Antisense Complementarity to Lin-14. Cell 75, 843-854.

Leeper, N.J., Raiesdana, A., Kojima, Y., Chun, H.J., Azuma, J., Maegdefessel, L., Kundu, R.K., Quertermous, T., Tsao, P.S., and Spin, J.M. (2011). MicroRNA-26a is a novel regulator of vascular smooth muscle cell function. Journal of cellular physiology 226, 1035-1043.

Lenga, Y., Koh, A., Perera, A.S., McCulloch, C.A., Sodek, J., and Zohar, R. (2008). Osteopontin expression is required for myofibroblast differentiation. Circ Res 102, 319-327.

Levenberg, S., Golub, J.S., Amit, M., Itskovitz-Eldor, J., and Langer, R. (2002). Endothelial cells derived from human embryonic stem cells. Proc Natl Acad Sci U S A 99, 4391-4396.

Lewis, B.P., Burge, C.B., and Bartel, D.P. (2005). Conserved seed pairing, often flanked by adenosines, indicates that thousands of human genes are microRNA targets. Cell 120, 15-20.

Lewis, B.P., Shih, I.H., Jones-Rhoades, M.W., Bartel, D.P., and Burge, C.B. (2003). Prediction of Mammalian MicroRNA Targets. Cell 115, 787-798.

Li, E., Zhang, J., Yuan, T., and Ma, B. (2014). MiR-145 inhibits osteosarcoma cells proliferation and invasion by targeting ROCK1. Tumour Biol 35, 7645-7650.

Li, G., Chen, S.J., Oparil, S., Chen, Y.F., and Thompson, J.A. (2000). Direct in vivo evidence demonstrating neointimal migration of adventitial fibroblasts after balloon injury of rat carotid arteries. Circulation 101, 1362-1365.

Li, J., Jiang, J., Yin, H., Wang, L., Tian, R., Li, H., Wang, Z., Li, D., Wang, Y., Gui, Y., et al. (2012). Atorvastatin inhibits myocardin expression in vascular smooth muscle cells. Hypertension 60, 145-153.

Li, S., Wang, D.Z., Wang, Z., Richardson, J.A., and Olson, E.N. (2003). The serum response factor coactivator myocardin is required for vascular smooth muscle development. Proceedings of the National Academy of Sciences of the United States of America 100, 9366-9370.

Lin, Y., Liu, X., Cheng, Y., Yang, J., Huo, Y., and Zhang, C. (2009). Involvement of MicroRNAs in hydrogen peroxide-mediated gene regulation and cellular injury response in vascular smooth muscle cells. The Journal of biological chemistry 284, 7903-7913.

Liu, H., Song, Z., Liao, D., Zhang, T., Liu, F., Zheng, W., Luo, K., and Yang, L. (2015). miR-503 inhibits cell proliferation and invasion in glioma by targeting L1CAM. Int J Clin Exp Med 8, 18441-18447.

Liu, J.Y., Peng, H.F., and Andreadis, S.T. (2008). Contractile smooth muscle cells derived from hair-follicle stem cells. Cardiovascular Research 79, 24-33.

Liu, J.Y., Peng, H.F., Gopinath, S., Tian, J., and Andreadis, S.T. (2010). Derivation of functional smooth muscle cells from multipotent human hair follicle mesenchymal stem cells. Tissue Eng Part A 16, 2553-2564.

Liu, J.Y., Swartz, D.D., Peng, H.F., Gugino, S.F., Russell, J.A., and Andreadis, S.T. (2007). Functional tissue-engineered blood vessels from bone marrow progenitor cells. Cardiovasc Res 75, 618-628.

Liu, X., Cheng, Y., Chen, X., Yang, J., Xu, L., and Zhang, C. (2011). MicroRNA-31 regulated by the extracellular regulated kinase is involved in vascular smooth muscle cell growth via large tumor suppressor homolog 2. The Journal of biological chemistry 286, 42371-42380.

Liu, X., Cheng, Y., Yang, J., Xu, L., and Zhang, C. (2012). Cell-specific effects of miR-221/222 in vessels: molecular mechanism and therapeutic application. J Mol Cell Cardiol 52, 245-255.

Liu, X., Cheng, Y., Zhang, S., Lin, Y., Yang, J., and Zhang, C. (2009). A necessary role of miR-221 and miR-222 in vascular smooth muscle cell proliferation and neointimal hyperplasia. Circ Res 104, 476-487.

Liu, Y., Sinha, S., and Owens, G. (2003). A transforming growth factor-beta control element required for SM alpha-actin expression in vivo also partially mediates GKLF-dependent transcriptional repression. The Journal of biological chemistry 278, 48004-48011.

Liu, Z.P., Wang, Z., Yanagisawa, H., and Olson, E.N. (2005). Phenotypic modulation of smooth muscle cells through interaction of Foxo4 and myocardin. Developmental cell 9, 261-270.

Llobet-Navas, D., Rodriguez-Barrueco, R., Castro, V., Ugalde, A.P., Sumazin, P., Jacob-Sendler, D., Demircan, B., Castillo-Martin, M., Putcha, P., Marshall, N., et al. (2014). The miR-424(322)/503 cluster orchestrates remodeling of the epithelium in the involuting mammary gland. Genes Dev 28, 765-782.

Lockman, K., Hinson, J.S., Medlin, M.D., Morris, D., Taylor, J.M., and Mack, C.P. (2004). Sphingosine 1-phosphate stimulates smooth muscle cell differentiation and proliferation by activating separate serum response factor co-factors. J Biol Chem 279, 42422-42430.

Long, J., Ou, C., Xia, H., Zhu, Y., and Liu, D. (2015). MiR-503 inhibited cell proliferation of human breast cancer cells by suppressing CCND1 expression. Tumour Biol 36, 8697-8702.

Long, J.L., and Tranquillo, R.T. (2003). Elastic fiber production in cardiovascular tissue-equivalents. Matrix Biol 22, 339-350.

Long, X., and Miano, J.M. (2011). Transforming growth factor-beta1 (TGF-beta1) utilizes distinct pathways for the transcriptional activation of microRNA 143/145 in human coronary artery smooth muscle cells. J Biol Chem 286, 30119-30129.

Lovett, M., Eng, G., Kluge, J.A., Cannizzaro, C., Vunjak-Novakovic, G., and Kaplan, D.L. (2010). Tubular silk scaffolds for small diameter vascular grafts. Organogenesis 6, 217-224.

Lu, J., Landerholm, T.E., Wei, J.S., Dong, X.R., Wu, S.P., Liu, X., Nagata, K., Inagaki, M., and Majesky, M.W. (2001). Coronary smooth muscle differentiation from proepicardial cells requires rhoA-mediated actin reorganization and p160 rho-kinase activity. Developmental biology 240, 404-418.

Lu, L.L., Liu, Y.J., Yang, S.G., Zhao, Q.J., Wang, X., Gong, W., Han, Z.B., Xu, Z.S., Lu, Y.X., Liu, D., et al. (2006). Isolation and characterization of human umbilical cord mesenchymal stem cells with hematopoiesis-supportive function and other potentials. Haematologica 91, 1017-1026.

Mack, C.P. (2011). Signaling mechanisms that regulate smooth muscle cell differentiation. Arteriosclerosis, thrombosis, and vascular biology 31, 1495-1505.

Mackenzie, N.C., Staines, K.A., Zhu, D., Genever, P., and Macrae, V.E. (2014). miRNA-221 and miRNA-222 synergistically function to promote vascular calcification. Cell Biochem Funct 32, 209-216.

Madsen, C.S., Hershey, J.C., Hautmann, M.B., White, S.L., and Owens, G.K. (1997). Expression of the smooth muscle myosin heavy chain gene is regulated by a negative-acting GC-rich element located between two positive-acting serum response factor-binding elements. The Journal of biological chemistry 272, 6332-6340.

Mah, S.M., Buske, C., Humphries, R.K., and Kuchenbauer, F. (2010). miRNA*: a passenger stranded in RNA-induced silencing complex? Crit Rev Eukaryot Gene Expr 20, 141-148.

Majesky, M.W. (2007). Developmental basis of vascular smooth muscle diversity. Arteriosclerosis, thrombosis, and vascular biology 27, 1248-1258.

Manabe, I., and Owens, G.K. (2001). Recruitment of serum response factor and hyperacetylation of histones at smooth muscle-specific regulatory regions during differentiation of a novel P19-derived in vitro smooth muscle differentiation system. Circulation research 88, 1127-1134.

Margariti, A., Winkler, B., Karamariti, E., Zampetaki, A., Tsai, T.N., Baban, D., Ragoussis, J., Huang, Y., Han, J.D., Zeng, L., et al. (2012). Direct reprogramming of fibroblasts into endothelial cells capable of angiogenesis and reendothelialization in tissue-engineered vessels. Proc Natl Acad Sci U S A 109, 13793-13798.

Margariti, A., Xiao, Q., Zampetaki, A., Zhang, Z., Li, H., Martin, D., Hu, Y., Zeng, L., and Xu, Q. (2009). Splicing of HDAC7 modulates the SRF-myocardin complex during stem-cell differentiation towards smooth muscle cells. J Cell Sci 122, 460-470.

Martin, K., Weiss, S., Metharom, P., Schmeckpeper, J., Hynes, B., O'Sullivan, J., and Caplice, N. (2009). Thrombin stimulates smooth muscle cell differentiation from peripheral blood mononuclear cells via protease-activated receptor-1, RhoA, and myocardin. Circulation research 105, 214-218.

Matsumura, G., Miyagawa-Tomita, S., Shin'oka, T., Ikada, Y., and Kurosawa, H. (2003). First evidence that bone marrow cells contribute to the construction of tissue-engineered vascular autografts in vivo. Circulation 108, 1729-1734.

Matsushita, R., Yoshino, H., Enokida, H., Goto, Y., Miyamoto, K., Yonemori, M., Inoguchi, S., Nakagawa, M., and Seki, N. (2016). Regulation of UHRF1 by dual-strand tumor-suppressor microRNA-145 (miR-145-5p and miR-145-3p): Inhibition of bladder cancer cell aggressiveness. Oncotarget 7, 28460-28487.

McAllister, T.N., Maruszewski, M., Garrido, S.A., Wystrychowski, W., Dusserre, N., Marini, A., Zagalski, K., Fiorillo, A., Avila, H., Manglano, X., et al. (2009). Effectiveness of haemodialysis access with

an autologous tissue-engineered vascular graft: a multicentre cohort study. Lancet 373, 1440-1446.

McKee, J.A., Banik, S.S., Boyer, M.J., Hamad, N.M., Lawson, J.H., Niklason, L.E., and Counter, C.M. (2003). Human arteries engineered in vitro. Embo Rep 4, 633-638.

Merlet, E., Atassi, F., Motiani, R.K., Mougenot, N., Jacquet, A., Nadaud, S., Capiod, T., Trebak, M., Lompre, A.M., and Marchand, A. (2013). miR-424/322 regulates vascular smooth muscle cell phenotype and neointimal formation in the rat. Cardiovasc Res 98, 458-468.

Miano, J.M. (2003). Serum response factor: toggling between disparate programs of gene expression. Journal of molecular and cellular cardiology 35, 577-593.

Miralles, F., Posern, G., Zaromytidou, A.I., and Treisman, R. (2003). Actin dynamics control SRF activity by regulation of its coactivator MAL. Cell 113, 329-342.

Mirza, A., Hyvelin, J.M., Rochefort, G.Y., Lermusiaux, P., Antier, D., Awede, B., Bonnet, P., Domenech, J., and Eder, V. (2008). Undifferentiated mesenchymal stem cells seeded on a vascular prosthesis contribute to the restoration of a physiologic vascular wall. J Vasc Surg 47, 1313-1321.

Mizuno, Y., Yagi, K., Tokuzawa, Y., Kanesaki-Yatsuka, Y., Suda, T., Katagiri, T., Fukuda, T., Maruyama, M., Okuda, A., Amemiya, T., et al. (2008). miR-125b inhibits osteoblastic differentiation by down-regulation of cell proliferation. Biochemical and biophysical research communications 368, 267-272.

Morrell, N.W., Yang, X., Upton, P.D., Jourdan, K.B., Morgan, N., Sheares, K.K., and Trembath, R.C. (2001). Altered growth responses of pulmonary artery smooth muscle cells from patients with primary pulmonary hypertension to transforming growth factor-beta(1) and bone morphogenetic proteins. Circulation 104, 790-795.

Nakao, A., Afrakhte, M., Moren, A., Nakayama, T., Christian, J.L., Heuchel, R., Itoh, S., Kawabata, M., Heldin, N.E., Heldin, C.H., et al. (1997). Identification of Smad7, a TGFbeta-inducible antagonist of TGF-beta signalling. Nature 389, 631-635.

Nalluri, J.J., Barh, D., Azevedo, V., and Ghosh, P. (2017). miRsig: a consensus-based network inference methodology to identify pan-cancer miRNA-miRNA interaction signatures. Sci Rep 7, 39684.

Neidert, M.R., Lee, E.S., Oegema, T.R., and Tranquillo, R.T. (2002). Enhanced fibrin remodeling in vitro with TGF-beta1, insulin and plasmin for improved tissue-equivalents. Biomaterials 23, 3717-3731.

Nieponice, A., Soletti, L., Guan, J., Deasy, B.M., Huard, J., Wagner, W.R., and Vorp, D.A. (2008). Development of a tissue-engineered vascular graft combining a biodegradable scaffold, muscle-derived stem cells and a rotational vacuum seeding technique. Biomaterials 29, 825-833.

Niklason, L.E., Gao, J., Abbott, W.M., Hirschi, K.K., Houser, S., Marini, R., and Langer, R. (1999). Functional arteries grown in vitro. Science 284, 489-493.

Ning, H., Lin, G., Lue, T.F., and Lin, C.S. (2011). Mesenchymal stem cell marker Stro-1 is a 75 kd endothelial antigen. Biochemical and biophysical research communications 413, 353-357.

Nishi, H., Ono, K., Iwanaga, Y., Horie, T., Nagao, K., Takemura, G., Kinoshita, M., Kuwabara, Y., Mori, R.T., Hasegawa, K., et al. (2010). MicroRNA-15b modulates cellular ATP levels and degenerates mitochondria via Arl2 in neonatal rat cardiac myocytes. J Biol Chem 285, 4920-4930.

Odorico, J.S., Kaufman, D.S., and Thomson, J.A. (2001). Multilineage differentiation from human embryonic stem cell lines. Stem Cells 19, 193-204.

Ohgushi, H., Goldberg, V.M., and Caplan, A.I. (1989a). Heterotopic osteogenesis in porous ceramics induced by marrow cells. Journal of orthopaedic research : official publication of the Orthopaedic Research Society 7, 568-578.

Ohgushi, H., Goldberg, V.M., and Caplan, A.I. (1989b). Repair of bone defects with marrow cells and porous ceramic. Experiments in rats. Acta orthopaedica Scandinavica 60, 334-339.

Okamura, K., Phillips, M.D., Tyler, D.M., Duan, H., Chou, Y.T., and Lai, E.C. (2008). The regulatory activity of microRNA* species has substantial influence on microRNA and 3' UTR evolution. Nat Struct Mol Biol 15, 354-363.

Olausson, M., Patil, P.B., Kuna, V.K., Chougule, P., Hernandez, N., Methe, K., Kullberg-Lindh, C., Borg, H., Ejnell, H., and Sumitran-Holgersson, S. (2012). Transplantation of an allogeneic vein bioengineered with autologous stem cells: a proof-of-concept study. Lancet 380, 230-237.

Olsen, P.H., and Ambros, V. (1999). The lin-4 regulatory RNA controls developmental timing in Caenorhabditis elegans by blocking LIN-14 protein synthesis after the initiation of translation. Dev Biol 216, 671-680.

Ørom, U.A., Nielsen, F.C., and Lund, A.H. (2008). MicroRNA-10a Binds the 5′ UTR of Ribosomal Protein mRNAs and Enhances Their Translation. Molecular Cell 30, 460-471.

Oswald, J., Boxberger, S., Jorgensen, B., Feldmann, S., Ehninger, G., Bornhauser, M., and Werner, C. (2004). Mesenchymal stem cells can be differentiated into endothelial cells in vitro. Stem Cells 22, 377-384.

Owen, M., and Friedenstein, A.J. (1988). Stromal stem cells: marrow-derived osteogenic precursors. Ciba Foundation symposium 136, 42-60.

Owens, G.K. (1995). Regulation of differentiation of vascular smooth muscle cells. Physiological reviews 75, 487-517.

Owens, G.K., Kumar, M.S., and Wamhoff, B.R. (2004). Molecular regulation of vascular smooth muscle cell differentiation in development and disease. Physiological reviews 84, 767-801.

Ozolanta, I., Tetere, G., Purinya, B., and Kasyanov, V. (1998). Changes in the mechanical properties, biochemical contents and wall structure of the human coronary arteries with age and sex. Med Eng Phys 20, 523-533.

Pan, Y., Balazs, L., Tigyi, G., and Yue, J. (2011). Conditional deletion of Dicer in vascular smooth muscle cells leads to the developmental delay and embryonic mortality. Biochemical and biophysical research communications 408, 369-374.

Papadimitriou, E., Kardassis, D., Moustakas, A., and Stournaras, C. (2011). TGFbeta-induced early activation of the small GTPase RhoA is Smad2/3-independent and involves Src and the guanine nucleotide exchange factor Vav2. Cell Physiol Biochem 28, 229-238.

Parmacek, M.S. (2007). Myocardin-related transcription factors: critical coactivators regulating cardiovascular development and adaptation. Circ Res 100, 633-644.

Parvizi, M., Bolhuis-Versteeg, L.A., Poot, A.A., and Harmsen, M.C. (2016). Efficient generation of smooth muscle cells from adipose-derived stromal cells by 3D mechanical stimulation can substitute the use of growth factors in vascular tissue engineering. Biotechnol J 11, 932-944.

Pashneh-Tala, S., MacNeil, S., and Claeyssens, F. (2016). The tissue-engineered vascular graft - Past, present, and future. Tissue Engineering - Part B: Reviews 22, 68-100.

Pasquinelli, A.E., Reinhart, B.J., Slack, F., Martindale, M.Q., Kuroda, M.I., Maller, B., Hayward, D.C., Ball, E.E., Degnan, B., Muller, P., et al. (2000). Conservation of the sequence and temporal expression of let-7 heterochronic regulatory RNA. Nature 408, 86-89.

Peng, H.F., Liu, J.Y., Andreadis, S.T., and Swartz, D.D. (2011). Hair Follicle-Derived Smooth Muscle Cells and Small Intestinal Submucosa for Engineering Mechanically Robust and Vasoreactive Vascular Media. Tissue Eng Pt A 17, 981-990.

Pipes, G.C., Sinha, S., Qi, X., Zhu, C.H., Gallardo, T.D., Shelton, J., Creemers, E.E., Sutherland, L., Richardson, J.A., Garry, D.J., et al. (2005). Stem cells and their derivatives can bypass the requirement of myocardin for smooth muscle gene expression. Developmental biology 288, 502-513.

Poh, M., Boyer, M., Solan, A., Dahl, S.L., Pedrotty, D., Banik, S.S., McKee, J.A., Klinger, R.Y., Counter, C.M., and Niklason, L.E. (2005). Blood vessels engineered from human cells. Lancet 365, 2122-2124.

Polioudakis, D., Abell, N.S., and Iyer, V.R. (2015). miR-503 represses human cell proliferation and directly targets the oncogene DDHD2 by non-canonical target pairing. Bmc Genomics 16, 40.

Poliseno, L., Cecchettini, A., Mariani, L., Evangelista, M., Ricci, F., Giorgi, F., Citti, L., and Rainaldi, G. (2006). Resting smooth muscle cells as a model for studying vascular cell activation. Tissue Cell 38, 111-120.

Prockop, D.J., and Olson, S.D. (2007). Clinical trials with adult stem/progenitor cells for tissue repair: let's not overlook some essential precautions. Blood 109, 3147-3151.

Qiu, P., Feng, X.H., and Li, L. (2003). Interaction of Smad3 and SRF-associated complex mediates TGF-beta1 signals to regulate SM22 transcription during myofibroblast differentiation. J Mol Cell Cardiol 35, 1407-1420.

Qiu, P., Ritchie, R.P., Fu, Z., Cao, D., Cumming, J., Miano, J.M., Wang, D.Z., Li, H.J., and Li, L. (2005). Myocardin enhances Smad3-mediated transforming growth factor-beta1 signaling in a CArG box-independent manner: Smad-binding element is an important cis element for SM22alpha transcription in vivo. Circulation research 97, 983-991.

Quintavalle, M., Elia, L., Condorelli, G., and Courtneidge, S.A. (2010). MicroRNA control of podosome formation in vascular smooth muscle cells in vivo and in vitro. The Journal of cell biology 189, 13-22.

Qureshi, H.Y., Ahmad, R., Sylvester, J., and Zafarullah, M. (2007). Requirement of phosphatidylinositol 3-kinase/Akt signaling pathway for regulation of tissue inhibitor of metalloproteinases-3 gene expression by TGF-beta in human chondrocytes. Cellular signalling 19, 1643-1651.

Ramakrishnan, V.M., and Boyd, N.L. (2017). The Adipose Stromal Vascular Fraction as a Complex Cellular Source for Tissue Engineering Applications. Tissue Eng Part B Rev.

Rangrez, A.Y., Massy, Z.A., Metzinger-Le Meuth, V., and Metzinger, L. (2011). miR-143 and miR-145: molecular keys to switch the phenotype of vascular smooth muscle cells. Circulation Cardiovascular genetics 4, 197-205.

Rao, X., Di Leva, G., Li, M., Fang, F., Devlin, C., Hartman-Frey, C., Burow, M.E., Ivan, M., Croce, C.M., and Nephew, K.P. (2011). MicroRNA-221/222 confers breast cancer fulvestrant resistance by regulating multiple signaling pathways. Oncogene 30, 1082-1097.

Rapoport, H.S., Fish, J., Basu, J., Campbell, J., Genheimer, C., Payne, R., and Jain, D. (2012). Construction of a tubular scaffold that mimics J-shaped stress/strain mechanics using an innovative electrospinning technique. Tissue Eng Part C Methods 18, 567-574.

Ratz, P.H., Berg, K.M., Urban, N.H., and Miner, A.S. (2005). Regulation of smooth muscle calcium sensitivity: KCl as a calcium-sensitizing stimulus. Am J Physiol Cell Physiol 288, C769-783.

Reinhart, B.J., Slack, F.J., Basson, M., Pasquinelli, A.E., Bettinger, J.C., Rougvie, A.E., Horvitz, H.R., and Ruvkun, G. (2000). The 21-nucleotide let-7 RNA regulates developmental timing in Caenorhabditis elegans. Nature 403, 901-906.

Ren, X., Feng, Y., Guo, J., Wang, H., Li, Q., Yang, J., Hao, X., Lv, J., Ma, N., and Li, W. (2015). Surface modification and endothelialization of biomaterials as potential scaffolds for vascular tissue engineering applications. Chem Soc Rev 44, 5680-5742.

Rhodes, L.V., Martin, E.C., Segar, H.C., Miller, D.F., Buechlein, A., Rusch, D.B., Nephew, K.P., Burow, M.E., and Collins-Burow, B.M. (2015). Dual regulation by microRNA-200b-3p and microRNA-200b-5p in the inhibition of epithelial-to-mesenchymal transition in triple-negative breast cancer. Oncotarget 6, 16638-16652.

Ries, J., Vairaktaris, E., Agaimy, A., Kintopp, R., Baran, C., Neukam, F.W., and Nkenke, E. (2014). miR-186, miR-3651 and miR-494: potential biomarkers for oral squamous cell carcinoma extracted from whole blood. Oncol Rep 31, 1429-1436.

Riha, G.M., Lin, P.H., Lumsden, A.B., Yao, Q., and Chen, C. (2005). Roles of hemodynamic forces in vascular cell differentiation. Annals of Biomedical Engineering 33, 772-779.

Rihani, A., Van Goethem, A., Ongenaert, M., De Brouwer, S., Volders, P.J., Agarwal, S., De Preter, K., Mestdagh, P., Shohet, J., Speleman, F., et al. (2015). Genome wide expression profiling of p53 regulated miRNAs in neuroblastoma. Sci Rep 5, 9027.

Rocco, K.A., Maxfield, M.W., Best, C.A., Dean, E.W., and Breuer, C.K. (2014). In vivo applications of electrospun tissue-engineered vascular grafts: A review. Tissue Engineering - Part B: Reviews 20, 628-640.

Rodriguez, L.V., Alfonso, Z., Zhang, R., Leung, J., Wu, B., and Ignarro, L.J. (2006). Clonogenic multipotent stem cells in human adipose tissue differentiate into functional smooth muscle cells. Proceedings of the National Academy of Sciences of the United States of America 103, 12167-12172.

Romanov, Y.A., Svintsitskaya, V.A., and Smirnov, V.N. (2003). Searching for alternative sources of postnatal human mesenchymal stem cells: candidate MSC-like cells from umbilical cord. Stem cells 21, 105-110.

Ross, R., and Glomset, J.A. (1976). The pathogenesis of atherosclerosis (first of two parts). The New England journal of medicine 295, 369-377.

Rothuizen, T.C., Kemp, R., Duijs, J.M., de Boer, H.C., Bijkerk, R., van der Veer, E.P., Moroni, L., van Zonneveld, A.J., Weiss, A.S., Rabelink, T.J., et al. (2016). Promoting Tropoelastin Expression in Arterial and Venous Vascular Smooth Muscle Cells and Fibroblasts for Vascular Tissue Engineering. Tissue Eng Part C Methods 22, 923-931.

Sabatini, F., Petecchia, L., Tavian, M., Jodon de Villeroche, V., Rossi, G.A., and Brouty-Boye, D. (2005). Human bronchial fibroblasts exhibit a mesenchymal stem cell phenotype and multilineage differentiating potentialities. Laboratory investigation; a journal of technical methods and pathology 85, 962-971.

Sabik, J.F., 3rd, Lytle, B.W., Blackstone, E.H., Houghtaling, P.L., and Cosgrove, D.M. (2005). Comparison of saphenous vein and internal thoracic artery graft patency by coronary system. Ann Thorac Surg 79, 544-551; discussion 544-551.

Sacchetti, B., Funari, A., Remoli, C., Giannicola, G., Kogler, G., Liedtke, S., Cossu, G., Serafini, M., Sampaolesi, M., Tagliafico, E., et al. (2016). No Identical "Mesenchymal Stem Cells" at Different Times and Sites: Human Committed Progenitors of Distinct Origin and Differentiation Potential Are Incorporated as Adventitial Cells in Microvessels. Stem Cell Reports 6, 897-913.

Salingcarnboriboon, R., Yoshitake, H., Tsuji, K., Obinata, M., Amagasa, T., Nifuji, A., and Noda, M. (2003). Establishment of tendon-derived cell lines exhibiting pluripotent mesenchymal stem cell-like property. Experimental cell research 287, 289-300.

Sandbo, N., Qin, Y., Taurin, S., Hogarth, D.K., Kreutz, B., and Dulin, N.O. (2005). Regulation of serum response factor-dependent gene expression by proteasome inhibitors. Molecular pharmacology 67, 789-797.

Sarkar, S., Dey, B.K., and Dutta, A. (2010). MiR-322/424 and -503 are induced during muscle differentiation and promote cell cycle quiescence and differentiation by down-regulation of Cdc25A. Mol Biol Cell 21, 2138-2149.

Sarkar, S., Salacinski, H.J., Hamilton, G., and Seifalian, A.M. (2006). The mechanical properties of infrainguinal vascular bypass grafts: Their role in influencing patency. European Journal of Vascular and Endovascular Surgery 31, 627-636.

Sartore, S., Chiavegato, A., Faggin, E., Franch, R., Puato, M., Ausoni, S., and Pauletto, P. (2001). Contribution of adventitial fibroblasts to neointima formation and vascular remodeling: from innocent bystander to active participant. Circulation research 89, 1111-1121.

Sata, M., Saiura, A., Kunisato, A., Tojo, A., Okada, S., Tokuhisa, T., Hirai, H., Makuuchi, M., Hirata, Y., and Nagai, R. (2002). Hematopoietic stem cells differentiate into vascular cells that participate in the pathogenesis of atherosclerosis. Nature medicine 8, 403-409.

Scalbert, E., and Bril, A. (2008). Implication of microRNAs in the cardiovascular system. Current opinion in pharmacology 8, 181-188.

Schuliga, M., Javeed, A., Harris, T., Xia, Y., Qin, C., Wang, Z., Zhang, X., Lee, P.V., Camoretti-Mercado, B., and Stewart, A.G. (2013). Transforming growth factor-beta-induced differentiation of airway smooth muscle cells is inhibited by fibroblast growth factor-2. Am J Respir Cell Mol Biol 48, 346-353.

Seifu, D.G., Purnama, A., Mequanint, K., and Mantovani, D. (2013). Small-diameter vascular tissue engineering. Nature Reviews Cardiology 10, 410-421.

Selbach, M., Schwanhausser, B., Thierfelder, N., Fang, Z., Khanin, R., and Rajewsky, N. (2008). Widespread changes in protein synthesis induced by microRNAs. Nature 455, 58-63.

Seo, B.M., Miura, M., Gronthos, S., Bartold, P.M., Batouli, S., Brahim, J., Young, M., Robey, P.G., Wang, C.Y., and Shi, S. (2004). Investigation of multipotent postnatal stem cells from human periodontal ligament. Lancet 364, 149-155.

Shankman, L.S., Gomez, D., Cherepanova, O.A., Salmon, M., Alencar, G.F., Haskins, R.M., Swiatlowska, P., Newman, A.A., Greene, E.S., Straub, A.C., et al. (2015). KLF4-dependent phenotypic modulation of smooth muscle cells has a key role in atherosclerotic plaque pathogenesis. Nat Med 21, 628-637.

Shen, G., Tsung, H.C., Wu, C.F., Liu, X.Y., Wang, X.Y., Liu, W., Cui, L., and Cao, Y.L. (2003). Tissue engineering of blood vessels with endothelial cells differentiated from mouse embryonic stem cells. Cell Res 13, 335-341.

Shen, X., Soibam, B., Benham, A., Xu, X., Chopra, M., Peng, X., Yu, W., Bao, W., Liang, R., Azares, A., et al. (2016). miR-322/-503 cluster is expressed in the earliest cardiac progenitor cells and drives cardiomyocyte specification. Proc Natl Acad Sci U S A 113, 9551-9556.

Shi, N., and Chen, S.Y. (2013). Cell division cycle 7 mediates transforming growth factor-beta-induced smooth muscle maturation through activation of myocardin gene transcription. The Journal of biological chemistry 288, 34336-34342.

Shi, S., and Gronthos, S. (2003). Perivascular niche of postnatal mesenchymal stem cells in human bone marrow and dental pulp. Journal of bone and mineral research : the official journal of the American Society for Bone and Mineral Research 18, 696-704.

Shimizu, K., Sugiyama, S., Aikawa, M., Fukumoto, Y., Rabkin, E., Libby, P., and Mitchell, R.N. (2001). Host bone-marrow cells are a source of donor intimal smooth- muscle-like cells in murine aortic transplant arteriopathy. Nature medicine 7, 738-741.

Shimizu, R.T., Blank, R.S., Jervis, R., Lawrenz-Smith, S.C., and Owens, G.K. (1995). The smooth muscle alpha-actin gene promoter is differentially regulated in smooth muscle versus non-smooth muscle cells. The Journal of biological chemistry 270, 7631-7643.

Shimokawa, H., Sunamura, S., and Satoh, K. (2016). RhoA/Rho-Kinase in the Cardiovascular System. Circ Res 118, 352-366.

Shin'oka, T., Imai, Y., and Ikada, Y. (2001). Transplantation of a tissue-engineered pulmonary artery. N Engl J Med 344, 532-533.

Shin'oka, T., Matsumura, G., Hibino, N., Naito, Y., Watanabe, M., Konuma, T., Sakamoto, T., Nagatsu, M., and Kurosawa, H. (2005). Midterm clinical result of tissue-engineered vascular autografts seeded with autologous bone marrow cells. J Thorac Cardiovasc Surg 129, 1330-1338.

Shin, C., Nam, J.W., Farh, K.K.H., Chiang, H.R., Shkumatava, A., and Bartel, D.P. (2010). Expanding the MicroRNA Targeting Code: Functional Sites with Centered Pairing. Molecular Cell 38, 789-802.

Shinoka, T., Shum-Tim, D., Ma, P.X., Tanel, R.E., Isogai, N., Langer, R., Vacanti, J.P., and Mayer, J.E., Jr. (1998). Creation of viable pulmonary artery autografts through tissue engineering. J Thorac Cardiovasc Surg 115, 536-545; discussion 545-536.

Shudo, Y., Cohen, J.E., Goldstone, A.B., MacArthur, J.W., Patel, J., Edwards, B.B., Hopkins, M.S., Steele, A.N., Joubert, L.M., Miyagawa, S., et al. (2016). Isolation and trans-differentiation of mesenchymal stromal cells into smooth muscle cells: Utility and applicability for cell-sheet engineering. Cytotherapy 18, 510-517.

Simmons, P.J., and Torok-Storb, B. (1991). Identification of stromal cell precursors in human bone marrow by a novel monoclonal antibody, STRO-1. Blood 78, 55-62.

Sivarapatna, A., Ghaedi, M., Le, A.V., Mendez, J.J., Qyang, Y., and Niklason, L.E. (2015). Arterial specification of endothelial cells derived from human induced pluripotent stem cells in a biomimetic flow bioreactor. Biomaterials 53, 621-633.

Solchaga, L.A., Penick, K., Porter, J.D., Goldberg, V.M., Caplan, A.I., and Welter, J.F. (2005). FGF-2 enhances the mitotic and chondrogenic potentials of human adult bone marrow-derived mesenchymal stem cells. J Cell Physiol 203, 398-409.

Song, R., Catchpoole, D.R., Kennedy, P.J., and Li, J. (2015). Identification of lung cancer miRNA-miRNA co-regulation networks through a progressive data refining approach. J Theor Biol 380, 271-279.

Sotiropoulou, P.A., Perez, S.A., Salagianni, M., Baxevanis, C.N., and Papamichail, M. (2006). Characterization of the optimal culture conditions for clinical scale production of human mesenchymal stem cells. Stem Cells 24, 462-471.

Spencer, J.A., and Misra, R.P. (1996). Expression of the serum response factor gene is regulated by serum response factor binding sites. The Journal of biological chemistry 271, 16535-16543.

Steinbach, S.K., El-Mounayri, O., DaCosta, R.S., Frontini, M.J., Nong, Z., Maeda, A., Pickering, J.G., Miller, F.D., and Husain, M. (2011). Directed differentiation of skin-derived precursors into functional vascular smooth muscle cells. Arterioscler Thromb Vasc Biol 31, 2938-2948.

Stenmark, K.R., Bouchey, D., Nemenoff, R., Dempsey, E.C., and Das, M. (2000). Hypoxia-induced pulmonary vascular remodeling: contribution of the adventitial fibroblasts. Physiological research / Academia Scientiarum Bohemoslovaca 49, 503-517.

Stone, D.H., Sivamurthy, N., Contreras, M.A., Fitzgerald, L., LoGerfo, F.W., and Quist, W.C. (2001). Altered ubiquitin/proteasome expression in anastomotic intimal hyperplasia. Journal of vascular surgery 34, 1016-1022.

Su, B., Mitra, S., Gregg, H., Flavahan, S., Chotani, M.A., Clark, K.R., Goldschmidt-Clermont, P.J., and Flavahan, N.A. (2001). Redox regulation of vascular smooth muscle cell differentiation. Circulation research 89, 39-46.

Sun, Q., Chen, G., Streb, J.W., Long, X., Yang, Y., Stoeckert, C.J., Jr., and Miano, J.M. (2006). Defining the mammalian CArGome. Genome research 16, 197-207.

Sun, S.G., Zheng, B., Han, M., Fang, X.M., Li, H.X., Miao, S.B., Su, M., Han, Y., Shi, H.J., and Wen, J.K. (2011). miR-146a and Kruppel-like factor 4 form a feedback loop to participate in vascular smooth muscle cell proliferation. EMBO reports 12, 56-62.

Sun, Y., Xu, J., Xu, L., Zhang, J., Chan, K., Pan, X., and Li, G. (2017). MiR-503 Promotes Bone Formation in Distraction Osteogenesis through Suppressing Smurf1 Expression. Sci Rep 7, 409.

Sundaram, S., Echter, A., Sivarapatna, A., Qiu, C., and Niklason, L. (2014a). Small-diameter vascular graft engineered using human embryonic stem cell-derived mesenchymal cells. Tissue Engineering - Part A 20, 740-750.

Sundaram, S., One, J., Siewert, J., Teodosescu, S., Zhao, L., Dimitrievska, S., Qian, H., Huang, A.H., and Niklason, L. (2014b). Tissue-engineered vascular grafts created from human induced pluripotent stem cells. Stem Cells Transl Med 3, 1535-1543.

Suzuki, H.I., Yamagata, K., Sugimoto, K., Iwamoto, T., Kato, S., and Miyazono, K. (2009). Modulation of microRNA processing by p53. Nature 460, 529-533.

Swartz, D.D., Russell, J.A., and Andreadis, S.T. (2005). Engineering of fibrin-based functional and implantable small-diameter blood vessels. American Journal of Physiology - Heart and Circulatory Physiology 288, H1451-H1460.

Swift, A.J., Rajaram, S., Campbell, M.J., Hurdman, J., Thomas, S., Capener, D., Elliot, C., Condliffe, R., Wild, J.M., and Kiely, D.G. (2014). Prognostic value of cardiovascular magnetic resonance imaging measurements corrected for age and sex in idiopathic pulmonary arterial hypertension. Circ Cardiovasc Imaging 7, 100-106.

Tamama, K., Sen, C.K., and Wells, A. (2008). Differentiation of bone marrow mesenchymal stem cells into the smooth muscle lineage by blocking ERK/MAPK signaling pathway. Stem Cells Dev 17, 897-908.

Taurin, S., Sandbo, N., Yau, D.M., Sethakorn, N., Kach, J., and Dulin, N.O. (2009). Phosphorylation of myocardin by extracellular signal-regulated kinase. The Journal of biological chemistry 284, 33789-33794.

Tay, Y., Zhang, J., Thomson, A.M., Lim, B., and Rigoutsos, I. (2008). MicroRNAs to Nanog, Oct4 and Sox2 coding regions modulate embryonic stem cell differentiation. Nature 455, 1124-1128.

Togliatto, G., Trombetta, A., Dentelli, P., Cotogni, P., Rosso, A., Tschop, M.H., Granata, R., Ghigo, E., and Brizzi, M.F. (2013). Unacylated ghrelin promotes skeletal muscle regeneration following hindlimb ischemia via SOD-2-mediated miR-221/222 expression. J Am Heart Assoc 2, e000376.

Toma, J.G., McKenzie, I.A., Bagli, D., and Miller, F.D. (2005). Isolation and characterization of multipotent skin-derived precursors from human skin. Stem cells 23, 727-737.

Tsutsumi, S., Shimazu, A., Miyazaki, K., Pan, H., Koike, C., Yoshida, E., Takagishi, K., and Kato, Y. (2001). Retention of multilineage differentiation potential of mesenchymal cells during proliferation in response to FGF. Biochem Biophys Res Commun 288, 413-419.

Uccelli, A., Moretta, L., and Pistoia, V. (2006). Immunoregulatory function of mesenchymal stem cells. Eur J Immunol 36, 2566-2573.

Uccelli, A., Moretta, L., and Pistoia, V. (2008). Mesenchymal stem cells in health and disease. Nat Rev Immunol 8, 726-736.

Urbich, C., Kuehbacher, A., and Dimmeler, S. (2008). Role of microRNAs in vascular diseases, inflammation, and angiogenesis. Cardiovasc Res 79, 581-588.

Vella, M.C., Choi, E.Y., Lin, S.Y., Reinert, K., and Slack, F.J. (2004a). The C. elegans microRNA let-7 binds to imperfect let-7 complementary sites from the lin-41 3'UTR. Genes Dev 18, 132-137.

Vella, M.C., Choi, E.Y., Lin, S.Y., Reinert, K., and Slack, F.J. (2004b). The C. elegans microRNA let-7 binds to imperfect let-7 complementary sites from the lin-41 3′ UTR. Genes and Development 18, 132-137.

Villaron, E.M., Almeida, J., Lopez-Holgado, N., Alcoceba, M., Sanchez-Abarca, L.I., Sanchez-Guijo, F.M., Alberca, M., Perez-Simon, J.A., San Miguel, J.F., and Del Canizo, M.C. (2004). Mesenchymal stem cells are present in peripheral blood and can engraft after allogeneic hematopoietic stem cell transplantation. Haematologica 89, 1421-1427.

Voorhees, A.B., Jr., Jaretzki, A., 3rd, and Blakemore, A.H. (1952). The use of tubes constructed from vinyon "N" cloth in bridging arterial defects. Ann Surg 135, 332-336.

Wamhoff, B.R., Bowles, D.K., McDonald, O.G., Sinha, S., Somlyo, A.P., Somlyo, A.V., and Owens, G.K. (2004). L-type voltage-gated Ca2+ channels modulate expression of smooth muscle differentiation marker genes via a rho kinase/myocardin/SRF-dependent mechanism. Circulation research 95, 406-414.

Wang, C., Cen, L., Yin, S., Liu, Q., Liu, W., Cao, Y., and Cui, L. (2010a). A small diameter elastic blood vessel wall prepared under pulsatile conditions from polyglycolic acid mesh and smooth muscle cells differentiated from adipose-derived stem cells. Biomaterials 31, 621-630.

Wang, C., Guan, S., Chen, X., Liu, B., Liu, F., Han, L., Un Nesa, E., Song, Q., Bao, C., Wang, X., et al. (2015). Clinical potential of miR-3651 as a novel prognostic biomarker for esophageal squamous cell cancer. Biochem Biophys Res Commun 465, 30-34.

Wang, C., Guo, F., Zhou, H., Zhang, Y., Xiao, Z., and Cui, L. (2013). Proteomic profiling of tissue-engineered blood vessel walls constructed by adipose-derived stem cells. Tissue Eng Part A 19, 415-425.

Wang, C., Yin, S., Cen, L., Liu, Q., Liu, W., Cao, Y., and Cui, L. (2010b). Differentiation of adipose-derived stem cells into contractile smooth muscle cells induced by transforming growth factor-beta1 and bone morphogenetic protein-4. Tissue Eng Part A 16, 1201-1213.

Wang, D.D., Li, J., Sha, H.H., Chen, X., Yang, S.J., Shen, H.Y., Zhong, S.L., Zhao, J.H., and Tang, J.H. (2016). miR-222 confers the resistance of breast cancer cells to Adriamycin through suppression of p27(kip1) expression. Gene 590, 44-50.

Wang, D.Z., Li, S., Hockemeyer, D., Sutherland, L., Wang, Z., Schratt, G., Richardson, J.A., Nordheim, A., and Olson, E.N. (2002). Potentiation of serum response factor activity by a family of myocardin-related transcription factors. Proceedings of the National Academy of Sciences of the United States of America 99, 14855-14860.

Wanjare, M., Kuo, F., and Gerecht, S. (2013). Derivation and maturation of synthetic and contractile vascular smooth muscle cells from human pluripotent stem cells. Cardiovasc Res 97, 321-330.

Weber, B., Kehl, D., Bleul, U., Behr, L., Sammut, S., Frese, L., Ksiazek, A., Achermann, J., Stranzinger, G., Robert, J., et al. (2016). In vitro fabrication of autologous living tissue-engineered vascular grafts based on prenatally harvested ovine amniotic fluid-derived stem cells. J Tissue Eng Regen Med 10, 52-70.

Weinberg, C.B., and Bell, E. (1986). A blood vessel model constructed from collagen and cultured vascular cells. Science 231, 397-400.

Wightman, B., Burglin, T.R., Gatto, J., Arasu, P., and Ruvkun, G. (1991). Negative Regulatory Sequences in the Lin-14 3'-Untranslated Region Are Necessary to Generate a Temporal Switch during Caenorhabditis-Elegans Development. Gene Dev 5, 1813-1824.

Wightman, B., Ha, I., and Ruvkun, G. (1993). Posttranscriptional Regulation of the Heterochronic Gene Lin-14 by Lin-4 Mediates Temporal Pattern-Formation in C-Elegans. Cell 75, 855-862.

Wong, M.M., Hong, X., Karamariti, E., Hu, Y., and Xu, Q. (2015). Generation and grafting of tissue-engineered vessels in a mouse model. J Vis Exp.

Writing Group, M., Mozaffarian, D., Benjamin, E.J., Go, A.S., Arnett, D.K., Blaha, M.J., Cushman, M., Das, S.R., de Ferranti, S., Despres, J.P., et al. (2016). Heart Disease and Stroke Statistics-2016 Update: A Report From the American Heart Association. Circulation 133, e38-360.

Wu, B., Li, C., Zhang, P., Yao, Q., Wu, J., Han, J., Liao, L., Xu, Y., Lin, R., Xiao, D., et al. (2013). Dissection of miRNA-miRNA interaction in esophageal squamous cell carcinoma. PLoS One 8, e73191.

Wu, W., Allen, R.A., and Wang, Y. (2012). Fast-degrading elastomer enables rapid remodeling of a cell-free synthetic graft into a neoartery. Nat Med 18, 1148-1153.

Wystrychowski, W., Cierpka, L., Zagalski, K., Garrido, S., Dusserre, N., Radochonski, S., McAllister, T.N., and L'Heureux, N. (2011). Case study: first implantation of a frozen, devitalized tissue-engineered vascular graft for urgent hemodialysis access. J Vasc Access 12, 67-70.

Wystrychowski, W., McAllister, T.N., Zagalski, K., Dusserre, N., Cierpka, L., and L'Heureux, N. (2014). First human use of an allogeneic tissue-engineered vascular graft for hemodialysis access. J Vasc Surg 60, 1353-1357.

Xiao, F., Zhang, W., Chen, L., Chen, F., Xie, H., Xing, C., Yu, X., Ding, S., Chen, K., Guo, H., et al. (2013). MicroRNA-503 inhibits the G1/S transition by downregulating cyclin D3 and E2F3 in hepatocellular carcinoma. J Transl Med 11, 195.

Xiao, Q., Luo, Z., Pepe, A.E., Margariti, A., Zeng, L., and Xu, Q. (2009). Embryonic stem cell differentiation into smooth muscle cells is mediated by Nox4-produced H2O2. Am J Physiol Cell Physiol 296, C711-723.

Xie, C., Huang, H., Sun, X., Guo, Y., Hamblin, M., Ritchie, R.P., Garcia-Barrio, M.T., Zhang, J., and Chen, Y.E. (2011a). MicroRNA-1 regulates smooth muscle cell differentiation by repressing Kruppel-like factor 4. Stem cells and development 20, 205-210.

Xie, C., Ritchie, R.P., Huang, H., Zhang, J., and Chen, Y.E. (2011b). Smooth muscle cell differentiation in vitro: models and underlying molecular mechanisms. Arteriosclerosis, thrombosis, and vascular biology 31, 1485-1494.

Xin, M., Small, E.M., Sutherland, L.B., Qi, X., McAnally, J., Plato, C.F., Richardson, J.A., Bassel-Duby, R., and Olson, E.N. (2009). MicroRNAs miR-143 and miR-145 modulate cytoskeletal dynamics and responsiveness of smooth muscle cells to injury. Genes & development 23, 2166-2178.

Xu, J., Li, C.X., Li, Y.S., Lv, J.Y., Ma, Y., Shao, T.T., Xu, L.D., Wang, Y.Y., Du, L., Zhang, Y.P., et al. (2011). MiRNA-miRNA synergistic network: construction via co-regulating functional modules and disease miRNA topological features. Nucleic Acids Res 39, 825-836.

Xu, J., Li, Y., Li, X., Li, C., Shao, T., Bai, J., Chen, H., and Li, X. (2013). Dissection of the potential characteristic of miRNA-miRNA functional synergistic regulations. Mol Biosyst 9, 217-224.

Xu, J., Lim, S.B., Ng, M.Y., Ali, S.M., Kausalya, J.P., Limviphuvadh, V., Maurer-Stroh, S., and Hunziker, W. (2012a). ZO-1 regulates Erk, Smad1/5/8, Smad2, and RhoA activities to modulate self-renewal and differentiation of mouse embryonic stem cells. Stem Cells 30, 1885-1900.

Xu, J., Shao, T., Ding, N., Li, Y., and Li, X. (2016). miRNA-miRNA crosstalk: from genomics to phenomics. Brief Bioinform.

Xu, Z., Ji, G., Shen, J., Wang, X., Zhou, J., and Li, L. (2012b). SOX9 and myocardin counteract each other in regulating vascular smooth muscle cell differentiation. Biochemical and biophysical research communications 422, 285-290.

Yahagi, K., Davis, H.R., Arbustini, E., and Virmani, R. (2015). Sex differences in coronary artery disease: pathological observations. Atherosclerosis 239, 260-267.

Yamasaki, M., Deb, S., Tsubota, H., Moussa, F., Kiss, A., Cohen, E.A., Radhakrishnan, S., Dubbin, J., Ko, D., Schwartz, L., et al. (2016). Comparison of Radial Artery and Saphenous Vein Graft Stenosis More Than 5 Years After Coronary Artery Bypass Grafting. Ann Thorac Surg 102, 712-719.

Yamashita, J., Itoh, H., Hirashima, M., Ogawa, M., Nishikawa, S., Yurugi, T., Naito, M., Nakao, K., and Nishikawa, S. (2000). Flk1-positive cells derived from embryonic stem cells serve as vascular progenitors. Nature 408, 92-96.

Yamashita, R., Sato, M., Kakumu, T., Hase, T., Yogo, N., Maruyama, E., Sekido, Y., Kondo, M., and Hasegawa, Y. (2015). Growth inhibitory effects of miR-221 and miR-222 in non-small cell lung cancer cells. Cancer Med 4, 551-564.

Yamazaki, T., Nalbandian, A., Uchida, Y., Li, W.L., Arnold, T.D., Kubota, Y., Yamamoto, S., Ema, M., and Mukouyama, Y.S. (2017). Tissue Myeloid Progenitors Differentiate into Pericytes through TGF-beta Signaling in Developing Skin Vasculature. Cell Rep 18, 2991-3004.

Yan, X., Liu, Z., and Chen, Y. (2009). Regulation of TGF-beta signaling by Smad7. Acta Biochim Biophys Sin (Shanghai) 41, 263-272.

Yang, J.S., Phillips, M.D., Betel, D., Mu, P., Ventura, A., Siepel, A.C., Chen, K.C., and Lai, E.C. (2011). Widespread regulatory activity of vertebrate microRNA* species. RNA 17, 312-326.

Yang, X., Du, W.W., Li, H., Liu, F., Khorshidi, A., Rutnam, Z.J., and Yang, B.B. (2013). Both mature miR-17-5p and passenger strand miR-17-3p target TIMP3 and induce prostate tumor growth and invasion. Nucleic Acids Res 41, 9688-9704.

Yang, Y.F., Wang, F., Xiao, J.J., Song, Y., Zhao, Y.Y., Cao, Y., Bei, Y.H., and Yang, C.Q. (2014). MiR-222 overexpression promotes proliferation of human hepatocellular carcinoma HepG2 cells by downregulating p27. Int J Clin Exp Med 7, 893-902.

Yao, L., Swartz, D.D., Gugino, S.F., Russell, J.A., and Andreadis, S.T. (2005). Fibrin-based tissue-engineered blood vessels: Differential effects of biomaterial and culture parameters on mechanical strength and vascular reactivity. Tissue Engineering 11, 991-1003.

Yin, H., Jiang, Y., Li, H., Li, J., Gui, Y., and Zheng, X.L. (2011). Proteasomal degradation of myocardin is required for its transcriptional activity in vascular smooth muscle cells. Journal of cellular physiology 226, 1897-1906.

Yokota, T., Ichikawa, H., Matsumiya, G., Kuratani, T., Sakaguchi, T., Iwai, S., Shirakawa, Y., Torikai, K., Saito, A., Uchimura, E., et al. (2008). In situ tissue regeneration using a novel tissue-engineered, small-caliber vascular graft without cell seeding. J Thorac Cardiovasc Surg 136, 900-907.

Yoshida, T., Gan, Q., and Owens, G.K. (2008). Kruppel-like factor 4, Elk-1, and histone deacetylases cooperatively suppress smooth muscle cell differentiation markers in response to oxidized phospholipids. American journal of physiology Cell physiology 295, C1175-1182.

Yoshida, T., Gan, Q., Shang, Y., and Owens, G.K. (2007). Platelet-derived growth factor-BB represses smooth muscle cell marker genes via changes in binding of MKL factors and histone deacetylases to their promoters. American journal of physiology Cell physiology 292, C886-895.

Yoshida, T., Hoofnagle, M.H., and Owens, G.K. (2004). Myocardin and Prx1 contribute to angiotensin II-induced expression of smooth muscle alpha-actin. Circulation research 94, 1075-1082.

Yoshida, T., and Owens, G.K. (2005). Molecular determinants of vascular smooth muscle cell diversity. Circulation research 96, 280-291.

Yu, S., Long, J., Yu, J., Du, J., Ma, P., Ma, Y., Yang, D., and Fan, Z. (2013). Analysis of differentiation potentials and gene expression profiles of mesenchymal stem cells derived from periodontal ligament and Wharton's jelly of the umbilical cord. Cells, tissues, organs 197, 209-223.

Zeidan, A., Nordstrom, I., Albinsson, S., Malmqvist, U., Sward, K., and Hellstrand, P. (2003). Stretch-induced contractile differentiation of vascular smooth muscle: sensitivity to actin polymerization inhibitors. American journal of physiology Cell physiology 284, C1387-1396.

Zhang, H., Jia, X., Han, F., Zhao, J., Zhao, Y., Fan, Y., and Yuan, X. (2013). Dual-delivery of VEGF and PDGF by double-layered electrospun membranes for blood vessel regeneration. Biomaterials 34, 2202-2212.

Zhang, J., Qi, H., Wang, H., Hu, P., Ou, L., Guo, S., Li, J., Che, Y., Yu, Y., and Kong, D. (2006a). Engineering of vascular grafts with genetically modified bone marrow mesenchymal stem cells on poly (propylene carbonate) graft. Artif Organs 30, 898-905.

Zhang, L., Ao, Q., Wang, A., Lu, G., Kong, L., Gong, Y., Zhao, N., and Zhang, X. (2006b). A sandwich tubular scaffold derived from chitosan for blood vessel tissue engineering. J Biomed Mater Res A 77, 277-284.

Zhang, L., Zhou, J.Y., Lu, Q.P., Wei, Y.J., and Hu, S.S. (2008). A novel small-diameter vascular graft: In vivo behavior of biodegradable three-layered tubular scaffolds. Biotechnology and Bioengineering 99, 1007-1015.

Zhang, X., Azhar, G., Zhong, Y., and Wei, J.Y. (2004). Identification of a novel serum response factor cofactor in cardiac gene regulation. The Journal of biological chemistry 279, 55626-55632.

Zhang, Y., Wang, Y., Wang, X., Zhang, Y., Eisner, G.M., Asico, L.D., Jose, P.A., and Zeng, C. (2011). Insulin promotes vascular smooth muscle cell proliferation via microRNA-208-mediated downregulation of p21. Journal of hypertension 29, 1560-1568.

Zhao, J., Liu, L., Wei, J., Ma, D., Geng, W., Yan, X., Zhu, J., Du, H., Liu, Y., Li, L., et al. (2012). A novel strategy to engineer small-diameter vascular grafts from marrow-derived mesenchymal stem cells. Artif Organs 36, 93-101.

Zhao, J., Wu, W., Zhang, W., Lu, Y.W., Tou, E., Ye, J., Gao, P., Jourd'heuil, D., Singer, H.A., Wu, M., et al. (2017a). Selective expression of TSPAN2 in vascular smooth muscle is independently regulated by TGF-beta1/SMAD and myocardin/serum response factor. Faseb J 31, 2576-2591.

Zhao, X., Song, H., Zuo, Z., Zhu, Y., Dong, X., and Lu, X. (2013). Identification of miRNA-miRNA synergistic relationships in colorectal cancer. Int J Biol Macromol 55, 98-103.

Zhao, Y., He, S., Liu, C., Ru, S., Zhao, H., Yang, Z., Yang, P., Yuan, X., Sun, S., Bu, D., et al. (2008). MicroRNA regulation of messenger-like noncoding RNAs: a network of mutual microRNA control. Trends Genet 24, 323-327.

Zhao, Y., Zhang, S., Zhou, J., Wang, J., Zhen, M., Liu, Y., Chen, J., and Qi, Z. (2010). The development of a tissue-engineered artery using decellularized scaffold and autologous ovine mesenchymal stem cells. Biomaterials 31, 296-307.

Zhao, Z., Fan, X., Jiang, L., Xu, Z., Xue, L., Zhan, Q., and Song, Y. (2017b). miR-503-3p promotes epithelial-mesenchymal transition in breast cancer by directly targeting SMAD2 and E-cadherin. J Genet Genomics 44, 75-84.

Zhou, J., Hu, G., and Wang, X. (2010). Repression of smooth muscle differentiation by a novel high mobility group box-containing protein, HMG2L1. The Journal of biological chemistry 285, 23177-23185.

Zhou, R., Gong, A.Y., Chen, D., Miller, R.E., Eischeid, A.N., and Chen, X.M. (2013). Histone deacetylases and NF-kB signaling coordinate expression of CX3CL1 in epithelial cells in response to microbial challenge by suppressing miR-424 and miR-503. PLoS One 8, e65153.

Zhou, R., Zhu, L., Fu, S., Qian, Y., Wang, D., and Wang, C. (2016a). Small Diameter Blood Vessels Bioengineered From Human Adipose-derived Stem Cells. Sci Rep 6, 35422.

Zhou, Y., Deng, L., Zhao, D., Chen, L., Yao, Z., Guo, X., Liu, X., Lv, L., Leng, B., Xu, W., et al. (2016b). MicroRNA-503 promotes angiotensin II-induced cardiac fibrosis by targeting Apelin-13. J Cell Mol Med 20, 495-505.

Zhu, X., Topouzis, S., Liang, L.F., and Stotish, R.L. (2004). Myostatin signaling through Smad2, Smad3 and Smad4 is regulated by the inhibitory Smad7 by a negative feedback mechanism. Cytokine 26, 262-272.

Zuk, P.A., Zhu, M., Ashjian, P., De Ugarte, D.A., Huang, J.I., Mizuno, H., Alfonso, Z.C., Fraser, J.K., Benhaim, P., and Hedrick, M.H. (2002). Human adipose tissue is a source of multipotent stem cells. Molecular biology of the cell 13, 4279-4295.

Zuk, P.A., Zhu, M., Mizuno, H., Huang, J., Futrell, J.W., Katz, A.J., Benhaim, P., Lorenz, H.P., and Hedrick, M.H. (2001). Multilineage cells from human adipose tissue: implications for cell-based therapies. Tissue engineering 7, 211-228.